# UVA Photosensitisers, Protein Oxidation and DNA Repair

**Matthew Peacock**

University College London

and

Cancer Research UK London Research Institute

PhD Supervisor: Peter Karran

A thesis submitted for the degree of

Doctor of Philosophy

University College London

August 2014

## Declaration

I, Matthew Peacock, confirm that the work presented in this thesis is my own. Where information has been derived from other sources, I confirm that this has been indicated in the thesis.

## Abstract

Pharmaceuticals can interact with sunlight to cause skin photosensitization and increase skin cancer risk. Interaction of drug molecules with solar UVA or visible radiation results in electronically excited states that damage biomolecules directly or indirectly *via* the formation of reactive species (RS). RS cause damage to DNA and its precursors, as well as to proteins and lipids.

I have devised methods to examine the induction of oxidative protein damage in cultured human cells and used these to investigate the effects of UVA-activated photosensitizing drugs on the formation of protein carbonyls and the oxidation of protein thiol groups. I examined the effects of 6-thioguanine (6-TG) (a surrogate for azathioprine, an immunosuppressant), fluoroquinolone antibiotics, and the malignant melanoma therapeutic vemurafenib, each of which is associated with clinical skin photosensitivity and increased skin cancer risk in patients. All of these drugs are shown to be synergistically cytotoxic with UVA in cultured human cells and toxicity is concurrent with the generation of RS. I identify singlet oxygen as a major component of these photochemically-generated RS and show that widespread protein oxidation is caused.

The Ku DNA repair heterodimer is identified as one of several targets for oxidation damage and I show using biochemical assays that damage to Ku compromises its function in the repair of DNA strand breaks. UVA irradiation of cells treated with the photosensitisers significantly compromises the removal of potentially mutagenic DNA lesions by the nucleotide excision repair pathway. Since this DNA repair pathway removes sunlight-induced DNA lesions and is the major protection against skin cancer, my findings have implications for the increased skin cancer risk associated with azathioprine. The ability of structurally dissimilar drugs to recapitulate the effects of 6-TG suggests that the observations may share a common mechanism.

## Acknowledgement

First and foremost, I'd like to express my gratitude to Dr Peter Karran for his unwavering support and guidance over the past four years. His patience, generosity and good humour made working in his lab an absolute pleasure from start to finish. I'd also like to thank him for introducing me to the sport of racketball and graciously letting me win to build my confidence. Secondly, I'd like to thank my thesis committee members Drs Simon Boulton and Yao Zhong Xhu for their support and for helpful suggestions throughout my PhD.

I'd especially like to thank the members of the Karran lab, past and present, for creating a fantastic working environment. Drs Quentin Gueranger and Reto Brem deserve special mention for dealing with an incompetent chemist with good grace and teaching me all of the techniques I used to carry out the work detailed herein. Mr Peter MacPherson was always willing to offer a helping hand despite having a packed schedule of his own. The company of Dr Lizzy McAdam-Gray and Miss Melisa Guven made my final two years in the lab far more enjoyable than they had any right to be. I'm especially grateful to Melisa for heroically polishing off the communal chocolate in a noble attempt to protect my waistline. My work stems from initial observations made by Drs Feng Li and Beatriz Montaner to whom I am also indebted.

I'm grateful to many other members of Clare Hall for their assistance. LRI Core Services, especially Cell Services, as well as the Clare Hall lab aides and admin staff, ensured that my working life ran as smoothly as possible. Dr David Frith was instrumental in the initial stages of the project. Mr Mark Johnson was always on hand to offer cheerful assistance despite possibly being the busiest person in Clare Hall. Rafal Lolo, in addition to being a great friend and driving companion, sacrificed many hours of his life to teach me how to use a microscope.

Finally I'd like to thank my Mum and grandparents for their continued love and support. Any success I've enjoyed is due to the start in life they gave me and I'll always be grateful to them.

# Table of Contents

# Table of figures

# List of tables

# Abbreviations

| | |
|---|---|
| $^1O_2$ | Singlet oxygen |
| 4-HNE | 4-hydroxynonenal |
| (6-4)PP | 6-4 pyrimidine:pyrimidone photoproduct |
| 6-MP | 6-mercaptopurine |
| 6-TG | 6-thioguanine |
| 8-oxoG | 8-oxoguanine |
| AFM | Alexa Fluor 647 Maleimide |
| ALE | Advanced Lipid Peroxidation End Product |
| BCC | Basal Cell Carcinoma |
| BER | Base Excision Repair |
| CMM | Cutaneous Malignant Melanoma |
| CPD | Cyclobutane pyrimidine dimer |
| DNPH | Dinitrophenylhydrazine |
| DSB | Double Strand Break |
| ELISA | Enzyme linked immunosorbent assay |
| EMSA | Electrophoretic mobility shift assay |
| FA | Fanconi Anaemia |
| FHA | Fluorescent hydroxylamine |
| FQ | Fluoroquinolone |
| GSH | Glutathione |
| $G^{SO2}$ | Guanine sulfinate |
| $G^{SO3}$ | Guanine sulfonate |
| HR | Homologous recombination |
| HO• | Hydroxyl Radical |
| MCO | Metal Catalysed Oxidation |
| MDA | Malondialdehyde |
| MED | Minimal erythemal dose |
| MMPP | Magnesium monoperoxyphthalate |
| MMR | Mismatch Repair |
| NEM | N-ethylmaleimide |

| | |
|---|---|
| NER | Nucleotide Excision Repair |
| NHEJ | Non-homologous end joining |
| NMSC | Non-melanoma skin cancer |
| NO• | Nitric Oxide |
| $O_2•^-$ | Superoxide |
| PDT | Photodynamic therapy |
| RNO | p-nitroso-N,N-dimethylaniline |
| RS | Reactive Species |
| ROS | Reactive Oxygen Species |
| SCC | Squamous Cell Carcinoma |
| SSB | Single Strand Break |
| TLS | Translesion Synthesis |
| XP | Xeroderma Pigmentosum |

# Chapter 1. Introduction

The central role of oxygen as a toxic, mutagenic gas that is nevertheless indispensible for all aerobic life is somewhat paradoxical. The chemical and physical properties that allow oxygen to participate in aerobic respiration also permit the formation of potentially damaging reactive species (RS). This duality is not exclusive to oxygen; RS also include both radical and non-radical species that result when cellular nitrogen, halogen and sulphur atoms transiently assume more reactive forms. This may not always be inadvertent on the cell's part and the traditional view of RS as inherently harmful has been supplanted as their essential cellular functions continue to be revealed. The extensive countermeasures employed by the cell, however, point to the potential threat that they pose.

## 1.1 Oxygen and reactive oxygen

Molecular oxygen is a diradical. Ground state oxygen exists in a triplet state; in other words, it contains two unpaired electrons with parallel spins. In contrast, most cellular macromolecules exist in singlet ground states and have electrons paired in molecular orbitals with antiparallel spins. A molecule in a triplet state cannot accept paired electrons due to the Pauli exclusion principle, which states that electrons in the same orbital must have different spins, and therefore reactions between triplet and singlet state molecules occur very slowly, if at all (they are said to be spin restricted). Although $O_2$ is essentially unreactive with cellular molecules, it does react very rapidly with other radical species.

In cells, the majority of oxygen is utilised as the terminal electron acceptor in oxidative phosphorylation. During this process, cytochrome c oxidase catalyses the concerted and complete, four-electron reduction of oxygen to yield water. As well as being completely reduced to water, oxygen can also exist as a number of intermediate species that are generated by successive one-electron reductions (Figure 1.1). These states are more reactive than molecular oxygen or water and are hence known as reactive oxygen species (ROS).

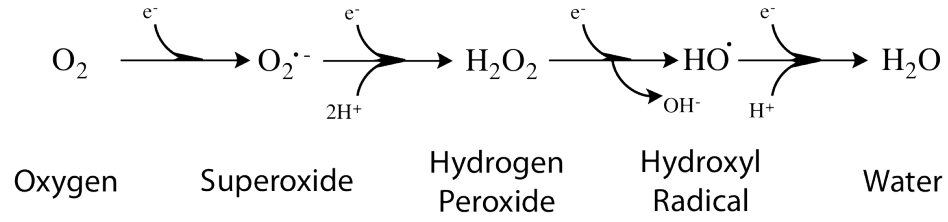


**Figure 1.1 Sequential single electron reductions of oxygen**

Successive one-electron reductions of oxygen yield the ROS illustrated above.

### 1.1.2 Hydroxyl Radical

The hydroxyl radical (HO•) is the most reactive known ROS and can take part in the widest range of reactions with cellular molecules. Reaction rates between HO• and most organic molecules are essentially diffusion-controlled and are limited only by how quickly HO• can be generated (Gaetke 2003). Its major modes of reaction are abstraction of hydrogen from hydrocarbons and addition to carbon-carbon double bonds (Valko et al. 2006).

There are several physiological and non-physiological sources of HO• with the most widely studied being the decomposition of $H_2O_2$ and the radiolysis of water(Halliwell & Gutteridge 2007). $H_2O_2$ decomposition can be induced by UV radiation. $H_2O_2$ absorbs strongly at shorter UV wavelengths(Holt et al. 1948) and UVC is most commonly used for generating HO• *in vitro*, for example, in water purification(Legrini et al. 1993).

The Fenton reaction (**1**) is the Fe(II) catalysed disproportionation of $H_2O_2$ to yield a hydroxyl radical and a hydroxyl anion. The catalytic Fe(II) can be regenerated by superoxide-mediated reduction of the resulting Fe(III) (**2**) however it is likely that other species can play this role in cells(Burkitt 2003). The Fenton reaction has been proposed as a source of HO• *in vivo*(Kehrer 2000).

$$Fe^{2+} + H_2O_2 \rightarrow Fe^{3+} + HO^{\bullet} + {}^{-}OH \quad \textbf{(1)}$$

$$Fe^{3+} + O_2^{\bullet -} \rightarrow Fe^{2+} + O_2 \quad \textbf{(2)}$$

$$\textbf{Net: } O_2^{\bullet -} + H_2O_2 \rightarrow HO^{\bullet} + {}^{-}OH + O_2 \quad \textbf{(3)}$$

The low bioavailability of potentially harmful iron in a redox-active form is an important constraint on Fenton chemistry in the cell. Specialised proteins mediate intracellular iron storage and transport; ferritin and transferrins being the best characterised. Historically, the presence of free iron was considered to reflect a pathological condition (haemochromatosis). More recently it has become apparent that, despite tight control of iron homeostasis, cells do maintain a "labile iron pool" for the synthesis of iron-containing proteins - a mixture of Fe(II) and Fe(III) weakly chelated by low Mw ligands including citrate, phosphate and nucleosides. Chelate oxidation can liberate free iron from iron-containing proteins. The best known example of this is superoxide-induced Fe(II) release from the iron sulphur cluster (4Fe-4S) of the mitochondrial protein aconitase which leads to HO• formation (Vasquez-Vivar 2000)). Oxidation can also release iron from ferritin (Rudeck et al. 2000). This indicates that free iron (and hence HO•) can be generated by less reactive forms of ROS thereby exacerbating their effects. Copper, chromium, cobalt and vanadium are all capable of Fenton-like chemistry although the low intracellular concentrations of these metals probably limit their ability to generate OH• (Gaetke 2003; Valko et al. 2006).

The interaction of water with ionizing radiation generates OH• *via* homolytic fission (**4**):

$$H_2O^* \rightarrow H^{\bullet} + HO^{\bullet} \quad \textbf{(4)}$$

where $H_2O^*$ is water excited by radiation.

HO• can also be generated during phagocytosis. The hypochlorous acid and superoxide produced by neutrophils can react rapidly to yield HO•(**5**):

$$HOCl + O_2^{\bullet -} \rightarrow O_2 + Cl^- + HO\bullet \qquad \textbf{(5)}$$

### 1.1.3 Hydrogen Peroxide

Hydrogen peroxide ($H_2O_2$) is a non-radical and relatively unreactive ROS. Its biological importance reflects its ubiquity and its ability to form reactive decomposition products. The chemistry of $H_2O_2$ is mediated by its labile oxygen-oxygen single bond and hence it has a propensity for disproportionation and oxidation reactions. Given that only a limited number of reactive substrates are oxidised by $H_2O_2$, the majority of adverse cellular effects caused by $H_2O_2$ actually result from HO• produced by $H_2O_2$ breakdown.

Intracellular steady-state concentrations of $H_2O_2$ are estimated to be micromolar (B. Chance et al. 1979). Most $H_2O_2$ derives from mitochondria but other organelles such as peroxisomes may contribute. The majority of mitochondrial $H_2O_2$ is formed from the enzyme-catalysed dismutation of superoxide (see Section 1.1.4). Many oxidases generate both $H_2O_2$ and superoxide as by-products(Halliwell & Gutteridge 2007). In addition, $H_2O_2$ is produced by auto- and metal-catalysed oxidation of various molecules including ascorbate and flavonoids(Halliwell 2008). $H_2O_2$ is an important intracellular signalling molecule and is transiently produced by NADPH oxidases in response to various extracellular stimuli such as growth factors and cytokines (Rhee 2003). $H_2O_2$ detoxifying enzymes ensure that signalling remains localised by destroying any $H_2O_2$ that diffuses away from the generation site(Rhee et al. 2000). It follows that excess $H_2O_2$, despite its lack of reactivity, can be deleterious by disrupting these signalling pathways.

#### *1.1.3.1 Antioxidant measures against $H_2O_2$*

Catalases, glutathione peroxidases and peroxiredoxins ensure that excess $H_2O_2$ is quickly destroyed. These enzymes are highly conserved and ubiquitous in aerobes. Their conservation highlights the inevitability of $H_2O_2$ production and the importance of resolving the threat it poses.

Catalase is mainly localised within peroxisomes. It disproportionates $H_2O_2$ to water and oxygen via the following steps (**6 & 7**):

$$\text{Catalase (Porphyrin-Fe}^{III}\text{)} + H_2O_2 \rightarrow \text{Compound I (Porphyrin}^{+\bullet}\text{-Fe}^{IV}\text{=O)} + H_2O \quad \textbf{(6)}$$

$$\text{Compound I (Porphyrin}^{+\bullet}\text{-Fe}^{IV}\text{=O)} + H_2O_2 \rightarrow \text{Catalase} + H_2O + O_2 \quad \textbf{(7)}$$

**Total** : $2H_2O_2 \rightarrow 2H_2O + O_2$

Since two $H_2O_2$ molecules are required in the catalytic cycle, catalase is not efficient at low $H_2O_2$ concentrations and probably only becomes significant under conditions of oxidative stress or when scavenging the $H_2O_2$ produced locally during signalling or within peroxisomes(Rhee et al. 2005). Loss of catalase (acatalasemia) only results in a mild phenotype illustrating the importance of other antioxidant measures.

Glutathione peroxidases (GPx) and peroxiredoxins (Prx) reduce $H_2O_2$ to $H_2O$. GPx are present in the cytosol and mitochondria of all mammalian cells. GPx uses glutathione (GSH) as a hydrogen donor to catalyse the reduction of $H_2O_2$. All GPx isoforms contain a selenocysteine in their active site. The lower pKa of selenocysteine means that it is deprotonated at physiological pH allowing it to react with peroxides to form selenic acid via the following reactions (**8, 9 & 10**):

$$\text{GPx-Se}^- + H_2O_2 + H^+ \rightarrow \text{GPx-SeOH} \quad \textbf{(8)}$$

$$\text{GPx-SeOH} + \text{GSH} \rightarrow \text{GPX-Se-GSH} + H_2O \quad \textbf{(9)}$$

$$\text{GPX-Se-GSH} + \text{GSH} \rightarrow \text{GPx-Se}^- + H^+ + \text{GSSG} \quad \textbf{(10)}$$

**Total**: $H_2O_2 + 2\text{GSH} \rightarrow \text{GSSG} + H_2O + H_2O$

GPx is not essential. Under normal conditions its absence in knockout mice is not associated with any overt phenotype although the mice are less able to cope with oxidative stress(Klivenyi et al. 2000).

Peroxiredoxins are extremely abundant and may comprise as much as 0.5% of total soluble protein. Despite exhibiting slower kinetics than catalase and GPx, they are thought to be the major effector of $H_2O_2$ disproportionation under normal conditions. All Prx isoforms have active site cysteines. Cysteine oxidation to sulfenic acid accompanies $H_2O_2$ reduction (**11**).

$$PrX - SH + H_2O_2 \rightarrow PrX - SOH + H_2O \qquad \textbf{(11)}$$

At high $H_2O_2$ concentrations, Prx can be inactivated by sulphinic acid formation or glutathionylation. Concomitantly, catalase and Gpx are upregulated. In this way, the three enzymes work in concert to manage antioxidant capacity over a range $H_2O_2$ concentrations(Rhee et al. 2005).

### 1.1.4 Superoxide

Like $H_2O_2$, superoxide ($O_2^{\bullet -}$) is a reduced form of molecular oxygen that is inevitably generated during aerobic metabolism and is utilised by the cell in a number of ways.

$O_2^{\bullet -}$ exhibits minimal reactivity with most biomolecules. This is partly due to the same spin restrictions that govern molecular oxygen reactivity and partly to its anionic nature that deters interaction with the electron rich centres that are the preferred targets of radicals(Winterbourn 2008).

The major source of $O_2^{\bullet -}$ in mammalian cells is thought to be electron leakage from Complexes I and III in the mitochondrial electron transport chain. Cells also produce $O_2^{\bullet -}$ intentionally via oxidases as part of cell signalling.

#### *1.1.4.1 Antioxidant measures against superoxide*

$O_2^{\bullet -}$ undergoes spontaneous dismutation under physiological conditions (Halliwell & Gutteridge 2007). Dismutation is a bimolecular process and proceeds via the hydroperoxyl radical ($HO_2^{\bullet}$), the protonated form of superoxide (pKa 4.8):

$$O_2\bullet^- + H^+ \leftrightarrow HO_2\bullet \quad \textbf{(12)}$$

$$HO_2\bullet + O_2\bullet^- + H^+ \rightarrow H_2O_2 + O_2 \quad \textbf{(13)}$$

or

$$HO_2\bullet + HO_2\bullet \rightarrow H_2O_2 + O_2 \quad \textbf{(14)}$$

Although spontaneous dismutation is fairly rapid, superoxide dismutases (SOD), which increase the rate of dismutation by around 3-4 orders of magnitude, are found in almost all eukaryotes.

$$M^{(n+1)} + O_2\bullet^- \rightarrow M^{n+} + O_2 \quad \textbf{(15)}$$

$$M^{n+} + O_2\bullet^- + 2H^+ \rightarrow M^{(n+1)} + H_2O_2 \quad \textbf{(16)}$$

$$\textbf{Total}: 2O_2\bullet^- + 2H^+ \rightarrow O_2 + H_2O_2$$

CuZnSOD (also known as SOD1) is a highly abundant (~$10^{-5}$ M), dimeric protein located primarily in the cytosol. The structurally unrelated tetrameric MnSOD (SOD2) is almost exclusively mitochondrial.

The extracellular CuZnSOD (EC-SOD or SOD3) - a tetrameric glycoprotein that is bound to cell surface carbohydrates and the extracellular matrix - shares 60% homology with SOD1. It is especially abundant in blood vessels, where it may play a role in mediating nitric oxide signalling(Fattman et al. 2003).

The phenotypes of SOD-deficient mice underline the importance of controlling $O_2\bullet^-$ levels. SOD1 knockout mice are hypersensitive to oxidants and show accelerated age-related deterioration. SOD2 knockout mice have cardiac abnormalities, mitochondrial dysfunction and dramatically shortened lifespans. Overexpression of SODs confers resistance to hyperbaric $O_2$.

### 1.1.5 Singlet Oxygen

The electronically excited singlet state of oxygen ($^1O_2$) occurs by energy transfer to molecular oxygen in its triplet ground state and consequent antiparallel alignment of its outer shell electrons (illustrated in Figure 1.2) ($^1O_2$).

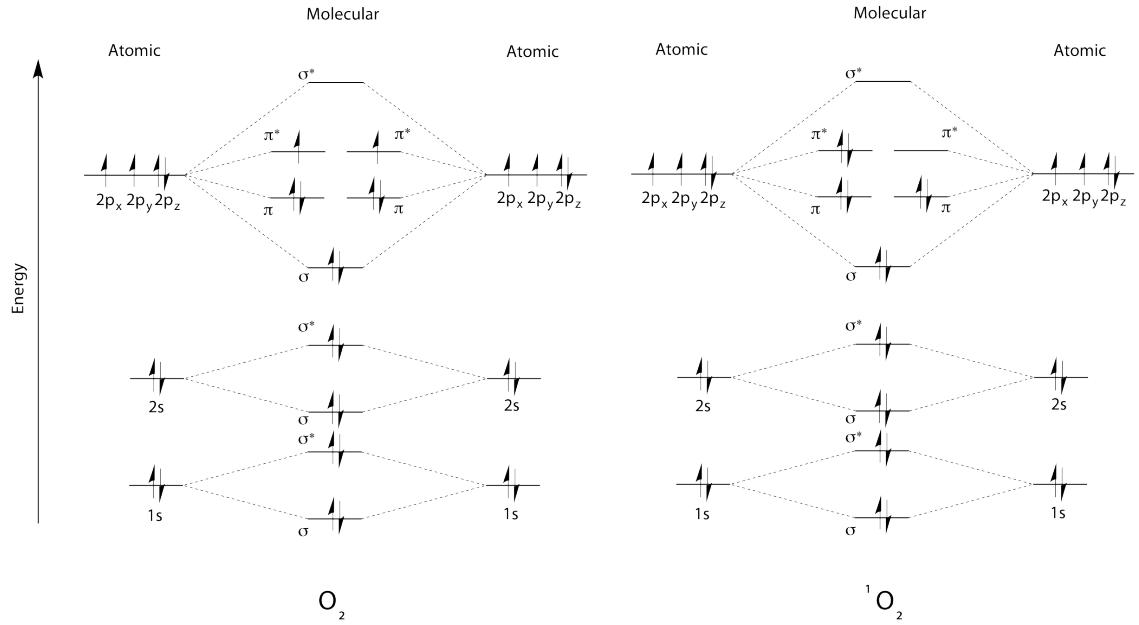


**Figure 1.2 Molecular orbital diagrams for molecular oxygen and singlet oxygen**
The molecular orbital energy levels of dioxygen (shown as short, horizontal lines) are flanked by their constituent atomic orbital energy levels. The energy levels increase from bottom to top. Electrons are depicted as arrows and the direction denotes their spin. The electrons in the outermost orbital of $O_2$ have the same spin and are in different orbitals (triplet). Excitation to singlet oxygen causes electrons to pair in one orbital with opposite spins.

#### *1.1.5.1 Chemistry of Singlet Oxygen*

The major $^1O_2$ source in biological systems is likely to be photosensitisation(M. J. Davies 2004) which is covered in Section 1.5.

Physical quenching by the solvent is the fate of most cellular $^1O_2$. It has a shorter lifetime in pure $H_2O$ (4 μs) than in pure $D_2O$ (68 μs). This isotope effect is also observed in cells saturated with $D_2O$ (lifetime ~30 μs). The short half-life of $^1O_2$ ($\leq$ 4 μs) means that its radius of diffusion is small (< 250 nm) and its primary effects will be localised to the immediate vicinity of its generation(Redmond & Kochevar 2006). Other molecules can also efficiently inactivate $^1O_2$. These include the azide ion, α-tocopherol,

β-carotene and ascorbate. In many cases the interaction of $^1O_2$ generates new products. Because the spin restrictions that limit the reactivity of $O_2$ no longer apply to $^1O_2$, it is much more reactive with cellular macromolecules. It is electrophilic and reacts mainly with aromatic groups, sulphur atoms and alkenes. Reactions with double bonds can result in three possible products: endoperoxides, hydroperoxides and dioxetanes (Detailed in Figure 1.3).

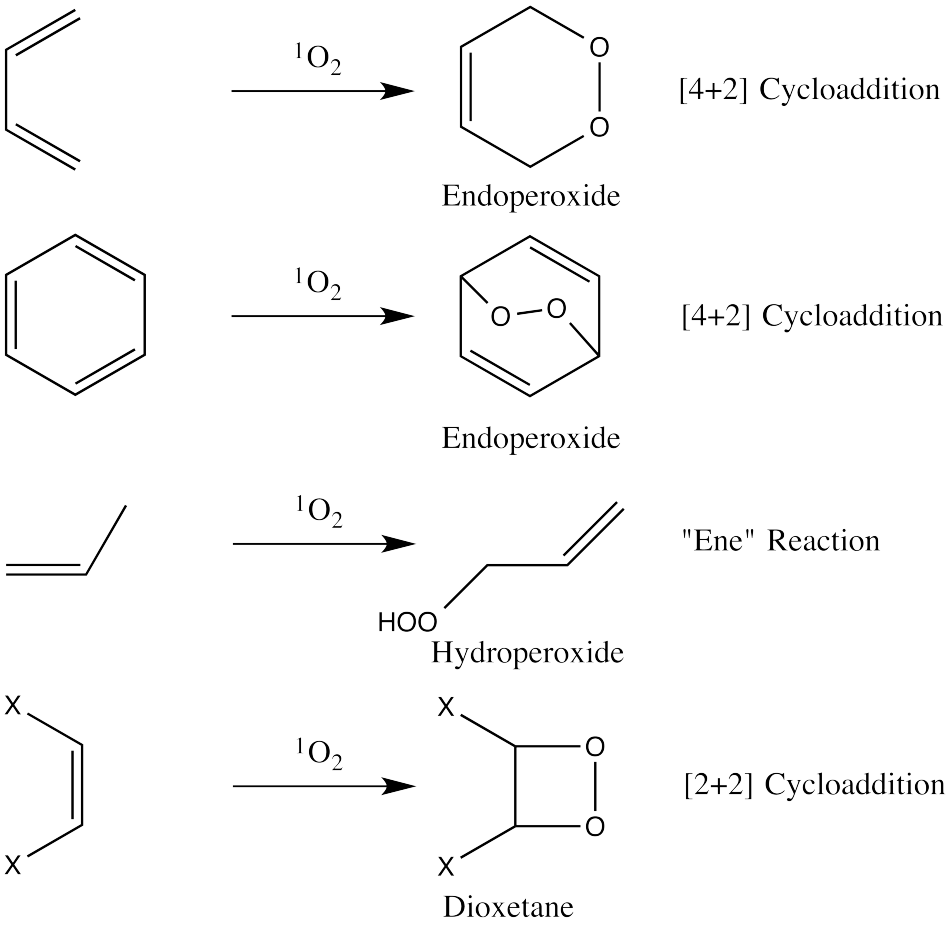


**Figure 1.3 Reactions of singlet oxygen with double bonds**
The products of $^1O_2$ reaction depend on the configuration of the double bonds plus the nature and arrangement of the other substituents. Endoperoxide formation occurs via [4+2] cycloaddition to conjugated cis-dienes (top) in a Diels-Alder like reaction. Endoperoxides are unstable and will decompose to yield other products including hydroperoxides. Allylic hydroperoxides can also be formed via the "ene" reaction with alkenes (middle). Reactants with electron-rich atoms adjacent to the double bond can also form unstable dioxetanes via [2+2] cycloaddition (bottom).

The interaction of $^1O_2$ with cellular thiols is almost entirely via chemical reaction (in contrast to the interaction with double bonds, 95% of which proceeds via physical quenching)(Breen & Murphy 1995; Devasagayam et al. 1991). The resulting products include disulphides and various sulphur oxyacids including sulfinate, sulfonate and sulfoxide.

No specialised enzymes have evolved to detoxify $^1O_2$. Because it is longer lived than HO•, $^1O_2$ can exert its influence over a wider area and cellular antioxidants may be important in minimising its harmful effects. Thiol quenching is likely to be most significant in a biological context owing to the high cellular concentrations of glutathione and cysteine(Di Mascio et al. 1990). Although carotenoids and tocopherols are more reactive, their lipophilic nature suggests that their protective effects will be confined to membranes. Other potential hydrophilic quenchers include ascorbic acid and aromatic amino acids, either free or within proteins. It has been estimated (Bisby et al. 1999) that the ability of cytoplasm to quench $^1O_2$ is 10 times greater than that of pure water. This suggests that the cellular lifetime of $^1O_2$ is around 0.4 μs. Overall, studies (Baker & Kanofsky 1992; Bisby et al. 1999) concur that cellular antioxidant defences are insufficient to protect proteins against damage by $^1O_2$ .

### 1.1.6 Other Cellular Reactive Species

Other RS containing a variety of heteroatoms have also been described. Like ROS, some RS arise naturally during the course of normal cellular function whilst others are induced by pathology or exogenous stimuli. Important examples include the non-radical RS hypochlorous acid (HOCl) that is generated by the enzyme myeloperoxidase within neutrophils and may assist in the killing of pathogens through oxidation or chlorination of DNA, proteins and lipids. HOCl modification of proteins has be detected in patients with inflammatory diseases(Pullar et al. 2000).

The nitric oxide radical (NO•) is generated by nitric oxide synthases (NOS) and regulates a variety of physiological processes ranging from blood pressure to inflammatory responses. It is an important signalling molecule that acts by modification

of its target proteins, usually by binding to transition metals or causing nitrosylation of susceptible cysteines. Many of the deleterious consequences originally ascribed to NO• are now known to be due to the peroxynitrite anion (OONO-), which forms extremely rapidly upon NO• reaction with $O_2$•$^-$. ONOO- is an extremely potent oxidant and causes DNA strand breaks, lipid peroxidation and protein oxidation. Its more selective reactivity enables ONOO- to diffuse 10000 times further than HO• (2-3 cell diameters vs the diameter of a small protein(Pacher et al. 2007)) whilst remaining extremely reactive. This property is reflected in the ability of ONOO- to kill cells at lower concentrations than HO•(Beckman 1994).

I will now consider some of the effects of the abovementioned reactive species on cells.

## 1.2 The actions of reactive species in cells

### 1.2.1 Oxidative Stress

The energetic cost of antioxidant systems, and the fact that some RS have roles in cell signalling means that the optimal RS level for a cell is not necessarily zero. Disruption of the oxidant/antioxidant balance, either through depletion or dysfunction of antioxidant defences or increased production of RS, leads to a condition termed oxidative stress. Unchecked RS are then able to damage cellular components. This undesirable state provokes a coordinated protective response.

### 1.2.2 Consequences of oxidative stress

Oxidative stress causes Nrf2 to upregulate transcription of genes involved in oxidant homeostasis. These include genes related to antioxidant synthesis such as glutathione-S-transferase and glutathione reductases, and antioxidant enzymes such as GPxs and Prxs(Ma 2013). The unifying feature of these genes is the presence of a 41-base-pair enhancer sequence, known as an antioxidant response element (ARE). Under normal conditions, Nrf2 is suppressed by Keap1, which marks Nrf2 for degradation and keeps

intracellular levels low. Oxidation of reactive cysteines within Keap1 results in inactivation, allowing Nrf2 to avoid degradation and enter the nucleus to bind AREs.

Oxidative stress also activates members of the MAP kinase superfamily. They can be subcategorised into three classes: extracellular-signal-related kinases (ERK), p38 kinases and c-Jun N-terminal kinases (JNK). Oxidation of reactive cysteines inactivates protein tyrosine phosphatases leading to ERK activation whilst oxidation of ASK1 cysteines leads to p38 and JNK activation(Runchel et al. 2011). These are just two examples and MAPK activation can result from numerous stimuli. Activation of ERK promotes phosphorylation of downstream transcription factors that induce proliferation whilst sustained p38 and JNK activation leads to apoptosis; the final outcome for the cell depends on the relative activation of these pathways(Sonntag 2006; Martindale & Holbrook 2002).

Some gene promoters such as γ-glutamyl transferase contain an ARE in addition to binding sites for AP-1 (stimulated by MAPK activation) and NFκB (another RS activated transcription factor) indicating complex interactions at play between these systems. By way of a multifaceted, dynamic response, low to moderate levels of RS can be tolerated by cells and in fact the increased antioxidant measures may persist for some time, equipping cells to better deal with future challenges.

If these adaptive measures cannot restore the oxidant/antioxidant balance, cells undergo senescence or cell death via apoptosis or necrosis. Moderate oxidative stress first results in cell cycle arrest by checkpoint activation. This can be achieved by many routes depending on the site of RS generation(Folkes et al. 1995; B. Liu et al. 2008), however one potential mechanism is p53 activation due to DNA damage. Prolonged MAPK stimulation leads to senescence (Halliwell & Gutteridge 2007; Boonstra & Post 2004). High levels of RS that disrupt essential cellular functions induce apoptosis. This is characterised by mitochondrial permeability transition, the release of pro-apoptotic factors and caspase activation. Necrosis may predominate at very high RS levels because caspases contain essential cysteines that are susceptible to oxidation. Apoptosis and necrosis represent the final recourse for the cell to prevent pathology arising from

oxidatively damaged cellular components; some examples of these products and their potential for deleterious effects are detailed in the following section.

### 1.2.3 Damage to cellular components

Oxidative damage can affect all cellular components however the precise nature of this damage depends on the chemistry of the RS and where they are generated. The most reactive RS such as HO• will react with the first molecule they encounter whereas less reactive RS will react with a more limited spectrum of targets and generate relatively specific products.

#### *1.2.3.1 Lipid Peroxidation*

Cellular membranes are a mixture of saturated and unsaturated fatty acids of varying chain lengths that contain embedded and attached proteins. Unsaturated bonds confer important membrane fluidity but polyunsaturated fatty acids (PUFAs) are vulnerable to attack by RS. Peroxidation occurs when an RS (usually HO•) abstracts a hydrogen atom from a lipid (LH) leaving a radical species (L•). This quickly reacts with $O_2$ to yield a peroxyl radical (LOO•) that then abstracts hydrogen to form a lipid hydroperoxide (LOOH) and a new L•. In this way, a chain reaction proceeds until terminated by an antioxidant or the meeting of two L•.

$$HO\bullet + LH \rightarrow L\bullet + H_2O \quad \textbf{(17)}$$

$$L\bullet + O_2 \rightarrow LOO\bullet \quad \textbf{(18)}$$

$$LOO\bullet + LH \rightarrow LOOH + L\bullet \quad \textbf{(19)}$$

Lipid peroxides can be formed in a non-radical reaction by the action of $^1O_2$, which reacts with unsaturated double bonds via the “ene” reaction shown in Figure 1.3.

Lipid peroxidation causes loss of membrane fluidity, reduces membrane integrity and, damages and inactivates membrane proteins. Importantly, chain cleavage adjacent to the peroxide moiety generates reactive aldehyde products that can form adducts with DNA and proteins. The most studied aldehydes are malondialdehyde (MDA) and 4-

hydroxynonenal (HNE) - both bifunctional electrophiles capable of reacting with DNA and proteins. Addition to DNA proceeds preferentially at guanine (the MDA-guanine adduct is known as $M_1G$ and has been identified in human DNA) whilst protein adducts form via a Schiff base resulting in protein dysfunction and aggregation(Negre-Salvayre et al. 2008) (Figure 1.4).

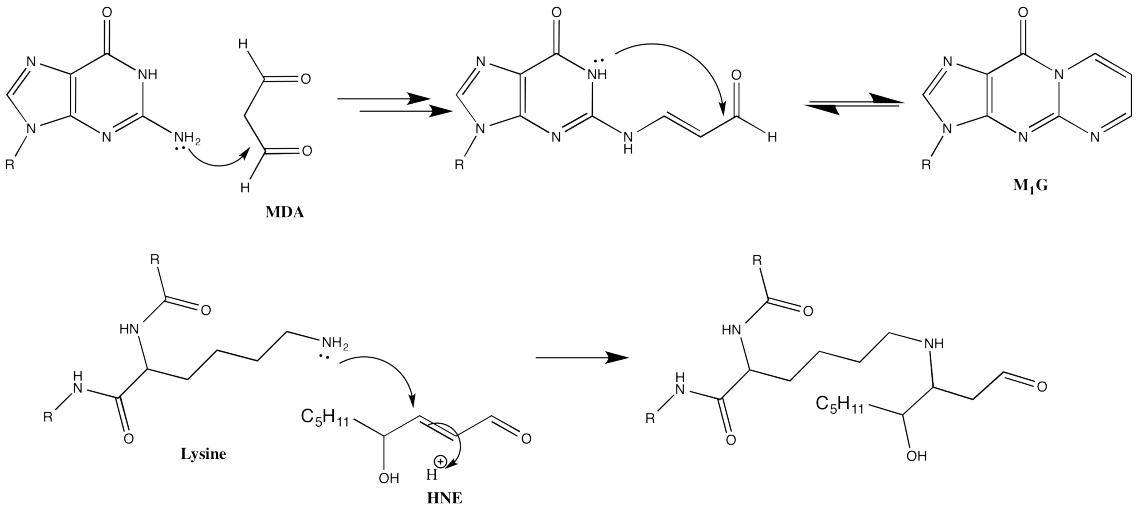


**Figure 1.4 Reactions of lipid peroxidation products**
**Top:** Malondialdehyde (MDA) can react with the nucleophilic N2 of guanine. The reaction product can then undergo ring closing to give $M_1G$. **Bottom:** HNE protein adduct formation via a Michael addition with a lysine residue. These reactions are examples and lipid peroxidation products will react with any appropriate nucleophile.

### *1.2.3.2 Protein oxidation*

Their abundance and the reactivity of their side chains make cellular proteins a significant target for reactive species. An extremely wide range of oxidation products are possible; the likelihood of formation is determined by the identity of the reactive species, the accessibility of protein side chains and the local redox environment.

Unsurprisingly, the hydroxyl radical exhibits the most extensive and complex pattern of modifications. Although HO• is sufficiently reactive to modify all amino acid side chains, reaction with electron rich amino acids is favoured. At physiological pH, direct H-abstraction from S-H and C-H bonds is the predominant reaction giving rise to thiyl

and alkyl radicals respectively(Xu & M. R. Chance 2007). Thiyl radicals go on to form disulphides and sulphur oxyacids.

Carbon centred radicals on α and β carbons can combine with oxygen to yield peroxyl radicals, eventually leading to cleavage of the protein backbone. Peroxyl species formed on side chains can yield a variety of residue-specific hydroperoxide, hydroxide and carbonyl products. The structure of some side chains makes protein carbonyl formation more favourable due to the presence of leaving groups (Figure 1.5, illustrated using arginine)(Xu & M. R. Chance 2007). The potential for chain reaction means that a single HO• radical can be responsible for the modification of up to 15 amino acids(Neuzil et al. 1993).

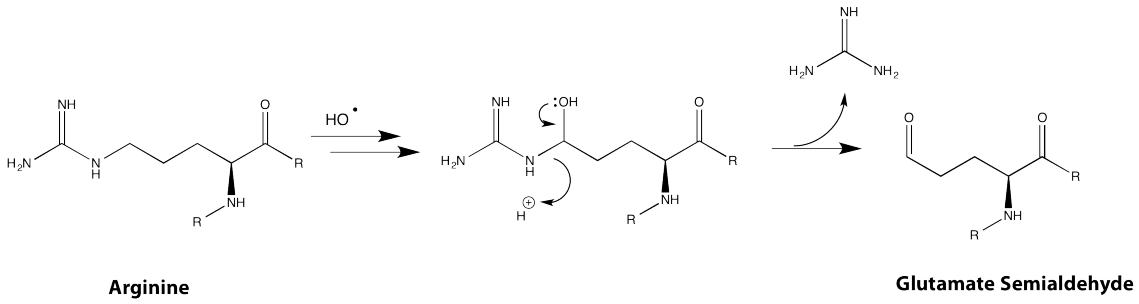


**Figure 1.5: Protein carbonyl formation from arginine**
After oxidation via HO• the resulting hydroxide can rearrange and eliminate the guanidino group to yield a protein carbonyl.

Hydrogen peroxide does not react with most proteins, even at mM concentrations(Halliwell & Gutteridge 2007). It can, however, inactivate a number of enzymes with active site cysteines including glyceraldehyde 3-phosphate dehydrogenase(Brodie & Reed 1987), phosphotyrosine protein phosphatase(Meng et al. 2002) and caspases(Borutaite & Brown 2001).
Some enzyme-$H_2O_2$ reactions may exacerbate oxidative stress. Heme oxidation with resultant release of iron(Gutteridge 1986) and activation of nitric oxide synthase and NADPH oxidase to increase $O_2^{\bullet -}$ levels(Coyle et al. 2006) are two examples.

$O_2^{\bullet -}$ is also generally unreactive toward proteins. An important exception is iron-sulphur cluster modification. Reaction with $O_2^{\bullet -}$ inactivates the enzyme and releases ferrous iron:

$$[4Fe\text{-}4S]^{2+} + O_2\bullet^- + 2H^+ \rightarrow [4Fe\text{-}4S]^{3+} + H_2O_2 \quad \textbf{(19)}$$

$$[4Fe\text{-}4S]^{3+} \rightarrow [3Fe\text{-}4S]^{+} + Fe^{2+} \quad \textbf{(20)}$$

Acontinase and dehydratases are particular targets and their inactivation leads to energy metabolism defects(Halliwell & Gutteridge 2007).

$^1O_2$ reacts predominantly with electron-rich aromatic residues and sulphur containing side chains(M. J. Davies 2003). The major products of tryptophan oxidation, N-formylkynurine and kynurine formed 2+2 cycloaddition (as seen in Figure 1.3) can act as photosensitisers, perhaps exacerbating damage by further $^1O_2$ production. Tyrosine modification proceeds *via* endoperoxide formation (Figure 1.3) leading to an unstable hydroperoxide, which may promote protein crosslinking. Hydroperoxide decomposition may also cause fragmentation and ring opening. Histidine oxidation occurs via endoperoxide formation on the imidazole ring, which then goes on to form a number of poorly characterized breakdown products, some of which may participate in His-His and His-Lys protein crosslinking. Oxidation of methionine leads to methionine sulfoxide whilst cysteine likely forms oxyacids and disulphides. Structures of singlet oxygen reaction products can be found in Figures 3.1 and 3.3.

In addition to protein carbonyl formation and thiol oxidation, peroxynitrite can form specific nitration products of aromatic residues(Ischiropoulos & al-Mehdi 1995). The formation of 3-nitrotyrosine may result in the downregulation of phosphotyrosine-dependent signalling as it is a poor tyrosine kinase substrate.

The numerous consequences that arise from protein oxidation are determined by the identities of the proteins and reactive species in question. Specific oxidative modification of key residues can reversibly regulate protein function as part of cell signalling or inactivate proteins in an uncontrolled or irreversible manner as part of RS-mediated pathology. Gross modification to protein structure caused by severe oxidative stress will cause loss of function as well as fragmentation, aggregation and proteasomal degradation.

Redox regulation of proteins, which almost always occurs via thiol oxidation, inactivates an enzyme if the thiol is necessary for catalytic activity (e.g. GapDH), or induces a conformational change that modulates activity. This modulation can be activating or inactivating and proceeds through a wide range of mechanisms including disrupting interaction with a repressor (Nrf2(Kansanen et al. 2013)), loss of metal binding (PKC(Korichneva 2005)) or reducing DNA binding (AP-1(Klatt et al. 1999)). Although less studied, methionine sulfoxide formation can also play a role in signalling. Methionine is considered a hydrophobic amino acid however addition of an oxygen atom renders it hydrophilic and can cause large scale conformational changes; in this way, methionine oxidation regulates calmodulin(Bigelow & Squier 2011). In the context of $H_2O_2$ signalling, the likelihood of a cysteine undergoing oxidation is determined in the first instance by accessibility but also by its pKa as the thiolate anion is much more nucleophilic. More reactive RS such as OH•, $^1O_2$ and $ONOO^-$ will be less selective in their reactions with protein thiols and more likely to form higher oxyacids. Thiol oxidation and the conformational changes it causes can also have deleterious effects on non-redox regulated proteins with susceptible cysteines and methionines.

Limited local oxidation leading to functional inactivation can also occur by the action of RS upon aromatic residues. Tyrosine nitration inactivates SOD2(Radi 2004), loss of tryptophan leads to inactivation of lysozyme(Jiménez et al. 2000) whilst histidine oxidation leading to loss of metal binding has been shown to inactivate the bacterial transcription factor PerR(Lee & Helmann 2006). The susceptibility of thiol and aromatic amino acids is consistent with their being the most reactive targets and thus multiple RS can modify them; modification of aliphatic residues will likely only be effected by OH•. As outlined previously, this generally proceeds via H-abstraction in addition of oxygen in some form. This alters the hydrophobicity of sidechains resulting in misfolding and exposure of hydrophobic domains leading to non-specific interaction and aggregation(Mirzaei & Regnier 2008). Aggregation can also occur through formation of interprotein cross links; these can be either radical mediated such dityrosine crosslinks, which can cause pathology *in* vivo(Souza 2000), or result from reaction between oxidation products such as those of histidine and a nucleophile

(Balasubramanian et al. 1999). Oxidation induced aggregation leading to inactivation may have implications for disease progression; aggregates may be inherently toxic regardless of their composition(Bucciantini et al. 2002). Severe oxidation or diminished removal capacity may result in the formation of lipofuscin, a persistant lipid-protein aggregate which may inhibit removal of other oxidised species and promote further oxidation through redox-metal binding.

Cells possess proteolytic systems that play roles in normal cellular function but are able to participate in the detoxification of oxidised proteins. The proteasome comprises a core (20S) subunit, which contains the proteolytic active sites. Its activity and specificity are modulated by the attachment of regulatory binding partners. The unmodified 20S subunit alone degrades oxidised proteins independently of ATP (oxidative stress actually causes dissociation of other proteasomal complexes, liberating 20S subunits). The mechanism by which oxidised proteins are targeted is still unclear but is thought to be via recognition of hydrophobic patches exposed by partial unfolding(Höhn et al. 2014) although Hsp90 has been shown to target oxidised but not native calmodulin for 20S degradation *in vitro* suggesting a role for chaperones(Whittier 2004). Proteasomal degradation peaks at a certain level of oxidation for each protein above which they can no longer be processed leading to lipofuscin formation and pathology. Proteasome concentrations are highest in the nucleus (mirroring total protein concentrations) which is likely a major factor in the lower relative levels of oxidised proteins found there (Jung et al. 2007). The proteasome is not expressed in mitochondria however they possess the specialised Lon protease for removal of oxidised proteins(Bota & K. J. A. Davies 2002). Lysosomal degradation is the other main route by which oxidised proteins are detoxified. Lysosomes contain the cathepsin proteases along with a wide range of other enzymes. Cathepsins (after activation by the low pH of lysosomes) can cleave at cysteines and aspartates depending on the isoform. Oxidative modifications may cause individual proteins to become substrates for microautophagy. Larger aggregates can be digested via macroautophagy; again there exists an upper limit of oxidation after which lipofuscin will accumulate in lysosomes.

## 1.3 DNA Repair

A variety of DNA modifications can arise due to the action of endogenous and exogenous damaging agents or spontaneous chemical and enzymatic reactions occurring during normal cellular function. Cells have evolved a number of different pathways to address these lesions and hence avoid the potential for lethality and mutagenesis. Continuing from the previous section, DNA damage by RS will be addressed first before moving on to other mechanisms of DNA damage and finally, how the cell processes this damage.

### 1.3.1 DNA Damage by RS

Radiation or chemical treatment of nucleosides *in vitro* generates more than 80 different base modifications. The majority have not been detected in cellular DNA either because they occur at levels below current detection limits or because conditions within the cell preclude their formation.

#### *1.3.1.1 HO• mediated damage*

HO• is a significant source of DNA damage. It reacts almost indiscriminately with all DNA bases at near diffusion-controlled rates. It can add to double bonds to generate an OH-adduct radical or it can abstract hydrogen. OH-adduct radicals can react with $O_2$ or become oxidised/reduced to yield stable products. Among the canonical DNA bases, guanine has the lowest reduction potential and therefore is most susceptible to oxidation(Sirbu & Cortez 2013; Steenken & Jovanovic 1997). Guanine OH adduct radicals can form at carbons 4, 5 or 8. The C4 and C5 adducts can rearrange to form C8 adducts or revert back to guanine. One electron oxidation of the C8-OH-adduct leads to formation of 8-hydroxyguanine (8-OH-G), the enol tautomer of 8-oxo-7,8-dihydroguanine (8-oxoG, Figure 1.6), which predominates in cellular DNA. The other possible fate of the C8-OH-adduct is ring opening and one electron reduction to give 2,6-diamino-4-hydroxy-5-formamidopyrimidine (FapyGua, Figure 1.6). Although the two products form in comparable yields *in vivo,* the ratio between them is influenced by redox environment (high $O_2$ levels favouring 8-oxo-G formation)(Dizdaroglu & Jaruga 2012). Historically, 8-oxo-G has received more attention. It is easier to detect and its

miscoding properties indicate an obvious potential for mutagenicity. Some authors believe that the contribution of other products (such as FapyGua) has been underestimated (Dizdaroglu et al. 2008). 8-oxo-G is detectable in urine and urinary 8-oxo-G is used as a biomarker for oxidative stress. The major products of DNA adenine oxidation, 4,6-diamino-5-formamidopyrimidine and 7,8-dihydro-8-oxoadenine (FapyAde and 8-oxo-A, Figure 1.6) are formed at levels an order of magnitude lower than those of DNA 8-oxoG. Reactions with thymine proceed *via* addition at C5 and C6 and to a lesser extent abstraction of the methyl H. The resulting radical adducts form a variety of hydroxy-thymine products including 5,6-dihydroxy-5,6-dihydrothymine (thymine glycol, Figure 1.6) and 5-hydroxymethyl-uracil (Figure 1.6), which are mutagenic and detectable in patient urine(Evans et al. 2010) and patient lymphocyte DNA(Halliwell 1998). Cytosine behaves similarly to thymine with a stronger preference for forming C5-OH-adduct radicals, which yield 5,6-dihydroxy-5,6-dihydrocytosine (cytosine glycol, Figure 1.6) and 5-hydroxy cytosine.

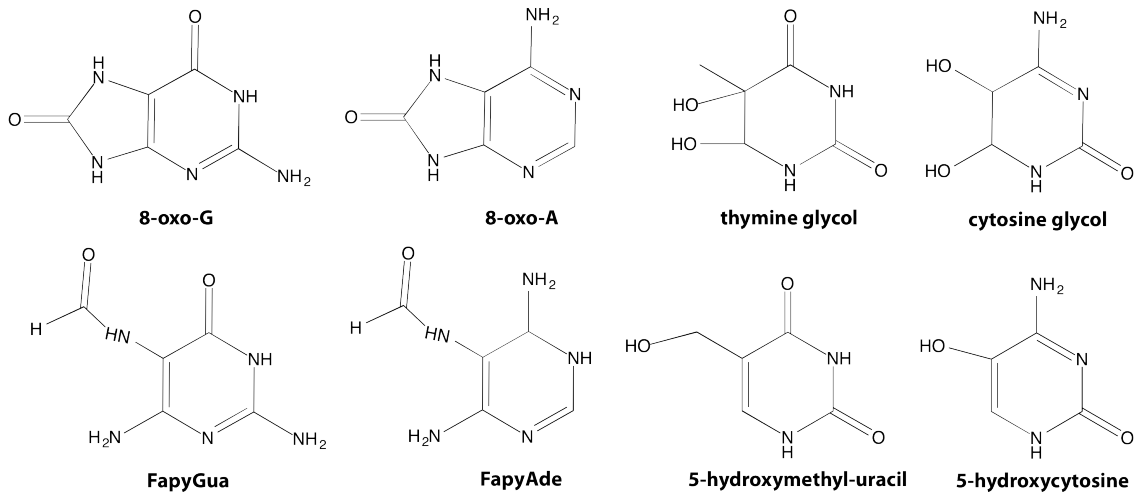


**Figure 1.6 Structures of common DNA base oxidation products**
**8-oxoG** ,8-oxo-7,8-dihydroguanine; **Fapy Gua**, 2,6-diamino-4-hydroxy-5-formamidopyrimidine; **8-oxoA**, 7,8-dihydro-8-oxoadenine; **Fapy Ade,** 4,6-diamino-5-formamidopyrimidine; **thymine glycol**, 5,6-dihydroxy-5,6-dihydrothymine, **5-hydroxymethyl-uracil; cytosine glycol**, 5,6-dihydroxy-5,6-dihydrocytosine, **5-hydroxycytosine**

### 1.3.1.2 $O_2^{\bullet -}$ and $H_2O_2$ mediated damage

Cellular DNA is unreactive towards $O_2^{\bullet -}$ or $H_2O_2$ although $O_2^{\bullet}$ may react with DNA radicals to yield peroxy products. More importantly, excess $O_2^{\bullet -}$ increases unbound iron levels and promotes Fenton chemistry (Keyer & Imlay 1996). The DNA strand breakage induced by treatment of cells with $H_2O_2$ is due to $OH^{\bullet}$ formation via the Fenton reaction. As $OH^{\bullet}$ is too reactive to diffuse, DNA breakage implies that metal ions are in close proximity to DNA. The overall negative charge of DNA allows it to chelate positively charged ions, although metal chelation by DNA *in vivo* has not been demonstrated.

### 1.3.1.3 $^1O_2$ mediated damage

$^1O_2$ can oxidise guanine directly. It does not oxidise other DNA bases and it cannot induce strand breaks(Cadet et al. 2006). The major observed DNA product resulting from the action of $^1O_2$ on cellular DNA is 8-oxo-G. It seems likely that secondary oxidation products resulting from [2+2] cycloaddition to the C4-C5 bond (Figure 1.7) will also be formed but they have not been detected in cellular DNA and their biological relevance, if any, is unclear (Neeley & Essigmann 2006).

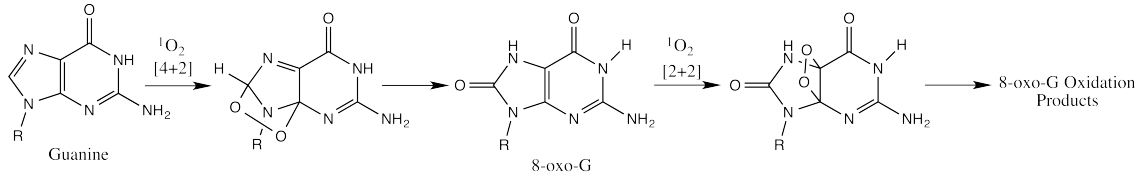


**Figure 1.7 Oxidation of guanine by singlet oxygen**
Guanine oxidation proceeds via a [4+2] cycloaddition to the imidazole ring, generating an unstable endoperoxide that decomposes to give 8-oxoG. 8-oxoG is still reactive towards $^1O_2$ and may form secondary oxidation products via [2+2] cycloaddition to the C4-C5 bond.

### 1.3.1.4 Other RS mediated damage

OONO- also forms DNA 8-oxo-G together with several other oxidation products. These include 8-nitroguanine and strand breakage *via* H abstraction(Burney et al. 1999). HOCl

mainly oxidizes pyrimidines (thymine glycol is the major product in cellular DNA) and also gives rise to chlorinated bases such as 5-chloro-uracil(Spencer et al. 2000).

DNA-protein crosslinks and DNA interstrand crosslinks can arise from RS by indirect mechanisms. These include DNA-radical/protein-radical coupling or attack of base radicals on susceptible amino acids such as tyrosine. Breakdown products of lipid peroxides (Section 1.2.3.1) can also generate indirect DNA damage.

### 1.3.2 Non-RS DNA damage

In addition to damage by excess RS, DNA can be damaged by other exogenous agents and during normal cellular function. Cells have evolved multiple pathways to address these DNA lesions and thereby avoid lethality and mutagenesis.

#### *1.3.2.1 Spontaneous damage*

The most common DNA damage under normal cellular conditions is spontaneous base loss *via* N-glycosyl bond hydrolysis. This reaction generates apurinic/apyrimidinic (AP) sites and occurs around 10000 times per cell per day(Lindahl 1993). Guanine is lost 1.5x faster than adenine whilst rates of depyrimidation are around 5% those of depurination. AP sites also arise from oxidative damage and as intermediates in base excision repair (BER, see Section 1.3.3 below). They can undergo mutagenic bypass by replicative polymerases with preferential insertion of adenine(Avkin et al. 2002). The deoxyribose that remains after base loss exists mainly in the closed ring furanose form but can tautomerise to give a ring-open aldehyde which can either undergo β-elimination, inducing cleavage of the 3'-phosphodiester bond, or react with nucleophiles to generate cross links. The ubiquity and conservation of AP endonucleases(Barzilay & Hickson 1995) emphasizes the potential dangers posed by AP sites and the need for their correct resolution.

DNA bases also undergo spontaneous hydrolytic deamination. Cytosine is deaminated to uracil which, in double-stranded DNA generates a U:G mispair. Cytosine deamination

occurs approximately 100-500 times per cell per day. To avoid GC→TA transition mutations, DNA uracil is removed (by BER, see below) thereby generating an AP site. Uracil can also be incorporated opposite adenine during DNA replication. These U:A pairings are also resolved by BER. Human DNA also contains 5-methylcytosine (5-meC). This normal epigenetic mark is confined to CpG sequences and 60-90% of cytosines in these dinucleotides are methylated. Methylation increases the rate of cytosine deamination by three to four fold. Deaminated 5-meC yields thymine and T:G mispairs in double-stranded DNA. If left uncorrected, this would cause a C→T transition mutation.

Oxidised DNA bases also arise spontaneously at baseline RS levels. 8-oxoG is the major product of endogenous RS (up to 2000 per cell per day(Friedberg et al. 2004)). It is mutagenic due to its ability to form a Hoogsteen base pair with adenine (Figure 1.8) leading to GC→TA transversion mutations upon strand replication. In addition to the RS-induced damage to DNA bases described in the previous section, the oxidized deoxynucleotide pool is also a source of DNA lesions. dNTPs are susceptible to oxidation and are substrates for incorporation by replicative DNA polymerases. 8-oxo-G incorporation opposite adenine directed by Hoogsteen base pairing leads to AT→CG transversion mutations if uncorrected(Pavlov et al. 1994). Mutation *via* incorporated oxidized bases is minimized by a nucleotide pool sanitizing system in which the MTH1 enzyme hydrolyses oxidised purine triphosphates thereby preventing their incorporation.

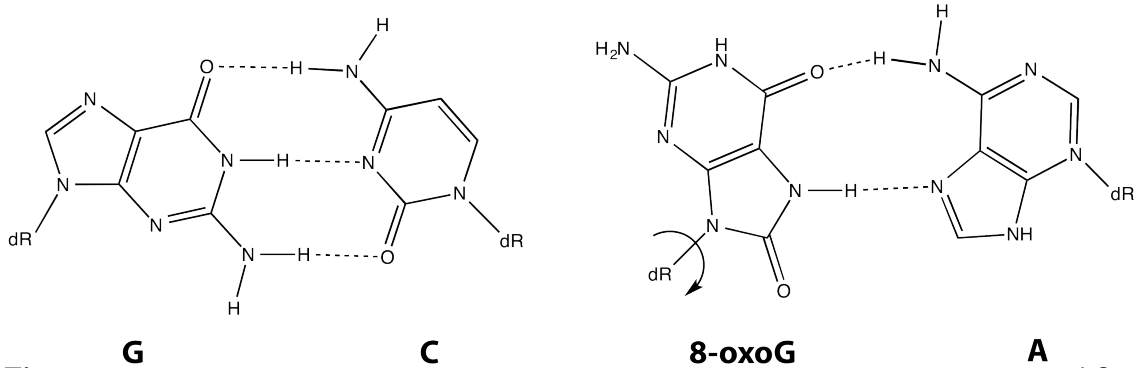


**Figure 1.8**
**Base pairing of 8-oxoG**
**Left:** Watson-Crick base pairing of guanine and cytosine. **Right:** Hoogsteen base pairing of 8-oxoG and adenine.

#### *1.3.2.2 Damage from exogenous sources*

DNA absorbs ultraviolet radiation (UVR) and this induces the formation of potentially mutagenic photoproducts. UVC (100-280nm) is absorbed most strongly but UVB (280-320nm) and UVA (320-400nm) are more relevant to terrestrial life. The most abundant DNA photoproducts of solar UVR are cyclobutane pyrimidine dimers (CPDs) (Figure 1-9). These lesions are formed via a [2+2] cycloaddition reaction between the C5-C6 double bonds of adjacent pyrimidine bases. Although various stereoisomers exist, the constraints of the B-DNA structure mean that the *cis-syn* dimer is the major product. The *trans-syn* form is observed in less structurally-constrained single stranded DNA. Although all possible CPDs (T<>T, C<>T, T<>C, C<>C) have been isolated from DNA irradiated *in vitro*, in cells, the T<>T dimer predominates, making up over 50% of photoproducts in DNA extracted from cells exposed to simulated sunlight(Douki et al. 2003). UVA also induces CPDs albeit 1000x less efficiently than UVB(S. Mouret et al. 2006). UVA can achieve this indirectly through triplet energy transfer via endogenous and exogenous photosensitisers(Cadet et al. 2012). In the past, this was thought to be the major mechanism by which UVA induces CPDs but recently, a direct excitation of DNA was shown to occur and, by assessing product distributions, judged to be the predominant mechanism in cells(S. Mouret et al. 2010).

Although the 5' residue hydrogen bonding is disrupted, CPDs remain stacked within the helix and induce a modest 9° DNA bend. Pyrimidine (6-4) pyrimidone photoproducts ((6-4)PPs) (Figure 1-9) are also generated by UVB and UVC irradiation of DNA. Like CPDs, (6-4)PPs can form between all combinations of pyrimidines. In DNA from UVB irradiated cells, TC products predominate followed by TT and CT. CC (6-4)PPs are not observed(Cadet et al. 2012). UVA irradiation does not induce significant numbers of (6-4)PPs, an observation that has implications for the mechanisms of formation of 6-4PPs and CPDs. The DNA distortion caused by (6-4)PPs is much greater than is caused by CPDs; the pyrimidine rings are almost perpendicular to each other and confer a 44° helical bend and loss of hydrogen bonding for the 3' base. This greater structural distortion is thought to facilitate more efficient recognition by repair factors and (6-4)PPs are repaired 5 to 10 times faster than CPDs. When (6-4)PPs absorb UVA, they undergo photoisomerisation to yield Dewar valence isomers (Figure 1.9). These bicyclic

β–lactam-containing pyrimidine isomers are repaired as rapidly as their (6-4)PP counterparts(Courdavault et al. 2005).

All 3 classes of UV photoproducts block DNA and RNA polymerases and must be removed or bypassed to allow replication and transcription to continue.

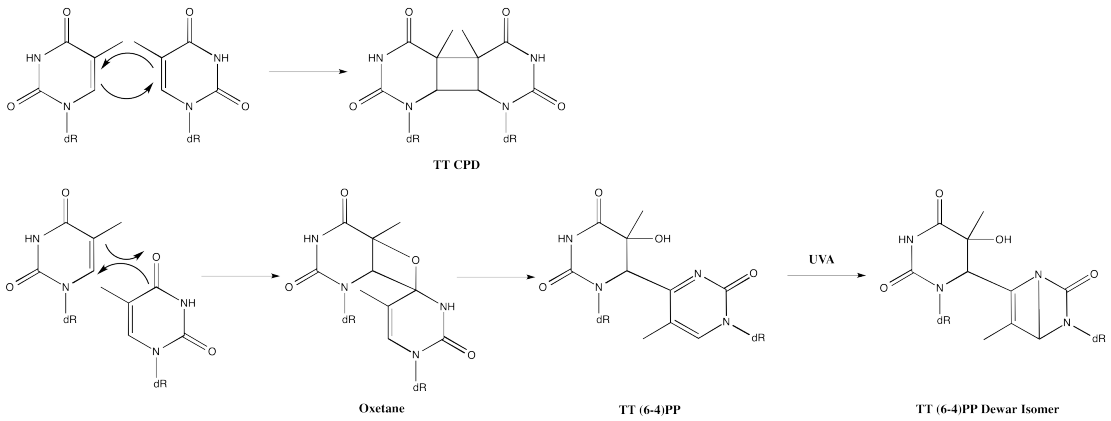


**Figure 1.9 DNA photoproducts and their mechanisms of formation**
**Top:** CPDs are formed via a [2+2] cycloaddition reaction between the C5-C6 double bonds of adjacent pyrimidine bases. **Bottom:** (6-4)PPs form *via* a photochemical [2+2] cycloaddition between a 5' C5-C6 pyrimidine double bond and a 3' C4 thymine carbonyl or C4 cytosine imine tautomer. This results in a covalent bond between 5'-C5 and 3'-C4 via an unstable oxetane or azetidine respectively. Upon absorption of UVA, (6-4)PPs photoisomerise to yield Dewar isomers.

### *1.3.2.3 Alkylation of DNA*

Numerous endogenous and exogenous electrophiles can add alkyl groups to nucleophilic centres in DNA. Endogenous alkylating agents include S-adenosylmethionine, which is a weak methylating agent, and lipid peroxidation products (as mentioned in Section 1.2.3.1). Exogenous alkylating agents include tobacco smoke components, therapeutics and various chemical weapons. The pattern of alkylation is dependent on the nucleophilic selectivity of the alkylating species and the properties of the bases. In general, alkylating agents with high nucleophilic selectivity preferentially react with nitrogens such as guanine N7 via an $S_N2$ mechanism. Less selective agents react via an $S_N1$ mechanism to yield O-alkylation and phosphotriester adducts in addition to the nitrogen products. 7-methylguanine (7meG) and 3-methyladenine (3meA) are the primary N-methylation products whilst $O^6$-methylguanine ($O^6$meG) is the major oxygen

adduct. Although 7meG is neither mutagenic nor cytotoxic, its N-glycosyl bond is labile and it is therefore more susceptible to depurination to generate an AP site. DNA 3meA is also highly susceptible to depurination. This potentially lethal DNA lesion also blocks DNA polymerases. $O^6$meG is responsible for the majority of mutagenesis and toxicity associated with $S_N1$ methylating agents. It mispairs with thymine and causes G→A transition mutations. $O^6$MeG can be directly reversed via a dedicated enzyme - $O^6$-methylguanine-methyltransferase (MGMT). MGMT transfers the methyl group to an active site cysteine to regenerate DNA guanine. Direct reversal of alkylation can also be achieved by AlkB and its homologues in a process termed oxidative DNA demethylation. AlkB hydroxylates the methyl group on 1-methyladenine and other lesions, which then rearranges and spontaneously eliminates to reform the undamaged base with loss of formaldehyde(Falnes et al. 2002).

N-methylated bases are excised by the BER pathway whereas more complex alkylation products are removed by NER. Bifunctional alkylating agents such as nitrogen mustards and mitomycin C can induce crosslinks by bridging two nucleophilic centres. Crosslinks can be DNA-protein crosslinks (DPCs) or intra- and interstrand DNA-DNA crosslinks (ICLs). These lesions all impede transcription and replication and must be repaired or bypassed.

#### *1.3.2.4 Strand Breakage*

In addition to modification of nucleobases, modification of the backbone can lead to strand breakage. Ionizing radiation (IR) can interact with DNA directly, through ionization of the DNA atoms, or indirectly, through the radiolytic decomposition products of water. The majority of cellular damage is due to indirect effects, mainly via the hydroxyl radical. Besides the addition products to DNA bases outlined in Section 1.3.1.1, OH• can also abstract a deoxyribose hydrogen although this accounts for < 20% of OH• reactions with DNA. Abstraction at C'4 and C'5 predominates due to greater accessibility and the resulting radicals can decompose with loss of the 3' or 5' phosphodiester or abasic site formation. If the ends derived from a single strand breaks consist of a 3'-OH and 5'-P then the nick can be simply repaired by direct DNA ligation.

This is rarely the case, however. More frequently, the ends must be processed and any lost bases replaced. For this reason, single strand break repair overlaps significantly with the post incision events of BER and will be discussed in more detail below. SSBs can also result from Fenton chemistry, as an intermediate in BER or due to abortive action of DNA topoisomerase 1. Unrepaired SSBs can result in stalled transcription and, more seriously, stalling and collapse of replication forks leading to double strand break (DSB) formation. DSBs are considered the most harmful DNA lesion; just one may be sufficient to induce apoptosis if left unrepaired(Ide et al. 2011; Khanna & Jackson 2001). Formation of two SSBs in close proximity (10bp) on opposing strands results in a DSB. Radiomimetic drugs such as bleomycin and topoisomerase inhibitors also induce DSBs. Aberrant repair of DSBs can lead to gross chromosomal rearrangements and mutation and as such cells devote significant resources to their repair.

### 1.3.3 Base Excision Repair

Small chemical modifications that do not significantly distort the helical structure of DNA are repaired by base excision repair (BER). These include most oxidative base modifications, uracil resulting from deamination, methylated and some other alkylated bases and AP sites. Furthermore, many of the main enzymes in BER are also involved in single strand break repair (SSBR). This section is informed by the recent review of BER by Krokan(Krokan & Bjoras 2013).

The initial step in BER is recognition and removal of the damaged base by one of 13 distinct DNA glycosylases that catalyse hydrolysis of the N-glycosyl bond. Each glycosylase has a preferred substrate although there is some degree of redundancy and many recognise multiple lesions (Table 1). Glycosylases bind to the minor groove and kink DNA at the damage site. The active sites of glycosylases can only accommodate extrahelical bases and so the damaged base must be flipped out of the major groove. It is unclear whether the enzyme induces this or captures temporarily extrahelical bases. Glycosyl bond hydrolysis is achieved *via* a water molecule activated by a catalytic acidic amino acid to generate an AP site. DNA glycosylases can be monofunctional or bifunctional. Bifunctional glycosylases also possess an AP lyase activity by which they cleave the DNA backbone *via* an elimination mechanism. BER initiated by

monofunctional glycosylases relies on the APE1 AP endonuclease to perform backbone incision. APE1 cleaves 5' to the AP site to generate a 3'OH and a 5' deoxyribose phosphate (5'dRP). AP sites generated by spontaneous base loss will also enter the BER pathway at this point. Bifunctional enzymes generate additional DNA end configurations that require further processing before the subsequent step can take place. This could entail removal of a 3'-phosphate or phosphorylation of a 5'-hydroxyl both of which can be performed by PNKP, which also participates end processing during NHEJ (see Section 1.3.5). At this stage, repair can proceed *via* the short or long patch BER subpathways. In the predominant short patch BER pathway, DNA Pol β removes the 5'dRP and fills the single nucleotide gap. In long patch BER, 2-8 nucleotides are added either by Polβ or replicative polymerases/PCNA, displacing the existing 3' strand. The resulting flap is cleaved by FEN1/PCNA. The factors that determine the selection of short or long patch BER are not fully understood but they may include ATP concentration, the nature of the 5'dRP (oxidised sugars cannot be removed by Pol β) and the proliferation status of the cell(Robertson et al. 2009). In the final step of both pathways, the resulting nick is sealed by DNA LigIII (complexed with XRCC1) or DNA LigI. BER functions are generally thought to be coordinated to avoid the persistence of potentially dangerous intermediates (AP sites, SSBs). After glycosylase recognition and hydrolysis, intermediate substrates remain sequestered until they are acted on by the next enzyme in the pathway(Prasad et al. 2011).

| Enzyme | Location | Mono/Bifunctional | Substrate |
|---|---|---|---|
| UNG2 | Nuclear | Mono | U, 5-FU, U:A, U:G |
| UNG1 | Mitochondrial | Mono | Like UNG2 |
| SMUG1 | Nuclear | Mono | 5-hmU, U:G, U:A, ssU, 5-FU |
| TDG | Nuclear | Mono | U:G, T:G, 5-hmU, 5-FU |
| MBD4 | Nuclear | Mono | U:G, T:G, 5-hmG |
| MPG | Nuclear | Mono | 3meA, 7meG, 3meG, |
| OGG1 | Nuclear | Bi | 8-oxoG:C, FapyG:C |
| MUTYH | Nuclear | Mono | A opposite 8-oxoG/C/G |
| NTHL1 | Nuclear | Bi | Tg, FapyG, 5-hC |
| NEIL1 | Nuclear | Bi | Tg, FapyG, FapyA, 8-oxoG, 5-hU |
| NEIL2 | Nuclear | Bi | Like NEIL1 |
| NEIL3 | Nuclear | Bi | FapyG, FapyA |

**Table 1.1 Mammalian DNA Glycosylases and some of their substrates**

Adapted from (Krokan & Bjoras 2013). Abbreviations: U, uracil; 5-FU, 5-fluorouracil; 5-hmU, 5-hydroxy-methyluracil; 3meA, 3-methyladenine; 7meG, 7-methylguanine; 3meG, 3-methylguanine; 5-hC, 5-hydroxycytosine; Tg, thymine glycol; 5-hU, 5-hydroxyuracil.

### 1.3.4 Nucleotide Excision Repair

Nucleotide excision repair (NER) is the other major pathway tasked with removing single strand lesions. NER is a more complex process than BER and involves more than 25 gene products. It acts upon a broad range of DNA lesions that, whilst chemically distinct, all have a destabilizing or distorting effect on the DNA helix. These include UV photoproducts and bulky lesions formed by environmental mutagens and pharmaceuticals. NER comprises two subpathways : global genome NER (GG-NER), which processes damage occurring throughout the genome, and transcription-coupled NER (TC-NER), which only removes lesions from the transcribed strands of active genes. This section is informed by the recent review of NER in eukaryotes by Schärer (Scharer 2013).

The two NER subpathways diverge at the initial damage recognition step. GG-NER utilises XPC (stabilised by RAD23B) to recognise damage and recruit repair factors, although the UV-DDB complex is necessary to facilitate the recognition of CPDs. XPC binds to the non-damaged strand and locates damaged sites by inserting a hairpin domain between the two strands and encircling the non-damaged strand. Hairpin insertion is facilitated by the loss of helical structure and attendant thermodynamic destabilisation caused by the lesion(Y. Liu et al. 2011). XPC-RAD23B also induces bending and local unwinding of the DNA that presumably aids in hairpin insertion. Because it recognises the distortion caused by the lesion rather than the lesion itself, XPC is able accommodate a wide range of structurally unrelated substrates. The accessory factor UV-DDB comprises two subunits DDB1 and DDB2. DDB1 binds to the CUL4-RBX1 complex and forms a ubiquitin ligase. DDB2 also uses a hairpin domain to sense damage but in this case DDB2 extrudes the lesion from DNA and binds to it. Lesion binding by UV-DDB2-CUL4 induces a 40° kink in DNA and facilitates its recognition by XPC(Scrima et al. 2008). This is especially important for CPDs, which induce minimal distortion and are poor XPC substrates. Mutations in DDB2 compromise CPD repair whilst 6-4 PP repair remains largely unaffected.

In TC-NER, damage recognition is a consequence of lesion-induced stalling of RNAPII. This in turn recruits TFIIH in a process that requires CSA, CSB and XAB2. The exact mechanism is unknown but the roles of some essential TC-NER proteins have been partly elucidated(Gaillard & Aguilera 2013). CSB tightly associates with stalled RNAPII and recruits various factors including CSA, TFIIH, XPA and XPF-ERCC1. CSA recruits XAB2, which binds XPA and may act as a scaffold. CSA also forms an E3 ligase with DDB1-CUL4 and can ubiquitylate CSB leading to its proteasomal degradation. This may be prevented by a deubiquitinase USP7, which is localised to the site by UVSSA - a CSB, CSA and RNAPII interaction partner. An important step in TC-NER is thought to be RNAPII backtracking to allow access by repair factors. One view is that by preventing CSB degradation, UVSSA/USP7 allows time for CSB to remodel the transcription complex(Schwertman et al. 2013). CSB also recruits chromatin remodelling factors p300 and HMGN1, which may loosen the chromatin structure behind the lesion to permit RNA backtracking(Hanawalt & Spivak 2008).

After recruitment of TFIIH and repair factors, the two NER subpathways converge. TFIIH comprises 10 subunits, including XPB and XPD, two essential NER proteins. XPB opens a 30-nucleotide stretch around the lesion in an ATP dependent manner that allows the XPD helicase to proceed along the damaged strand until it reaches the lesion and stalls due to a damage-sensing domain(Mathieu et al. 2013). Confirmation by TFIIH of both the presence and location of the lesion precedes formation of the preincision complex. Following recruitment of XPA, XPG and RPA, XPC-RAD23B departs. XPA interacts with many NER factors and is thought to ensure their correct localisation. It binds to the 5' end of the open DNA bubble where it can interact with RPA and ERCC1-XPF(Krasikova et al. 2010). The RPA heterotrimeric single stranded binding protein has at least two roles in NER. It binds to the undamaged strand and protects it from nuclease activity. RPA also assists in the orientation of the incision nucleases XPG and ERCC1-XPF(de Laat et al. 1998). The XPG endonuclease, which is recruited through an interaction with TFIIH binds 3' to the lesion and specifically cuts at double strand/single strand junctions with 3' ssDNA overhangs. ERCC1-XPF completes the pre-incision complex and is positioned 5' to the lesion by its interactions with XPA and RPA. ERCC1-XPF makes the first incision followed by XPG-mediated incision 3' to the lesion. The ERCC1/XPF complex is also involved in other DNA repair pathways although its function is not always known in detail(Kirschner & Melton 2010).

Dual incision by ERCC1-XPF and XPG is followed by release of the cleaved oligonucleotide and repair DNA synthesis. Three different polymerases - Pol δ, Pol ε and Pol κ - can carry out this resynthesis step(Lehmann 2011). All require PCNA for recruitment (PCNA must be monoubiquitinated in the case of Pol κ, which is a Y family, translesion polymerase) but the clamp loader differs in each case. Pol δ requires RFC, Pol ε a variant RCF and Pol κ requires XRCC1. Depletion studies reveal that Pols δ and κ probably work on the same pathway and Pol ε in another. The criteria that determine the selection of one polymerase over another remain an area of active research. Non-proliferating cells reveal a preference for Pols δ and κ whilst proliferating cells also utilise Pol ε suggesting that cell cycle effects such as polymerase or dNTP concentrations may influence polymerase choice. The ligase that seals the nick depends

on the polymerase used; LigIII with Pols δ and κ and LigI with Pol ε. LigIII is the major NER ligase in non-dividing cells.

### 1.3.5 Double strand break repair

Mammalian cells have two main DSB repair pathways: non-homologous end-joining (NHEJ) and homologous recombination (HR). HR requires the presence of a sister chromatid to serve as a template for repair and so can only operate in S or G2 phase of the cell cycle. NHEJ is the major DSB repair pathway in G1 phase. The two pathways also have roles in addition to their DNA repair function. HR is involved in meiotic division whilst NHEJ is involved in antibody generation and telomere maintenance. NHEJ is considered the more error prone of the two pathways as it does not rely on sequence homology. In contrast, HR is considered to be essentially error free. A backup end-joining system known as alt-NHEJ operates through minimally resected ends. Although suppressed under normal conditions, there is evidence to suggest that it is responsible chromosomal translocations linking it to carcinogenesis(Kehrer 2000; Bunting & Nussenzweig 2013).

NHEJ is initiated *via* rapid detection of DSBs by the Ku70:Ku80 heterodimer. Ku is an abundant ($1 \times 10^6$ molecules per cell) nuclear protein that avidly binds free DNA ends by threading the broken strand through its double ring structure (Grundy 2014). Ku binding protects ends from nucleolytic activity and also serves as a platform for recruitment of other NHEJ factors. The ends of DSBs are structurally diverse and must be processed before they can be ligated. The essential NHEJ proteins: Ku, DNA PKcs, XRCC4, DNA Ligase IV and XLF make up a core complex to which processing factors are recruited. These end-processing factors include nucleases (Artemis, APLF, TDP1), polymerases (λ and μ) and phosphatases (PNKP and aprataxin). A model of core complex assembly based on interaction studies envisages sequential recruitment of Ku, followed by DNA PKcs, then XRCC4-Lig4 and XLF. More recent real time imaging suggests that after initial DSB detection by Ku, the remaining factors are recruited simultaneously to form the core complex(Yano et al. 2009). DNA PKcs binds to Ku in a DNA dependent manner by threading DNA through its N-terminal channel to form a stable holoenzyme known as DNA PK. Ku and DNA binding activates the kinase

activity of DNA PKcs allowing it to phosphorylate other NHEJ factors and itself. DNA PK phosphorylation (either by ATM or itself) is essential for NHEJ activity and induces conformational changes that regulate access to DNA ends by processing factors(Waters et al. 2014). DNA-PKcs is also thought to be involved in the initial tethering of the two ends known as synapsis(Weterings 2003). XRCC4-Lig4 is recruited as a preformed complex. Lig4 is a NHEJ-specific DNA ligase that rejoins the ends once processing has taken place. XRCC4 stabilises Lig4 and forms long filaments with XLF that may play a structural role in stabilising synapsis(Chiruvella et al. 2013).

It has been suggested that the processing of DNA ends is iterative with NHEJ factors binding and departing multiple times until the ends are ready for ligation(Lieber 2010). Lesion complexity (i.e. the amount of processing needed) may be a deciding factor in the likelihood of processing errors(Schipler & Iliakis 2013) which can cause deletion (by nuclease action), insertion ( by template-independent polymerisation) or aberrant synapsis. Ligation-appropriate ends can actually be joined in a rapid DNA-PKcs independent mechanism that requires only Ku, XRCC4, LigIV and XLF(Reynolds et al. 2012).. Current thinking frames NHEJ as taking place within a dynamic, multi-subunit complex with Ku mediating the recruitment of repair factors as needed(Radhakrishnan et al. 2014).

Rejoining of DSBs by HR can be divided into 3 stages – pre-synapsis, synapsis and post-synapsis. The initial stage in pre-synapsis is resection of the 5’ ends to yield 3’ single stranded DNA. Resection is carried out by MRN in conjunction with CtIP, Exo1, Dna2 and BLM. The MRN heterotrimer comprises Mre11, which possesses both endonuclease and 3’-5’ exonuclease activity, Rad50, which mediates DNA binding and tethers broken ends through a flexible hinge, and Nbs1, which recruits Mre11 and Rad50 to DSBs via its interaction with γH2AX and both recruits and is a target of ATM and ATR(Y. Zhang et al. 2006). The current working model of rejoining is a two-step process in which the Mre11 endonuclease first nicks the 5’ strand at a site distant from the DSB and then uses its 3’-5’ exonuclease activity to resect towards the end, possibly displacing Ku in the process. Resection is extended by the 5’-3’ nuclease activity of Exo1 and the combined action of helicase/endonuclease activity of BLM/Dna2. CtIP mediates this process via its

interaction with BRCA1 (discussed below). The resulting single stranded region is quickly coated with RPA, which is then displaced by the recombinase Rad51, a process requiring BRCA2 and Rad52. Rad51 forms a nucleoprotein filament, in a process that also requires five mammalian Rad51 paralogues, and this initiates the search for the undamaged homologous duplex. Rad51 contains two DNA-binding sites, one binds the resected single stranded DNA and the second binds to target strands to be probed for homology. More rapid repair at less stable AT-rich regions supports the notion that target strand binding occurs at transitory ssDNA bubbles resulting from DNA "breathing". DNA stretching within the Rad51 filament results in 3 bp segments of DNA that retain B-DNA conformation separated by extended internucleotide regions. In order to interact with the extended DNA-Rad51 filament, target DNA must deform and stable binding can only be achieved if the energy required for deformation is offset by base pairing and thus only the homologous region is targeted(Renkawitz et al. 2014).

Once the homologous region has been found, HR enters the synaptic phase and strand exchange leads to the formation of a D-loop that comprises the newly formed heteroduplex and the displaced strand. In the post-synaptic phase, repair synthesis by Pol η commences from the broken 3' end(McIlwraith et al. 2005). In mitotic cells, the primary outcome is displacement of the newly synthesised strand by helicase action and re-annealing with the original broken DNA end in a process termed synthesis-dependent strand annealing. An alternative outcome is capture of the other DNA end by the D-loop to form a double Holliday junction which is cleaved by resolvases to yield crossover products (favoured in meiotic cells) or non-crossover (favoured in mitotic cells) products, or dissolved by the BLM-TopoIIIα-RMI1-RMI1 complex.

alt-NHEJ can perform Ku- and Lig4- independent end-joining. In view of the severe consequences of NHEJ and HR loss, alt-NHEJ is unlikely to make a major contribution to overall DSB repair. Alt-NHEJ is thus far poorly characterised. Current knowledge presents the following model, which consists of three key steps – recognition and tethering, processing, and ligation(Frit et al. 2014). All alt-NHEJ factors are repurposed from other repair pathways including BER, NER, HR and TLS. The initial recognition of the break is carried out by PARP1 (PARP inhibitors suppress alt-NHEJ), which both

tethers the ends and recruits other factors including XRCC1, Lig3, PNK and MRN, which may also assist in tethering the ends. If present, Ku can outcompete PARP1 for ends thus suppressing alt-NHEJ if classical NHEJ is functional. The next step is short-range resection of the ends by HR factors MRN and CtIP (knockout of either supresses alt-NHEJ) to expose regions of microhomology (6-8bp), which may aid in synapsis through annealing. Although not absolutely essential to all alt-NHEJ reactions, microhomology use seems to predominate. Tumours that show reduced Ku activity have increased evidence of microhomology around rejoining sites and are subject to gross chromosomal rearrangements(Bentley et al. 2009). Pol λ is the most likely candidate for gap filling whilst FEN1 and PNK process the ends ready for ligation; XRCC1-Lig3 seems to be the prime candidate for this role but Lig1 can substitute. There is by no means a definitive list of factors owing to alt-NHEJ's apparent flexible and opportunistic nature.

End resection seems to be a key determinant in the choice of DSB repair pathway. Selection is mediated by an antagonistic relationship between 53BP1, which promotes NHEJ, and BRCA1, which positively regulates HR. Upon detection of a DSB by MRN, ATM is recruited and histone H2AX is phosphorylated. The product, γH2AX, is recognised by MDC1, which in turn recruits more MRN and ATM, in a positive feedback loop. Another consequences of MDC1 binding is 53BP1 recruitment to chromatin, where it cooperates with RIF1 to oppose end resection. This blocking mechanism can be counteracted in S phase via CtIP phosphorylation and association with BRCA1. BRCA1-CtIP mediates the exclusion of 53BP1-RIF1 from chromatin thus allowing end resection and hence HR to take place(Panier & Boulton 2013). End resection is also a necessary step in alt-NHEJ initiation. Deletion of 53BP1 leads to excessive end resection and an increase in alt-NHEJ. It can also rescue genomic instability associated with BRCA1 deficiency by promoting HR, thereby highlighting the delicate balance between NHEJ and HR(J. R. Chapman et al. 2012). More extensive resection and formation of Rad51 filaments are both refractory to alt-NHEJ thus suppression occurs on multiple fronts provided that primary repair pathways are functional.

### 1.3.6 Mismatch Repair (MMR)

Replicative DNA polymerases incorporate a non-complementary nucleotide every $10^5$ to $10^6$ base pairs. Intrinsic proofreading activity of the polymerase improves fidelity by a further two orders of magnitude. Post-replicative DNA mismatch repair (MMR) corrects insertion errors missed by proofreading and reduces the overall replication error rate to around $10^{-9}$ nucleotide. Insertion/deletion loops (IDLs) generated by strand slippage during DNA replication of repeated mono- or dinucleotide sequences (microsatellites) are also corrected by MMR. MMR failure is associated with a mutator phenotype and an approximately 100-fold increase in the rate of spontaneous mutation. Mismatches represent a unique challenge for DNA repair as they are only apparent in duplex DNA and the lesion is lost as soon as the strands are no longer annealed. This section summarises the content of the 2013 review by Jiricny(Jiricny 2013).

MMR consist of three steps – recognition, degradation of the error containing strand, and error-free resynthesis. MMR must recognise a range of different distortions and ensure that the mismatched (i.e. nascent) strand is degraded. The recognition step is performed by heterodimers of MSH proteins. Each has a conserved C-terminal ATPase domain that controls key conformational changes. The ability to utilise different combinations of subunits give the cell scope to recognise a wider variety of substrates. For example, the MSH2-MSH6 heterodimer (known as MutSα) recognises single base mismatches (eg G:T) and 1/2 nucleotide IDLs most efficiently whereas larger IDLs are more efficiently recognised by the MSH2-3 dimer (MutSβ). The current proposed model of mismatch recognition begins with MutSα loosely bound to DNA, hydrolysing ATP as it translocates along the helix. When it encounters a mismatch (perhaps identified through unfavourable electrostatic or H-bonding interactions), a conformational change is triggered. A phenylalanine residue is inserted into the helix where it stacks with the aberrant base. At this point, after a final ADP→ATP exchange, the ATPase domain of MSH6 is inhibited. A similar ADP-ATP exchange in MSH2 triggers removal of the phenylalanine and transition to a more tightly bound clamp that is free to slide along DNA. The MutLα (MLH1: PMS2 heterodimer) is recruited to form a ternary MutSα/MutLα/DNA complex. The exact timing of this interaction is unknown although MutSα can assume its sliding clamp form in the absence of MutLα suggesting that their

association follows mismatch recognition. MutLα also encircles DNA via an ATP-driven conformational change. MutLα was initially thought simply to serve as a "matchmaker" to assemble MMR factors. The more recent discovery of its endonuclease ability, activated by the interaction between the ternary complex and PCNA, has forced reconsideration of its role.

Degradation of the incorrect strand follows mismatch recognition. To accomplish this, Exo1, the 5'→3' nuclease associated with MMR, has to be loaded onto the nascent strand, 5' to the mismatch. Exo1 loading occurs at nascent strand discontinuities which allow MMR to distinguish it from the template strand. Okazaki fragments provide many opportunities for Exo1 loading on the lagging strand. On the leading strand, the endonuclease activity of MutLα introduces nicks 5' to the mismatch. More distant, replication related nicks facilitate RFC-mediated PCNA loading onto DNA. The MutSα/MutLα complex can diffuse along DNA in either direction until it reaches a loaded PCNA forming a quaternary complex. If the PCNA is 5' to the mismatch, Exo1 can be loaded and degradation can begin. If PCNA is 3', the complex must travel back past the mismatch and Exo1 loading is accomplished at nicks introduced by MutLα. The defective DNA strand can then be replaced in an error-free manner by Pol δ.

In the case of a template nucleotide without a complementary base (e.g. $O^6$meG), repair synthesis directed to the nascent strand will retrigger MMR. This cycle occurs repeatedly leading to the formation of a persistent SSB, which will be converted to a potentially lethal DSB upon attempted replication. This is a mode of cell killing for many methylating agents and MMR deficient cells are highly resistant to this family of drugs. Loss of MMR also greatly increases mutation frequency. Lynch syndrome patients who inherit a mutated MMR allele have a high predisposition toward colon cancers that are characterised by early onset, complete loss of MMR and high mutation rates.

### 1.3.7 Translesion Synthesis (TLS)

Although classified as a DNA damage tolerance mechanism rather than a repair pathway, TLS is integral to maintaining genome stability.

The high fidelity exhibited by replicative polymerases is a consequence of rigorous steric and electrostatic constraints imposed by their active sites. These constraints render them unable to process template distortions resulting from DNA lesions, some of which inevitably are not removed prior to replication. In contrast, TLS polymerases possess a more accommodating active site capable of accepting a variety of templates. This relaxed tolerance carries the unwelcome consequence of potential mutagenesis and deployment of TLS must be tightly regulated. The Y family is the most abundant class of TLS polymerases. Y family members include Rev1 and Pols η,ι and κ. These are the primary exponents of TLS and also significant contributors to DNA damage–induced mutagenesis(Sale et al. 2012).

In addition to the less stringent active site, the Y family polymerases also lack 3'-5' exonuclease proofreading activity. They are less processive owing to fewer contacts with both the template and incoming nucleotide. Each of these factors contributes to their decreased fidelity.

Pol η is able to bypass T<>T CPDs with higher fidelity than any other known polymerase albeit with slightly higher chance for misinsertion at for the 3'T(McCulloch et al. 2004). It does, however, exhibit low fidelity when acting upon undamaged DNA. The risk is minimised by the reduced processivity of Pol η that disengages from the template after the addition of three bases(Biertümpfel et al. 2010). A Pol η defect in XPV patients is associated with increased UV induced mutagenesis due to the cooperative action of the alternative TLS polymerases Pol ι and Pol κ together with Pol ζ on CPDs. Replication past (6-4)PPs proceeds normally in XPV cells suggesting another polymerase is responsible for their bypass(Yoon et al. 2010). Pol ι can accurately bypass 8-oxo-G (avoiding Hoogsteen pairing with A) and contributes to UV photoproduct bypass(Kirouac & Ling 2011). Pol κ can bypass a limited spectrum of alkylation products. It is also an efficient extender from mismatched primer termini although this

role is likely played by Pol ζ (discussed below). Rev1 inserts dCMP opposite a wide range of lesions although it has another important function as an adaptor for the recruitment of the other Y-family polymerases to PCNA, for which its catalytic domain is dispensable.

Pol ζ, a B family polymerase related to δ and ε, is inefficient at lesion bypass but is highly efficient at extending mismatched termini. It is able to participate in a two-step mechanism for lesion bypass in which Pol ζ binds and extends the initial nucleotide inserted by a stalled Y family polymerase at a damage site. This concerted action is thought to be the major mode of lesion bypass and this Pol η-mediated bypass of CPDs is somewhat atypical(Shachar et al. 2009).

Upon encountering a lesion on the leading strand, the replication fork stalls. This halts replication and also increases the risk of DSB formation upon fork collapse(Aguilera & Gómez-González 2008). Lesions on the lagging strand present less of a problem as a polymerase can disengage and reengage downstream(Fu et al. 2011), leaving a single-strand gap between two Okazaki fragments. Leading strand blockages result in uncoupled replication as template unwinding and lagging strand synthesis can continue. Historically, all leading strand synthesis was thought to be continuous. Re-priming has now been observed in yeast suggesting that downstream re-initiation occurs in eukaryotes as well as prokaryotes, which possess dedicated replication restart proteins(Yeeles et al. 2013). In these cases, post-replicative TLS is required to fill in the tracts of single-strand DNA on both leading and lagging strands.

The need for extensive gap-filling can be avoided and fork progression maintained by the transient recruitment of a TLS polymerase by the replication machinery. The TLS polymerase bypasses the lesion and then departs allowing the replicative polymerase to resume synthesis. The post-replicative gap filling and fork-associated lesion bypass polymerases are recruited by mono-ubiquitination of PCNA and Rev1 respectively(Edmunds et al. 2008). Following replication arrest, RAD18 and RAD6, an E3 ubiquitin ligase and an E2 ubiquitin conjugating enzyme respectively, are activated by interaction with RPA at single-stranded DNA and mono-ubiquitinate PCNA. This

PCNA modification serves to recruit Y-family polymerases via their C-terminal ubiquitin-binding domains. Mutation of K164 causes a defect in gap filling although some TLS activity appears to be independent of PCNA ubiquitination. PCNA can also be poly-ubiquitinated at the same site. This serves as a signal to commence an error-free repair mechanism that functions via recombination.

### 1.3.8 Crosslink Repair

Bifunctional electrophiles can induce DNA mono-adducts plus covalent DNA-protein, DNA intrastrand, and DNA interstrand crosslinks (ICLs). DNA monoadducts impede polymerases and impair both replication and transcription. In common with other bulky and polymerase-blocking lesions, most are resolved by BER and NER and can be bypassed by TLS. ICLs form an absolute block to replication and transcription as they prevent separation of the DNA strands by helicases and as a consequence an estimated 20-40 ICLs are lethal to cells deficient in ICL repair(Clauson et al. 2013). Fanconi anaemia (FA), a disorder characterized by defective ICL repair, results from mutation of one of sixteen members of the FA pathway. Many DNA repair gene mutations sensitise cells to crosslinking agents as the proteins are repurposed for ICL repair by the coordinated action of FA factors.

Following ICL-induced stalling of a replication fork, FANCM, FAAP24 and MHF are recruited to DNA. The replication fork is remodelled *via* the ATP-dependent translocase activity of FANCM, which leads to RPA recruitment to ssDNA at the damage site and subsequent ATR and checkpoint activation. Damage signalling is amplified by phosphorylation of FAND2 and FANCI by ATR, which also activates the MRN complex and CtIP. FANCM, FAAP24 and MHF form part of a larger complex with FANCs A, B, C, E, F, G and L and FAAP20, which is necessary for monoubiquitination of phosphorylated FANCD2-FANCI by the E3 ligase FANCL. FANCD2-FANCI phosphorylation is essential for ICL repair and coincides with the complex localising to chromatin where it recruits the nucleases and polymerases - including SLX4 FAN1 and Pol ν - involved in subsequent repair steps. SLX4 interacts with XPF-ERCC1, which is thought to make the 3’ incision in the lagging strand required for crosslink unhooking.

XPF mutants are much mores sensitive to crosslinking agents than other NER mutants and the XPA binding site of XPF is dispensable for its role in crosslink repair. Incision 5' to the crosslink allowing unhooking of the crosslink and generates a DSB(Clauson et al. 2013). The nuclease responsible for the 5' incision remains unidentified. The unhooked crosslink attached to the leading strand is bypassed by a TLS polymerase. This restores the double stranded template and allows repair of the lagging strand DSB by HR. Mutations of Pol ζ and Rev1 sensitise cells to crosslinking agents as do mutations of Pol η, Pol κ and Pol ν, suggesting polymerase selection may be lesion dependent. Strand invasion by the 3' lagging strand, begins HR-mediated repair, which restores the lagging strand and allows the replication fork to proceed. The remaining half of the ICL (now effectively a monoadduct) can be removed by NER. Thus, the FA pathway effectively routes ICL repair through HR and NER. In FA cells, erroneous attempts to fix ICLs by NHEJ generate chromosome breaks and radials; inhibition of NHEJ improves the survival of FA cells upon exposure to crosslinking agents(Adamo et al. 2010).

### 1.3.9 DNA Damage Response

DNA repair is one facet of a complex system that minimises the potential genotoxic effects of DNA damaging agents. This system, the DNA damage response (DDR), is a signal transduction pathway that coordinates attempted repair of DNA damage with apoptosis. The DDR has three tiers (signal sensors, transducers and effectors) and DDR signalling via a kinase cascade ultimately modulates various processes with links to genomic stability. These processes include DNA replication and repair, and cell cycle progression(Marechal & L. Zou 2013).

The serine/threonine kinases ATM, ATR and DNA-PKcs sense DNA damage and serve as transducers for the DDR. ATM and ATR mediate the phosphorylation of hundreds of targets in a DNA damage-dependent manner whilst DNA-PKcs targets proteins involved in NHEJ. The active form of ATM is a monomer that originates from inactive ATM dimers and oligomers that dissociate upon DSB sensing. ATR activation is induced by the presence of ssDNA, a signal that is produced by many types of DNA damage. In

addition to direct phosphorylation and transcriptional control of DNA repair factors, ATM and ATR activation regulates other cellular processes to promote conditions that are conducive to repair. Local chromatin structure is modified via H2AX-dependent and -independent mechanisms to make lesions more accessible and increase recruitment of repair factors. More global changes to the cellular environment are also effected. Among these alterations, checkpoint activation is the most important. It is achieved through phosphorylation of the effector kinases Chk1 and Chk2 by ATR and ATM respectively. Cell cycle progression can be halted at various checkpoints, depending on cell cycle phase (G1/S, intra-S, G2/M). One important consequence of checkpoint activation is that it postpones the interaction between damaged DNA and replication or mitosis. This effectively increases the time the cell has to repair DNA the initial damage and thereby avoids the formation of more complex and potentially lethal lesions. ATM and Chk2 knockout mice are viable whereas disruption of ATR or Chk1 is embryonic lethal(J. Smith et al. 2010). These findings suggest that the ATR-Chk1 branch plays a wider and more generalised role in repair and checkpoint response whilst ATM-Chk2 has a more specialised function in the DDR following direct DSB induction. The DDR also controls deoxynucleotide (dNTP) levels through increased activity of ribonucleotide reductase (RNR) and may target RNR to sites of damage to provide dNTPs for repair processes(Sirbu & Cortez 2013).

The MRN complex senses DSBs and activates ATM. MRN binds free DNA ends where NBS1 interacts with ATM and localises it to the break. The histone variant H2AX is an important early target of ATM; its phosphorylation occurs within minutes of DSB formation and propagates >500kb into the flanking chromatin. Spreading of phosphorylated H2AX is facilitated by the action of Mdc1 that recruits RNF8 followed by RNF168, an E3 ligase that polyubiquitinates H2A and H2AX. This modification results in the association of BRCA1 and 53BP1, two factors integral to DSB repair (discussed in more detail in Section 1.3.5). The p53 protein is another important target of ATM (and also ATR, DNA-PKcs, Chk1 and Chk2). Phosphorylation of the p53 N-terminus prevents the ubiquitination and degradation that occur in the absence of DNA damage. p53 binds DNA in a sequence specific manner and regulates expression of numerous target genes by interacting with transcription factors. Outcomes of p53

activation include cell cycle arrest, senescence, autophagy and apoptosis(Zilfou & Lowe 2009).

The RPA-coated ssDNA regions that activate ATR can be formed by DSB end resection by HR factors. The more extensively resected ends become, the more likely they are to activate ATR rather than ATM, and there is a shift from Chk2 to Chk1 activation over time. RPA coated ssDNA also arises during the course of repair and during replication stress, when helicase-polymerase progression is uncoupled by DNA lesions. ATR binds to RPA via its interacting partner ATRIP and is activated by autophosphorylation. ssDNA-dsDNA junctions are recognised by Rad17-Rfc2-5, which in turn loads the Rad9-Rad1-Hus1 (9-1-1) clamp. Assisted by the recently identified RHINO protein, the 9-1-1 clamp recruits TopBP1, which binds to the auto-phosphorylated site of ATR, increasing its kinase activity. Claspin, a target of ATR and a key mediator in Chk1 activation, is also recruited. Chk1 phosphorylates BRCA1 whilst ATM and ATR can phosphorylate BRCA2 promoting HR repair. ATR also phosphorylates many members of the FA pathway and plays an important role in ICL repair(Sirbu & Cortez 2013).

DNA repair is an integral part of the DDR. Defective DNA repair is responsible for the hereditary disorders XP and FA. Defective DDR signalling is also a feature of much human pathology including cancer and neurological disorders. An inability to respond appropriately to DNA damage as a consequence of hereditary ATM defects in ataxia telangiectasia and mutated p53 in Li-Fraumeni syndrome result in cancer predisposition. The role of the DDR in localising DNA damage, signalling its presence and activating and up-regulating the various repair pathways puts it at the center of cell maintenance. Its successful operation requires the optimal interactions between large numbers of component proteins. Damage to this extensive protein family carries the risk of compromising cellular well-being and, like DNA, the DDR proteome presents a significant target for inactivation by environmental insults.

## 1.4 Solar radiation

Much like oxygen, the sun is a double-edged sword. On one hand, its energy allows life on earth to exist, both by providing habitable conditions and serving as the driving force for the food chain *via* photosynthesis. On the other hand, solar radiation can have deleterious consequences for biological systems through its interaction with, and subsequent modification of, biomolecules.

### 1.4.1 The solar radiation spectrum

Solar radiation comprises wavelengths from across the electromagnetic spectrum although predominantly between 100 and $10^6$ nm. This band contains the ultraviolet (UVR), visible and infrared regions (IR) (red line, Figure 1-10), all of which have biological relevance. The visible region (400-700nm) is required for photosynthesis whilst the IR (700-$10^6$ nm) imparts the majority of solar thermal energy to the earth's surface. Historically, the deleterious effects of solar radiation were solely ascribed to the UVR region (Diffey 1991) but more recent findings suggest contributions from visible and IR(Zastrow et al. 2009). The UVR region is arbitrarily subdivided into three wavelength categories: UVA (400-320nm), UVB (320-280nm) and UVC (280-100nm). Absorption by the canonical nucleic acid bases peaks at around 260nm whilst proteins absorb maximally at around 280nm. As a result, shorter wavelengths of UVR are more damaging to cells.

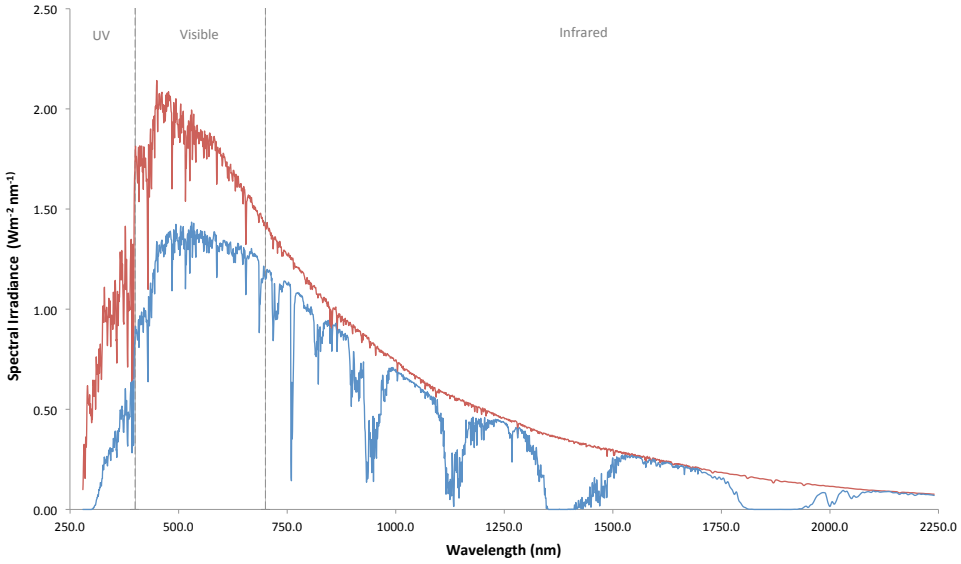


**Figure 1.10 Incoming solar wavelengths**
Solar radiation at the top of the atmosphere (red) is selectively attenuated by atmospheric constituents resulting in an altered wavelength profile at the Earth's surface. American Society for Testing and Materials: Terrestrial Reference Spectra.

Interaction with the atmosphere significantly alters the wavelength profile of solar radiation arriving at the Earth's surface, (blue line, Figure 1-10). For living organisms, the most important consequence of this is the loss of shorter UVR wavelengths. Atmospheric oxygen absorbs wavelengths below 240nm, triggering photolysis and the formation of ozone. The resulting stratospheric ozone layer absorbs UVR with wavelengths ≤ approximately 310nm. These two processes ensure that the Earth's surface is entirely shielded from UVC and the majority of UVB radiation(de Gruijl & van der Leun 2000). UVR comprises around 5% of incident sunlight. Approximately 95% of this is UVA and 5% UVB. Visible light comprises 45% and infrared around 50%(Svobodová & Vostálová 2010). The ratio of UVA to UVB is not fixed and varies with latitude, season, time of day and cloud cover.

### 1.4.2 Solar radiation and Cellular Components

The skin is the main target for solar radiation where its effects are mediated by interactions with DNA, proteins and lipids. The wavelength of the incident radiation determines the nature of the interactions. Cellular macromolecules can be modified directly *via* absorption of radiation, or as a consequence of interactions with endogenous chromophores (photosensitisers) and the formation of RS. Historically, the

action spectrum of radiation in mammalian cells has focused studies on the interaction between DNA and UVC. In recent years, recognition of the contribution of other wavelengths and macromolecules has increased.

#### *1.4.2.1 UVB*

UVB induces DNA photoproducts in the form of CPDs and 6-4 PPs. The yields and relative frequencies of these lesions can be found in Table 1-2. Other products (cytosine hydrates, adenine containing dimers) have been generated in model systems but have not been observed in skin DNA(Cadet et al. 2012). 8-oxoG is present in skin DNA and its formation suggests indirect RS production by UVB. Since photoproducts account for 99% of UVB modifications, 8-oxoG is probably not a significant contributor to the genotoxicity of these wavelengths(Kielbassa et al. 1997).

Some amino acid side chains (Trp, Tyr, Phe, His, Met, Cys) also absorb UVB and undergo oxidation (Pattison et al. 2011). UVB absorption generates radical cations that react with oxygen to give peroxyl products(M. J. Davies & Truscott 2001). Tryptophan is the most significant UVB chromophore and is converted to the tryptophan oxidation products outlined in Figure 3-3. Other endogenous UVB photosensitisers such as fatty acids and vitamins can generate $^1O_2$ and other RS(Regensburger et al. 2012). Nitric oxide and $H_2O_2$ are also an integral part of the signal transduction pathways activated by UVB. Nitric oxide is crucial for melanogenesis(Romero-Graillet et al. 1996) whilst $H_2O_2$ is produced as part of apoptotic signalling(Peus et al. 1999). UVB can also cause lipid peroxidation in keratinocytes albeit at doses that exceed natural conditions(Morliere et al. 1995).

#### *1.4.2.2 UVA*

UVA can damage DNA by direct photoexcitation of DNA or by indirect triplet energy transfer from excited photosensitisers. UVA-induced CPDs are overwhelmingly (79%) T<>T and since the levels are similar in DNA irradiated *in vitro* and extracted from irradiated cells, the former mechanism appears to predominate (S. Mouret et al. 2010). Exogenous photosensitisers such as xenobiotics can shift this balance, however. UVA-induced 6-4PPs have not been detected in mammalian cells(Sage et al. 2011) possibly

due to the nature of the excited state induced by UVA(Banyasz et al. 2011). Although CPD induction by UVA is 1000 times less efficient than by UVB, the higher proportion of UVA in sunlight together with its greater penetration into the dermis, means that up 10% of CPDs in sun-exposed skin may be UVA-induced(Sage et al. 2011).

| | T<>T | 6-4 TT | T<>C | 6-4 TC | C<>T | C<>T |
|---|---|---|---|---|---|---|
| **UVA** | 0.69 | - | 0.12 | - | 0.06 | - |
| **Yield** | 79% | - | 14% | - | 7% | - |
| **UVB** | 2.06 | 0.19 | 1.58 | 0.72 | 0.56 | 0.44 |
| **Yield** | 37% | 3% | 28% | 13% | 10% | 8% |

**Table 1.2 Photoproduct induction in human skin by UVA and UVB**

Values are lesions/ $10^4$ bases per kJ/cm$^2$ for UVA and per J/cm$^2$ for UVB. Modified from Cadet et al(Cadet et al. 2012).

UVA also causes oxidative DNA damage and 8-oxoG is the major oxidative DNA lesion. Approximately 80% is produced from $^1O_2$ and the remainder from OH• derived from $O_2^{\bullet-}$ (Cadet & Douki 2011). The production of OH•, also accounts for the SSBs and oxidised pyrimidines that constitute minor products of UVA irradiation. OH• generation may be amplified by Fenton chemistry involving UVA-induced iron release from ferritin(Pourzand et al. 1999). 8-oxo-G was previously considered the signature lesion of UVA irradiation but it has since been shown that CPDs are induced at five-fold higher levels (S. Mouret et al. 2006). Within skin, the CPD:8-oxoG ratio is cell-type dependent and is reduced from 5.2 in keratinocytes to around 1.4 in melanocytes, possibly as a result of $^1O_2$ produced by melanin photosensitisation(S. Mouret et al. 2011a).

UVA induces protein oxidation(Vile & Tyrrell 1995) and this is mediated by $^1O_2$. Protein carbonyls and oxidised sulfhydryls(Vile & Tyrrell 1995)have been detected after UVA irradiation of human fibroblasts(Sander et al. 2002). Examples of UVA damage to specific proteins include PCNA(Montaner et al. 2007) and XRCC3(Girard et al. 2011). High UVA doses inactivate SOD and catalase in mouse skin but not SOD irradiated *in vitro* (Shindo et al. 1994). In human fibroblasts, SOD is unchanged immediately after irradiation but catalase activity is depleted and only recovers upon

synthesis of new enzyme(Shindo & T. Hashimoto 1997). UVA also inactivates enzymes in intact human lenses irradiated *in vitro*(Linetsky et al. 2003). Protein carbonyls are detectable in dermis but not the epidermis of normal skin (Dimon-Gadal et al. 2000). This may reflect the higher epidermal antioxidant capacity(Rhie et al. 2001). Depletion of non-enzymatic antioxidants may also promote protein oxidation as endogenous RS levels are not longer controlled(Rhie et al. 2001).

UVA also induces lipid peroxidation, which appears to coincide with the upregulation of MMP-1, a collagenase, providing another potential route to photoaging in addition to protein oxidation(Polte & Tyrrell 2004). Numerous other genes such as antioxidant and stress response factors are also upregulated by UVA in a $^1O_2$ dependent manner(Tyrrell 2011). UVA also stimulates NADPH oxidase at sub-lethal doses, which besides the increasing cellular RS burden, results in the synthesis of prostaglandin E2, in important immunosuppressive factor(Kalinski 2011)

### 1.4.3 Solar radiation and the skin

The above-mentioned cellular effects of UVR result in a number of adverse consequences for skin including photoaging and skin cancer.

Photoaging is characterised by dermal dyspigmentation, laxity, yellowing, wrinkles, telangiectasia and cutaneous malignancies(Yaar & Gilchrest 2007). This correlates with decreasing and disordered collagen and the accumulation of partially degraded elastin in the upper dermis. UVA is thought to make the main contribution to photoaging due to its relative abundance and penetration. There may also be contributions from visible and IR wavelengths(Holzer et al. 2010).

Skin malignancies occur frequently and incidence rates continue to increase in the Western world as changes in human behaviour and increasing life expectancy result in greater exposure to UVR, the main risk factor. They are classified in the first instance as either cutaneous malignant melanoma (CMM) or non-melanoma skin cancer (NMSC); the two main classifications of NMSC are basal cell carcinoma (BCC) and squamous cell carcinoma (SCC).

#### *1.4.3.1 Cutaneous Malignant Melanoma (CMM)*

CMM describes a range of melanocytic neoplasms that can be further subdivided depending on growth patterns and site of occurrence(Bastian 2014). Incidence rates have increased more than any other cancer over the last 30 years(Parkin et al. 2011). Risk factors include large numbers of moles, organ transplantation and family history of melanoma. UVR exposure is a risk factor with the nature and timing seemingly most important; more than one severe sunburn in childhood causing a two-fold increase in melanoma risk(Narayanan et al. 2010). CMM shows limited dependence on cumulative sun exposure(S. Wu et al. 2014). Metastatic melanoma has a median survival of 6-10 months after diagnosis and is responsible for the vast majority of skin cancer deaths. In 2011, there were 13348 diagnoses of MM in the UK and 2209 deaths (Cancer Research UK). Two drugs, ipilimumab and vemurafenib (Section 4.1.4), showed promise in clinical trials and have now been approved for use although their survival benefits are still under assessment.

#### *1.4.3.2 Non Melanoma Skin Cancer (NMSC)*

NMSCs are keratinocyte-derived malignancies for which UVR exposure is an acknowledged risk factor. They are the most frequent cancers in Caucasian populations and account for 90% of all skin cancers and 20% of total malignancies in the UK (NCIN Data Briefing 2013). There were 102628 cases of NMSC in the UK in 2011, of which 74% were basal cell carcinomas (Section 1.4.3.3) and 23% squamous cell carcinomas (Section 1.4.3.4). Mortality rates are low as most lesions are curable. NMSCs can be disfiguring, however, and this is exacerbated by their propensity to appear on the face. The BCC:SCC ratio in immunocompetent individuals is around 4:1 but this ratio is inverted in immunosuppressed patients(Mudigonda et al. 2012). Risk factors which are common to both BCCs and SCCs include fair skin, UV exposure and exposure to chemical carcinogens(Emmert et al. 2013).

#### *1.4.3.3 Basal cell carcinoma*

BCCs are slow growing, translucent malignancies that form *de novo* with no detectable precursor lesion(Epstein 2008). They can cause morbidity by local invasion and multiple recurrences but less than 0.1% metastasise. BCCs are normally surgically excised which is curative in most cases with minimal recurrence. Other treatment options include curettage, cryosurgery, laser ablation and photodynamic therapy.

Aberrant signalling is implicated in the development of BCCs. Signalling by Sonic Hh (SHh), the only Hh protein expressed in human skin, coordinates hair growth and stem cell proliferation and is usually turned off in adult skin(Saran 2010). The signalling cascade is mediated by the SMO receptor, which is repressed under normal circumstances by Ptch1; SHh lifts the repression upon binding to Ptch1 and permits SMO signalling resulting in activation of the Gli transcription factors, which target cell cycle regulators and itself, turning off the signal. Hh signalling can become pathologically activated by Ptch1 loss-of-function mutations (70% of sporadic BCCs) or SMO activating mutations (10-20%)(De Zwaan & Haass 2009)..

UVR is the primary etiologic agent of BCC genesis although the precise nature of the relationship remains unclear. There appears to be a similarity to melanoma induction by UVR (i.e. a history of childhood and intermittent extreme exposure) although there is a also correlation with total UVR exposure albeit less strong than that of SCC (Dessinioti et al. 2010).

#### *1.4.3.4 Squamous Cell Carcinoma (SCC)*

SCC is the second most common cancer amongst Caucasians however unlike BCC, it carries a risk of metastasis and is therefore associated with greater morbidity and the majority of NMSC mortalities. Primary cutaneous SCCs are generally cured through excision but metastatic SCC has ten-year survival rates of less than 20%(Alam & Ratner 2001). SCC primarily occurs in the elderly with 70 years being the mean age of onset(Emmert et al. 2013). Long-term immunosuppressed patients have a 100-250 fold increased risk of SCC and the rate of metastasis exceeds 10%(Euvrard et al. 2003).

SCCs mainly develop from precursor lesions, principally actinic keratoses (AK). The vast majority of AKs do not progress to SCC and 26% may spontaneously regress(Emmert et al. 2013). Much like BCC, surgical excision remains the best option for SCC treatment although topical alternatives exist(Bahner & Bordeaux 2013).

SCCs are thought to occur via a multistep process. 60-90% of AKs and SCCs have C→T transitions in p53. UV-exposed but morphologically normal skin contains patches with p53 mutations that potentially represent an even earlier stage in carcinogenesis than AKs(de Gruijl & Rebel 2008). Loss-of-function NOTCH mutations are found in around 75% of SCCs however these are considered a stage progression rather than an initiatory event (N. J. Wang et al. 2011). Other pathways frequently dysregulated in SCC include ERK and EGFR/Fyn via RAS mutation, which affect proliferation and invasion respectively. Cell cycle inhibitor p16INK4a is also mutated in some tumours. One study showed that just two mutations (RAS in combination with CDK4 or RAS and NF-κB) may be sufficient for SCC formation(Dajee et al. 2003).

#### *1.4.3.5 Signature mutations in skin tumours*

Recent advances in whole exome sequencing have offered unprecedented insight into the genetics of cancer. In the most comprehensive study of SCC genetics to date, South et al found that 82% of sporadic SCCs contained a NOTCH mutation, confirming the earlier work of Wang et al, with a high (68%) proportion of C→T transition mutations, confirming an etiologic role for UVR(South et al. 2014). Also notable was the extremely high mutational burden of SCCs (around 50 mutations per Mb DNA) which far exceeded the next highest cancer with metastatic potential (lung squamous cell carcinoma, 8.1 per Mb, (Hammerman et al. 2012)); only BCCs reach comparable levels (around 75 mutations per Mb(Jayaraman et al. 2013)). The mutational burden of both skin cancers suggests that skin possesses an extraordinary capacity to withstand tumour formation likely conferred by tumour suppressors such as NOTCH and PTCH1.

The link between skin cancer and DNA repair is made starkly apparent by the autosomal recessive disorder, xeroderma pigmentosum (XP). XP is characterised by mutagenic inactivation of one of 8 genes, 7 of which coordinate the NER response (XP-A to XP-G) and the other (XP-V) which corresponds to loss of Pol η, the TLS polymerase responsible for bypassing unrepaired UVR photoproducts. XP patients have a 10,000 fold increased risk of NMSC with first onset at a median age of 9 vs. 67 in the general population(DiGiovanna & Kraemer 2012). Melanoma risk is also 2000-fold higher than average. Cells taken from XP patients can be defective in GG-NER (XP-C and XP-E), defective in both forms of NER (XP-A, XP-B, XP-D, XP-F or XP-G) or NER-proficient but with a defect in TLS (XP-V). It is clear that UVR mediated DNA damage and its persistence in the genome are key determinants of carcinogenesis.

## 1.5 Photosensitisers

Photosensitisers are molecules that potentiate the effects of radiation by the formation of RS upon photonic excitation. Many UVR and visible photosensitisers are present endogenously within cells and are responsible for some of the cutaneous effects of solar radiation described above. These effects can be exacerbated by the introduction of xenobiotics, usually in the form of pharmaceuticals, which act as exogenous PS and increase the RS burden on the cells resulting in an abnormal response to sunlight in patients.

### 1.5.1 Mechanisms of photosensitisation

The initial step in photosensitisation is absorbance of UVR or visible light by the photosensitiser (red arrow, Figure 1-11) to form an excited singlet state which can then undergo intersystem crossing to the first excited triplet state (purple arrow, Figure 1-11). This triplet state can decay back to the ground state (phosphorescence, orange arrow, Figure 1-11) or damage cellular targets by one of two mechanisms, known as type I and type II photosensitisation. Type I damage involves electron transfer or hydrogen abstraction by the excited photosensitiser and formation of photosensitiser and substrate radicals. Electrons can be transferred to suitable acceptors such as disulphides or oxygen, yielding $O_2^{\bullet-}$ (Silvester et al. 1998; M. J. Davies & Truscott 2001). Radicals can

react with $O_2$ to give peroxyl products that can decompose to give HO•, which is also formed via the $H_2O_2$ generated by dismutation of the photosensitiser-derived $O_2^{\bullet-}$. Type I mechanisms can proceed in anoxic conditions via direct reaction of the excited PS for example the photocycloaddition of psoralen to DNA. Type II reactions are oxygen dependent and result from energy transfer to ground state oxygen to give $^1O_2$ (blue arrows, Figure 1-11) which then reacts with targets within the cell. Type II reactions comprise the majority of endogenous photosensitisation occurring within the cell upon solar irradiation. An efficient PS must have a high quantum yield for a long-lived triplet state and for type II reactions, the energy of the triplet state must be ≥95kJ $mol^{-1}$. Taking fluorescein as an example, intersystem crossing is inefficient and hence fluorescence predominates with no $^1O_2$ production; halogenation of fluorescein to give Rose Bengal, increases ISC efficiency thus giving a high quantum yield for $^1O_2$ generation with minimal fluorescence(Wondrak et al. 2006). Generally photosensitisers act via both type I and type II mechanisms concurrently; the mechanism that predominates is determined by the photochemistry of the chromophore and the reaction conditions although $^1O_2$ formation is usually the faster process(M. J. Davies 2004).

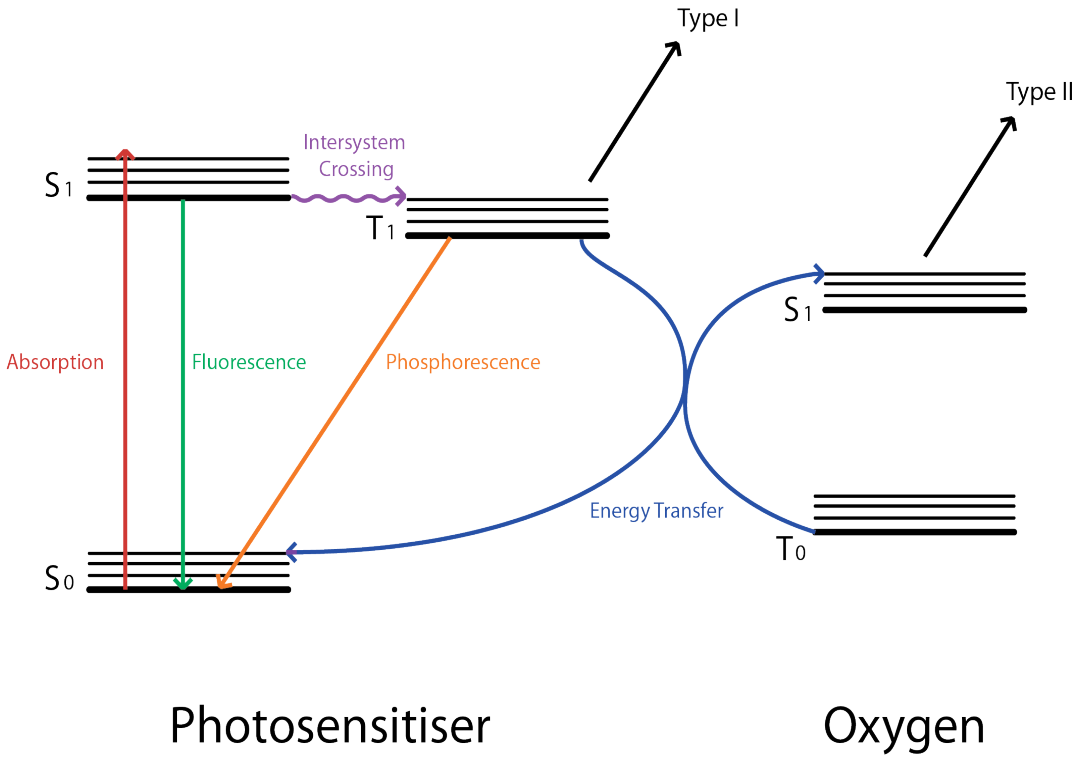


**Figure 1.11 Electronic transitions in photosensitisation**

Upon absorption of radiation (red arrow), the photosensitiser is excited from the singlet ground state ($S_0$) to the first excited singlet state ($S_1$). Fluorescence is the direct return to the ground state with emission of light (green arrow). The photosensitiser can transition to an excited triplet state ($T_1$) via intersystem crossing (purple arrow). The excited triplet state can engage in electron transfer with other molecules (type I) or energy transfer to oxygen (blue arrow, type II), exciting it to its excited singlet state ($^1O_2$).

### 1.5.2 Photosensitisers and their effects

The outcome of photosensitisation is determined by a number of PS characteristics including quantum yield, excitation wavelength and cellular and subcellular localisation. The reactions of any generated RS with biomolecules (Sections 1.2.3 and 1.3.1) will also govern which targets are modified and how; the chemistry of the PS excited state will affect type I reactions. Ultimately the chemical modifications to DNA, protein and lipids within the abovementioned parameters determine the consequences of photosensitisation. The importance of localization and reaction mechanism can be illustrated by comparison of two dermatological procedures; photodynamic therapy

(PDT) and psoralen-UVA treatment (PUVA). Both cause apoptosis in their target cells upon UVA irradiation but the proposed mechanisms are different in each case.

PDT utilises the photosensitising ability of porphyrins, which are synthesized by the cell to serve as prosthetic groups for various proteins. Porphyrins act as classical type II photosensitisers and their pathological accumulation in the skin (disease states known as cutaneous porphyrias) are characterised by skin fragility and necrosis. By topical application of a compound that induces porphyrin accumulation, localised photosensitisation can be achieved upon exposure to a UVA light source; PDT is used in the treatment of BCCs, AKs and other skin disorders. The burst of singlet oxygen produced upon irradiation triggers immediate apoptosis in a manner reminiscent of high doses of UVA alone(Godar 1999), possibly via the activation of p38/JNK (R. W. K. Wu et al. 2011). The action of porphyrins is oxygen dependent(Carraro & Pathak 1988). Psoralen derivatives, the active compound of PUVA, have a furocoumarin structure, which intercalates with DNA. Upon UVA irradiation, a 2+2 photocycloaddition occurs between the C5-C6 double bond of thymine and the 4,5 double bond of the furan of psoralen to give a DNA-monoadduct. Absorption of a second photon leads to another cycloaddition and yields an ICL(Bethea et al. 1999). PUVA also causes apoptosis but with a slower time course which is more akin to DNA damaging agents such as UVC and ionizing radiation(Godar 1999). Psoralens can also form adducts with double bonds in proteins and lipid and also produces $^{1}O_2$ and $O_2^{\bullet-}$ however DNA crosslinking is not oxygen dependent(Carraro & Pathak 1988). A recent study posits that transcription and replication blockage by ICLs is the major factor in apoptosis(Derheimer et al. 2009). The DNA damaging effects of PUVA likely underlie the increased risk of NMSC(Archier et al. 2012); in contrast, PDT has no reported carcinogenesis(Ibbotson 2011).

Photosensitisation is the key component of PDT and PUVA but photosensitivity can also arise as an undesired side effect of a wide range of pharmaceuticals(Drucker & Rosen 2011).

## 1.6 Aims

At the outset of my work, 6-thioguanine, a potent UVA photosensitiser that becomes incorporated into DNA, was known to act via type I and type II mechanisms leading to a variety of DNA lesions. Little was known about the effects on cellular proteins caused by 6-TG treatment and UVA although previous work in the lab suggested that DNA repair proteins are damaged. My aims were to:

- Establish a robust protocol for examining protein oxidation in cultured cells and use it to identify proteins reproducibly oxidised by 6-TG photosensitisation.
- Examine the effects of protein oxidation on DNA repair capacity.
- Apply the developed assays to other photosensitisers to provide information on the mechanism that underlies the effects of 6-TG.

# Chapter 2. Materials & Methods

## 2.1 Chemicals and reagents

Unless otherwise stated, all chemicals and reagents were sourced from Sigma-Aldrich.

Standard solutions of 1 M Tris-HCl, 0.5 M EDTA, 1 M $MgCl_2$, 5 M NaCl, 10x Tris-Borate-EDTA (TBE) and phosphate buffered saline (PBS) were provided by Cancer Research UK London Research Institute (LRI) Central Services.

### 2.1.1 $^{32}$P Labelling of Oligonucleotides

Oligonucleotides were diluted to a concentration of 0.5pmoles/µl. 4µl of oligonucleotide solution was added to 1µl of T4 kinase buffer, 1µl of T4 PNK (New England Biolabs) and 4.5µl γ-ATP (Amersham Pharmacia). This was incubated at 37$^{o}$C for 40 minutes, and then labelled oligonucleotide separated from residual γ-ATP and ADP in a G50 spin column (Amersham Pharmacia). Labelled oligonucleotides were stored at 4$^{o}$C.

### 2.1.2 Annealing of Complementary Oligonucleotides

Equimolar amounts of the complementary oligonucleotides were mixed. An appropriate volume of 10X Annealing Buffer (0.1M Tris-HCl, pH7.5, 0.1M $MgCl_2$) was added. The solution was heated to 80$^{o}$C for 5 minutes followed by incubation for 1 hour at room temperature.

| | Sequence 5' – 3' | Supplier |
|---|---|---|
| **A** | GATCTGATTCCCATCTCCTCAGTTTCACTTCTGCACCGCATG | atdbio |
| **B** | CATGCGGTGCAGAAGTGAAACTGAGGAGATGGGAATCAGATC | atdbio |
| **C** | CCTGACTGTATGATGAAGATGCTGACGAG | Sigma |
| **D** | CTCGTCAGCATCTTCATCATACAGTCAGG | Sigma |
| **E** | CTCGTCAGCATCXACATCATACAGTCAGG | Sigma |
| **F** | CCTGACTGTATGATGAAGATGCTGACGAG | Sigma |

**Table 2-1: Oligonucleotides used in this work.**

X= 6-TG

## 2.2 Cell Biology

### 2.2.1 Cell culture and cell maintenance

| Cell Line | Organism | Origin | Gene Mutated | DNA repair status |
|---|---|---|---|---|
| CCRF-CEM | Human | Leukemic T cell Lymphoblast | MLH1 | MMR deficient |
| CHO – K1 | Hamster | Ovary | - | Proficient |
| CHO – xrs6 | Hamster | Ovary | Ku80 | NHEJ deficient |

**Table 2-2: Cell lines used in this work.**

DMEM (CHO) and RPMI (CCRF-CEM) media were obtained from Life Technologies, antibiotics from CRUK LRI Central Cell Services. Sterile plastic ware was from Corning, Becton Dickinson and BD Pharmingen. CCRF-CEM cells were maintained in RPMI medium, supplemented with antibiotics (penicillin and streptomycin prepared by Cancer Research UK LRI Central Services) and 10% Foetal Calf Serum, at 37°C in a humidified atmosphere containing 5% CO2. CHO cell lines were maintained in DMEM medium supplemented with antibiotics and 10% Foetal Calf Serum (Invitrogen) at 37°C in a humidified atmosphere containing 10% CO2. Cell numbers were determined using a haemocytometer or Cellometer AutoT4 (Biotechnologie GmbH).

### 2.2.2 Drug Treatments

6-TG treatment: 6-TG stock solution (1mM in 0.1 M NaOH, filter sterilised) was added to cells growing exponentially at around 500,000 cells/ml and incubated for 24 hours.

Fluoroquinolones: All fluoroquionolones were prepared as stock solutions (50mM in 0.1M NaOH). They were added to exponentially growing cells at around 500,000 cells/ml and incubated for 1 hour.

Vemurafenib: As for 6-TG but with vemurafenib stock solution (100mM in DMSO).

After drug treatment, cells were washed twice with PBS, and resuspended, generally at 1-2.5 x $10^6$ cells/ml in 10ml PBS for irradiation.

### 2.2.3 Irradiation

#### *2.2.3.1 UVA irradiation*

Cells were generally irradiated in PBS in 10cm dishes. UVA irradiation was carried out using a UVH 250W iron bulb (UVLight Technologies) fitted with a black filter glass with a low range cut off at 320 nm, and high range cut off at 400 nm (Fig 2.1). The standard dose rate, as measured using a UVA Light Meter dosimeter (UVLight Technologies), was 0.1 kJ/$m^2$/s and was used throughout. A temperature control unit, coupled to the irradiation chamber maintains the temperature at between 10~15°C during irradiation.

#### *2.2.3.2 UVC irradiation*

UVC irradiation was performed using the built in 254-nm UV light bulbs in a Stratalinker UV Crosslinker (Stratagene). The dose rate for irradiation was approximately 10 J/$m^2$/s and the preset dose was delivered automatically by the calibrated crosslinker.

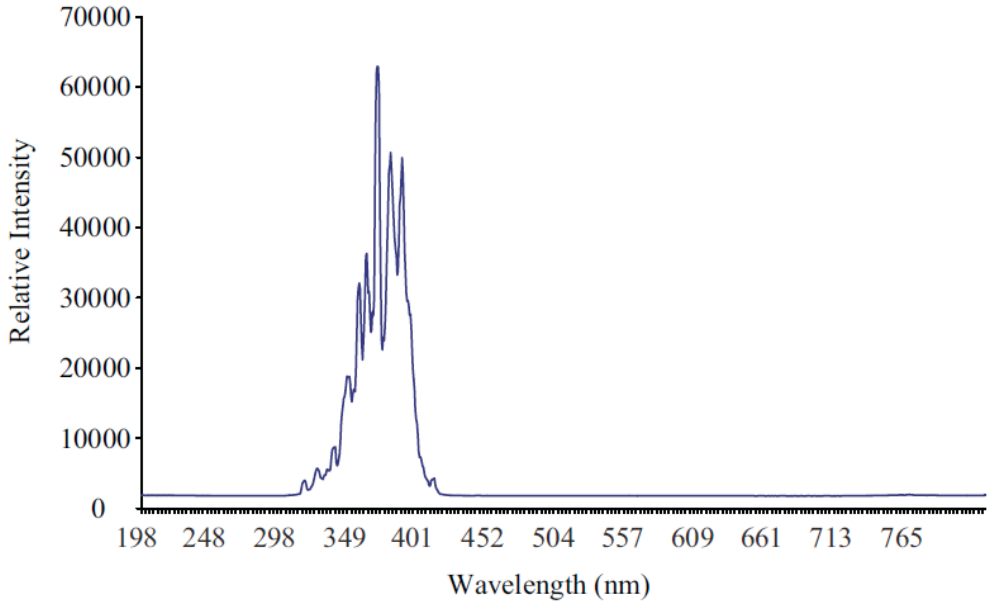


**Figure 2.1 Emission spectrum of the UVA light source.**
Emission spectrum for iron doped metal halide UV bulb fitted with a black filter glass with a low range cut off at 320 nm and high range cut off at 400 nm. (Adapted from UVLight Technologies).

### 2.2.4 Proliferation Assay

Approximately $10^7$ cells were that had been treated with drug and/ or UVA were resuspended at 200,000 cells/ml in fresh growth medium. Cell growth was monitored by cell counts taken at 24 and 48 hours.

## 2.3 Biochemical Techniques

### 2.3.1 RIPA cell extracts

Three pellet volumes of RIPA (Radioimmunoprecipitation Assay) buffer, 50mM Tris pH 7.5, 150 mM NaCl, 0.1% SDS, 0.5% sodium deoxycholate, 1% Triton X 100) was added to approximately $10^8$ cells that were then disrupted by vortexing. After 20 min on ice with intermittent vortexing, extracts were centrifuged at 14,000 x g for 10 mins. Aliquots of the supernatant were stored at -80°C.

### 2.3.2 Protein Gel Electrophoresis

Nu-PAGE 10-well Bis-Tris 10% polyacrylamide gels (Life Technologies) were electrophoresed in X-cell SureLock Mini Cells. Samples (25µl max) were electrophoresed at 200V until the dye front reached the bottom of the gel. Each gel was run with RPN-800 Full Range Rainbow Markers (5µl) (GE Lifesciences).

### 2.3.3 Immunoblot

Separated proteins were transferred to a PVDF membrane (Immobilon-P, Millipore) overnight at 20V using a Biorad wet transfer apparatus. Following transfer, membranes were washed and blocked for 90 minutes with 10% (w/v) non-fat powdered milk in PBST (PBS + 0.1% Tween-20) at room temperature. Primary antibodies (Table 2-3 for dilutions and suppliers) were incubated for 1h at room temperature or overnight at 4°C All antibodies were diluted in 5% milk in PBST. Membranes were washed 3 x with PBS-T then incubated with the appropriate secondary antibody (Table 2-3, 1:5000). Membranes were washed 3 x with PBS-T and detected using ECL substrate (GE Healthcare) and proteins visualised using Amersham Hyperfilm ECL (GE Lifesciences).

### 2.3.4 FHA derivatisation

Aliquots of Alexa Fluor Hydroxylamine 647 (FHA) (Invitrogen) 1 mg/ml in distilled water were stored at -20°C. 1 µl of this stock was added to 20µg protein to give a final concentration of 0.05µg/µl FHA in 20µl. Following incubation at 37°C for 2 hours 5µl 5x SDS loading buffer was added and the mixture left to stand at room temperature for 5 minutes before gel loading and electrophoresis. Following electrophoresis, the dye front was excised from the bottom of the gel (to remove highly fluorescent unincorporated FHA) which was then rinsed in distilled water. At this point, if total protein content was to be examined, gels were fixed and stained with Sypro Ruby (Life Technologies) according to the manufacturer's "Quick" protocol. Gels were imaged

using the Typhoon 9400 scanner (GE Healthcare) at "Normal" sensitivity at 633nm and 488nm concurrently. Western blotting was carried out on unfixed gels.

| | Supplier | Dilution |
|---|---|---|
| **Ku 70/80** | Stratech | 1:1000 |
| **Ku 70** | Abcam | 1:400 |
| **Ku 80** | Abcam | 1:1000 |
| **MCM 4** | Abcam | 1:1000 |
| **MCM 6** | Abcam | 1:1000 |
| **MCM 7** | Abcam | 1:1000 |
| **RPA 32** | Abcam | 1:1000 |
| **PCNA** | Santa Cruz | 1:2000 |
| **DDB1** | Abcam | 1:1000 |
| **DDB2** | Abcam | 1:250 |
| **Goat Anti Mouse HRP** | Biorad | 1:5000 |
| **Goat Anti Rabbit HRP** | Biorad | 1:5000 |

**Table 2-3: Antibodies used in this work**

### 2.3.5 AFM derivatisation

The protocol of Baty et al(Baty et al. 2002) was followed with the exception of the derivatisation reagent, which was substituted by Alexa Fluor 647 Maleimide (AFM, Invitrogen). Briefly, 25 x 106 treated cells were resuspended in 200µl extract buffer (100 mM N-ethyl maleimide (NEM), 40 mM HEPES pH 7.4, 50 mM NaCl, 1 mM EDTA, protease inhibitors,) and incubated at room temperature for 15 minutes. Cells were lysed by the addition of CHAPS at a final concentration of 1% w/v and the extract was vortexed and incubated for a further 15 min at room temperature. Insoluble material was separated by centrifugation at 8000 g for 5 min. Excess NEM was removed by passage through a spin column that had been equilibrated with 40 mM HEPES pH 7.4, 50 mM NaCl, 1 mM EDTA, protease inhibitors, and 1% CHAPS w/v. DTT (1 mM) was

added to the column eluate a and the extract incubated for 10 min at room temperature. This step reduces the oxidized thiols. AFM (10 mM in DMSO) was added to the extract to a final concentration of 100µM and the mixture was incubated in the dark at room temperature for 10 min. Excess AFM and salts were then removed by passage through a second spin column equilibrated with PBS. Samples were subsequently processed as for FHA derivatised extracts.

### 2.3.6 2-D PAGE

To 250µg FHA-derivatised cell extract protein, 2.5 µl IPG buffer (GE Healthcare, broad range) and 237.5 µl rehydration buffer (8M Urea, 2% CHAPS, 5% glycerol, bromophenol blue) was added for a final volume of 250 ml. This mixture was loaded onto a 13cm ceramic strip holder. An Immobiline DryStrip (pH 3-10 NL, 13cm) strip was added to the sample and the strip holder placed in an Ettan IPGphor apparatus. Isoelectric focussing (IEF) was carried out overnight under the conditions described in Table 2-4.

| | Voltage (V) | Volt Hours | Step & Hold / Gradient |
|---|---|---|---|
| **Step 1** | 30 | 480 | Step & Hold |
| **Step 2** | 500 | 500 | Step & Hold |
| **Step 3** | 1000 | 800 | Gradient |
| **Step 4** | 8000 | 11325 | Gradient |
| **Step 5** | 8000 | 4400 | Step & Hold |

**Table 2-4: Conditions used during isoelectric focussing**

Following IEF, proteins were reduced by incubating the strips for 15 mins at room temperature in 5ml equilibration buffer (0.1M? Tris pH 8.8, 6M Urea, 30% glycerol, 2% SDS, bromophenol blue) containing 1% DTT. Strips were then transferred to 5ml equilibration buffer containing 4% iodoacetamide and proteins were alkylated for a further 15 min. Processed strips were loaded onto 10% Bis-Tris gels (BioRad) and electrophoresed at 125V until the dye front had exited the gel. SyproRuby staining and fluorescence imaging were preformed as described above.

Gel spot excision was performed under blue light illumination using a scale image as a guide. Excised spots were analysed by mass spectrometry by the LRI Department of Protein Analysis & Proteomics.

### 2.3.7 EMSA

#### *2.3.7.1 Ku*

Approximately $10^8$ cells were resuspended in extraction buffer (20mM HEPES, pH 7.9, 1mM $MgCl_2$, 5mM EDTA, protease inhibitors, 1% Triton X-100), incubated on ice for 30mins, and then centrifuged at 20,000 x g. 20µg extract was incubated with 10 fmol radiolabelled oligonucleotide duplex A+B (Table 2.1) for 15 minutes at RT in binding buffer (20mM Tris.HCl pH 8.0, 2mM $MgCl_2$, 0.1mM EDTA, 0.25mM DTT, 200mM KCl) in 12.5µl reaction volume. For antibody supershift analysis, 1µl Ku Polyclonal 70/80 (Stratech) was added and incubation continued for a further 10 mins. To each sample, 2.5 µl 6x DNA loading buffer (300mM Tris.HCl, pH8, 60% glycerol, 12mM EDTA, bromophenol blue) was added and electrophoresis performed on a 5% polyacrylamide gels. Running buffer was 0.25x TBE at 100V. The gel was dried and then exposed to a Storage Phosphor Screen (GE Healthcare) and imaged using a Storm scanner (GE Healthcare).

#### *2.3.7.2 DDB2*

Extracts were prepared in the DDB2 EMSA binding buffer (Wittschieben et al. 2005) (20 mM Tris-HCl, pH 7.5, 5 mM DTT, 150 mM NaCl, 1 mM $MgCl_2$, 0.2 mM EDTA, and 5% glycerol) with the addition of 1% Triton X-100 (Invitrogen) and protease inhibitors (Roche). Oligonucleotide D (Table 2-1) was irradiated with 5000 J/$m^2$ UVC. Oligonucleotide E was either irradiated with 100 kJ/$m^2$ UVA or MMPP in a 10:1 MMPP:oligonucleotide ratio. Treated oligonucleotides were annealed to radiolabelled complementary strands. Control duplexes were assembled from untreated oligonucleotides D and E. For EMSA assays, 10 fmol duplex probes were incubated with 20µg extract for 15 minutes at room temperature in binding buffer (20 mM Tris-

HCl, pH 7.5, 5 mM DTT, 150 mM NaCl, 1 mM $MgCl_2$, 0.2 mM EDTA, 5% glycerol). Electrophoresis and analysis was performed as described in the previous section.

### 2.3.8 NHEJ Assay

The assay was adapted from Baumann & West(Baumann & West 1998). The substrate is an XhoI-digested plasmid. pFastBac Dual (Invitrogen) plasmid was digested with Xho1 (NEB) and gel purified. 400ng linearised plasmid was end-labelled with ATP-[$\gamma$ - $^{32}$P].

Extracts were prepared from 5 x $10^7$ treated and pelleted cells by resuspension and freeze thaw in three pellet volumes of LB buffer (25mM Tris.HCl, pH 7.5, 333mM KCl, 1.3mM EDTA, 4mM DTT, protease inhibitors (Roche), phosphatase inhibitor cocktail II (Sigma)). Following 20 mins incubation on ice, extracts were centrifuged at 14,000 x g for 20 mins. The supernatant was dialysed overnight at 4°C against E buffer (20mM Tris.HCl, pH8, 100mM K(OAc), 0.5mM EDTA, 1mM DTT, 20% glycerol). Aliquots were stored at -20$^o$C.

For NHEJ assay, 10ng DNA substrate and 20µg extract were combined in a final volume of 10µl ligation buffer (50mM Tris. HCl, pH 8.0, 60mM K(OAc), 0.5mM $Mg(OAc)_2$, 1mM ATP, 1mM DTT, 0.1mg/ml BSA) for 2 hours at 37°C.
2.5µl buffer (10mg/ml Proteinase K, 2.5% SDS, 50mM EDTA, 100mM Tris.HCl, pH7.5) was then added and digestion carried out for 30mins at 55°C. 2.5 µl 6x DNA loading buffer (30% glycerol, 0.25% w/v bromophenol blue) was added and electrophoresis performed on a 0.7% agarose gel in TBE. The gel was dried, exposed to a Phosphor Screen and imaged using a Typhoon 9400 Scanner.

For complementation, 1µl aliquots of appropriate dilutions of recombinant Ku 70/80 (Trevigen) was added to the initial reaction mixture.

### 2.3.9 CM-H2DCFDA Assay

Drug-treated cells ($5.10^6$) were resuspended in 1ml CM-H2DCFDA (Life Technologies solution (final concentration 7.2μM) and incubated at 37°C for 30 minutes. Cells were harvested, resuspended in PBS and UVA irradiated. They were then resuspended in 1ml PBS in 12 x 75mm tubes with cell strainer caps. FACS analysis was performed on a Beckton Dickinson FACScan using the FL1 channel for green fluorescence. Data acquisition and analysis was performed using CellQuest v3.3 software.

### 2.3.10 RNO assay

100μM p-nitroso-N,N-dimethylaniline was prepared in 0.1M sodium phosphate buffer pH 7.0 prepared with water or $D_2O$. Stock solutions of each drug (10mM) and histidine (100mM) were prepared in phosphate buffer. These solutions were combined in a final volume of 800μl in triplicate wells of duplicate 96 well plates. One plate was kept in the dark whilst the other was irradiated with UVA (100 kJ/$m^2$). Sample absorbance was then measured at 440nm using a plate reader. Mean values for the $A_{440}$ remaining were calculated.

In the modified assay all component were dissolved at the same concentrations in DMSO except histidine, which could only be dissolved in water-based buffer.

### 2.3.11 Enzyme-linked immunosorbent assay

The induction and persistence of CPDs and 6-4PPs in cellular DNA was determined by enzyme-linked immunosorbent assays (ELISA) performed according to the manufacturer's (Cosmo Bio Co) instructions.
Genomic DNA was extracted from treated cells using the QiaAMP DNA Mini Kit according to the manufacturer's instructions, diluted in PBS and quantified using the Nanodrop spectrophotometer (NanoDrop Technologies). 96-well plates were pre-coated with 50 μl/well protamine sulphate (0.003% in $H_2O$), dried at 37°C overnight, and washed with $H_2O$. Triplicate samples of DNA: 200ng per well for 6-4PP detection or

10ng per well for CPD detection were added to the pre-coated plates which were dried overnight at 37°C. 6-4PPs or CPDs were detected using anti-6-4PP(Cosmo Bio Co LTD, 1:1500 dilution) or anti-CPD (Cosmo Bio Co LTD, 1:1000 dilution) primary antibodies respectively, the biotin- F(ab')$_2$ fragment of goat antimouse IgG (H+L) (Invitrogen, 1:2000 dilution) and streptavidin-coupled peroxidase (Invitrogen, final concentration 0.1 µg/ml). Plates were incubated for 30 min at 37°C followed by five washes with PBST (0.05% Tween-20 in PBS). To the wells were was added 150µl citrate-phosphate buffer (pH 5.0) followed by 100µl substrate (8 mg o-Phenylene diamine/4 µl $H_2O_2$ (35%) in 20 ml citrate-phosphate buffer, pH 5.0) and incubated at 37°C for approximately 10 min to allow colour development. The absorbance of each well was measured at 492 nm in a plate reader.
To determine NER efficiency, treated cells were also irradiated with UVC (20 J/m$^2$) and returned to full growth medium before DNA extraction and ELISA.

### 2.3.12 DNA immobilisation for DDB2 binding

DNA was extracted from treated cells using the QiaAMP Mini kit. Cell X-100 extracts were prepared from approximately $10^8$ cells using the DDB2 EMSA binding buffer (Wittschieben et al. 2005) (5 mM DTT, 150 mM NaCl, 20 mM Tris-HCl, pH 7.5, 1 mM MgCl2, 0.2 mM EDTA, and 5% glycerol) with the addition of 1% Triton X-100 (Invitrogen) and protease inhibitors (Roche). Cells were resuspended in 3 pellet volumes of buffer, incubated on ice for 20 mins and then centrifuged at 20,000 x g. Aliquots were stored at -80°C.

Genomic DNA, diluted in 200µL 0.1M sodium citrate, pH5, was immobilised on a positively charged nylon membrane (Immobilon ny+, Millipore) using a slot blot apparatus attached to a vacuum manifold. The membrane was dried overnight at 37°C and then washed once with PBS-T. The membrane was blocked with 10% milk, then cut into narrow strips and incubated in 1ml of the X-100 extract for 15 min at room temperature to allow DDB2 binding. The membrane was then washed five times with PBS-T and probed with DDB2 antibody as described for the immunoblot procedure.

# Chapter 3. Protein oxidation by 6-TG/UVA

## 3.1 Introduction

### 3.1.1 Protein oxidation by reactive species

The relative abundance of cellular proteins (they account for 70% of dry mass) and the kinetic favourability of RS-reactions with amino acid side chains(M. J. Davies 2005) makes them a major target for oxidative damage. Protein oxidation usually compromises protein function although a few examples of activating oxidation also exist, most notably activation of protein kinase C by cysteine oxidation(Cosentino-Gomes et al. 2012). Inactivating oxidation is not invariably detrimental and RS and protein oxidation are now seen as key features of cell signalling. Accumulation of oxidised proteins is associated with aging and with a number of disease states including diabetes, atherosclerosis and cancer (reviewed in (Berlett & Stadtman 1997)).

Despite the ostensive chaos of unchecked RS production that characterises oxidative stress, protein oxidation exhibits a degree of specificity that has both chemical and biological underpinnings. The products of protein oxidation depend on the identities of the RS and the chemistry of the amino acids. Multiple products can be formed from side chain oxidation and these may undergo secondary reactions with other cellular molecules. Products from the oxidation of non-protein cellular components such as lipids can also modify proteins. All these factors combine to make the oxidised fraction of the proteome a chemically heterogeneous mixture.

### 3.1.2 Factors affecting likelihood of oxidation

Each RS has a specific profile of amino acid reactivity. At one extreme, typified by $O_2^{\bullet-}$ and $H_2O_2$, reaction can only occur with activated protein thiols. At the other extreme, HO• will react with any amino acid although the reaction rates span three orders of magnitude(Xu & M. R. Chance 2007). The reaction between an RS and an amino acid side chain is affected by multiple variables. Firstly, adjacent residues can influence the nucleophilicity of an amino acid, which makes it more attractive to many RS as they are generally electrophilic. Secondly, nearby bound metal atoms increase the likelihood of

Fenton chemistry. In addition, protein structure affects RS access - buried amino acids are less easily oxidised(Lundeen & McNeill 2013) and non-polar microenvironments within a protein can impede the formation of charged transition states. On a larger scale, protein reactivity can be influenced by subcellular location and its proximity to the source of RS as well as local pH.

Given the diverse chemistry of amino acid side chains and RS, myriad oxidative modifications are possible. To simplify analysis, general markers of oxidation are frequently used and the two most common are discussed below.

### 3.1.3 Thiol oxidation

Protein thiols are a major target of oxidation *in vivo*(Conte & Carroll 2013). The sulphur atom can occupy various oxidation states and cysteine can function as a redox switch, as well as an active site nucleophile and structural element. Thiol oxidation is more kinetically favourable than the majority of oxidative modifications; in this way, preferential oxidation of methionine in particular may serve as an intrinsic antioxidant system as its first oxidation product, methionine sulfoxide, can be reduced enzymatically(Stadtman & Levine 2001). A number of enzymes (e.g. thiol proteases) utilise nucleophilic cysteines in their active sites. These are activated by hydrogen bond formation or deprotonation mediated by adjacent residues. This activation also increases their susceptibility to oxidation.

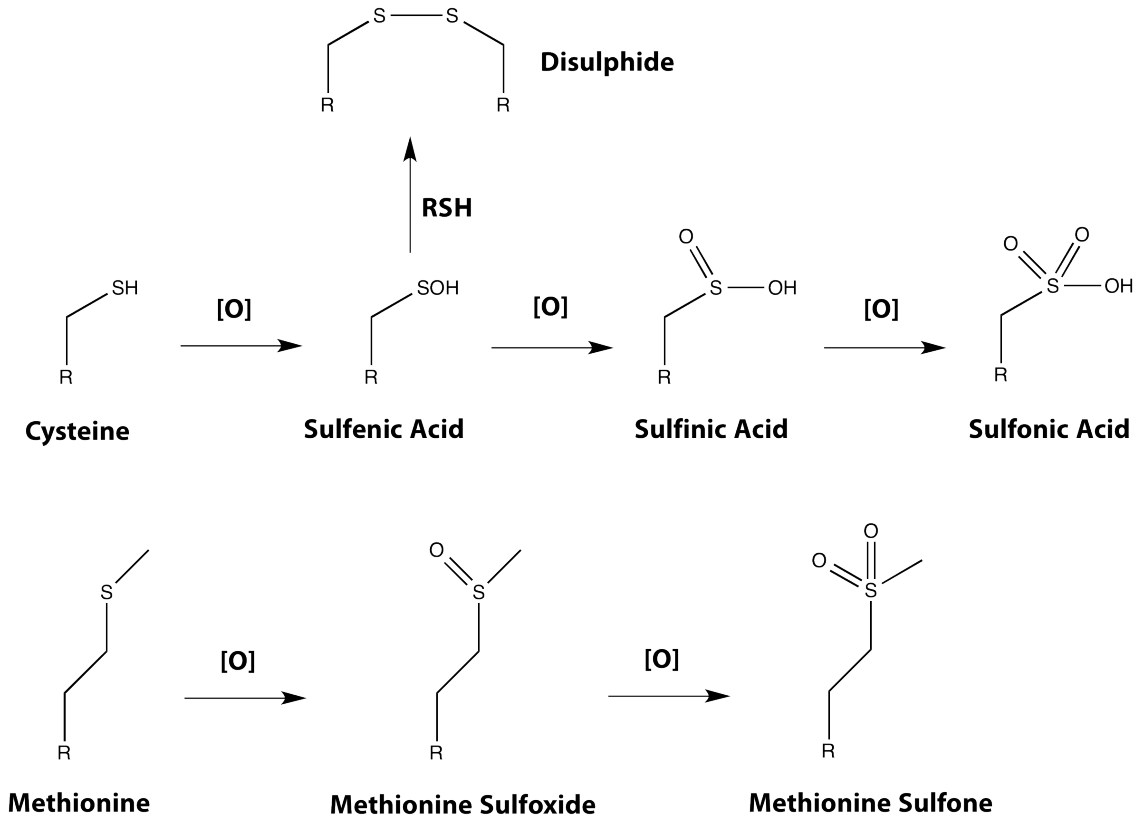


**Figure 3.1 Oxidation products of cysteine and methionine**
Sequential oxidation of cysteine yields the cysteine oxyacids, sulfenic, sulfinic and sulfonic acid. Sulfenic acid can also react with an reduced thiol to yield a new disulphide bind. Methionine is sequentially oxidized to give the sulfoxide and sulfone products. [O] denotes an unspecified oxidant.

Cysteine oxidation(Figure 3.1) generally proceeds via a short-lived intermediate, sulfenic acid. Sulfenic acid can be reduced by another thiol to yield a new disulphide bond or further oxidised to sulfinic acid. Disulphides can be intramolecular or intermolecular, for example protein-protein or protein-glutathione. Thioredoxins and glutaredoxin catalytically reduce disulphides and thus restore cysteine to its reduced state. Although initially considered to be a protective measure, protein glutathionylation is now recognised as a regulatory post translational modification(Dalle-Donne et al. 2007). Further oxidation of sulfinic acid yields sulfonic acid. Sulfinic and sulfonic acids are generally stable and irreversible.

Reversible thiol oxidation (sulfenic acid and disulphides) plays a role in cell signalling and is usually studied by the “switch” strategy (Figure 3.2). Mass spectrometry can

identify the oxidised proteins labelled by the switch method and may pinpoint individual oxidised cysteines.

Studying irreversible thiol oxidation is more challenging as their relative chemical inertness precludes selective tagging with currently available probes. One approach used antibodies generated against a sulfonic acid-containing peptides modelled on the active sites of various proteins(Woo & Rhee 2010). Although both sulfinate and sulfonate can be detected directly by mass spectrometry, inefficient ionisation and ambiguous fragment masses complicate analysis(Murray & Van Eyk 2012). The negative charge of sulfonate may provide a route to affinity purification but this has only been demonstrated for model peptides(Y.-C. Chang et al. 2010). A sulfinic acid-specific probe has been developed and is currently being evaluated(Conte & Carroll 2012).

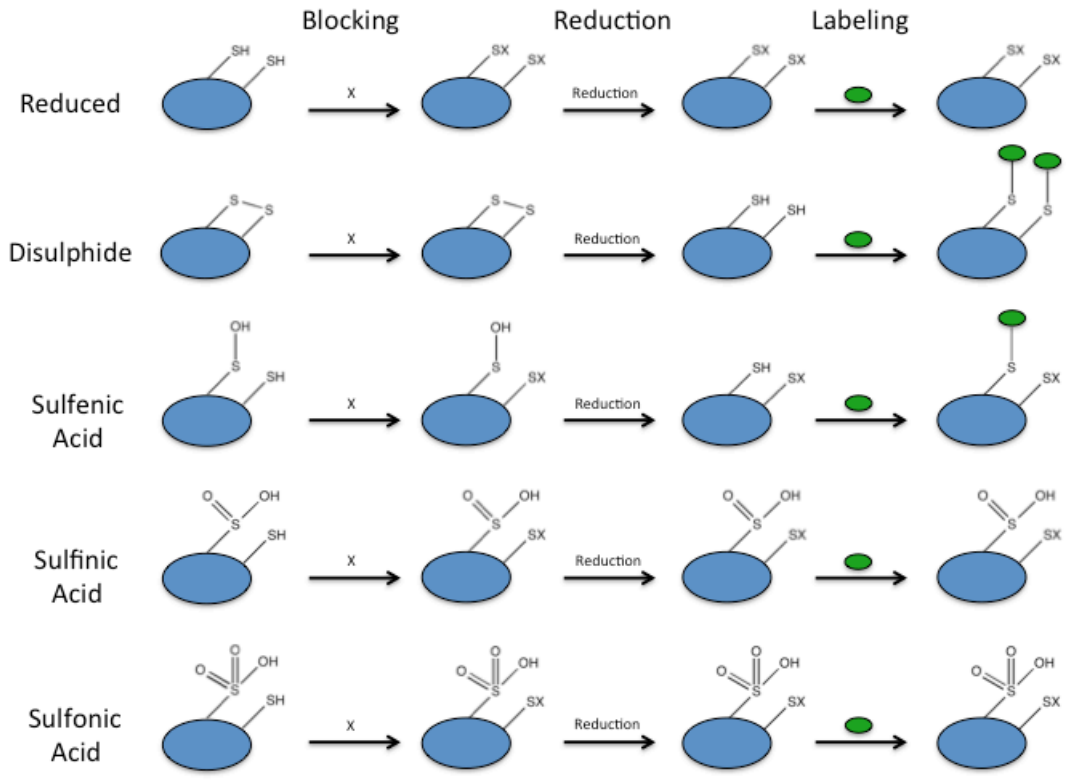


**Figure 3.2 The "switch" method for derivatising reversibly oxidised cysteines.**
Reduced thiols in the sample are irreversibly blocked with an alkylating agent denoted X (common reagents include N-ethyl maleimide and iodoacetamide). Samples are then treated with a reducing agent, returning any reversibly oxidised cysteines to their original state. These can then be irreversibly alkylated allowing derivatisation with a range of probes that facilitate

detection. Examples include probes detectable by fluorescence and immunoblot or probes that facilitates identification by mass spectrometry.

### 3.1.4 Protein carbonyls

Protein aldehydes and ketones are the most widely-used general oxidation marker. They are less prone to artefactual induction during cell lysis than thiol modifications and as they cannot be repaired chemically or enzymatically, they are effectively irreversible. Under non-stressed conditions, the basal level of protein carbonyls is around one for every ten proteins. During oxidative stress, this increases to around one in every three with deleterious consequences for cellular function(Stadtman & Levine 2001).

Carbonyls can form directly on susceptible side chains by reaction with RS. Metal catalysed oxidation (MCO), the combination of $H_2O_2$, Fe(II) and a reducing agent, is probably the most relevant in a biological setting. Lysine, arginine, proline and threonine residues are the most likely targets. Glutamic and aminoadipic semialdehydes (Figure 3.3), the products of arginine and proline, and lysine oxidation respectively, constitute 60% of carbonyls induced by MCO(Requena et al. 2001). Carbonyl formation is not limited to MCO and different carbonyl containing products can occur by direct reaction between $^1O_2$ and aromatic amino acids (Figure 3.3). The residues that are carbonylated by a given treatment is therefore determined by the specific oxidant (Temple et al. 2006).

Protein carbonyls can also be introduced indirectly *via* covalent adducts of bifunctional electrophiles derived from lipids and sugars. The altered proteins are known as advanced lipid peroxidation end products (ALEs) and advanced glycation end products respectively (AGEs). Levels of 4-HNE and MDA protein adducts (Figure 1.4), the most common ALEs, increase with a wide range of disease states(Negre-Salvayre et al. 2008). AGEs are especially indicative of hyperglycaemia in diabetics(Vistoli et al. 2013).

#### *3.1.4.1 Carbonyl Detection*

The carbon atom of protein carbonyls can be derivatised with an appropriate nucleophile (Figure 3.4). 2,4-dinitrophenylhydrazine (DNPH)(Levine et al. 1990), the first carbonyl probe to be developed is still routinely used. DNPH-derivatized proteins can be detected spectrophotometrically by absorbance at365nm or immunochemically using anti-DNP antibodies (the Oxyblot kit). The Oxyblot kit is by no means ideal. Identified concerns include loss of sensitivity on storage(P. Wang & Powell 2010), artefactual oxidation(S. Luo & Wehr 2009) and possible cross-reaction with sulfenic acids(Dalle-Donne et al. 2009). DNPH-derivatisation combined with mass spectrometry has been used to identify proteins carbonylated during various disease states(Pignatelli et al. 2001; Telci et al. 2000) (Cocciolo et al. 2012), as a product of aging(Breusing et al. 2009) or after oxidant treatment of cells(Bollineni et al. 2014).

In recent years, other carbonyl probes have become available. These include fluorophore and biotin conjugates. Fluorescent hydroxylamine (FHA) has been used in conjunction with mass spectrometry to identify oxidised proteins(Poon et al. 2004). It is superior to the Oxyblot because it avoids the need for immunoblotting. This permits the visualization of both oxidised and total protein content on a single gel. Biotin conjugates have been used to affinity purify carbonylated proteins prior to mass spectrometric identification(Madian & Regnier 2010).

Carbonylation of a protein is often correlated with inactivation but it is important not to conflate an increase in any given marker with functional significance. This was demonstrated by Jimenéz et al who showed that increased protein carbonyl content broadly correlated with inactivation of lysozyme but that oxidation of an active site tryptophan was actually the underlying cause(Jiménez et al. 2000).

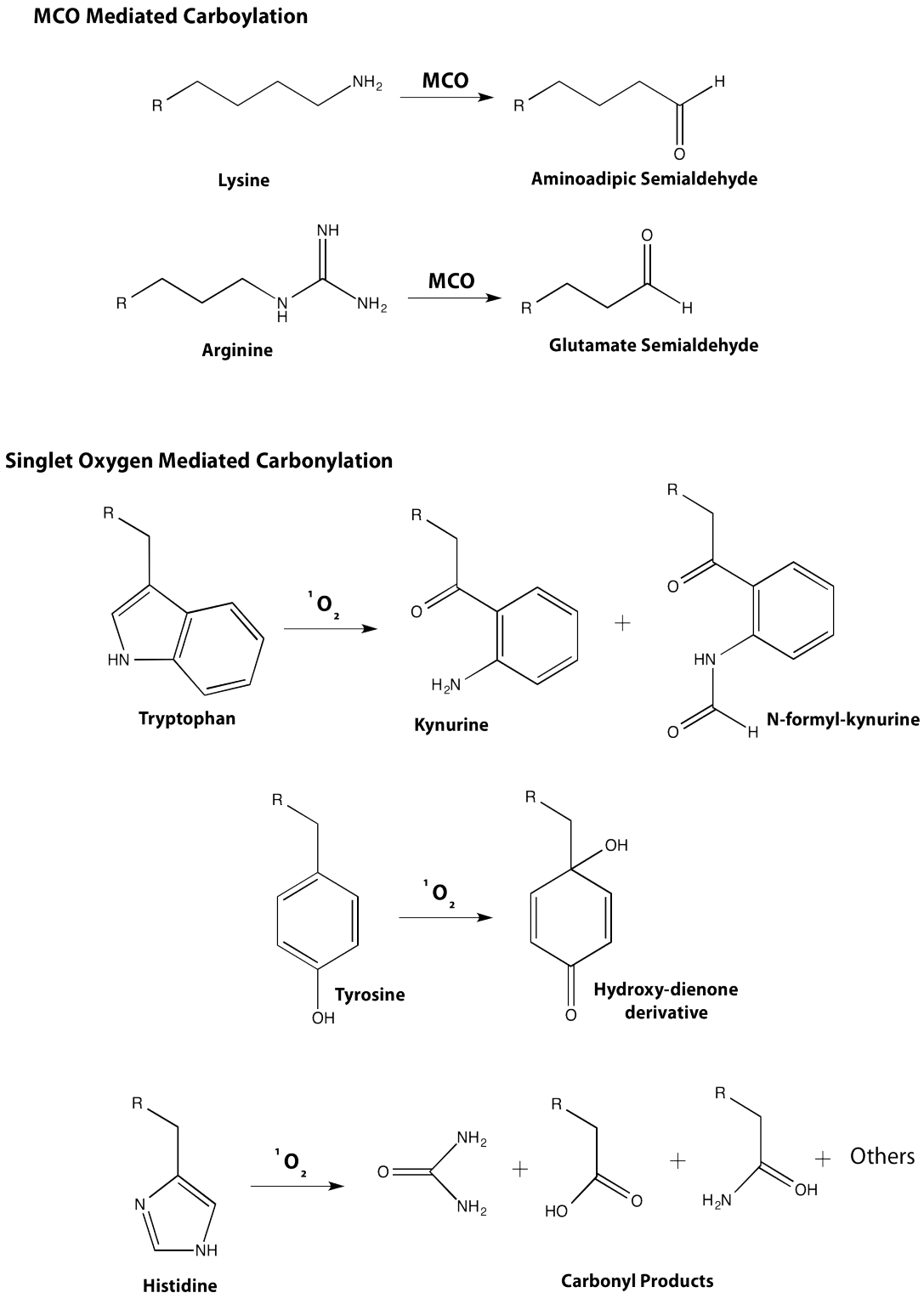


**Figure 3.3 Carbonylation by MCO and $^1O_2$.**
The two most common carbonyl products of MCO are shown although many others are possible. Glutamate semialdehyde can also result from proline oxidation. Carbonyl containing products on aromatic amino acids derive from the cycloaddition products shown in Figure 1.3

### 3.1.5 Protein oxidation by photosensitisers

Protein oxidation during PDT (Chapter 1.5.2) mainly results from the action of $^1O_2$ (M. J. Davies 2004). The main protein residues found to be oxidised after *in vitro* photosensitised reactions are the known targets of $^1O_2$: tryptophan, histidine, methionine and to a lesser extent tyrosine (Oleinick et al. 2009; Silvester et al. 1998). Protein carbonyls are formed, predominantly the oxidation products of aromatic amino acids (Silvester et al. 1998). These are the most commonly studied modifications in photosensitised cells(Szokalska et al. 2009; Sakharov et al. 2003; Tsaytler et al. 2008).

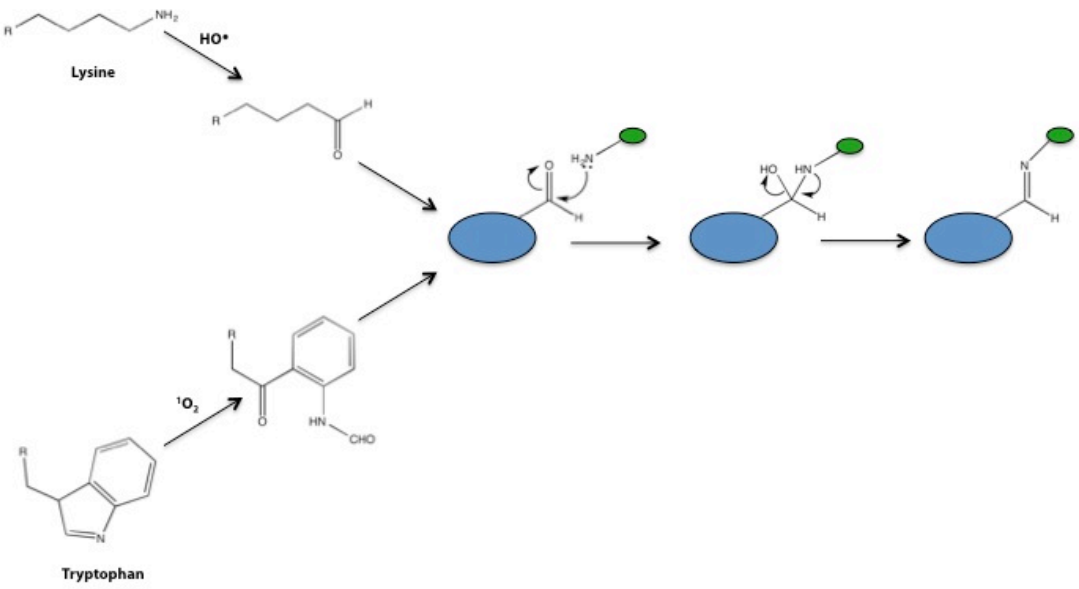


**Figure 3.4 Derivatisation of protein carbonyls.**
Protein carbonyls resulting from both MCO and $^1O_2$ can be derivatized with a nucleophilic probe (depicted in green). Nucleophilic nitrogen attacks the electrophilic carbonyl carbon resulting in covalent binding of the probe. Detection strategies include fluorescence, immunoblot and mass spectrometry.

Photosensitised reactions inactivate several enzymes including catalase, superoxide dismutases(J. Luo et al. 2006) and mitochondrial enzymes(Benov et al. 2010); Benov et al demonstrated the importance of photosensitiser subcellular localisation. Increasing

the lipophilicity of a porphyrin derivative causes localisation to membrane and results in enhanced phototoxicity. Photosensitisation can also induce widespread protein-protein crosslinking. This can occur between two histidines(Shen, Spikes, C. J. Smith & Kopeček 2000a), a histidine and a lysine (Shen et al. 1996) or two tyrosines(Shen, Spikes, C. J. Smith & Kopeček 2000b).

The purine analogue 6-thioguanine (6-TG) is a known photosensitiser(O'Donovan et al. 2005). At the inception of this study some of the photosensitised reactions of DNA 6-TG had been identified. Among these, photosensitized crosslinking of PCNA(Montaner et al. 2007) suggested that protein oxidation might be widespread and determining the extent of 6-TG/UVA-mediated protein oxidation was the initial focus of my project.

## 3.2 Results

I opted to focus on carbonylation as a marker of photosensitised protein oxidation. Carbonyls are also less susceptible than oxidized thiols to artefactual oxidation obviating the possible need for a low oxygen environment. Depending on exposed residues, any protein that is carbonylated is also likely to be subject to thiol oxidation. My aim at the outset was to develop a robust detection protocol that could be combined with two-dimensional polyacrylamide gel electrophoresis (2D-PAGE) and mass spectroscopy to identify putative oxidation targets in cultured human cells.

### 3.2.1 Detecting protein carbonyls

DNPH derivatisation combined with immunoblotting (Oxyblot kit) is the most widely used detection system for protein carbonyls. Based on my initial experience with this kit, I decided that derivatisation with fluorescent hydroxylamine (FHA) might offer a number of advantages. Firstly, fluorescent in-gel detection removes the need for blotting. Oxidised proteins can be identified and excised from a single gel thereby eliminating inter-gel variation as a potential source of error (matching spots between blotted and non-blotted gels is often problematic). The approach was a modification of

the method of Poon et al(Poon et al. 2007). The original study measured basal carbonyl levels but adapting the procedure to measure pathological RS resulting from photosensitisation seemed a realistic goal. By altering the procedure for use with FHA containing Alexa Fluor 647 rather than Alexa Fluor 488, I was able to use Sypro Ruby to stain for total protein, which is an order of magnitude more sensitive than the commonly used Coomasie Blue and more compatible with mass spectrometry than silver staining(Lopez et al. 2000). The excitation spectra (Figure 3.5) exhibit little overlap and essentially none at 633nm, the wavelength for AlexaFluor excitation.

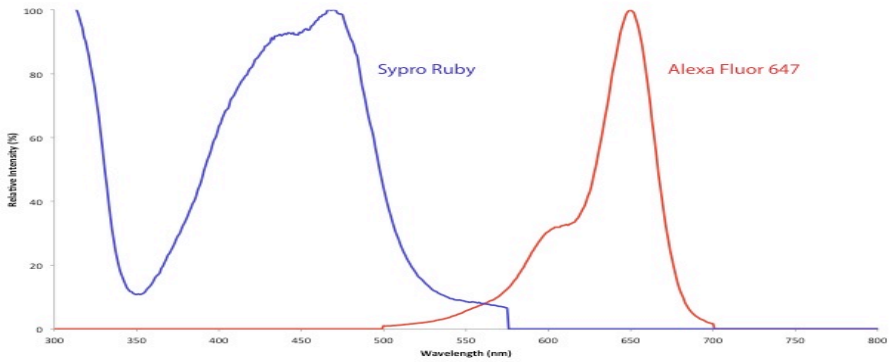


**Figure 3.5 Excitation spectra for Sypro Ruby and Alexa Fluor 647.**
Sypro Ruby shown in blue, Alexa Fluor 647 in red. Fluorophore data obtained from Invitrogen Spectraviewer (Invitrogen.com).

I optimised the reaction conditions for FHA derivatisation using bovine serum albumin (BSA) that had been oxidised *in vitro via* MCO (detailed in Materials and Methods). BSA treated with $NaBH_4$ to reduce all carbonyl groups to alcohols served as a negative control. Figure 3.6 (top) illustrates that FHA derivatisation of oxidized BSA produced a robust fluorescent signal. The sensitivity was comparable to that of the DNPH-based Oxyblot kit and the clear specificity for protein carbonyls was evidenced by the minimal response for reduced BSA. Refinements to the reaction conditions (Figure 3-6, bottom) improved the sensitivity still further and reduced the detection limit to considerably below that of the Oxyblot (<50ng of oxidised BSA). The optimised protocol of 0.05mg/ml (~40µM) FHA in PBS (pH7.4) at 37°C for 2 hours was used for all subsequent experiments. Another significant advantage of FHA over DNPH is that derivatisation does not need to be carried out in 1M HCl (which can affect protein

solubility) although lowering pH did improve sensitivity (data not shown). The compatibility of FHA with cell extracts and Sypro Ruby was examined (Figure 3-7). Extracts from 6-TG/UVA treated cells showed a strong signal indicating that the optimised protocol is compatible with cell extracts (Figure 3-7, left). No bleedthrough into the 633nm channel was observed reducing the likelihood of false positives. With a robust method for detecting both total protein and protein carbonyls in place, I then investigated the effects of UVA sensitization of 6-TG.

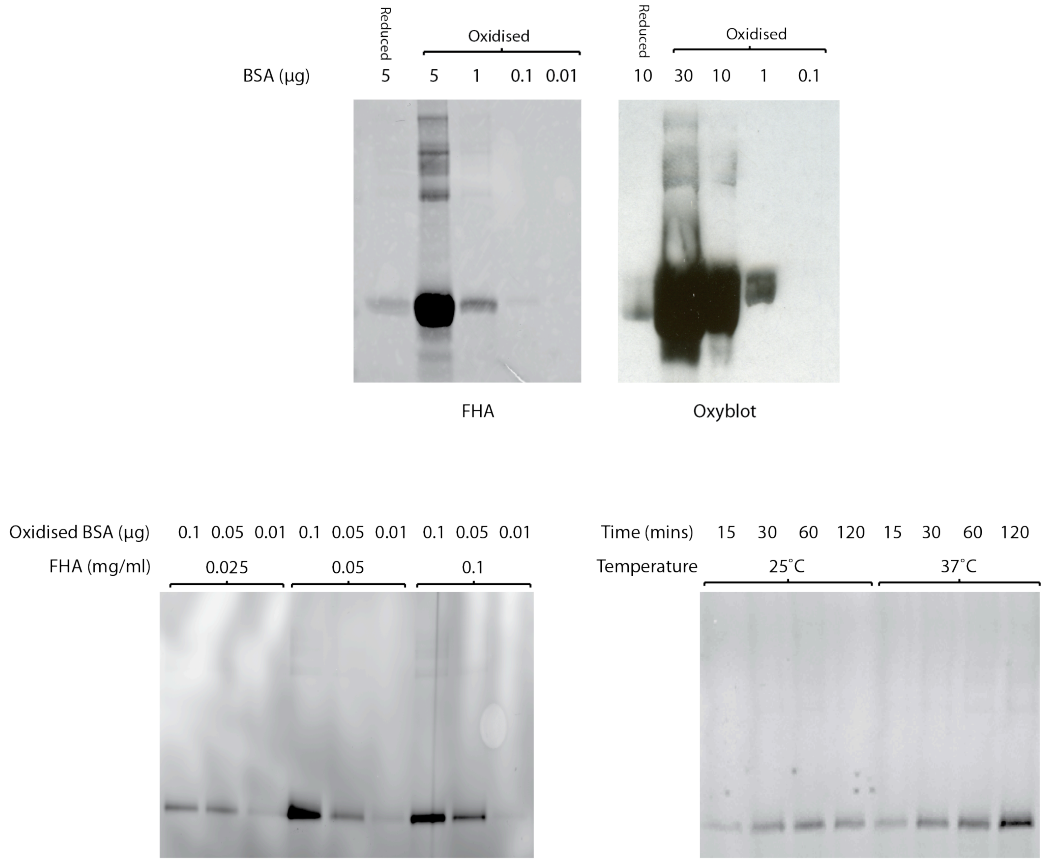


**Figure 3.6 Optimization of FHA derivatisation**

**Top:** BSA, oxidised *in vitro* as outlined in Materials and Methods, served as a model protein. BSA reduced with $NaBH_4$ was used as a negative control. Decreasing amounts of oxidised BSA were treated with 0.025mg/ml AlexaFluor647-fluorescent hydroxylamine (FHA, Invitrogen) for 120mins in PBS (pH7.4) at room temperature. Electrophoresis was performed and the gel (10% Bis-Tris) imaged at 633nm. A similar experiment performed using the Oxyblot kit (Millipore) following the manufacturer's protocol is provided for comparison. **Bottom, left**: Decreasing amounts of oxidised BSA were treated as above over a range of FHA concentrations. **Bottom, right:** 0.05 µg oxidised BSA was treated with 0.05mg/ml FHA at 25 or 37°C over a range of incubation times.

### 3.2.2 The effects of 6-TG/UVA on carbonylation

CCRF-CEM (CEM) cells that had been grown in the presence of 6-TG were UVA irradiated. Whole cell extracts were treated with FHA according to the conditions established in Section 3.2.1 and derivatised proteins separated by SDS-PAGE. Gels were stained with Sypro Ruby and scanned at 633nm and 488nm concurrently. Figure 3.7 (right) demonstrates a 6-TG- and UVA-dependent increase in protein carbonyls. There is some background derivatisation in extracts from untreated cells. This presumably reflects the steady-state level of protein carbonylation. It was not increased significantly by this UVA dose (20kJ/m$^2$) although higher doses of UVA (>100kJ/m$^2$) do induce detectable carbonylation (not shown). Treatment with the highest 6-TG dose (0.75 µM) increased carbonylation slightly but the effect of 6-TG and UVA are clearly more than additive. The azide ion ($N_3^-$) is a known $^1O_2$ scavenger(Klotz et al. 2003). Preincubation with sodium azide prior to irradiation induces a loss of FHA signal suggesting carbonylation is $^1O_2$-mediated (Figure 3.8).

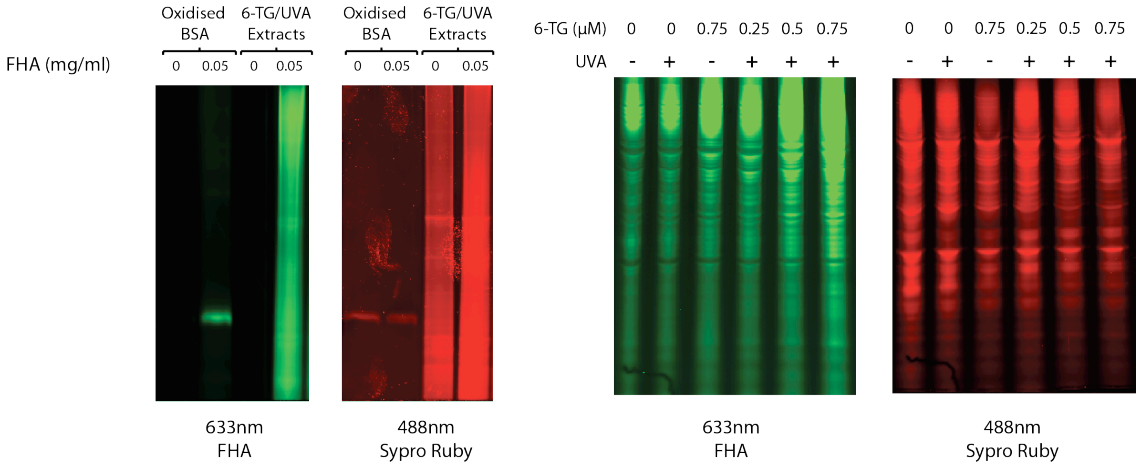


**Figure 3.7: Protein carbonylation induced by 6-TG/UVA treatment**
**Left:** Oxidised BSA (0.05µg) and extracts from cells treated with 6-TG (1µM/24h) and UVA (20kJ/m$^2$) were treated using the optimised FHA protocol. Samples were subject to SDS-PAGE and gels were scanned at 633nm and 488nm concurrently. The FHA and Sypro Ruby signals are shown in green and red respectively. **Right:** CEM cells were treated with 6-TG (24h) at the indicated doses and UVA irradiated (20kJ/m$^2$) as indicated. Cell extracts were prepared, derivatised with FHA and processed as above.

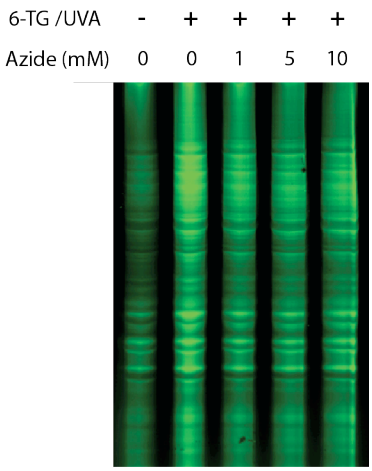


**Figure 3.8 Treatment with azide reduces carbonylation by 6-TG/UVA**
CEM cells were treated with 6-TG (0.6µM/24h) and UVA (20 kJ/m$^2$) or left untreated. Prior to irradiation, cells were incubated with $NaN_3$ in PBS at the indicated concentration for 10 minutes.

### 3.2.3 Thiol oxidation

Reversible thiol oxidation was investigated using the "switch" methodology outlined in Figure 3.2. The protocol was based on Baty et al (Baty et al. 2002) with the inclusion of a Sypro Ruby-compatible detection reagent. Briefly, treated cells are incubated with N-ethylmaleimide (NEM). This cell-permeable alkylating agent blocks all free SH groups prior to cell lysis. Following cell lysis, all oxidized thiols - disulphides and sulfenates - are reduced with dithiothreitol and then derivatised with Alexa Fluor 647 maleimide (AFM). The samples are then processed as for carbonyl detection. Figure 3-9 (left) shows that 6-TG/UVA significantly increased the level of thiol oxidation. Thus, my experiments reveal that, by the two commonly used criteria of oxidative protein damage, carbonylation and thiol oxidation, UVA sensitized 6-TG is a significant threat to the proteome.

In Figure 3.9 (left), it is apparent that widespread thiol oxidation coincided with reduced Sypro Ruby signal indicating protein loss during processing, probably due to precipitation. A titration of AFM concentrations (Figure 3.9, right) confirmed that protein losses were proportional to the extent of thiol derivatisation. This drawback meant that the technique was not pursued further but the approach clearly provides a

clear qualitative indication of widespread thiol oxidation by this photosensitizing treatment.

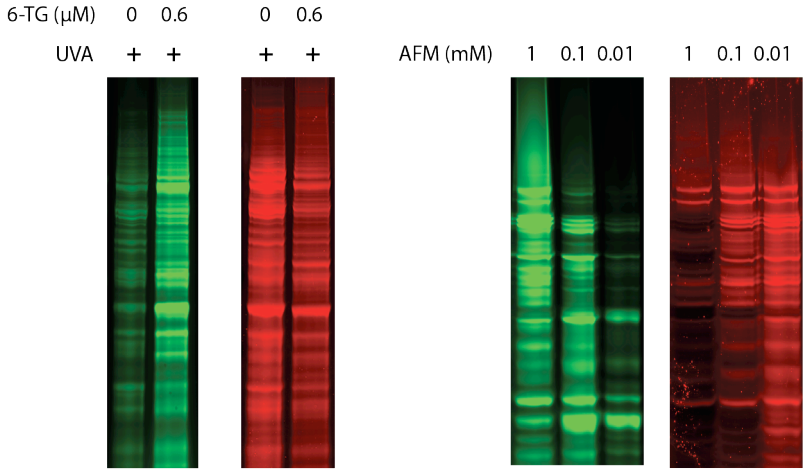


**Figure 3.9 Detecting thiol oxidation**
**Left:** CEM cells were treated with 6-TG (0.6μM) for 24 hours and irradiated with UVA (20kJ/m$^2$) as indicated. Cells were then processed according to the AFM protocol (Materials and Methods). **Right:** NEM-blocked, DTT-reduced extracts from 6-TG/UVA treated cells were incubated with decreasing amounts of AFM and then processed according to the standard protocol.

### 3.2.4 Identification of carbonylated proteins

Extracts from 6-TG/UVA treated cells were separated by 2D-PAGE in order to identify individual carbonylated proteins. Figure 3.10 shows the gel image of one of three independent experiments in which untreated and 6-TG/UVA treated cell extracts are compared.

FHA derivatisation appeared to be broadly compatible with 2D-PAGE (Figure 3.10) and indicated the presence of relatively few oxidized proteins (green spots) in the untreated or UVA treated extract. Inspection of the gel from the 6-TG/UVA treated extracts revealed an increase in FHA signal as expected but a number of issues were apparent. Most obviously, treatment was associated with vertical and horizontal streaking, which reflects protein precipitation during electrophoresis and incomplete isoelectric focusing, respectively. This made spot location and comparison between replicates less straightforward than anticipated. Mass spectrometry analysis (carried out by Dr David Frith of the Proteins and Proteomics Department, Clare Hall) of protein spots excised from the 2D gels revealed that they were frequently heterogeneous,

possibly resulting from deposition of aggregated proteins and/or inaccurate excision. Since streaking was only observed in extracts from treated cells, it seems likely that the intrinsic inferior solubility of carbonylated proteins exacerbated by derivatisation with a bulky chromophore is responsible for the precipitation. Furthermore, the presence of unincorporated FHA in the sample may prevent proper isoelectric focussing.

MS analysis of the excised FHA fluorescent spots identified the presence of numerous proteins with >80% certainty. RPA32 and p53 were identified in all three replicate analyses whilst RPA70, Ku70, MCM4 and PCNA were identified in two of the three. Although clearly not optimal, this approach identified DNA repair/replication-associated proteins (including PCNA that was known to be damaged by this treatment). At this point, I elected to focus on the effects of photosensitisation on these identified proteins rather than to further refine the 2D gel procedure.

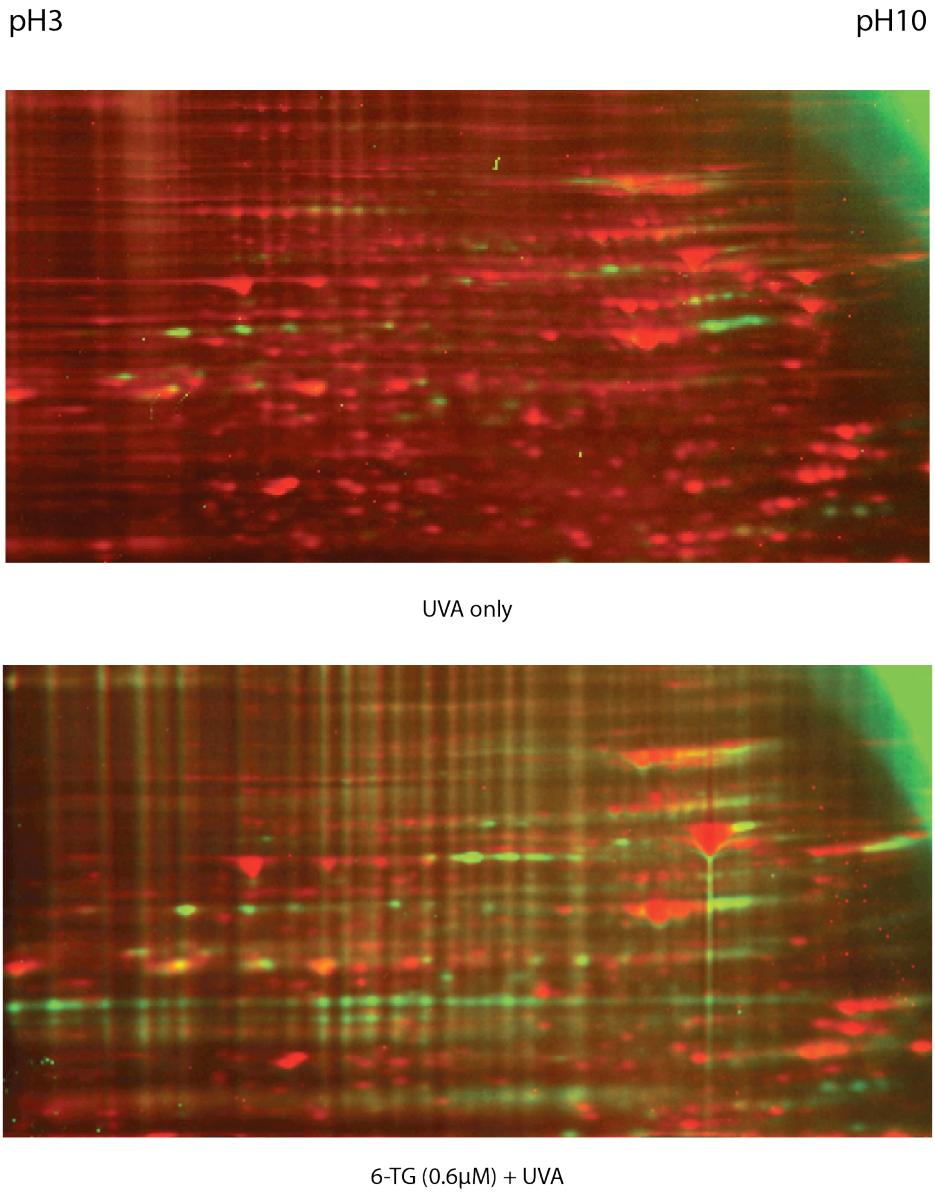


**Figure 3.10 Two dimensional gel electrophoresis of the FHA treated samples**
Samples were FHA derivatised and subjected to 2D-PAGE as outlined in Materials and Methods. FHA spots were excised and analysed by mass spectrometry. This an example of one of three replicates. **Top:** UVA (20 kJ/m$^2$) **Bottom:** 6-TG (0.6µM, 24h) plus20 kJ/m$^2$.

### 3.2.5 Ku oxidation

Western blot analysis of identified proteins Ku70, MCM4 and RPA32 revealed the presence of treatment-dependent slower migrating species in each case (Figure 3.11). The subunits adjacent to MCM4 in the MCM complex (MCMs 6 and 7) exhibited a similar migration pattern strongly suggesting the formation of inter-subunit crosslinks. Due to its abundance and important role in DNA repair, I chose to investigate the effects of 6-TG/UVA on the Ku protein complex. Western blot analysis revealed that the slowly migrating forms of Ku70 cross-reacted with a monoclonal Ku80 antibody indicating that both partners of the Ku complex were present (Figure 3.12).

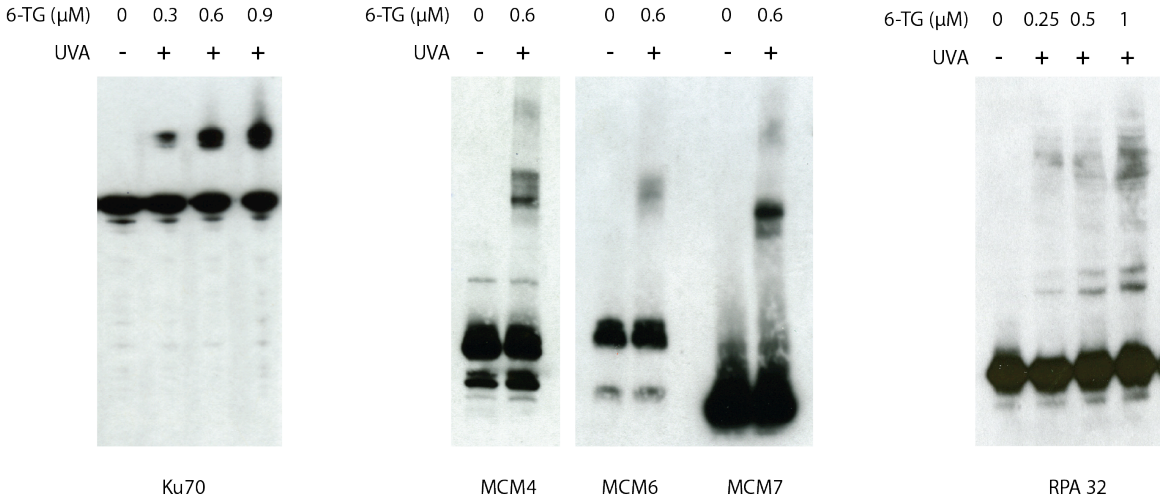


**Figure 3.11 Effects of 6-TG/UVA on identified proteins from 2D gels**
Cells were treated with 6-TG and irradiated with UVA (20kJ/m$^2$) as indicated. Extracts were analysed by western blotting **Left:** CEM cell extracts Ku70 probe **Centre:** MCM4/6 or 7 probes as indicated **Right:** RPA 32 probe (performed by Melisa Guven).

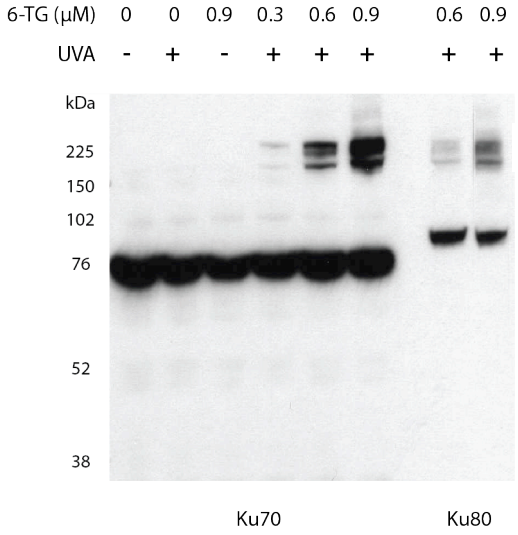


**Figure 3.12 Crosslinking of the Ku Complex**
CEM cells were treated with 6-TG(24h) and irradiated with UVA (20kJ/m$^2$) as indicated. Cell extracts were prepared and analysed by western blot with Ku70 or Ku 80 probe as indicated.

The complexes were resistant to the denaturing conditions in western blot sample preparation (100mM DTT, 5 mins, 95°). This rules out S-S formation and suggests crosslinking is covalent. The mass as judged by molecular weight markers is approximately the size of the sum of the Ku70 and Ku80 subunits. I concluded that the complexes represent covalent crosslinking of the subunits of the Ku heterodimer. The crosslinked species decreased with time, suggesting proteolytic degradation (Figure 3.13).

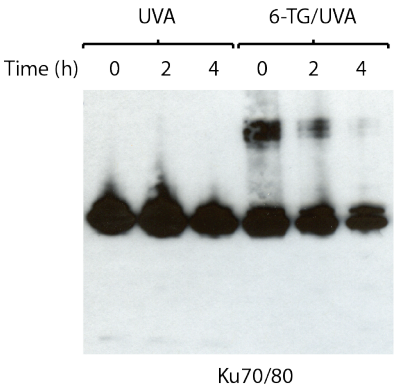


**Figure 3.13 Persistence of Ku crosslinking**
CEM cells were UVA (20 kJ/m$^2$) irradiated with or without 24h 6-TG (0.6μM) treatment. Cell extracts were prepared at the indicated time after irradiation and analysed by western blot with a Ku70/80 antibody.

The functional impact of photochemical Ku damage was explored. An electrophoretic mobility shift assay (EMSA) using a radiolabelled dsDNA probe and extracts from 6-

TG/UVA treated cells indicated that Ku-mediated DNA binding was impaired in a 6-TG concentration-dependent manner (Figure 3.14, top).

The EMSA was validated and the Ku dependence of binding was confirmed in two ways. Firstly, anti-Ku antibody induced a supershift of the entire complex (Figure 3.14, middle left). Secondly, the complex was not observed when extracts from the Ku80 deficient xrs6 cell line were used (Figure 3.14, middle right). In addition, when recombinant Ku70:80 was incubated with 6-TG and UVA irradiated *in vitro* it was also crosslinked (Figure 3.14, bottom left). *In vitro* Ku crosslinking was also associated with reduced DNA binding activity (Figure 3.14, bottom right).

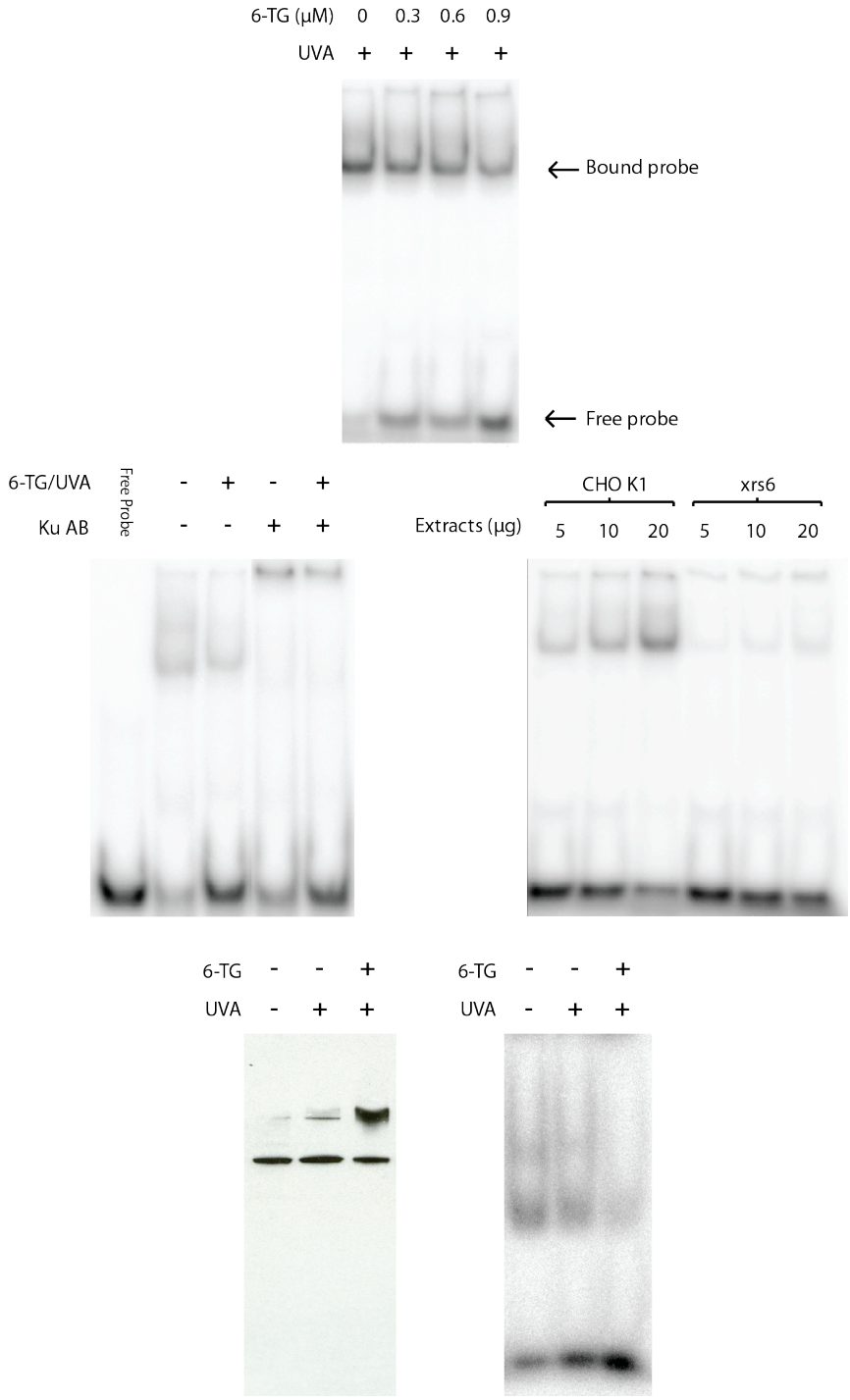


**Figure 3.14 Electrophoretic mobility shift assays of Ku binding.**
**Top:** CEM cells were treated with 6-TG as indicated and UVA irradiated (20kJ/m$^2$). Extracts were prepared and EMSA performed (see Materials and Methods). **Middle, left:** Cell were treated with 6-TG/UVA (0.6μM/20kJ/m$^2$). Extracts were prepared and EMSA was performed following a 10-minute incubation with polyclonal Ku70/80 antibody (Stratech, 1μl) prior to electrophoresis. **Middle, right:** EMSA analysis of extracts from the Ku80 deficient hamster cell line xrs6 and its parent cell line CHO K1. **Bottom, left:** Western blot analysis of recombinant Ku70/80 (Trevigen) treated with UVA (20kJ/m$^2$) or 6-TG(100μM) and UVA. **Bottom, right:** EMSA analysis of the 6-TG/UVA treated recombinant Ku samples

### 3.2.6 Ku damage and NHEJ

The Ku heterodimer is an essential component of non-homologous end joining (NHEJ), the major pathway of DNA double strand break repair. The effect of 6-TG/UVA on NHEJ activity was examined. Cell extracts prepared by freeze-thaw lysis were incubated with an end-radiolabelled, linearised 5237bp plasmid probe. Products of ligation were separated by agarose gel electrophoresis and detected by autoradiography. In the first instance, I determined the optimum ratio of DNA probe to cell extract for NHEJ activity (Figure 3.15, top) Based on these data, 10 fmol radiolabelled DNA with 20μg extract were used for the remaining experiments.

Since the DNA probe contains complementary ends, a number of steps were taken to ensure that the assay reflected true NHEJ and not simple plasmid recircularisation. Wortmannin, an inhibitor of DNA-PKcs(M. Hashimoto et al. 2003), inhibited oligomerisation in a dose-dependent fashion. (Figure 3.15, middle left). Incubation of the probe with T4 DNA ligase generated a distinct pattern of ligation products compatible with expected recicularisation (Figure 3.15, middle right). Finally, depletion of Ku70 via immunoprecipitation abolished NHEJ activity confirming that the assay is Ku dependent (Figure 3.15, bottom). The assay therefore provides a true reflection of the NHEJ capacity of the extracts.

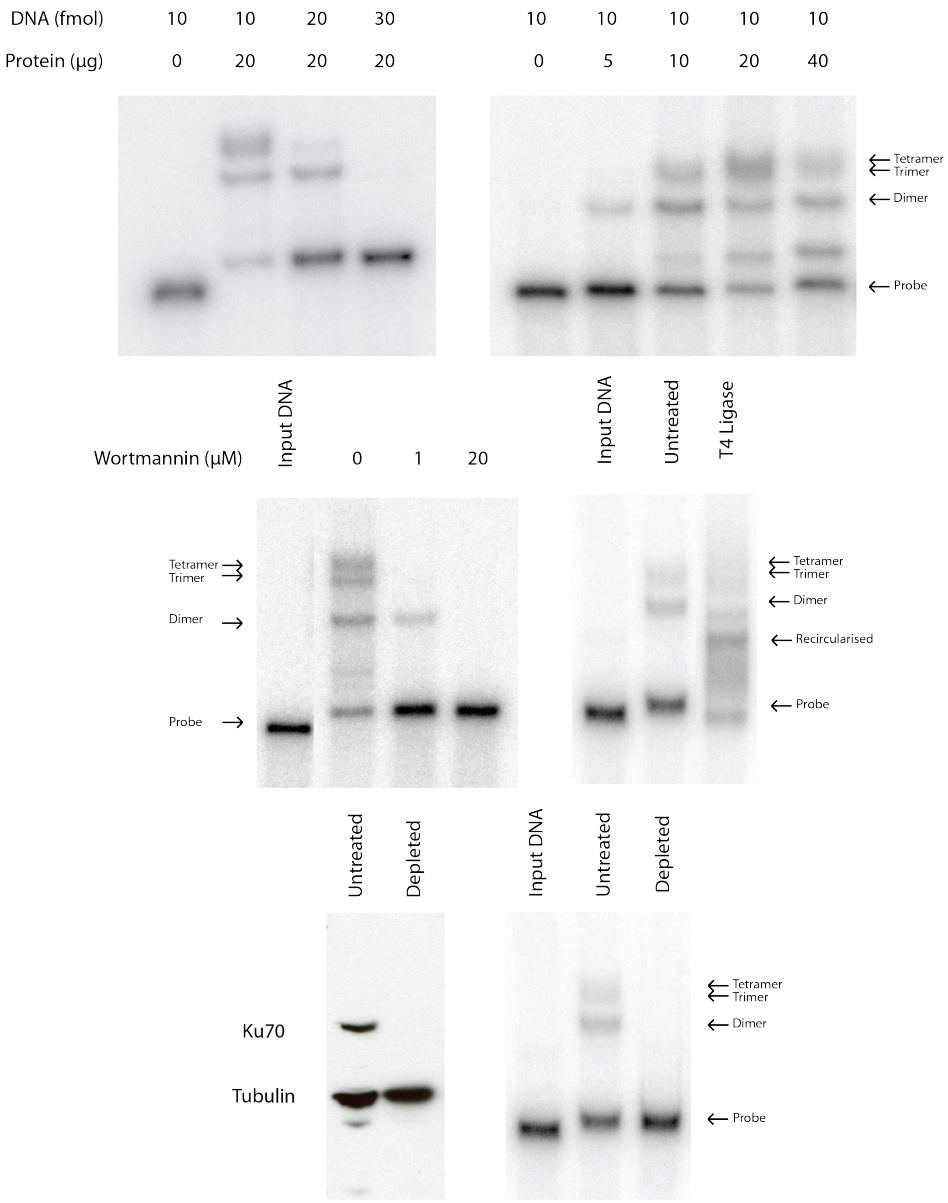


**Figure 3.15 Optimisation and validation of the NHEJ assay**
**Top:** Optimising DNA protein ratios. Extracts from untreated CEM cells were combined with end-radiolabelled linearized plasmid DNA as indicated. Following incubation, end-joined products were separated by agarose gel electrophoresis and detected by autoradiography. Ligation products are indicated. **Middle, left:** Inhibition by wortmannin. Wortmannin was included in the NHEJ assay at the concentrations shown. **Middle, right:** Recircularisation by T4 DNA ligase. **Bottom, Left:** Ku was removed from CEM extracts by immunoprecipitation with a polyclonal Ku70/80 antibody. Ku depletion was verified by western blotting. **Bottom, right:** NHEJ was assayed in non-depleted and Ku depleted extracts as indicated.

Extracts prepared from CEM cells treated with 6-TG (0.1μM) and UVA (20kJ/m$^2$) were deficient in NHEJ whereas extracts from cells treated with either this low 6-TG concentration or UVA alone were fully NHEJ-proficient (Figure 3.16, left). Following treatment with 6-TG concentrations higher than 0.1μM TG, NHEJ activity was reduced, even in the absence of UVA irradiation (Figure 3.16, right). Thus the dynamic range for this assay as a test for photosensitisation is rather small.

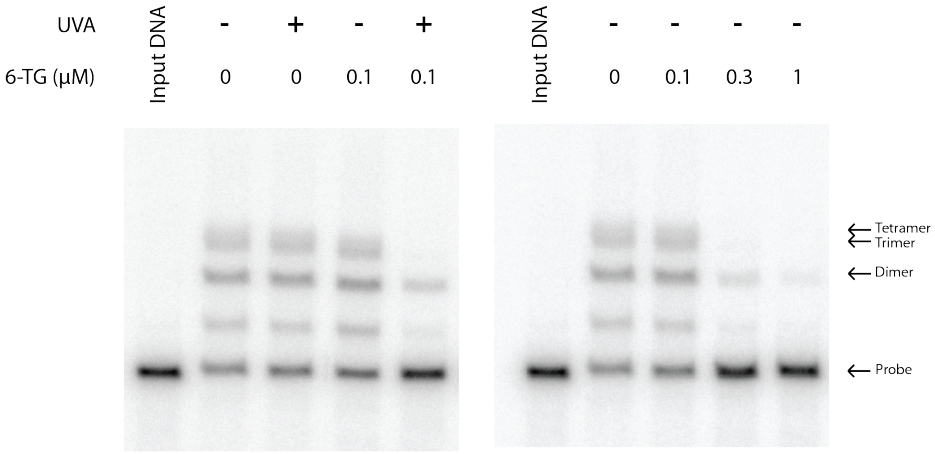


**Figure 3.16 The effect of 6-TG/UVA on NHEJ *in vitro***
Extracts were prepared from CEM cells treated with 6-TG at the indicated concentrations (24h) with and without UVA (20kJ/m$^2$) irradiation. The NHEJ assay was performed as described in Materials and Methods.

Defective NHEJ in cell extracts could be complemented by the addition of recombinant Ku and full end-joining activity was restored (Figure 3.17, left ). High Ku concentrations were inhibitory, however. Addition of Ku to extracts from untreated cells also slightly stimulated end-joining activity (Figure 3.17, right). This rather surprising observation suggests that, despite its abundance, Ku may be limiting for end-joining in this *in vitro* assay

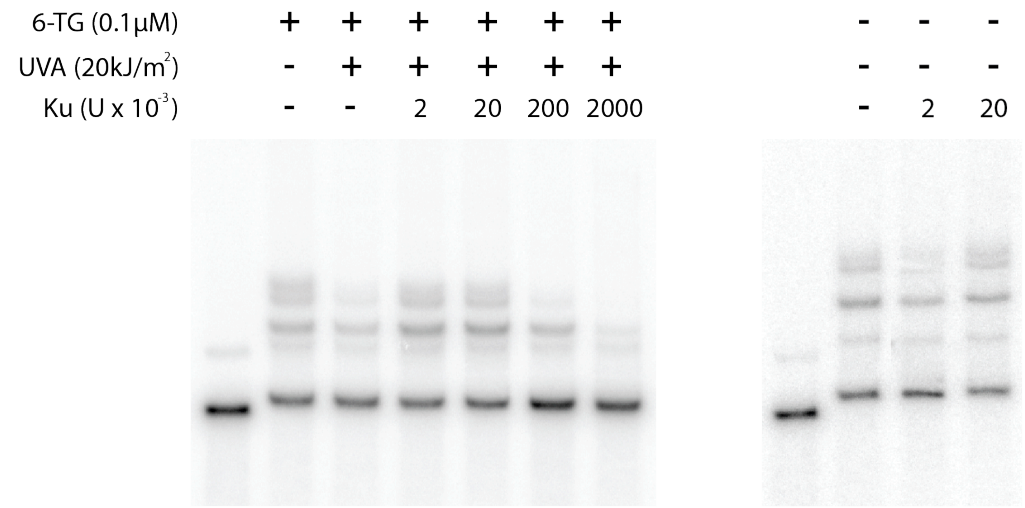


**Figure 3.17 Complementation of *in vitro* NHEJ.**
NHEJ extracts were prepared from CEM cells treated with 6-TG and UVA (20kJ/m$^2$) as indicated. **Left:** treated, **right:** untreated. NHEJ activity was assayed with the addition of recombinant Ku70/80 (Trevigen) at the indicated amounts**.**

## 3.3 Discussion

### 3.3.1 Detecting protein oxidation

The protocol I devised for FHA derivatisation offers a number of advantages over the more commonly used DNPH-based immunoblot (Oxyblot kit). These include: in-gel detection, Sypro Ruby compatibility, neutral derivatisation conditions and simpler sample processing (no need for neutralisation). In its current form, the procedure provides a sensitive and reproducible indication of protein carbonylation when used with one-dimensional electrophoresis. The problems that became evident upon application to 2D-PAGE may be tractable and possible solutions will be discussed below.

### 3.3.2 FHA and 2D-PAGE

Protein insolubility leading to gel streaking and a negative impact on experiment repeatability are frequently reported problems in 2D-PAGE analysis of carbonylated

proteins(Baraibar et al. 2013). Although FHA was used successfully to measure basal levels of oxidation in mouse brain(Poon et al. 2007), it is possible that this analysis is not appropriate for more severely oxidised samples. FHA is a fairly large molecule (~1200Mw) that carries a negative charge and as such its presence will affect both isoelectric focussing and gel migration. This problem will be particularly acute if multiple FHAs are bound to a single protein. This is a possible explanation for the identification of multiple proteins in a single spot in my experiments.

Due to this limitation, no FHA spot can be reliably attributed to an individual protein and therefore its oxidation status cannot be assessed by this technique. The observed modifications to Ku70, MCM4, RPA32 and PCNA by photosensitization provide a retrospective validation of their identification. However, the majority of proteins identified are among the most abundant proteins in the cell according to a recent quantitative analysis of a human cell line(Beck et al. 2011). PCNA and Ku70 are 96$^{th}$ and 115$^{th}$ in a list of over 7000 proteins organised by abundance; each is present at over 1 x $10^6$ copies per cell and therefore their identification could be entirely serendipitous. An unbiased and validated list of proteins damaged by the action of photosensitisers may be a useful tool in understanding their effects. Populating this list would have been a significant investment of time and effort and my preferred approach was rather to investigate possible functional consequences of tentatively identified oxidation changes.

I have considered a number of alternative approaches to alleviate these problems. A recent study by Tamarit et al (Tamarit et al. 2012) used a BODIPY hydrazide conjugate, to study proteins carbonylated after $H_2O_2$ treatment of yeast. BODIPY is a relatively small fluorophore with no net charge and its derivatisation results in greatly improved spot alignment.

In principle, derivatisation with a biotinylated probe followed by affinity purification offers the best approach since the use of gels is avoided entirely. A reagent originally designed for labelling abasic sites in DNA, aldehyde reactive probe (ARP), has been used to purify and identify carbonylated proteins resulting from MCO in rat mitochondria(Chavez et al. 2010). In addition to permitting enrichment of oxidised

proteins, detection of ARP-containing fragments during mass spectroscopic analysis can identify specific carbonylation sites. Using ARP I was able to confirm the 6-TG/UVA-induced increase in carbonylation (Figure 3.18). Although further attempts at enrichment were hindered by excessive non-specific binding and these efforts were discontinued, these problems appear to be tractable.

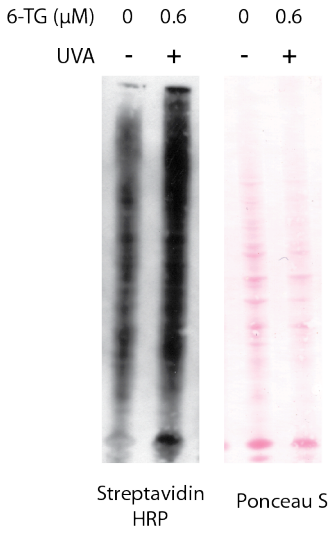


**Figure 3.18 ARP derivatisation**
Extracts from 6-TG/UVA treated and untreated cells were derivatised with ARP (Materials and methods) and separated using SDS-PAGE. After blotting, proteins carrying ARP were detected using Streptavidin-HRP. Ponceau S detected total protein content.

### 3.3.3 6-TG/UVA and protein carbonylation

6-TG-induced protein carbonylation was essentially all UVA dependent within the normal working dose range. High 6-TG doses (≥ 0.75 μM) induced a small increase in protein damage. This might reflect oxidative stress induced in the absence of UVA(Brem & Karran 2012).

6-TG can photosensitise via type I and type II mechanisms(O'Donovan et al. 2005). $O_2^{-\bullet}$ and $H_2O_2$ resulting from type I photosensitisation are unable to induce carbonylation directly and any type I-mediated carbonylation is probably via HO•. The most probable mechanism is MCO with its intrinsic preference for carbonyl formation at arginine, lysine, proline and threonine. (HO• does react with other amino acids but mainly forms hydroxy-addition products with aliphatic and aromatic side chains).

Singlet oxygen (type II) is significantly reactive with only five amino acids: cysteine, methionine, tryptophan, histidine and tyrosine(M. J. Davies 2003) (Table 3-1). Carbonyls will form predominantly from oxidation of tryptophan, histidine and tyrosine. Although $^1O_2$ is much less reactive than HO•, its greater lifetime and consequent ability to diffuse far greater distances compensate for its reduced activity and $^1O_2$ poses a major threat to cellular proteins. The oxidising species could subtly affect response to carbonyl derivatisation as MCO will mainly induce aldehydes, which are more electrophilic than the ketone products of $^1O_2$ oxidation. Figure 3-8 shows a decrease of FHA signal after incubation with sodium azide prior to irradiation. This suggests that carbonylation is at least in part $^1O_2$-mediated although levels do not return to those of untreated cells. Whether this represents a type I component to carbonylation or incomplete scavenging cannot be determined from this experiment, although increasing the dose ten-fold had no effect which supports the former conclusion.

| | **Rate Constant for Reaction ($M^{-1}$ $s^{-1}$)** | |
|---|---|---|
| **Residue** | **$^1O_2$** | **HO•** |
| Histidine | $3.2 \times 10^7$ | $4.8 \times 10^9$ |
| Tryptophan | $3.0 \times 10^7$ | $1.3 \times 10^{10}$ |
| Methionine | $1.6 \times 10^7$ | $8.5 \times 10^9$ |
| Tyrosine | $0.8 \times 10^7$ | $1.3 \times 10^{10}$ |
| Cysteine | $8.9 \times 10^6$ | $3.5 \times 10^{10}$ |
| Arginine | - | $3.5 \times 10^9$ |
| Proline | - | $6.5 \times 10^8$ |
| Threonine | - | $5.1 \times 10^8$ |
| Lysine | - | $3.5 \times 10^8$ |

**Table 3-1: Rate constants for reaction of selected amino acids with $^1O_2$ and HO•**
$^1O_2$ data reproduced from Davies et al(M. J. Davies 2003) . HO• reproduced from Xu and Chance(Xu & M. R. Chance 2007)

My experiments do not exclude the possibility of 6-TG/UVA-induced secondary carbonyl formation ALEs and AGEs. $^1O_2$ lifetime is increased in the non-aqueous environment of the lipid bilayer and it is known to be a potent inducer of peroxidation(Gaboriau et al. 1995). Specific antibodies for MDA and 4-HNE protein adducts could address this possibility.

To summarise, for standard SDS-PAGE, this protocol offers numerous advantages over the more commonly used DNPH-derivatisation and is a simple, specific way to demonstrate treatment-related increases in protein carbonylation. My adaptation of existing an FHA protocol for use with Sypro Ruby makes it simple to assess total and oxidised protein levels concurrently.

### 3.3.4 Thiol oxidation

My data indicate that, as expected, thiol oxidation occurs concurrently with carbonyl formation in cells treated with 6-TG/UVA. Oxidized thiol detection therefore provided an approach to measuring the effects of oxidative stress. Although somewhat limited as an analytical tool, visualisation of oxidized thiols highlighted another facet of protein oxidation. Heavily oxidised proteins bearing sulfinate and sulfonate modifications would not give a fluorescent signal as they cannot be reduced (see Figure 3.2) which could limit the utility of thiol oxidation to studying harsh oxidising conditions.

### 3.3.5 Ku oxidation

The covalently crosslinked forms of Ku were visualised as a series of proteins with apparent molecular weights of around 200 kDa all of which contained both Ku70 and Ku80. This is larger than the ~150 kDa expected for the Ku heterodimer. Their migration properties might reflect a non-linear (possibly multiply) crosslinked structure with anomalous electrophoretic properties. The involvement of another unidentified crosslinked protein, whilst possible, seems less likely.

Sitte et al(Sitte et al. 1998) demonstrated that oxidized proteins are removed by the 20S proteasome. I observed a reduction in the crosslinked species with time after irradiation consistent with the degradation of oxidised protein. High carbonylation levels are associated with attenuated proteasomal activity although the underlying mechanism is currently unclear. Possibilities include inhibition of the proteasome by crosslinked proteins or direct damage to proteasomal factors; alternatively, high levels of carbonylation may be a symptom rather than a cause of proteasome inhibition.

6-TG/UVA treatment is a known source of $^1O_2$ and hence aromatic amino acids will be preferentially oxidised. One of the products of histidine oxidation by $^1O_2$, a hydroxyimidazolone is susceptible to nucleophilic attack at C5 (Figure 3.19). Visual inspection of the crystal structure of the Ku heterodimer suggests a number of potential crosslinking sites. Most obvious are the three Ku70 lysine-Ku80 histidine pairs (highlighted in Figure 3.20, inset). A Ku70 histidine-Ku80 lysine pair, a histidine-histidine pair and a tyrosine-tyrosine pair (not shown) could also potentially react. (Since HO• can also form this product with histidine(Xu & M. R. Chance 2007), type I photosensitisation could also induce crosslinking although there is a high probability that HO• would be intercepted before reaching the susceptible amino acid). In sum, there are several plausible sites at which photochemical crosslinking between these two subunits might occur.

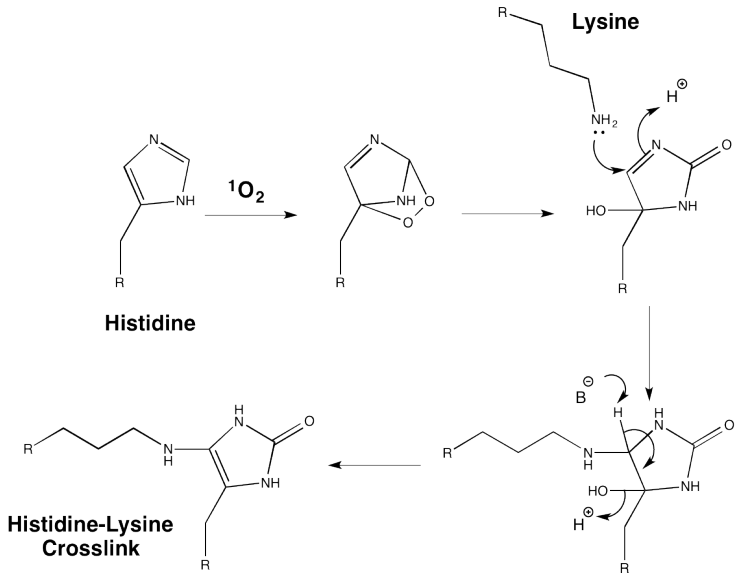


**Figure 3.19 Mechanism of histidine-lysine crosslink formation mediated by $^1O_2$.**
Histidine forms a short-lived endoperoxide upon attack by $^1O_2$ that rearranges to give a hydroxy-imidazolone species. This is a target for nucleophilic addition (lysine is shown here but histidine or cysteine could substitute). Water is eliminated from the addition product to give the stable covalent crosslink.

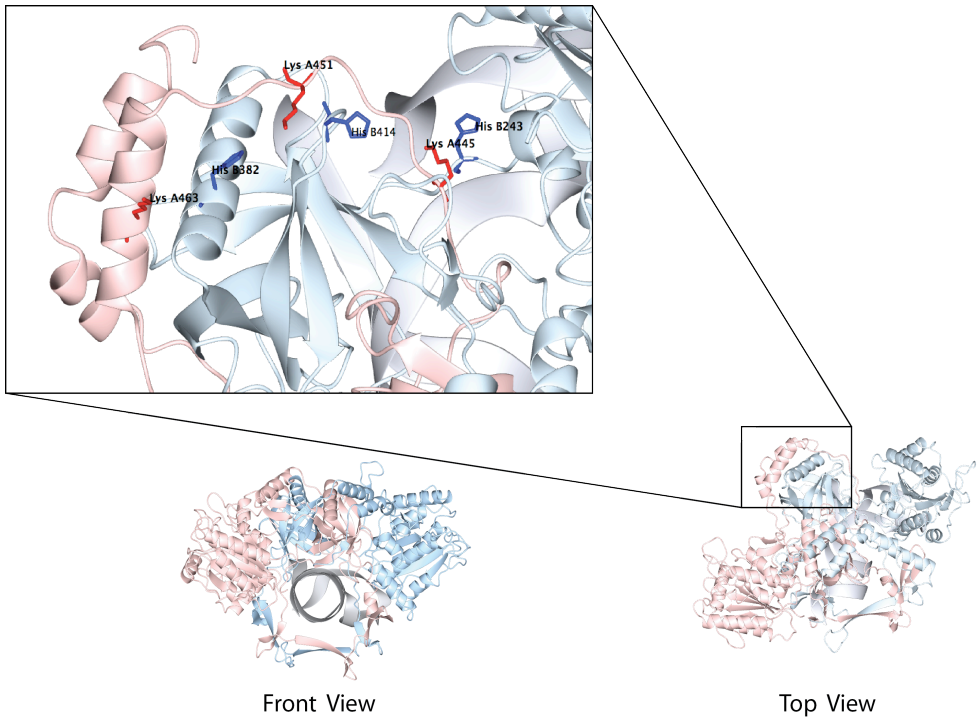


**Figure 3.20 Ku heterodimer structure with highlighted candidate residues for crosslinking.**

3D model of Ku bound to DNA. Ku 70 is shown in pink and Ku80 in blue. **Inset**: Spatially proximate lysines (Ku70) and histidines (Ku80) are highlighted in red or blue respectively. Crystal structure from Walker et al (Walker et al. 2001). Image rendered using CCP4mg (McNicholas et al. 2011).

Ku was identified as a target for sulfenate modifications(Leonard et al. 2009) and in keeping with this its DNA binding activity is regulated by oxidation(Andrews et al. 2006). Oxidation of thiols by diamide causes a conformational change that increases $k_{off}$ rates thereby reducing DNA binding. The oxidised thiol(s) that triggers the switch is not known although cysteine 249 is the current leading candidate (Dolan et al. 2013). It is therefore likely that crosslinked Ku is symptomatic of inactivation rather than uniquely causative and that inactivation could plausibly occur before crosslinked Ku is detectable.

Attenuated Ku binding could result in promotion of alt-NHEJ with mutagenic consequences. Oxidative stress reduces the assembly of DNA-PK at DNA ends with a consequent inhibition of NHEJ (Bacsi et al. 2005) –an observation that is consistent with Ku damage and reduced end-binding. Remarkably, other DNA repair proteins including OGG1(Bravard et al. 2006), RPA(Men et al. 2007), MGMT and XRCC3(Girard et al. 2013) are also inactivated by thiol oxidation and experiments from this laboratory have shown that OGG1 activity is lower in extracts from cells treated with 6-TG/UVA ((Gueranger et al. 2014)). Quite why this functional vulnerability has evolved is unclear as it would appear antithetical to an efficient DNA damage response.

### 3.3.6 Ku damage and NHEJ

Having identified Ku as target of oxidative damage, I was prompted to examine NHEJ which was achieved using an *in vitro* extract-based assay, based on the protocol published by Baumann and West(Baumann & West 1998). After extensive validation of the assay, I demonstrated that 6-TG caused a synergistic inhibition of NHEJ with UVA, which potentiated otherwise non-inhibitory drug treatments. High 6-TG concentrations caused UVA-independent inhibition of NHEJ. One possible explanation is transcription modulation caused by treatment with 6-TG although none of the gene products reported to be down-regulated seem especially relevant to NHEJ(F. Zhang et al. 2013). In addition, higher 6-TG concentrations are a source of RS (by depleting antioxidant levels)(Brem & Karran 2012) thus the effect could still be redox-mediated.

The complementation of defective NHEJ extracts with recombinant Ku firstly strengthens the link between Ku damage and NHEJ inactivation and secondly, suggests that sufficient levels of other NHEJ factors remain functional at least after treatment with 0.1μM 6-TG/UVA.

On the basis of my findings, NHEJ activity in 6-TG/UVA treated cells was examined and found to be diminished (performed by Quentin Gueranger, Figure 3.21). Neutral comet assays with treated HeLa cells, which are less susceptible to 6-TG than CEM cells, revealed that 1 μM 6-TG and 50 kJ/m$^2$ UVA significantly inhibited repair of double strand breaks *in vivo*. Thus UVA-dependent inhibition of NHEJ is detected both in cells and in an *in vitro* assay. If photoactivation of DNA-6-TG can induce significant oxidative stress in patient skin, a chronic reduction in NHEJ capacity may result. This could have adverse consequences for genome stability.

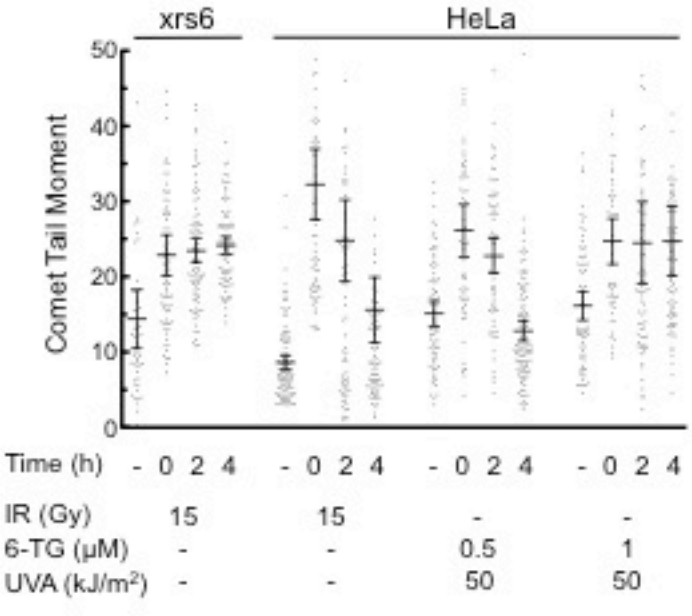


**Figure 3.21 Neutral comet assay of 6-TG/UVA treated cells**
Hela or CHO xrs6 (Ku80-deficient) cells were synchronised at G1/S by double thymidine block. HeLa cells were grown in 6-TG containing medium between thymidine treatments. Maintaining the block, cells were irradiated with IR (15Gy) or UVA (50kJ/m$^2$) and DSBs remaining were assessed via neutral comet assay over a 4-hour time course. Each dot represents a single comet measurement. Performed by Quentin Gueranger, taken from (Gueranger et al. 2014).

## 3.4 Summary

I have developed a robust detection method for assessing the carbonylation of proteins induced by photosensitisation that offers a number of advantages over commercially available options. Its compatibility with 2D gels is currently limited although these problems could be overcome. An increase in thiol oxidation due to treatment was also detected.

Several important DNA repair/replication proteins were identified in a screen for carbonylation. Among these, the essential NHEJ heterodimer, Ku, was crosslinked and functionally inactivated by 6-TG/UVA treatment. DNA binding and NHEJ activity in extracts were both impaired. Activity was restored by the addition of recombinant Ku.

With protocols in place to examine a number of different markers of protein oxidation, I was able to turn my attention to the effects of other known photosensitisers.

# Chapter 4. Other photosensitisers and protein oxidation

## 4.1 Introduction

### 4.1.1 Photosensitisers and their effects

Upon absorption of characteristic wavelengths of light, photosensitisers participate in photochemical reactions that damage biomolecules and in so doing potentiate the effects of incident radiation. Their presence in human skin leads to an exaggerated skin response to sun exposure.

This reactivity has been harnessed therapeutically as part of PDT (Section 1.5) but is also an undesired side effect of a wide range of pharmaceuticals(Drucker & Rosen 2011). The experimental work described in this chapter compares the photosensitizing effects of DNA 6-TG with those of selected pharmaceuticals.

### 4.1.2 Thiopurines

#### *4.1.2.1 Treatment with thiopurines*

DNA-6-TG is one of the end products of the metabolism of the thiopurine group of pharmaceuticals. Originally developed in the 1950's for cancer therapy, the thiopurines are now mainly prescribed as anti-inflammatory and immunosuppressive agents although 6-mercaptopurine (6-MP) remains one of the main treatments for childhood acute lymphoblastic leukaemia(McLeod et al. 2000). The 6-MP prodrug azathioprine has long been used as an immunosuppressant in organ transplant patients, often in combination with a calcineurin inhibitor and/or corticosteroids(Kasiske et al. 2009). The use of azathioprine has declined markedly with advent of newer immunosuppressants such as mycophenolate mofetil(Karran & Attard 2008) but it is nevertheless still taken by thousands of patients worldwide. Azathioprine continues to be prescribed for the management of inflammatory bowel disease and other disorders(Carter 2004). In total,

azathioprine was prescribed 814,000 times in the UK in 2012. 6-MP (49,000) and 6-TG (100) prescriptions were less frequent (Centre 2013).

All thiopurines require metabolic conversion to their common active metabolite, 6-thioguanine nucleosides (TGN). The metabolic process is detailed in Figure 4.1. Notably, 6-MP, 6-TG, thioinosine monophosphate (TIMP) and thio-guanine monophosphate (TGMP) are all inactivated by thiopurine S-methyltransferase (TPMT) and patients with low activity variants of TPMT are a risk of effective thiopurine overdose and require careful monitoring. Methylated TIMP (meTIMP) is an effective inhibitor of *de novo* purine biosynthesis and this has been proposed as an explanation for thiopurine cytotoxicity but the anti-proliferative and immunosuppressive activities of thiopurines are more likely a consequence of TGN formation and incorporation into DNA (discussed in (Karran & Attard 2008)).

The mechanism of thiopurine cytotoxicity is still not fully understood. TGN are efficiently incorporated into replicating DNA and DNA-6-TG comprises 0.01%-0.03% total DNA guanine in patient skin and lymphocytes(Attard & Karran 2011). A low level of incorporated DNA-6-TG does not block polymerases and is not significantly toxic or mutagenic. The cytotoxic activity of DNA-6-TG is thought to reflect its *in situ* chemical methylation, replication and recognition of me6-TG-containing base pairs by post-replicative mismatch repair(Swann et al. 1996) (Detailed in Figure 4.2).

#### *4.1.2.2 6-TG and UVA*

6-TG absorbs maximally at 342nm (Figure 4.3) and its presence in DNA shifts the DNA absorption profile into the wavelength range of incident solar radiation. Various DNA lesions are produced upon excitation of DNA-6-TG by UVA (reviewed in(Brem & Karran 2011)). These include guanine-6-sulfinate ($G^{SO2}$) and guanine-6-sulfonate ($G^{SO3}$)(Ren et al. 2010), DSBs, DNA interstrand crosslinks (ICLs)(Brem et al. 2011) and DNA-protein crosslinks(Gueranger et al. 2011). ICLs are important contributors to lethality and FA-deficient cells are very sensitive to 6-TG/UVA. NER-deficient cells are not hypersensitive indicating that toxic 6-TG/UVA DNA lesions are not excised by

NER. Oxidative DNA damage occurs by the action of $^1O_2$ on guanine to give 8-oxoG(COOKE et al. 2008).

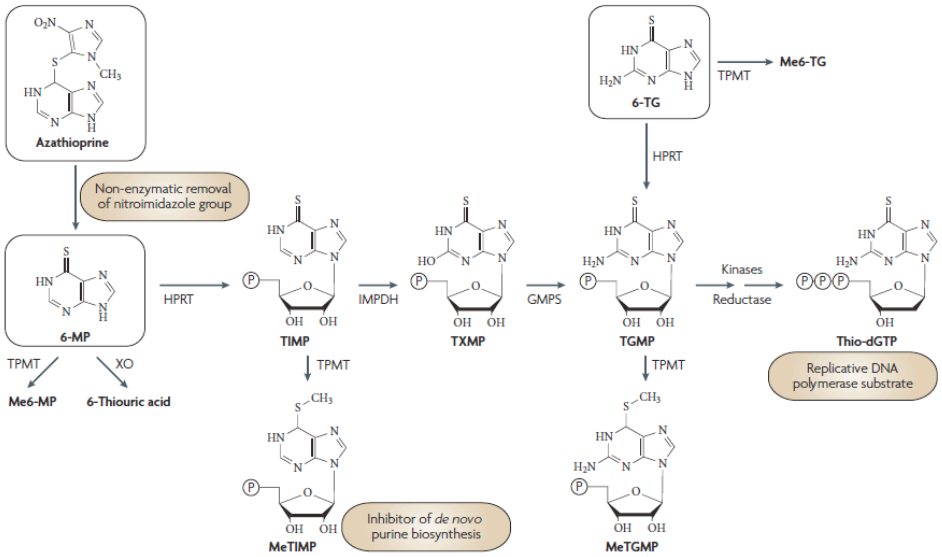


**Figure 4.1 Metabolism of thiopurines**
The substituted imidazole ring is non-enzymatically removed from azathioprine to yield 6-MP, which, along with 6-TG, is actively transported into cells(Conklin et al. 2012). Once within the cell, it enters the purine salvage pathway. Hypoxanthine-guanine phosphoribosyl transferase (HPRT) catalyses the addition of ribose-5-phosphate to 6-MP to generate thioinosine monophosphate (TIMP). TIMP is then further metabolised via a two-step process catalysed by inosine-5'-monophosphate dehydrogenase (IMPDH) and guanine monophosphate synthetase. This yields thioguanine monophosphate (TGMP), which can also be formed directly via the action of HPRT on 6-TG, which reduced and phosphorylated to yield TGN, a substrate for DNA polymerases. 6-MP is also subject to a competing catabolic reaction with xanthine oxidase and thus allopurinol, an XO inhibitor, potentiates thiopurine effects. Reproduced from Karran and Attard(Karran & Attard 2008).

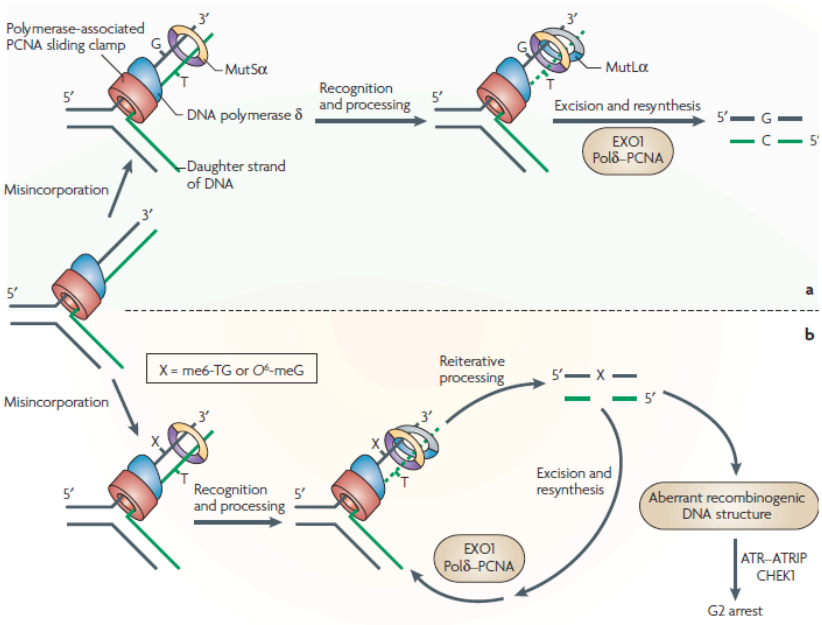


**Figure 4.2 Toxicity of thiopurines**
Non-enzymatic S-methylation of DNA-6-TG by S-adenosylmethionine occurs at 1 in $10^4$ DNA-6-TGs. Methylation of incorporated 6-TG promotes the formation of me6-TG:T which is recognised by MutSα-MutLα, triggering MMR. As the lesions cannot be correctly paired, MMR is unsuccessful and the strand opposing the lesion is left as a SSB. Upon replication forks meeting SSBs during a subsequent round of replication, cells enter ATR-Chk1 mediated G2 arrest with aberrant DNA structures. Reproduced from Karran and Attard (Karran & Attard 2008).

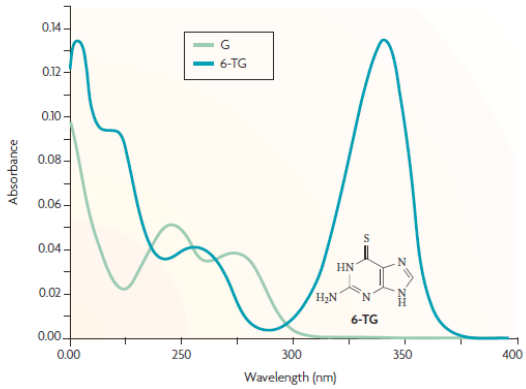


**Figure 4.3 Absorption spectra of guanine and 6-TG**
The absorption spectrum of guanine (green) shows little absorption above>300nm whilst the absorbance maximum of 6-TG (blue) peaks at 342nm. Reproduced from Karran and Attard (Karran & Attard 2008).

Replication-arresting 6-TG/UVA-induced DNA lesions cause PCNA monoubiquitination (Montaner et al. 2007), ATR-Chk1 checkpoint activation and subsequent G2/M arrest(Brem et al. 2010). Montaner et al also demonstrated a UVA and 6-TG dose-dependent formation of a crosslinked form of PCNA termed PCNA*, which they attributed to oxidative modification. PCNA* was most apparent in S-phase cells suggesting intimate association with DNA may place proteins at increased risk of DNA-6-TG-mediated oxidation.

#### *4.1.2.3 Therapy-related cancer*

As organ transplant rates and patient and organ survival increased over the latter half of the 20$^{th}$ century, a susceptibility of organ transplant recipients (OTRs) to NMSC became apparent. A recent 22-year cohort study in the UK found that after 30 years of immunosuppression 74% of patients had developed malignancies of which 73% were SCCs and 24% were BCCs(Harwood et al. 2012). SCCs occur 150-fold times more frequently relative to the general population thus inverting the usual BCC:SCC ratio. SCC in OTRs seems to be qualitatively different from SCC occurring in the general population; onset is earlier plus metastasis and mortality are significantly increased(Euvrard et al. 1995).

Epidemiological analysis has identified sun exposure and the duration and level of immunosuppression as risk factors for NMSC development. Since the immune system is important in cancer prevention, chronic immunosuppression is an inherently oncogenic intervention. Cancers with viral aetiologies have greatly increased incidence rates in pharmacologically immunosuppressed patients(Buell et al. 2005). A comparison of cancer incidence rates in HIV/AIDS patients and OTRs suggests the immunosuppressants have oncogenic properties in addition to their immunosuppressive abilities(Grulich et al. 2007). In particular, although virus-associated malignancies are increased in both HIV/AIDS patients and OTRs, NMSCs are disproportionally associated with the latter patient group(Grulich et al. 2007).

### 4.1.3 Fluoroquinolones

The fluoroquinolones (FQs), a diverse group of antimicrobial agents, are derived from nalidixic acid. Structural modifications to the nalidixic acid structure resulted in a wide range of compounds with improved pharmacological properties and diverse activities versus different bacterial species (Figure 4-4). Addition of a fluorine atom to C6 increased efficacy by up to two orders of magnitude and created the FQ class. A C7 piperazine group (norfloxacin and ciprofloxacin) inhibited drug efflux and yielded improved activity versus Gram-negative bacteria (Andersson 2003). A second fluorine atom at C8 (lomefloxacin) improves potency but increases the innate photoactivity of FQs(Martínez et al. 1998). Despite later iterations with improved pharmacokinetics, ciprofloxacin remains the most prescribed FQ in the UK by a wide margin (789,100 prescriptions in 2012). It was also the 4$^{th}$ most prescribed antibiotic in the USA in 2010(Hicks et al. 2013). Ciprofloxacin is a first line treatment for many UTIs and STDs and frequently used as an alternative to penicillin if a patient is allergic. Levofloxacin, the active enantiomer of ofloxacin, is indicated for community-acquired pneumonia due to its action against *S. Pneumoniae* and is the second most frequently prescribed FQ in the UK.

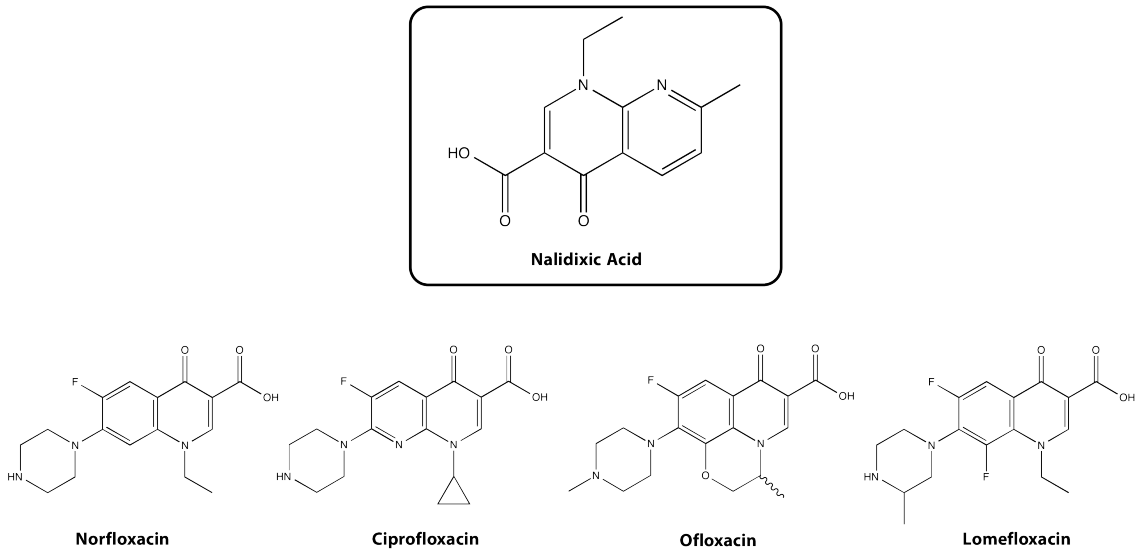


**Figure 4.4 Structures of nalidixic acid and notable fluoroquinolones.**
Nalidixic acid, the parent compound of the FQs, is highlighted. Norfloxacin was one of the first FQs synthesized but has been largely supplanted by ciprofloxacin, which is currently the most prescribed FQ. Ofloxacin is supplied as a racemic mixture (its levo- enantiomer is the second most prescribed FQ). Use of lomefloxacin, a difluoroquinolone, is limited due to phototoxic effects.

#### *4.1.3.1 Action of fluoroquinolones*

FQs are potent inhibitors of bacterial DNA gyrase and topoisomerase IV, both of which are essential for bacterial DNA replication(Blondeau 2004). Both enzymes create a DSB (stabilised by covalent binding between a phosphotyrosine and the 5'-P), pass another duplex through the break and then reseal the original strands. By these actions, DNA gyrase relaxes supercoiling ahead of the replication fork and topoisomerase IV decatenates the replicated daughter chromosomes to permit segregation. In Gram-negative bacteria the primary target is DNA gyrase whereas in Gram-positive bacteria, it is topoisomerase IV. FQs bind the enzyme-DNA complex by intercalating into DNA at the newly formed nick and trapping the complex in the cleaved form by blocking the phosphotyrosine from the active site(Wohlkonig et al. 2010).

#### *4.1.3.2 Fluoroquinolones and UVA*

Treatment with ciprofloxacin is associated with very mild phototoxicity in <2.4% of patients(Ferguson 1995). Phototoxicity associated with the difluoroquinolone, lomefloxacin, occurs more frequently (4-10%) and is more severe(Ferguson 1995) and it is only used topically.

The UVA MED of patients taking ciprofloxacin is reduced by around 50%, which correlates with an absorbance peak at around 340nm, and thus it is a weak UVA photosensitiser(Ferguson & Dawe 1997). In mice, UVA photosensitisation of various FQs, including ciprofloxacin and ofloxacin induced a modest increase in benign papillomas. The effect of photosensitised lomefloxacin was more severe and resulted in multiple SCCs(Klecak et al. 1997).

The higher photocarcinogenic risk associated with lomefloxacin is supported by increased SCC formation in UVA-irradiated XPA-/- mice treated with lomefloxacin but not ofloxacin (Itoh et al. 2005).

In practice, FQ-mediated phototoxicity is generally mild and short course lengths minimise the risk of phototumourigenesis in patients although ciprofloxacin has been recommended as a prophylactic antibiotic which requires extended course lengths (10 weeks)(Hart & Beeching 2001).

### 4.1.4 Vemurafenib

#### *4.1.4.1 Treatment with Vemurafenib*

Vemurafenib is an inhibitor of the BRAF protein kinase. It was recently approved for advanced metastatic melanoma patients carrying the BRAF V600E mutation, which is found in around 60% of cases(Roberts & Der 2007). It is currently the first-line treatment for advanced melanoma with a >50% response rate and a median survival of 16 months (vs. 6-10 months with previous best treatments)(Sosman et al. 2012). Resistance to vemurafenib invariably develops and can arise by several mechanisms including upregulation CRAF, activating Ras mutation and BRAF truncation to yield a constitutively dimerised protein that is resistant to inhibition(Bollag et al. 2012). Importantly, cutaneous SCCs are diagnosed in 26% of patients treated with vemurafenib(Sosman et al. 2012).

#### *4.1.4.2 Action of Vemurafenib*

The RAF/MEK/ERK pathway is a sub pathway of the larger MAPK family that plays a regulatory role in cellular growth, differentiation and survival. Upon stimulation by growth factors, mitogens or cytokines, cell surface receptors prompt membrane-bound Ras to recruit and activate RAF. The complex activation procedure involves phosphorylation, dephosphorylation and disruption of autoinhibitory binding. Importantly, it also forms a side-to-side dimer, which is essential for activation. RAF is present in three isoforms A, B and C although in practice, the RAF B-C heterodimer is most prevalent followed by RAF B homodimers(Freeman et al. 2013). BRAF exhibits significantly higher activity than the other RAF isoforms and is considered to be the main RAF transducer. RAF activates MEK by phosphorylation of its catalytic domain, which then goes on to activate ERK. ERK phosphorylates over 160 cytoplasmic and

nuclear targets. Nuclear targets of ERK lead to altered gene expression through the action of numerous transcription factors including NF-κB, c-Myc and AP-1. (McCubrey et al. 2007).

Mutational upregulation of the ERK pathway occurs in around 30% of human cancers(Wellbrock et al. 2004). Ras is mutated in 15% of all cancers whilst BRAF is mutated in 8%(H. Davies et al. 2002). Strikingly BRAF mutation is found in 70% of malignant melanomas; a T→A transversion that leads to V600E, accounts for 90% of these(Roberts & Der 2007). V600E is effectively a phosphomimetic mutation that exchanges a hydrophobic Val for a charged Glu, causing a conformational change that destabilises inactive BRAF and promotes constitutive activation(Cantwell-Dorris et al. 2011). In contrast to wild-type RAF, V600E mutants are kinase active in the absence of dimerization(Freeman et al. 2013) thus ERK activation is promoted in the absence of Ras or upstream signalling.

Vemurafenib inhibits V600E BRAF at doses more than ten times lower than wild type BRAF and shows even greater discrimination against other kinases(Tsai et al. 2008). The drug is complementary to RAF-specific structural features and its binding induces a conformational change that only inactivates the V600E mutant.

#### *4.1.4.3 Vemurafenib and UVA*

Photosensitivity and SCC formation were among the reported side effects in the initial clinical trials of vemurafenib(P. B. Chapman et al. 2011). A more recent collation of 3 trial data sets reported photosensitive reactions 35-63% of patients and development of SCCs in 19-26%(Lacouture et al. 2013). Of these SCCs, 41% were HRAS mutated. The photosensitivity associated with vemurafenib is UVA dependent(Dummer et al. 2012). Although the precise action spectrum has not yet been elucidated, it is clear that vemurafenib is a UVR photosensitiser.

Whilst vemurafenib blocks ERK signalling in cells carrying the V600E mutation, it causes paradoxical ERK activation in cells with wild type BRAF. The mechanism is

still not fully understood but it seems that upon binding to the active site of one RAF in a dimer, it transactivates the binding partner (Poulikakos et al. 2011). The effect requires the presence of CRAF and an activated Ras to induce RAF dimer formation. Sequencing of SCCs arising during vemurafenib treatment reveals that 60% contain a Ras mutation(Su et al. 2012). The speed of SCC development (weeks) suggests that vemurafenib potentiates pre-existing Ras mutations via ERK activation. Although the development of SCCs is likely distinct from vemurafenib-mediated photosensitisation, little information is available regarding vemurafenib as a photosensitiser.

In these experiments, I sought to further characterize the as yet poorly understood phototoxic effects of vemurafenib. As non-DNA incorporated type II photosensitisers, FQs were chosen to offer a point of comparison to 6-TG such that the effects of its RS generation might be decoupled from its incorporation into DNA. The techniques developed in Chapter 3 in conjunction with other assays detailed below were used to assess the similarities and differences between known UVA photosensitisers.

## 4.2 Results

### 4.2.1 Phototoxicity in CEM-CCRF cells

The ability of DNA-6-TG(O'Donovan et al. 2005) and the FQs(Zhao et al. 2010) to sensitise cultured cells to sub-lethal UVA doses has previously been documented. At the time my experiments were performed, UVA photosensitisation by vemurafenib had been observed only in patients but its effect on cultured mouse cells has since been reported(Boudon et al. 2013). To examine the *in vitro* photosensitising effects of the drug and the concentration range over which they are effective in the CEM cells, drug-treated cells were UVA irradiated at 20 $kJ/m^2$ and the outgrowth of surviving cells was determined over 48 hours. (20 $kJ/m^2$ is a relatively mild UVA dose and is equivalent to around 30 minutes of midday sun in the British summertime).

6-TG requires less metabolic processing prior to its incorporation into DNA and was used as an azathioprine proxy. Cells were allowed to incorporate 6-TG into DNA by growth in medium supplemented with the free base for 24 hours. Following washing

and resuspension in PBSA, cells were UVA irradiated in a closed Petri dish. Irradiated cells were returned to fresh growth medium and proliferation was monitored for 48 hours. As expected, 6-TG and UVA were synergistically toxic to CEM cells (Figure 4-5, top left). Low 6-TG concentrations (0.1, 0.3 μM) that had no detectable effect on cell proliferation were cytostatic in conjunction with UVA. A higher 6-TG dose (0.6 μM) was required to cause even minor retardation of growth in the absence of irradiation.

Photosensitisation by FQs was investigated using ciprofloxacin and ofloxacin. CEM cells were treated with the drug for 60 minutes. In all other respects, the procedure described for 6-TG was followed. Ciprofloxacin (Figure 4-5, top right) was a more potent photosensitiser than ofloxacin (Figure 4-5, bottom left). Cells treated with 50 μM ciprofloxacin survived 20 kJ/m$^2$ UVA irradiation whereas irradiated cells treated with 100 or 250 μM drug showed no sign of recovery. In contrast, irradiated cells treated with higher (500, 1000 μM) ofloxacin concentrations showed some signs of recovery. Neither drug detectably affected growth in the absence of UVA.

Vemurafenib is also a UVA photosensitiser in CEM cells. 20 kJ/m$^2$ UVA resulted in partial inhibition of growth in cells treated for 24 h with 5 μM vemurafenib (Figure 4-5, bottom right). Treatment with 20 μM vemurafenib and UVA abolished proliferation. Neither dose affected proliferation of unirradiated cells. Thus DNA 6-TG, ciprofloxacin and ofloxacin, and vemurafenib are all UVA photosensitisers in CEM cells over the examined dose ranges.

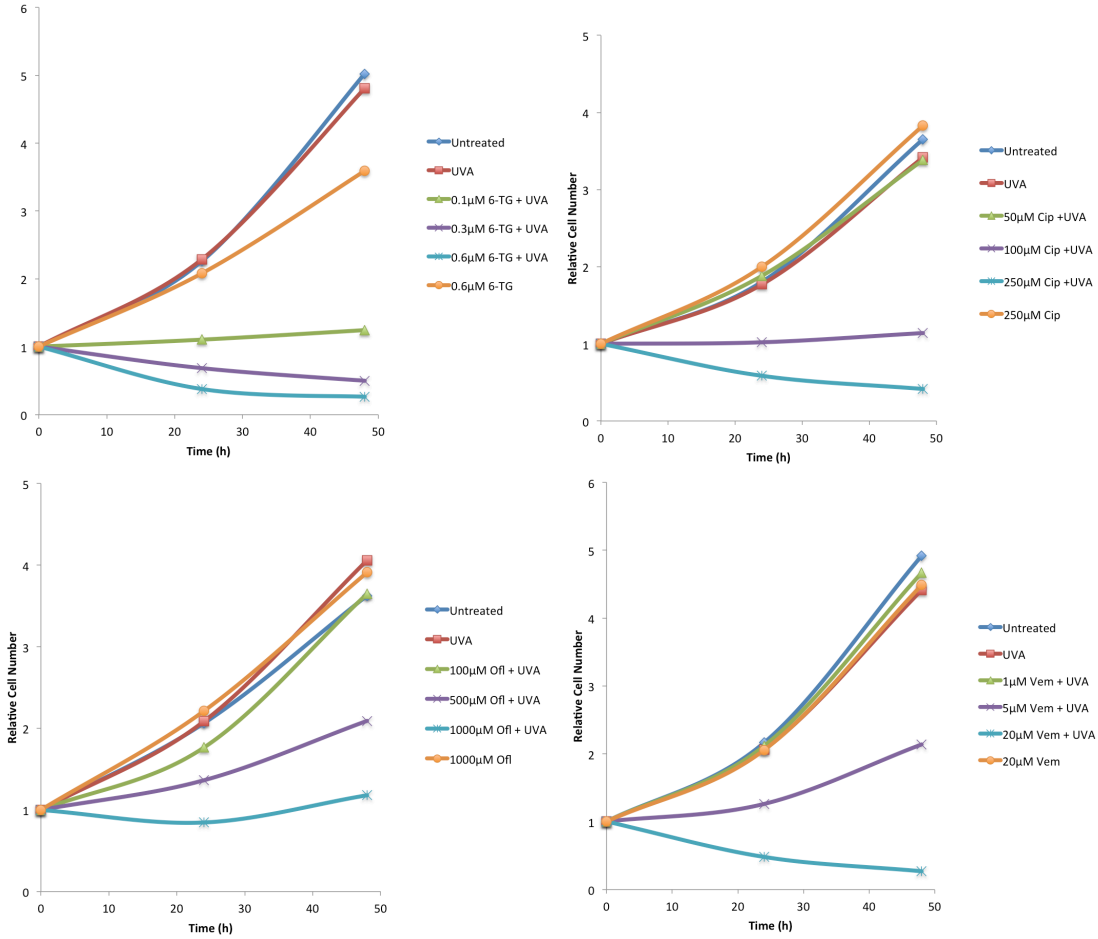


**Figure 4.5 Proliferation of CEM cells after photosensitisation**
CEM cells were drug treated (6-TG & Vem 24h/ FQs 1h) and irradiated with UVA (20 kJ/m$^2$) as indicated. After irradiation, cells were collected and resuspended in fresh growth medium. Cells were counted at 24 and 48 hours after irradiation. **Top, left:** 6-TG. **Top, right:** Ciprofloxacin. **Bottom, left:** Ofloxacin. **Bottom, right:** Vemurafenib

### 4.2.2 Generation of RS

Photosensitisation frequently involves generation of RS. UVA can produce RS from unincorporated 6-TG or following its incorporation into cellular DNA(X. Zhang et al. 2007; O'Donovan et al. 2005). The ability of FQs to generate intracellular RS can be inferred by formation of 8-oxoG in genomic DNA following UVA irradiation of treated cells(Sauvaigo et al. 2001). The relationship between vemurafenib phototoxicity and RS in cultured cells has not been characterised.

Intracellular RS generation can be assayed using a suitable fluorescent probe in conjunction with fluorescent-activated cell sorting (FACS). 5-(and-6)-chloromethyl-2',7'-dichlorodihydrofluorescein diacetate, acetyl ester (CM-$H_2$DCFDA) is a reduced fluorescein derivative that becomes fluorescent upon oxidation (Figure 4.6).

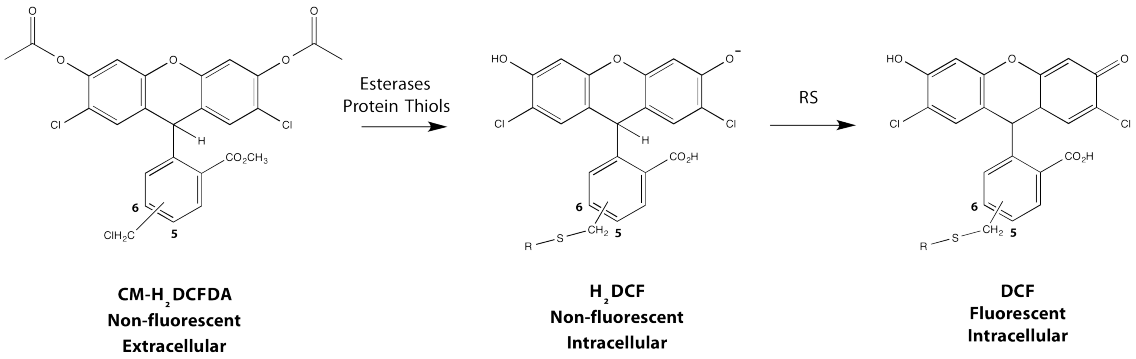


**Figure 4.6 Mechanism of CM-$H_2$DCFDA function**
CM-$H_2$DCFDA penetrates cells whereupon the acetate groups are cleaved by cellular esterases to give a charged form that is less able to cross cell membranes. The chloromethyl derivative used in these experiments reacts with cellular thiols to further increase retention. Oxidation by intracellular RS results in a fluorescent form that can be detected by FACS.

After treatment with a range of drug concentrations (24 h 6-TG and vemurafenib, 1 h ciprofloxacin and ofloxacin), cells were incubated with CM-$H_2$DCFDA and UVA irradiated. FACS analysis yields a frequency distribution as a function of fluorescence intensity, which is proportional to RS generation. Figure 4.7 shows that drug and UVA treatments are also synergistic for RS generation. In each case, there is a positive correlation between RS and drug concentration. A maximum response is reached at the highest doses of 6-TG and ciprofloxacin suggesting that the dynamic range of the assay is limited to around 50x the response of the untreated control. As a result, it is difficult to compare RS generating ability. Ciprofloxacin (Figure 4.7, top right) appears to be the most powerful RS source. The highest ciprofloxacin doses (250, 500 μM) and 6-TG (0.5μM) all gave maximal fluorescence values whereas this level was not reached following vemurafenib or ofloxacin treatment.

It is apparent from these findings that RS generation and cell killing are not related in a simple way. This is illustrated in Figure 4-8 in which approximately equitoxic treatments are compared. Ciprofloxacin and ofloxacin generate significantly more RS than the approximately equitoxic doses of 6-TG and vemurafenib. The discrepancies between RS formation and cytotoxicity may reflect differential contributions from type I and type II photosensitisation, different localisation of the photosensitiser within the cell, or drug-mediated alterations to cellular function that otherwise modulate UVA sensitivity

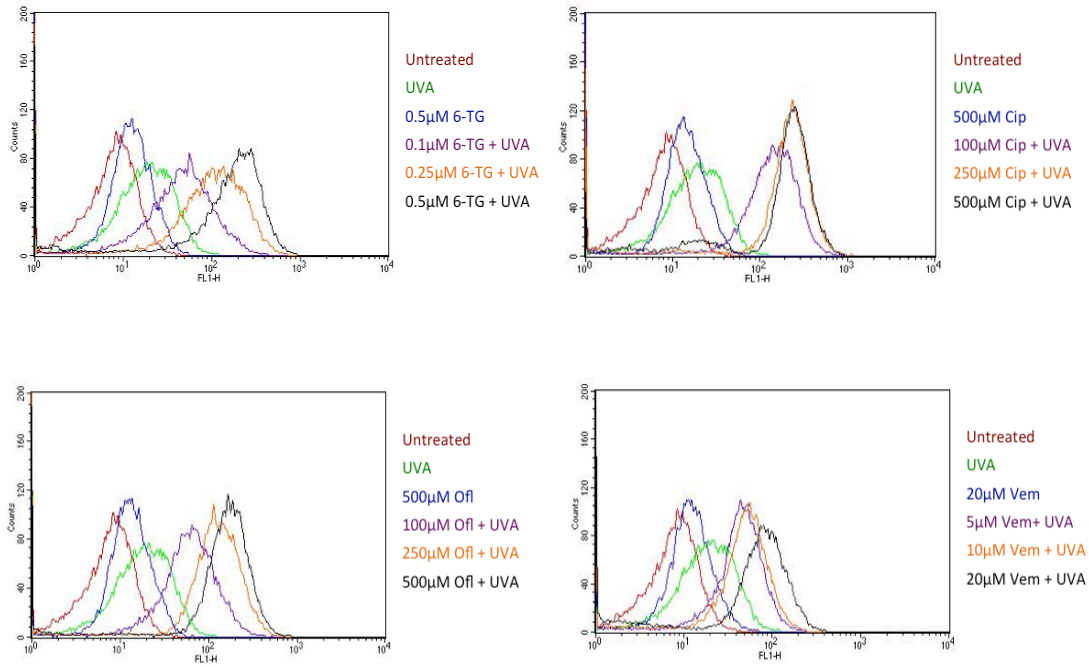


**Figure 4.7 FACS analysis of intracellular RS by CM-$H_2$DCFDA**
Cells were drug treated and UVA irradiated as indicated. Cells were incubated with 7.5µM CM-$H_2$DCFDA for 15 minutes prior to irradiation. They were then collected, washed and resuspended in PBS and subject to FACS analysis. **Top, left:** 6-TG. **Top, right:** Ciprofloxacin. **Bottom, left:** Ofloxacin. **Bottom, right:** Vemurafenib

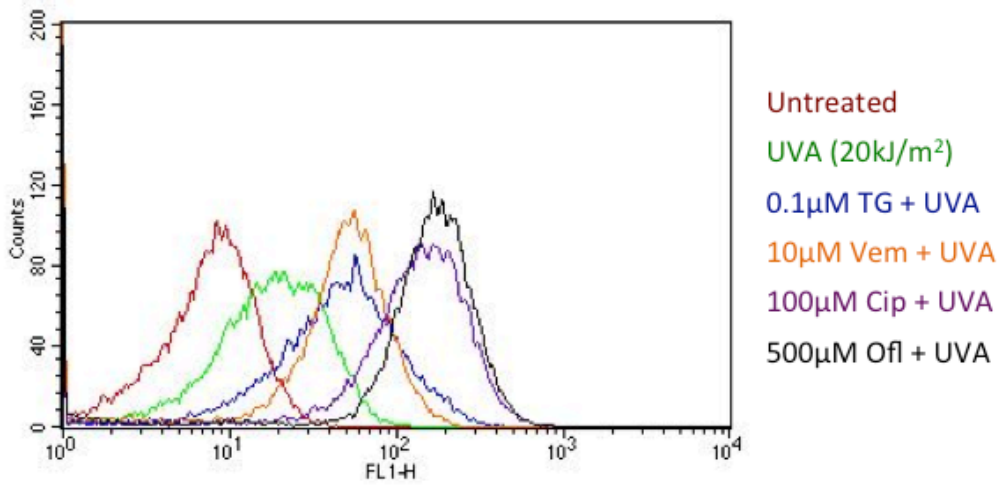


**Figure 4.8 RS produced at equitoxic doses of photosensitiser**
Selected histograms from Figure 4.7 are replotted to allow easier comparison.

To gain an insight into the relative photosensitising potency as well as the potential contribution of type I and II photosensitisation for each PS, *in vitro* photosensitising ability was assessed by secondary bleaching of p-nitroso-N,N-dimethylaniline (RNO) (Kraljić & Mohsni 1978). RNO is a yellow dye that becomes colourless upon oxidation (Figure 4.9). $^1O_2$ cannot oxidise RNO directly. RNO does, however, react with endoperoxides formed by reaction of $^1O_2$ with a diene (as seen in Figure 1.3) and $^1O_2$ – dependent bleaching can therefore only occur in the presence of an appropriate mediator, such as histidine. Strong oxidants such as HO• oxidise RNO directly. Thus in the assay, histidine dependent RNO bleaching can be attributed to $^1O_2$ production and histidine-independent bleaching to type I photosensitisation. Although semi quantitative, the assay does give an indication as to whether RS are produced and, if they are, whether $^1O_2$ represents a significant proportion.

Samples were treated in accordance with the RNO assay protocol in Materials and Methods. An RNO/drug mixture with or without histidine in phosphate buffer is loaded into duplicate 96-well plates. One plate is UVA irradiated (100kJ/m$^2$) whilst its partner is shielded from light. Absorbance at 440nm is then measured and the extent of bleaching is calculated relative to its unirradiated counterpart.

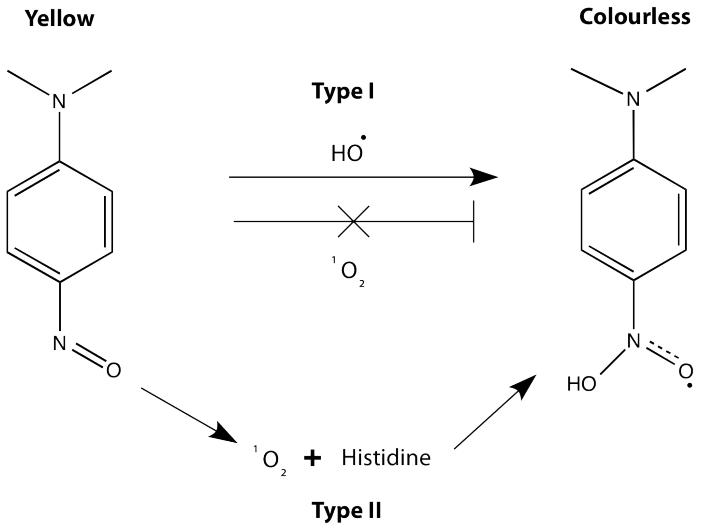


**Figure 4.9 Reaction scheme for RNO bleaching**
Yellow dye molecule, RNO, can be converted to its colourless oxidised form by direct reaction with HO• or via histidine mediated reaction with $^1O_2$. Histidine dependence of bleaching indicates type II photosensitisation and histidine independence, type I.

Figure 4.8 shows the data for 6-TG. The ratio of His-dependent to His-independent bleaching is around 2.5 indicating a significant production of $^1O_2$. This ratio is increased to ≥3.0 when the reaction mixtures were prepared in $D_2O$, which prolongs $^1O_2$ lifetime, thereby confirming histidine dependence as indicative of $^1O_2$ production. As expected, histidine-independent bleaching is largely unaffected by $D_2O$.

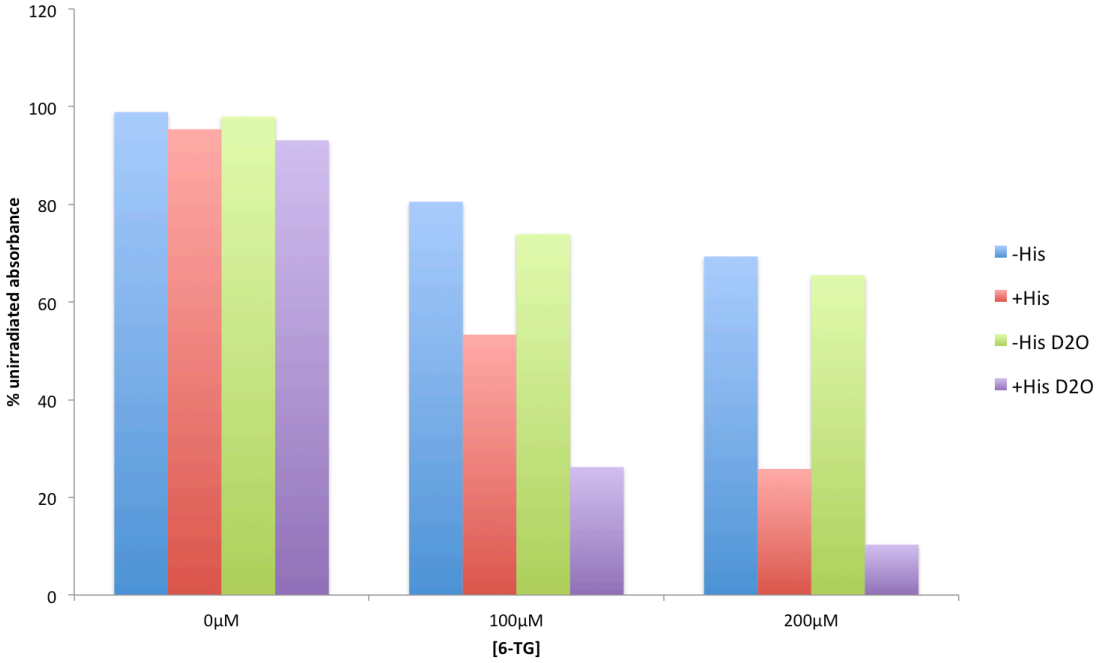


**Figure 4.10 RNO assay for 6-TG**
6-TG (0-300 μM) was assayed according to the RNO assay protocol (Materials and Methods). Values represent absorbance at 440nm relative to unirradiated sample. Samples without histidine are shown in blue, with histidine shown in red, without histidine and with $D_2O$ shown in green and with histidine and with $D_2O$ depicted in purple.

In agreement with published data(Dall'Acquaa et al. 2007), ciprofloxacin was a significant source of $^1O_2$. In contrast to 6-TG, a much higher proportion of RNO bleaching was histidine-dependent (the independent to dependent ratio was approximately 4.0) suggesting a larger role for singlet oxygen in its bleaching ability (Figure 4.11). I thus conclude that although 6-TG is an efficient producer of $^1O_2$, it has a more significant type I component than ciprofloxacin. Both histidine-dependent and independent bleaching is significantly higher for 6-TG at lower concentrations suggesting that it is more effective at both type I and type II photosensitisation. Published data support this conclusion. The $^1O_2$ quantum yield, quantitatively related to type II photosensitising ability, is around 5x greater for 6-TG than for ciprofloxacin (0.5 vs. 0.092 – for comparison, the quantum yields of most clinical photosensitisers are between 0.7 and 0.9 (DeRosa & Crutchley 2002)).

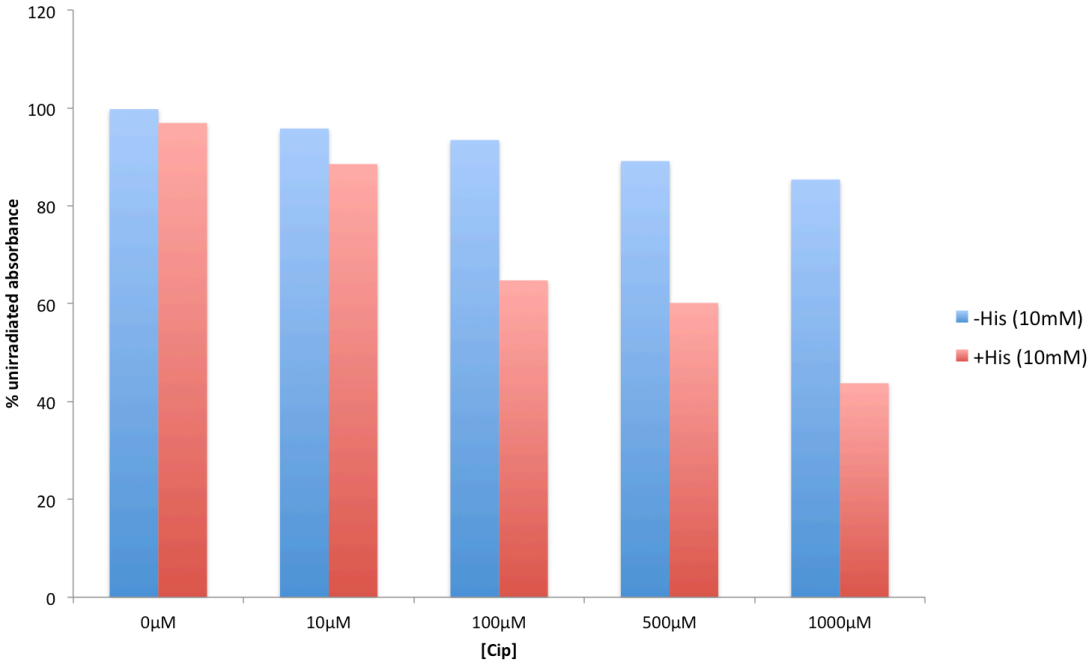


**Figure 4.11 RNO assay for ciprofloxacin**
Ciprofloxacin (0-1000 μM) was assayed according to the RNO assay protocol (Materials and Methods). Values represent absorbance at 440nm relative to unirradiated sample. Samples without histidine are shown in blue and with histidine shown in red.

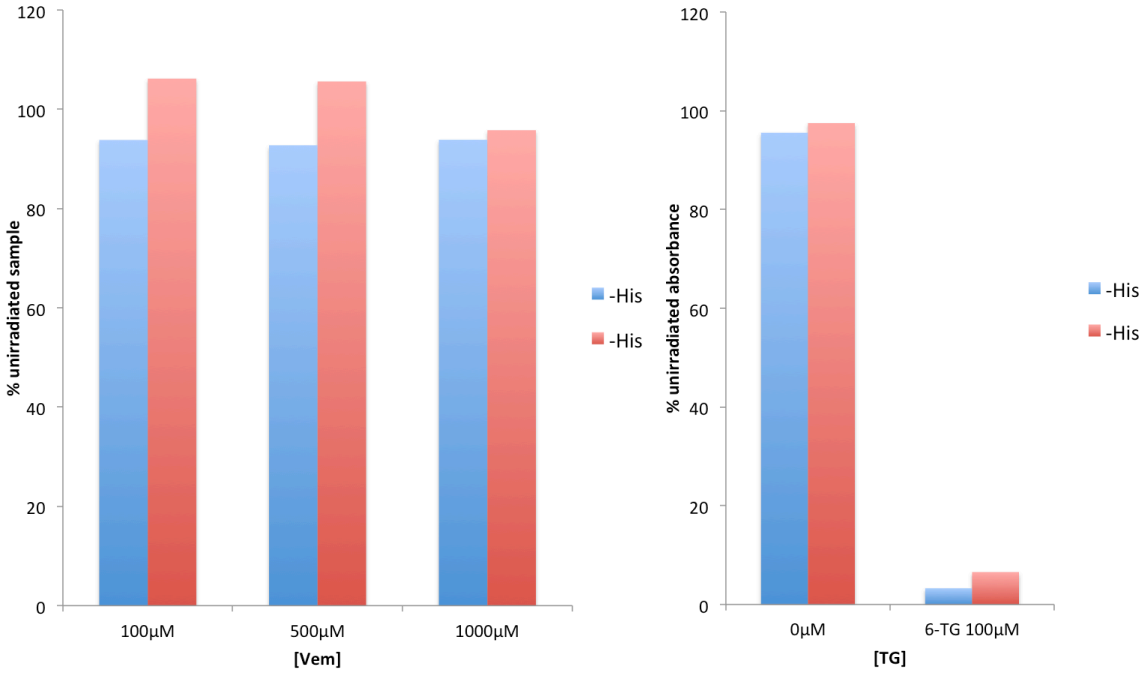


**Figure 4.12 Modified RNO assay for vemurafenib**
**Left:** Vemurafenib (0-1000 μM) was assayed in a modified RNO assay prepared in DMSO (Materials and Methods). Samples without histidine are shown in blue and with histidine shown in red. **Right:** Samples prepared as for vemurafenib but with 6-TG (100μM).

Vemurafenib is very poorly soluble in aqueous solvents. To solve this problem, I carried out the RNO bleaching assay in DMSO. There are no previous reports of RNO bleaching in a non-aqueous solvent but since the lifetime of $^1O_2$ in DMSO is around 6x longer than in $H_2O$(Wilkinson & Brummer 1981) and triplet state lifetime are also extended, an increase in both type I and type II photosensitisation might be expected. DMSO is, however, a radical scavenger and this prevents detection of any HO• mediated effects. Despite the anticipated increase in sensitivity, vemurafenib did not induce either histidine-dependent or independent photobleaching of RNO (Figure 4.12, left). I did observe extensive histidine-dependent and –independent bleaching by irradiated 6-TG in DMSO (Figure 4.12, right). This control indicated that using a non-protic solvent does not prevent RNO bleaching and confirmed the predicted increase in sensitivity. Although not entirely definitive, these observations suggest that the effects of vemurafenib on cells are likely not $^1O_2$ mediated and that it has no ability to act as a type II photosensitiser.

### 4.2.3 Protein oxidation by UVA photosensitisers

The effects of the non-DNA incorporated photosensitisers on protein oxidation were assessed using the endpoints identified in the previous chapter and the previously reported crosslinking of PCNA (Figure 4.13). FHA derivatized extracts from 6-TG/UVA, ciprofloxacin/UVA and ofloxacin/UVA treated cells are shown in Figure 4.13, top. As the RS induction observed in the previous section predicted, a UVA and dose-dependent increase in carbonylation was observed in each case. Western blot analysis of Ku70 and PCNA revealed formation of the crosslinked species in a UVA and drug-dose dependent manner. Taken together these results indicate that the fluoroquinolones recapitulate the protein oxidation behaviour of 6-TG. I conclude that extensive protein oxidation can also occur via non DNA-embedded UVA chromophores.

Protein oxidation by vemurafenib presents a somewhat different picture. Carbonylation appears fairly modest (Figure 4.14, top left). A slight increase can be discerned in extracts from cells treated with 20 μM vemurafenib and UVA irradiated. Attempts to visualise this increase with a very high dose (50 μM) lead to significant UVA-

independent carbonylation, which increased substantially upon irradiation (Figure 4.14, top right). Gels were western blotted (rather than Sypro Ruby stained) to interrogate the Ku oxidation status (Figure 4.14, middle). Crosslinking could not be perceived after any treatment, even in the heavily carbonylated samples, again suggesting a different mechanism may underlie vemurafenib photosensitisation. PCNA crosslinking was also minimal although the signal was often slightly increased over that observed with UVA alone (Figure 4.14, bottom). (These experiments also highlighted the automatic signal adjustment that the acquisition software performs when saturated by highly fluorescent samples meaning that comparison between separately scanned gels is not necessarily meaningful).

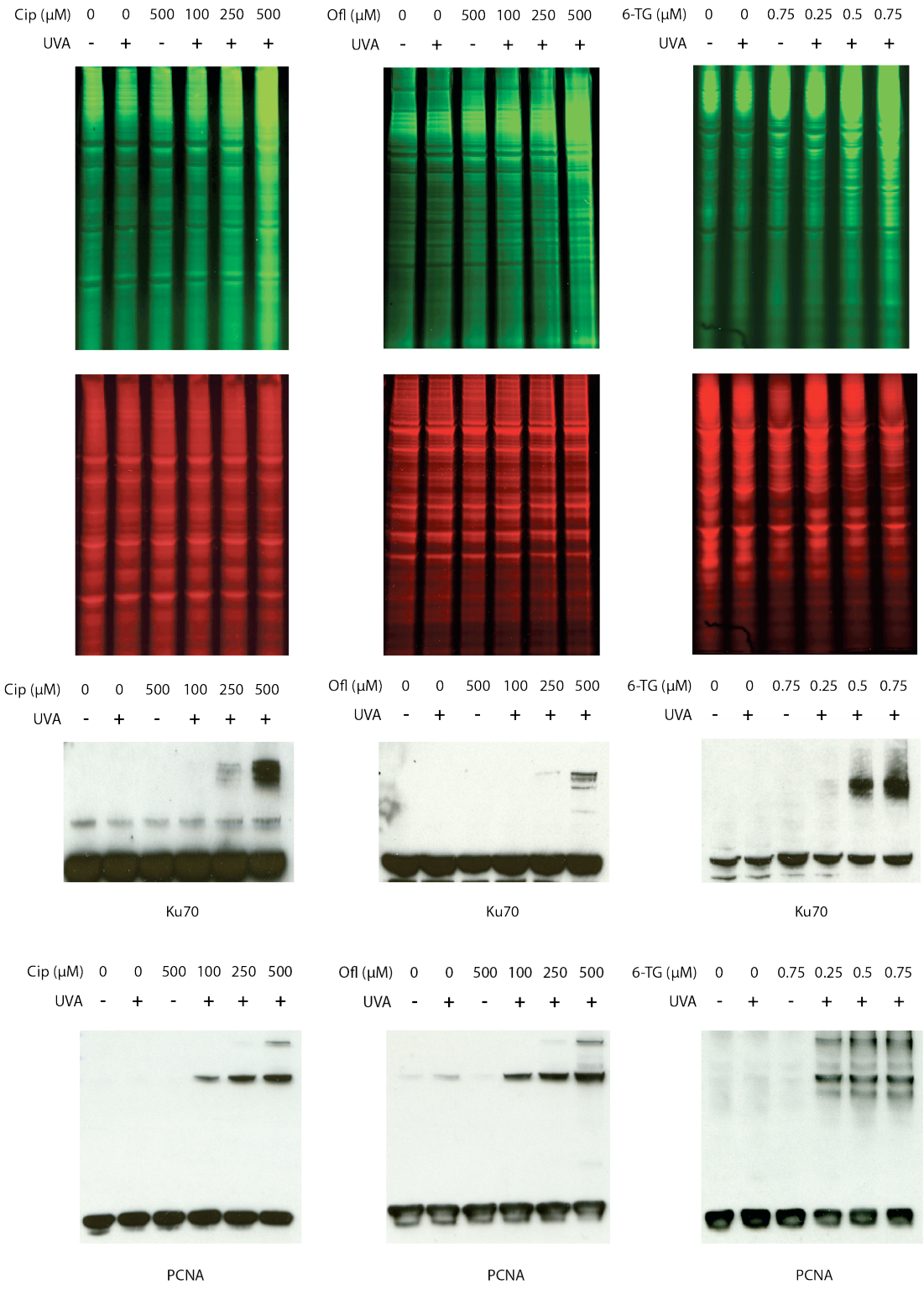


**Figure 4.13 Fluoroquinolones replicate the protein oxidation characteristics of 6-TG**
CEM cell extracts were prepared from cells drug treated (ciprofloxacin & ofloxacin/1 h, 6-TG/24 h) and UVA irradiated (20 kJ/m$^2$) as indicated. **Left column:** Ciprofloxacin **Middle column**: Ofloxacin. **Right column:** 6-TG. **Top row:** FHA gels and corresponding Sypro Ruby gels prepared according to FHA protocol in Materials and Methods. **Middle row:** Western blot analysis of Ku70. **Bottom row:** Western blot analysis of PCNA.

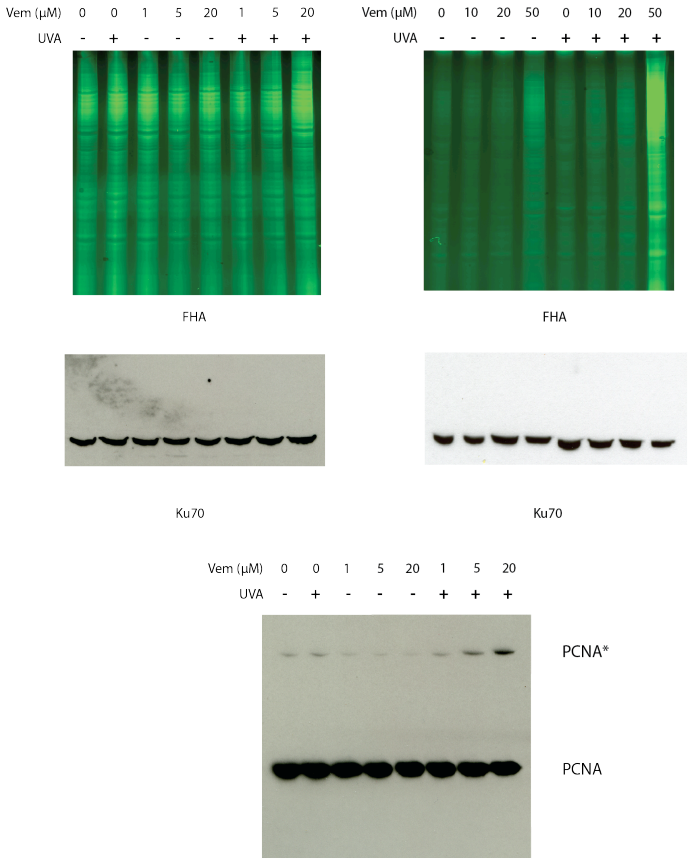


**Figure 4.14 Protein oxidation by vemurafenib.**
RIPA extracts were prepared from cells treated with vemurafenib (24 h) and UVA irradiated (20 kJ/m$^2$) as indicated. **Top:** Extracts were derivatised with FHA according to the FHA protocol in Material and Methods. **Middle:** The FHA gels were western blotted after scanning and probed with Ku70 antibody. **Bottom:** Samples from same extracts used to prepare the left-hand FHA gel were western blotted and probed for PCNA.

Incubation in PBS prepared using $D_2O$ prior to irradiation, exacerbated crosslinking of PCNA and Ku by 6-TG, ciprofloxacin and ofloxacin but not vemurafenib where it remained almost undetectable (Figure 4.15). This indicated that both phenomena were at least partially $^1O_2$ mediated. As with, 6-TG/UVA treatment, levels of oxidised proteins decreased with time (Figure 4.16) consistent with proteolysis of the crosslinked material.

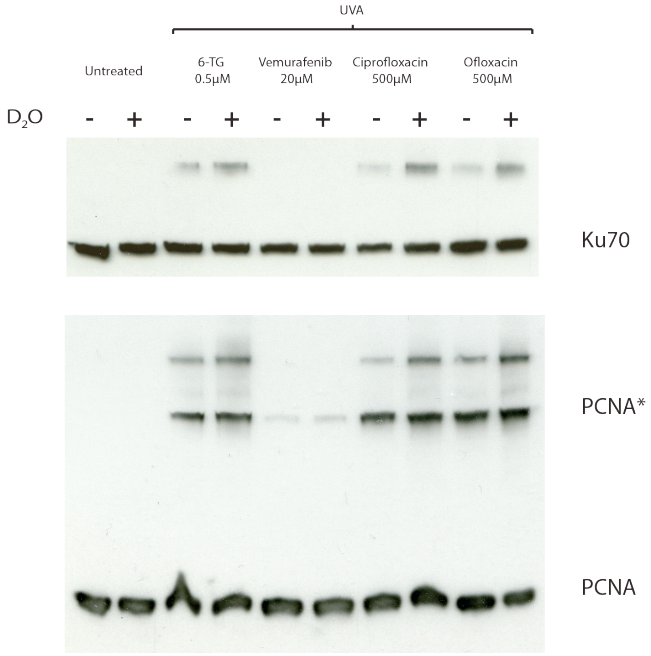


**Figure 4.15 $D_2O$-PBS incubation exacerbates Ku and PCNA crosslinking**
CEM cells were drug treated and UVA (20 kJ/m$^2$) irradiated with and without 15 minute pre-incubation with PBS prepared using $D_2O$. **Top:** RIPA extracts were prepared and western blotted with anti-Ku70 primary antibody. **Bottom:** The same membrane was stripped and probed with anti-PCNA.

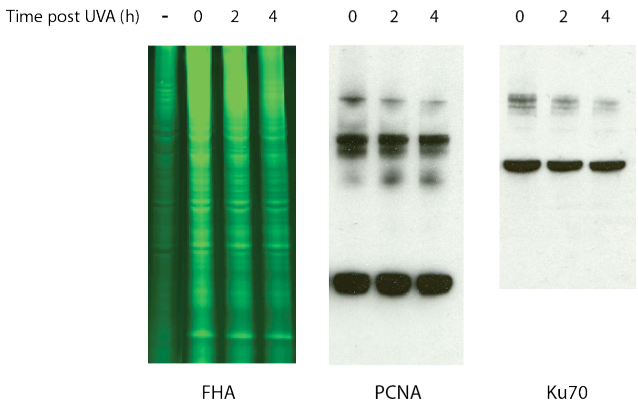


**Figure 4.16 Persistence of ciprofloxacin protein oxidation.**
CEM cells were treated with 500μM ciprofloxacin and 20 kJ/m$^2$ UVA and returned to fresh growth medium. Samples were taken at 0, 2 and 4 hours after irradiation then subjected to FHA analysis and western blot analysis as detailed above.

### 4.2.4 The effects of UVA photosensitisation on NHEJ

The fluoroquinolones ciprofloxacin and ofloxacin both combined with UVA to inhibit NHEJ (Figure 4.17). Ofloxacin did so less effectively than ciprofloxacin as evidenced by the presence of a dimer band in the lane corresponding to ofloxacin/UVA extracts that was not generated by extracts from ciprofloxacin/UVA treated cells.

Like higher doses of 6-TG, vemurafenib inhibited NHEJ independently of UVA irradiation (Figure 4.18). Despite several attempts, I was unable to find a vemurafenib concentration that produced only UVA-dependent inhibition of NHEJ.

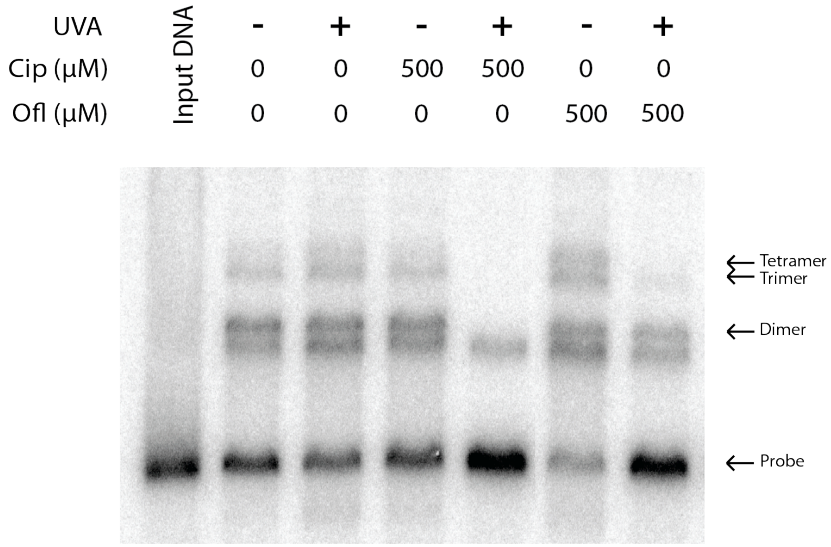


**Figure 4.17 *In vitro* NHEJ assay of extracts from FQ/UVA treated cells**
Extracts were prepared from CEM cells that had been treated with ciprofloxacin (500 µM, 1h), Ofloxacin (500µM, 1h) and UVA (20 kJ/m$^2$) as indicated. NHEJ was assayed as described in Materials and Methods. A representative autoradiograph from two independent experiments is shown.

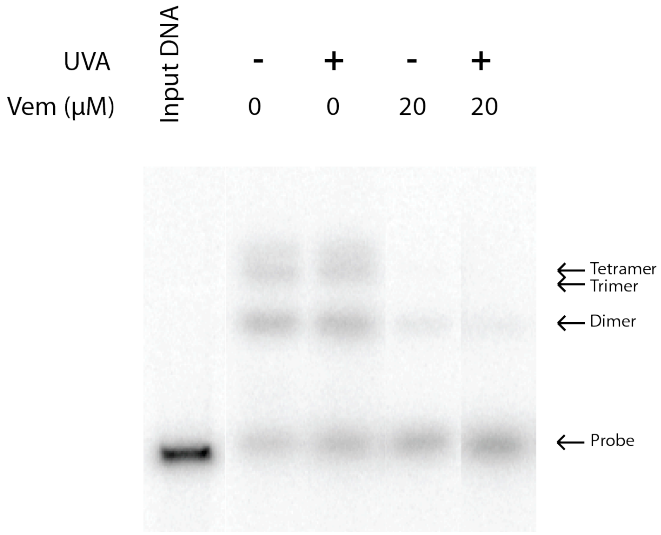


**Figure 4.18 *In vitro* NHEJ assay of extracts from vemurafenib/UVA treated cells**
Extracts were prepared from CEM cells that had been treated with vemurafenib (20 μM) and UVA (20 kJ/m$^2$) as indicated. NHEJ was assayed as described in Materials and Methods. A representative autoradiograph from two independent experiments is shown.

### 4.2.5 The effects of UVA photosensitisation on NER

Treatment with 6-TG/UVA inhibits NER in MRC5VA and HeLa cells (Li 2010; Gueranger et al. 2014). I began by examining this combination in CEM cells. Cells were treated with 6-TG (0.6μM), irradiated with UVA (20 kJ/m$^2$) followed immediately by UVC (20 J/m$^2$). Genomic DNA was isolated at different times after irradiation and (6-4)PP levels were measured by ELISA. The half-time for (6-4)PP repair in untreated cells was 2-3 h and this was unaffected by either UVA or 6-TG treatment. In contrast, 6-TG/UVA treated cells performed no detectable repair during the 4-hour time course (Figure 4.19, top left). Having confirmed that 6-TG/UVA causes NER inhibition in CEM cells, I examined the effect of the other photosensitisers on (6-4)PP removal.

Ciprofloxacin/UVA inhibited NER in a similar manner to 6-TG/UVA and no (6-4)PP excision was observed over 4 hours (Figure 4.19, top right). The effects of ofloxacin were less marked. Although NER was inhibited over 2 hours following irradiation the cells recovered and excised (6-4)PP efficiently thereafter (Figure 4.19, bottom left). These findings also reflect the trend observed in the growth curves and RS

measurements, namely that the effects of ofloxacin are similar to those of ciprofloxacin but somewhat attenuated. The recovery of NER in ofloxacin/UVA treated cells demonstrates that that repair inhibition is potentially reversible, at least in the case of ofloxacin.

A 24-hour treatment with vemurafenib (20 μM) combined with UVA also inhibited NER (Figure 4.19, bottom right). In this case, as with 6-TG/UVA and ciprofloxacin/UVA, there was no indication of recovery of NER. UVA alone or 6-TG, ciprofloxacin, ofloxacin or vemurafenib alone did not detectably affect repair. Taken together these results demonstrate that photosensitisers that are not incorporated into DNA can sensitise UVA toxicity and mimic the effects on NER inhibition of DNA-embedded 6-TG.

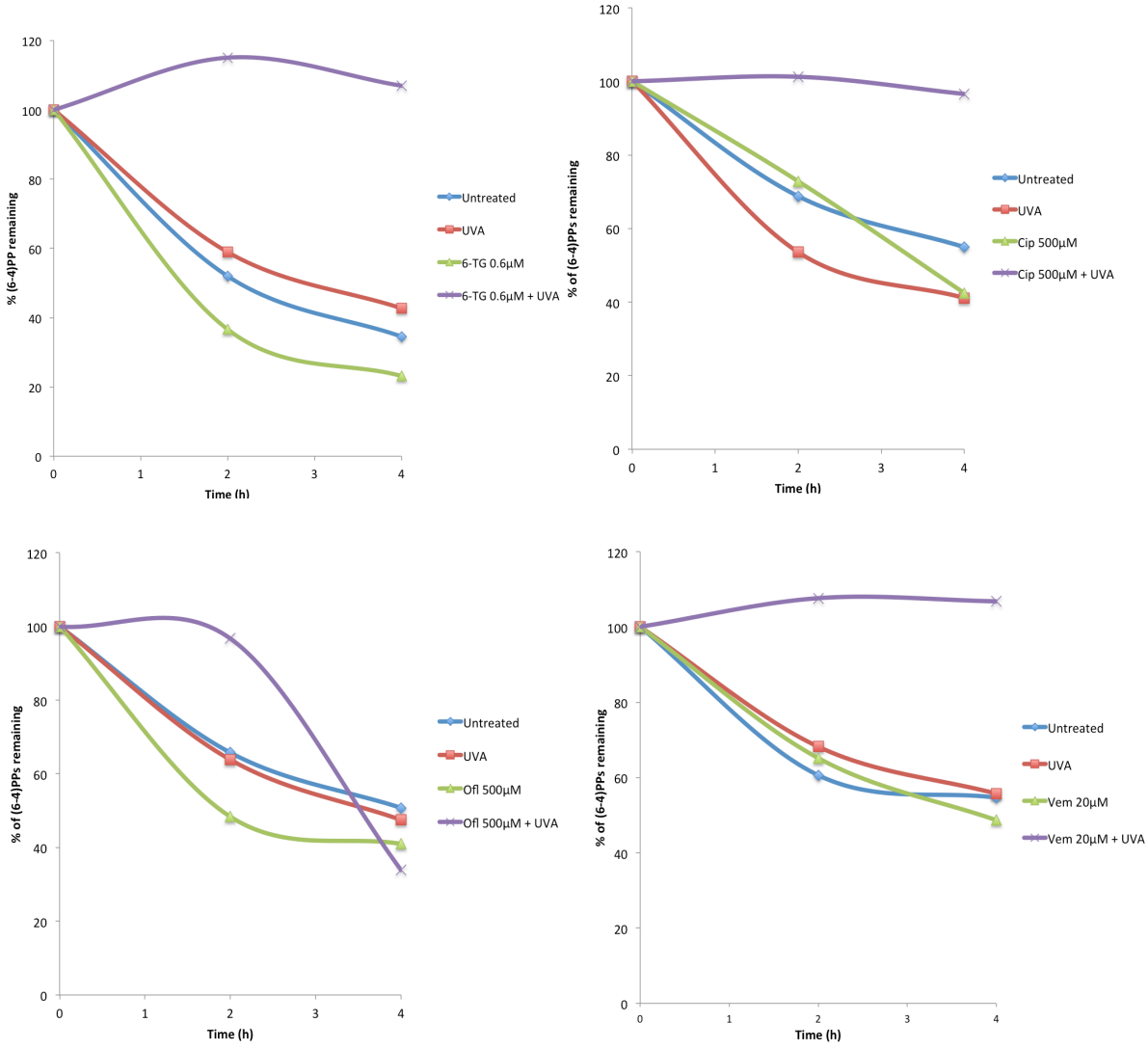


**Figure 4.19 Inhibition of NER by photosensitisers**
CEM cells were treated with drugs (6-TG and vemurafenib 24 h/ ciprofloxacin and ofloxacin 1 h) and UVA (20 kJ/m$^2$) as indicated and then immediately irradiated with UVC (20 J/m$^2$). Irradiated cells were returned to fresh growth medium, genomic DNA was extracted at the indicated times and (6-4)PP levels measured by ELISA. Levels immediately after irradiation are set to 100%. A representative of two independent experiments is shown. Values shown are the mean of triplicate measurements.

## 4.3 Discussion

### 4.3.1 Assessing phototoxicity in the CEM-CCRF cell line

Azathioprine (a DNA 6-TG precursor), ciprofloxacin, ofloxacin and vemurafenib are all pharmaceuticals known to sensitise patient skin to UVA to greater or lesser degrees. Consistent with this property, all were synergistically phototoxic with UVA in CEM

cells. The choice of CEM cells was initially dictated by their resistance to 6-TG (they are MMR-deficient and thus can proliferate in the presence of relatively high concentrations of the thiopurine). An additional advantage of using suspension cells such as CEM is that it facilitates the preparation of extracts for *in vitro* assays for which large quantities of cells are required. On the basis of the growth curves, a working dose range for phototoxicity was established for use in subsequent experiments, although I sometimes worked with supra lethal doses to demonstrate certain effects more conclusively.

### 4.3.2 Generation of RS

To measure intracellular RS, I elected to use the CM-$H_2$DCFDA fluorescent probe. This has been the laboratory standard and enabled me to more easily compare my findings with previous results. Using the CM-$H_2$DCFDA fluorescent probe, I demonstrated that all the compounds tested caused an increase in cellular RS when combined with UVA, although the magnitude of this effect varied. Over the tested dose ranges (taken from the proliferation assays), ciprofloxacin reached the maximal fluorescence value most quickly, followed by 6-TG. Ofloxacin and vemurafenib did not reach this maximum although vemurafenib is a notably weaker RS inducer than ofloxacin. Although CM-$H_2$DCFDA is by far the most commonly used probe for interrogating oxidative stress in cells, there are often misconceptions regarding its specificity. An important but often unheeded caveat when using CM-$H_2$DCFDA is that most primary RS (i.e. the products of initial RS forming reactions) such as $O_2^{\bullet-}$, $H_2O_2$ and $^1O_2$ cannot oxidise the probe directly(Wardman 2007). More reactive secondary RS such as HO•, $NO_2$• (the product of reaction between NO• and $O_2$) and $CO_3^{\bullet-}$ (from $ONOO^-$) oxidise CM-$H_2$DCFDA as does the thiyl radical resulting from GSH deprotonation. Radical cations arising from type I photosensitisation may also be sufficiently reactive. The mechanism of probe oxidation is outlined in Figure 4.20 along with some putative routes through which photosensitisation may give rise to fluorescence. For the purposes of this thesis, CM-$H_2$DCFDA can be said to provide a general indication of cellular redox status. Each of the drug/UVA combinations increases intracellular RS to some degree although this technique can give no information with respect to their identity.

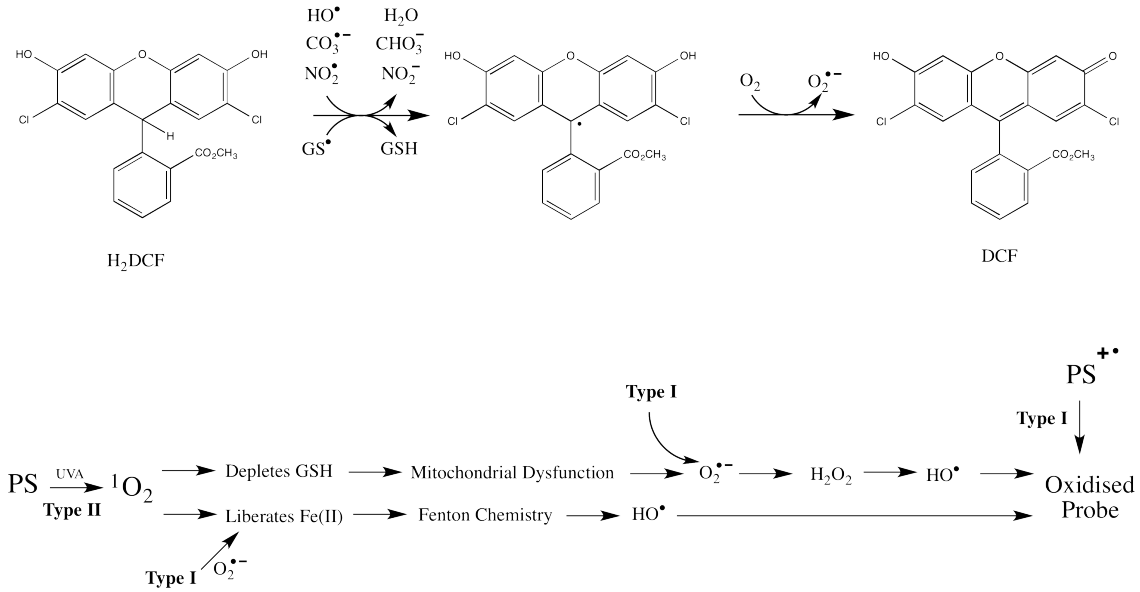


**Figure 4.20 Chemistry of CM-$H_2$DCFDA oxidation**
**Top:** Mechanism of $H_2$DCF oxidation (Chloromethyl- and acetate esters omitted for clarity): The first step towards fluorescence is one electron oxidation or H abstraction by a radical species to give a radical probe intermediate which loses an electron to oxygen to give the oxidised fluorescent probe and $O_2^{\bullet-}$. **Bottom:** Some putative mechanisms by which photosensitisation may give rise to CM-$H_2$DCFDA oxidation are presented. $^1O_2$ may upset the redox state of the cell by depleting antioxidants or liberating free iron, which can then lead to HO• formation and causing probe oxidation. Type I photosensitisation could contribute in a similar fashion through $O_2^{\bullet-}$ generation or directly via a radical cation state.

One additional concern regarding CM-$H_2$DCFDA use applies particularly to vemurafenib. Although the charged form of the probe generated intracellularly cannot traverse membranes by diffusion, it can be actively exported by multidrug-resistant efflux pumps(Wardman 2007). The recently reported stimulation of the MDR-1 efflux pump by vemurafenib(Michaelis et al. 2014) may lead to underestimation of the induced RS, although subsequent results do not suggest this is the case.

The RNO bleaching assay partially addresses some of the limitations of CM-$H_2$DCFDA and serves as a complementary approach to shed light on the likely nature of RS and provide qualitative information on the balance between type I and type II oxidation. The assay indicated that photosensitisation by 6-TG had a more significant type I component than that of ciprofloxacin; this has some bearing on the relative phototoxicities of these two compounds. From Figure 4-8, it is apparent that equitoxic treatments do not correspond to intracellular RS levels. A combination of 6-TG's incorporation into DNA

and its type I photoreactivity means that it can induce lethal damage such as strand breaks, ICLs and DNA-protein crosslinks directly. For photosensitisers with greater type II character, $^1O_2$ mediated damage must accumulate until enough biomolecules are oxidised to cause disruption to cellular processes hence the requirement for greater RS levels to achieve equitoxicity.

Whilst the RS assays described in this section revealed notable differences between 6-TG and ciprofloxacin, vemurafenib gave somewhat unexpected results. In accordance with previous findings(Boudon et al. 2013), I found vemurafenib to be phototoxic in CEM cells. CM-$H_2$DCFDA staining indicated that vemurafenib/UVA treatment was toxic with little concomitant RS generation in a similar fashion to 6-TG. The main conclusion drawn from the RNO assay is that vemurafenib does not produce $^1O_2$ and this finding was later supported by its inability to induce significant Ku or PCNA crosslinking. Taken together, these results suggest vemurafenib photosensitises exclusively by a type I mechanism. Its lipophilicity suggests it will localise to membranes and organelles once inside the cell, which has to be shown increase lethality of photosensitisers (Benov et al. 2010). Within a membrane, a type I photosensitiser can initiate lipid peroxidation which occurs via a chain reaction (Section 1.2.3.1) leading to carbonyl stress via ALEs and release of pro-apoptotic factors from disrupted organelles, a possible route to vemurafenib mediated cell death. Similar low RS, high toxicity, no $^1O_2$ behaviour is also seen in Crystal Violet, which mainly photosensitises via type I and localises to mitochondria(Oliveira et al. 2011).

A more “exotic” route to cellular damage became apparent upon comparing the structures of vemurafenib and lomefloxacin. Lomefloxacin is noted to undergo defluorination upon UVA irradiation(Fasani et al. 1997).; an amine adjacent to the fluorine site stabilises the resulting reactive carbene species (outlined in Figure 4.21 (bottom)). Carbenes are very reactive and would form adducts with biomolecules via the modes of reactivity outlined in Figure 4.21 (top). Vemurafenib contains a similar structure and therefore an interesting alternative mechanism for photosensitisation arises, which would not be detected by the abovementioned techniques.

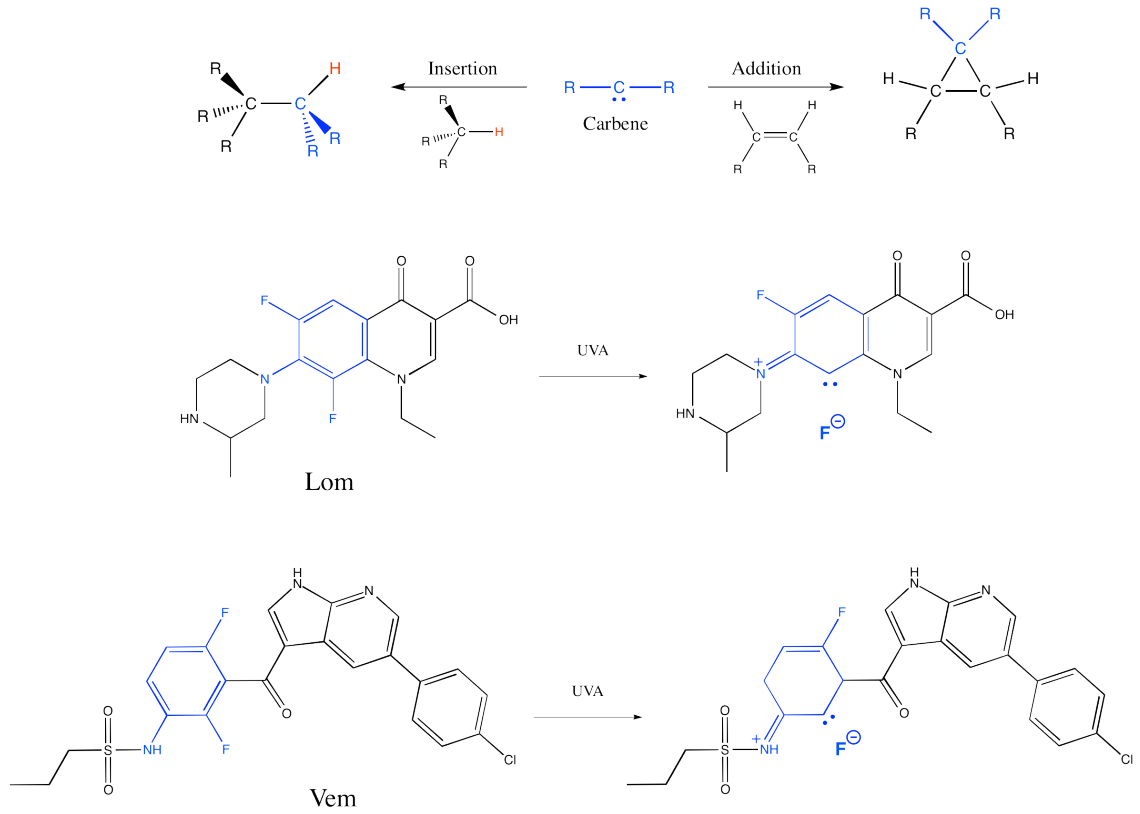


**Figure 4.21 A potential route to carbene formation by vemurafenib**
**Top:** The major reactions of carbenes are addition to double bonds and insertion into C-H bonds; **Middle:** The fluorinated ring with adjacent amine (blue) predisposes lomefloxacin towards defluorination; **Bottom:** Vemurafenib posses structural similarity to lomefloxacin that may also lead to formation of reactive carbenes that could damage cellular components.

### 4.3.3 Protein oxidation by UVA photosensitisers

Photosensitisers with significant type II character as judged by RNO bleaching (i.e. 6-TG and FQs) exhibit a similar suite of effects in combination with UVA including efficient carbonyl induction and the ability to crosslink susceptible multi-protein complexes. Vemurafenib, in contrast, gives a weak carbonyl response across the range of doses corresponding to its proliferation assay. A strong FHA signal occurs after treatment with 50 µM vemurafenib and UVA, 2.5x higher than the dose needed to abolish proliferation. UVA independent protein oxidation is also seen after 50 µM treatment which could be a result of transcriptional modulation. Vemurafenib can activate and inhibit the ERK pathway in a biphasic dose response(Poulikakos et al. 2011), which controls the numerous antioxidant genes with AP-1 promoter sites.

Shorter vemurafenib incubation times should elimination identification of transcription-mediated effects and these experiments are currently underway in the lab.

Ciprofloxacin and ofloxacin mirror 6-TG in their UVA-dependent generation of crosslinked Ku species (Figure 4-13). Vemurafenib induced no significant Ku crosslinking, even at 50 μM/UVA (Figure 4-14), which is associated with significant protein carbonylation. This suggests that Ku crosslinking is not a general marker for protein oxidation but rather a specific response to certain photosensitisers.

A similar pattern is observed for crosslinking of PCNA. Since Montaner et al's initial observation(Montaner et al. 2007), other labs have reported crosslinking of PCNA as a result of photosensitisation by non-DNA incorporated compounds(Bae et al. 2008; Bracchitta et al. 2013). These later reports importantly demonstrated $^1O_2$ dependence of the effect through $D_2O$ potentiation (and histidine inhibition). PCNA is more readily crosslinked than Ku and appears to be a more sensitive measure of intracellular $^1O_2$ production. The $D_2O$ exacerbation shown in Figure 4-15 supports the conclusion that crosslinking of these complexes by 6-TG, ciprofloxacin and ofloxacin is $^1O_2$-mediated. The functional consequences of PCNA crosslinking remain to be determined. The inability of vemurafenib to induce significant PCNA or Ku crosslinking further supports the likelihood, suggested by the RNO bleaching assay, that it is not a type II photosensitiser. Overall, study of protein oxidation elucidated fundamental differences between UVA photosensitisers and provides an indication as to how they photosensitise.

### 4.3.4 The effects of UVA-induced phototoxicity of NHEJ

Like 6-TG, ciprofloxacin and ofloxacin cause UVA-dependent inhibition of NHEJ. Inhibition was synergistic and UVA potentiated the effects of non-inhibitory drug treatments. Photosensitisation with ofloxacin produced an attenuated version of the effects seen with ciprofloxacin. The FQs provided a useful comparison to 6-TG and the findings demonstrate that NHEJ inhibition is not dependent on the specific photochemistry of 6-TG.

Vemurafenib also causes NHEJ inhibition but unfortunately UVA-dependence was not established. At sufficiently high doses, vemurafenib inhibits the ERK pathway in cells that do not have the target V600E mutated BRAF. This alters transcription profiles and proliferation(Poulikakos et al. 2011). ERK pathway inhibition has previously been shown to reduce expression of DNA-PKcs(Marampon et al. 2011) and MEK inhibitors sensitise cells to ionising radiation. In light of these data, vemurafenib might influence NHEJ through an effect on DNA PKcs expression. Reducing treatment time to 1 hour should minimise any effects on transcription and allow photosensitising effects to be assessed.

### 4.3.5 The effects of UVA induced phototoxicity on NER

All tested compounds caused UVA-dependent inhibition of NER. Firstly, this confirms the finding of Dr Feng Li(Li 2010) that UVA activation of DNA-embedded 6-TG inhibits NER. My findings also indicate that the vulnerability of NER to photochemical inhibition extends to other photosensitisers, yielding new mechanistic insight.

The two most obvious mechanisms by which 6-TG/UVA might cause NER inhibition are:

- The introduction of competing or obstructing DNA lesions
- Oxidation and inactivation of repair proteins

DNA-6-TG photoactivation induces $G^{SO2}$ and $G^{SO3}$. These two polymerase-blocking lesions are not themselves NER substrates(Li 2010). They may however, prevent access of repair factor to UVC photoproducts. Photoactivated DNA 6-TG forms ICLs that prevent strand segregation(Brem et al. 2011). ICLs and DNA-6-TG related DNA-protein crosslinks(Gueranger et al. 2011) might hinder access to lesions. The observation that XPA is among the crosslinked proteins suggests further that depletion of repair factors might also play a role in inhibiting NER. Thus all the available evidence of the effects of 6-TG/UVA is compatible with a DNA lesion-mediated NER inhibition. These findings do not, however, exclude non-DNA related mechanisms.

My finding that structurally unrelated photosensitisers are also able to inhibit NER establishes the principle the DNA incorporation is not essential for UVA sensitised inhibition of NER and provides more evidence for a DNA-independent mechanism. Evidence for an important contribution of protein-damage to NER inhibition was obtained from an *in vitro* NER assay that examines the ability of nuclear extracts from treated cells to excise a cisplatin intrastrand crosslink from plasmid DNA (Figure 4.22, top). Nuclear extracts from 6-TG/UVA treated cells have reduced NER activity in this assay(Gueranger et al. 2014)(Figure 4.22, middle left). Extracts prepared from UVA irradiated cells treated with ciprofloxacin or ofloxacin are also deficient in NER (these experiments were performed by Peter Macpherson, Figure 4.22 bottom), confirming the link to protein damage. In agreement with the generally more severe biological effects of ciprofloxacin/UVA that I have observed, this combination was more severely inhibitory than ofloxacin/UVA.

Surprisingly, extracts from cells treated with vemurafenib/UVA appear to retain undiminished NER activity, contradicting the results from the ELISA. Although the reasons for this apparent discrepancy are not clear at present, there are several possibilities:

- Altered UVA dosimetry. Large numbers of cells are required to make the active extracts, which could lead to shielding effects. Although measures are taken to minimise dose attenuation due to different irradiation conditions, it is possible that these are not sufficient and the UVA dose received by the cells used to prepare the extracts is sub-inhibitory for vemurafenib/UVA but not the other compounds.
- The inherent artificiality of the *in vitro* assay. In preparing nuclear extracts, it is essential that high protein concentrations be maintained, as dilute extracts are invariably inactive. It is therefore possible that by concentrating levels of NER proteins that would be sub-optimal *in vivo*, it is possible to prepare an active nuclear extract. In addition, inclusion of high concentrations of reducing agent is essential during extract preparation. Partial restoration of enzyme activity by artefactual reduction of oxidised proteins is also a possibility. One could envisage a scenario in which strong (e.g. ciprofloxacin) and weak (e.g. vemurafenib) RS-generating photosensitisers both inhibit NER in cells through thiol oxidation, with the more potent photosensitiser leading to formation of irreversible sulphur oxidation

products (i.e. sulfinates and sulfonates). Exposure to reducing agents upon extract preparation would be able to reduce disulphides and restore activity in extracts from the weaker photosensitiser hence giving a discrepant response between *in vivo* and *in vitro* experiments, whilst the stronger photosensitiser would give a negative result in both cases.

- Chromatin effects. The *in vitro* NER substrate is naked plasmid DNA. Any effects related to chromatin will not be apparent in the assay.

Further experimental work is required to test the various possibilities and reconcile these discrepant observations.

Although some of the finer mechanistic details are yet to be elucidated, the available data indicate that oxidation of key proteins is responsible for the inhibition of NER. NER can restored *in vitro* by complementation of extracts with purified RPA(experiment performed by Quentin Gueranger, in collaboration with Annabel Larnicol-Fery, Figure 4-22, middle right), which is known to be redox-sensitive(Men et al. 2007) (Further discussion of enzyme susceptibilities in Chapter 6). The *in vitro* assay does not entirely recapitulate the situation within cells and contributions from other oxidised NER factors or DNA damage that inhibits repair cannot be excluded.

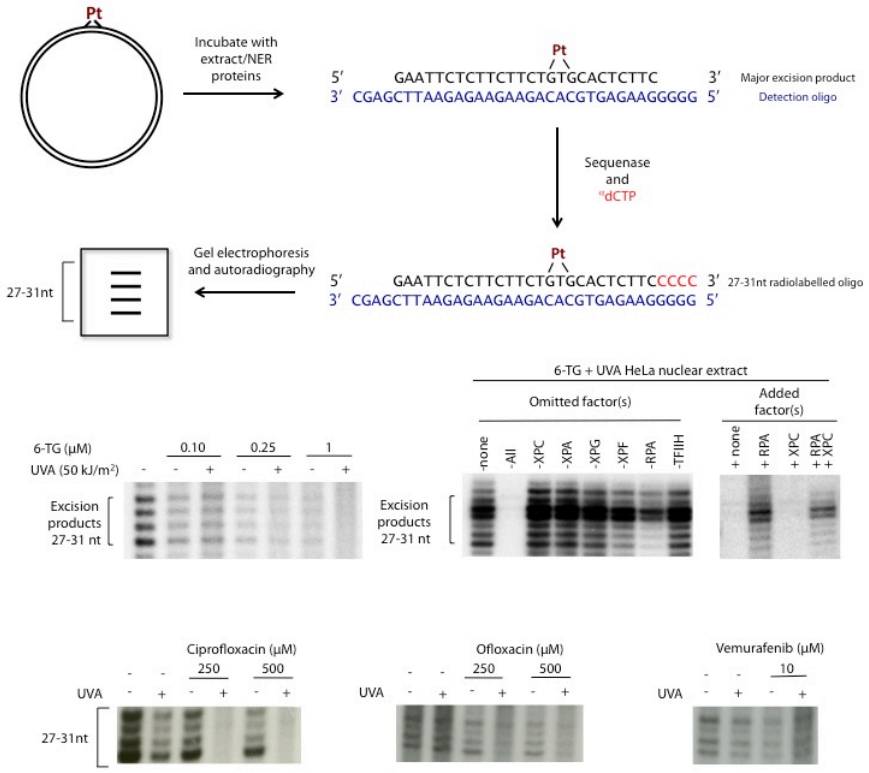


**Figure 4.22 Nucleotide excision repair *in vitro***
**Top:** Schematic of the *in vitro* NER assay. A circular duplex DNA substrate containing a single cisplatin intrastrand crosslink is incubated with nuclear extracts or purified NER proteins. Excision products are detected by hybridization to a complementary oligonucleotide with a 5'-GGG overhang that permits radiolabelling with Sequenase and α-$^{[32]}$P labeled dCTP. Labeled products are resolved by denaturing PAGE. **Middle, left:** The detected products of the *in vitro* assay for nuclear extracts from HeLa cells treated with 6-TG and UVA as indicated. **Middle, right:** Nuclear extracts from 6-TG/UVA treated cells replace omitted factors in a reconstituted NER system. Extracts cannot fully complement a reaction missing RPA. In the reciprocal experiment, purified RPA is able to complement defective extracts. **Bottom:** The detected products of the NER assay for extracts made from CEM cells treated with FQs/UVA and Vem/UVA as indicated.

## 4.4 Summary

I have demonstrated a number of consequences arising from UVA-dependent photosensitisation of cultured cells. Comparative measurements of phototoxicity and RS production suggest that different mechanisms could operate in the three different drug classes. The FQs replicated the protein oxidation behaviour of 6-TG characterised in Chapter 3 whereas vemurafenib did not and appears to be mechanistically distinct from the other tested compounds.

Extracts from 6-TG and ciprofloxacin treated cells showed significant UVA-dependent abrogation of NHEJ activity. The effect of ofloxacin/UVA is less dramatic, in keeping with generally less severe photosensitisation in other assays. Vemurafenib affected NHEJ in a UVA-independent fashion that may reflect its influence on transcription.

My findings, together with those of other lab members, provide strong evidence that NER is compromised in photosensitised cells and that this reflects, at least in part, damage to repair proteins, including RPA. As such, the link between protein oxidation and DNA damage repair seems worthy of further investigation.

In the final results chapter, a potential mechanism for repair inhibition without the direct damage to repair factors seen here is explored.

# Chapter 5. Possible sequestration of an NER factor by 6-TG/UVA photoproducts

## 5.1 Introduction

The *in vitro* assays discussed in the previous chapter indicate that protein damage induced by oxidative stress conditions can inhibit DNA repair in cultured cells. DNA damage-related events may also contribute to this inhibition in intact cells. The preliminary experiments described in this chapter were performed to investigate whether NER capacity may be affected by interference with lesion recognition.

### 5.1.1 Lesion recognition in NER

NER is a versatile system that can excise a variety of DNA lesions in addition to UVR photoproducts. Rather than recognising the structure of a particular lesion, the NER damage sensing factors, XPC (with its partner HR23B) and UV-DDB, utilise a β-hairpin to probe for helical distortion and thermodynamic destabilisation induced by the lesion. They do this *via* subtly different mechanisms. XPC binds to the strand opposite the lesion, inserting the hairpin to flip out and bind the undamaged bases opposite the lesion whilst loosely binding the lesion itself(Min & Pavletich 2007). Provided that disruption of base pairing is sufficient to permit extrusion of the damaged base pair, XPC can perform lesion recognition. The most abundant UVR photoproducts, CPDs, are poor XPC substrates probably due to their relatively mild effect on duplex structure and $T_m$(Jing et al. 1998). Localisation of the XPC complex to CPDs is stimulated by DDB2, the product of the XPE gene(Fitch, Nakajima, et al. 2003b). DDB2 is the DNA binding element in a larger, constitutively assembled complex that also contains DDB1, CUL4A and RBX1(Scrima et al. 2008). In contrast to XPC binding, the DDB2 complex binds to the damaged DNA strand. This binding induces a 40° kink and it is this enhanced distortion that is thought to stimulate subsequent recruitment of XPC. The β-hairpin of DDB2 displaces the lesion into a shallow recognition pocket that appears to be optimised for binding to CPDs(Fischer et al. 2011). Thus, the current consensus is that DDB2 selectively enhances CPD recognition by XPC. Consistent with this

possibility, XP-E cells, which lack functional DDB2, have normal TC-NER but are defective in repair of CPDs by GG-NER(Hwang et al. 1999). Since repair of the more distorting (6-4)PPs occurs predominantly through direct recruitment of XPC, (6-4)PP excision by XP-E cells is normal although rates may be somewhat reduced especially at low UV doses(Nishi et al. 2009; Moser et al. 2005).

The ubiquitin ligase activity of the DDB2-DDB1-CUL4-RBX1 complex plays an important role in orchestrating repair events. It is activated by binding to DNA and catalyses the ubiquitination of DDB2, XPC and other targets, including histones(Fischer et al. 2011). Histone ubiquitination is responsible for the chromatin remodelling activity of DDB2(Luijsterburg et al. 2007) which may be important for access by repair factors especially in nucleosomes. Importantly, ubiquitination reduces DDB2's affinity for DNA and marks it for degradation. In contrast, XPC ubiquitination increases its affinity for DNA. The differential effects of this modification may underlie the handover of lesions from DDB2 to XPC for subsequent processing(Sugasawa et al. 2005).

Although DDB2 binds a variety of non-photoproduct lesions *in vitro* including abasic sites and mismatches (Wittschieben et al. 2005) as well as adducts induced by nitrogen mustard, N-methyl-N'-nitroso-N-nitrosoguanidine and cisplatin(Payne & Chu 1994), it probably does not participate in their repair. Indeed, cisplatin does not induce XPC ubiquitination suggesting that *in vitro* recognition by DDB2 is not necessarily a good indication of *in vivo* recognition(Sugasawa 2006); cisplatin intrastrand crosslinks are a good substrate for *in vitro* NER assays suggesting that direct XPC recognition may predominate.

In principle, the effectiveness of NER in preventing mutation by sunlight might be compromised if skin cells sustain DNA damage that competes at the initiating recognition step. UVA irradiation of cells containing DNA 6-TG leads to the formation of bulky sulfinate and sulfonate lesions (Figure 5. 1) that impede replicative polymerases but can be bypassed by lower fidelity translesion polymerases. The biological consequences of this type of DNA damage are unclear.

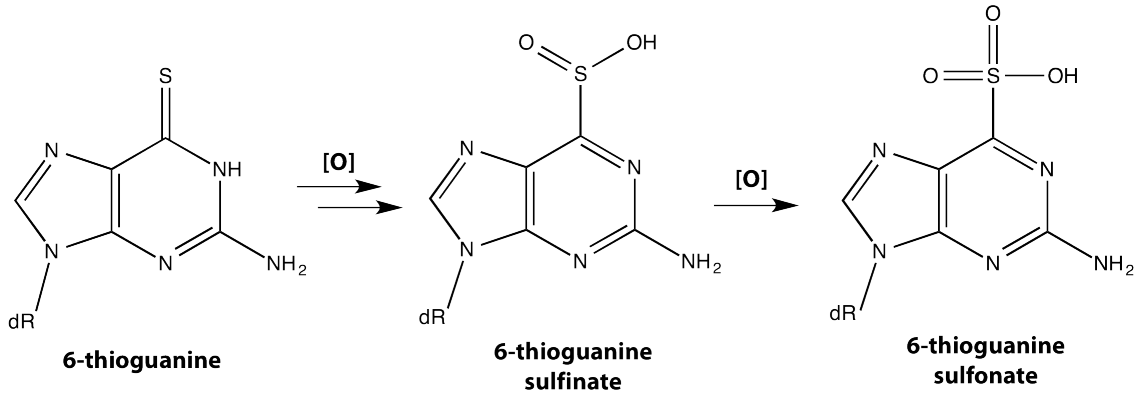


**Figure 5.1 6-Thioguanine and its oxidation products**
UVA irradiation of DNA-6-TG leads to the formation of the 6-TG photoproducts, guanine sulfinate ($G^{SO2}$) and sulfonate ($G^{SO3}$).

These lesions appear not to be processed by TC-NER as CSB mutant cells are no more sensitive to 6-TG than their repair proficient counterparts(Brem et al. 2009). This is also true of XPG mutants but cells lacking XPF or polymerases Polη, Polι, and Polζ are all sensitive to 6-TG/UVA presumably reflecting the role of translesion synthesis in processing 6-TG-mediated ICLs or other lesions(Brem et al. 2011). $G^{SO2}$ and $G^{SO3}$ do not appear to be good substrates for removal by NER and the levels of these lesions decrease at similar rates in NER proficient and deficient (XPA) cells (around 60% remained after 24 hours)(Li 2010). UVA activation of some FQs induces T<>T CPDs by a triplet energy transfer mechanism, which could increase the burden on the NER system. The ability of vemurafenib to cause DNA damage has not been investigated.

To examine whether these photosensitising treatments might compromise lesion recognition, I first assessed their ability to provoke a DDB2 response.

## 5.2 Results

### 5.2.1 UVC and DDB2

The effects of UVC on DDB2 have been widely studied(Rapić-Otrin et al. 2002). Figure 5-2 (top) shows that DDB2 is detectable by western blotting of low-salt extracts

of CEM cells and that following UVC treatment it is no longer extractable under low salt conditions. This is in accordance with previously published data that indicate a damage-dependent DDB2 relocalisation to chromatin, and a requirement for high salt extraction for its removal(Otrin et al. 1997). DDB2 levels remained low for 1-2h but recovered within 3 hours. During this period, DDB1 levels remain unchanged and are included as a loading control. Although p53 status is known to affect DDB2 expression levels(Hwang et al. 1999) and CEM is a p53-negative cell line, this is only likely to become important at time points later than 24h(Rapić-Otrin et al. 2002) and it appears, at least at early time points, CEM cells have a the normal DDB2 response to UVC. Figure 5-2 (bottom) shows loss of extractable DDB2 can be induced at doses of UVC as low as 1-5 J/m$^2$. High doses of UVA are needed (200kJ/m$^2$) to see even partial loss of DDB2 from extracts, in keeping with the relative DNA damaging abilities of these wavelengths.

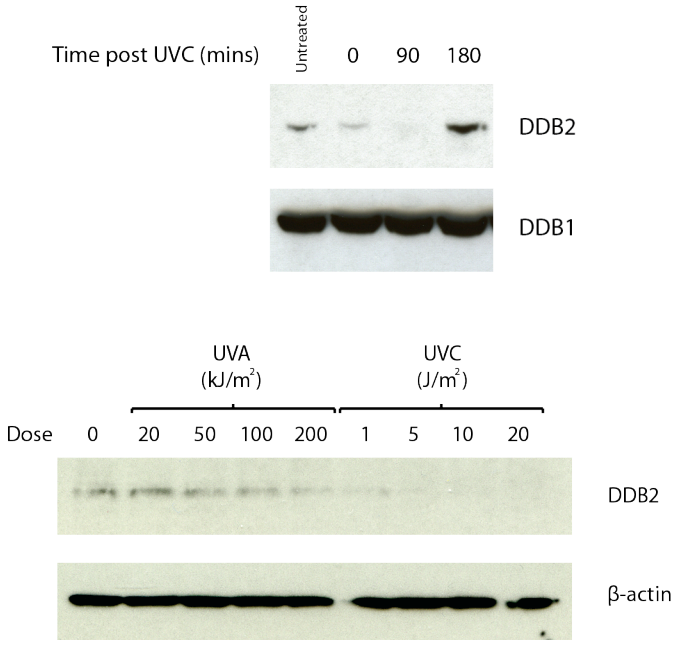


**Figure 5.2 Effects of UVC and UVA on DDD2 on CEM cells**

**Top:** CEM cell extracts prepared at the indicated time after UVC (20 J/m$^2$) irradiation were analysed by western blot with DDB2 and DDB1 primary antibodies.
**Bottom:** Extracts prepared immediately after the indicated dose of UVA or UVC were analysed by western blot.

### 5.2.2 DDB2 relocalisation induced by photosensitisers

Figure 5-3 shows a western blot analysis of the effects of 6-TG, ciprofloxacin and vemurafenib treatment with and without UVA irradiation. In the absence of UVA, none of the drug treatments affected the levels of extractable DDB2. After irradiation with UVA, DDB2 is not recovered in extracts from cells treated with 6-TG or ciprofloxacin whereas vemurafenib had no discernable effect. The 6-TG dose was titrated to determine the minimum needed to induce DDB2 relocalisation (Figure 5-4). The minimum dose required to yield a visible effect lies between 0.03 μM and 0.1 μM in growth medium concentration. Thus, the loss of extractable DDB2 one of the most sensitive indicators of 6-TG photosensitisation found to date.

The kinetics of DDB2 relocalisation after 6-TG/UVA were also examined. Figure 5-5 confirms that DDB2 in 6-TG treated cells becomes resistant to low salt buffer extraction immediately after UVA irradiation. No recovery of extractable DDB2 was apparent during subsequent 3 h incubation in full growth medium. Including the recombinant endonuclease Benzonase in the extraction buffer leads to partial recovery of DDB2. Since Benzonase degrades chromatin DNA and releases bound proteins, this observation confirms that the treatment induces tight binding of DDB2 to DNA.

### 5.2.3 DNA Damage

Some FQs are known to induce T<>T CPDs by a Type I UVA photosensitised reaction. This provides a possible explanation for the ability of ciprofloxacin/UVA to induce DDB2 relocalisation although there appear to be no reported data for CPD induction by ciprofloxacin. Ofloxacin is reported not to photosensitise this type of DNA damage(Cuquerella et al. 2011). Whether 6-TG/UVA induces these lesions is not known.

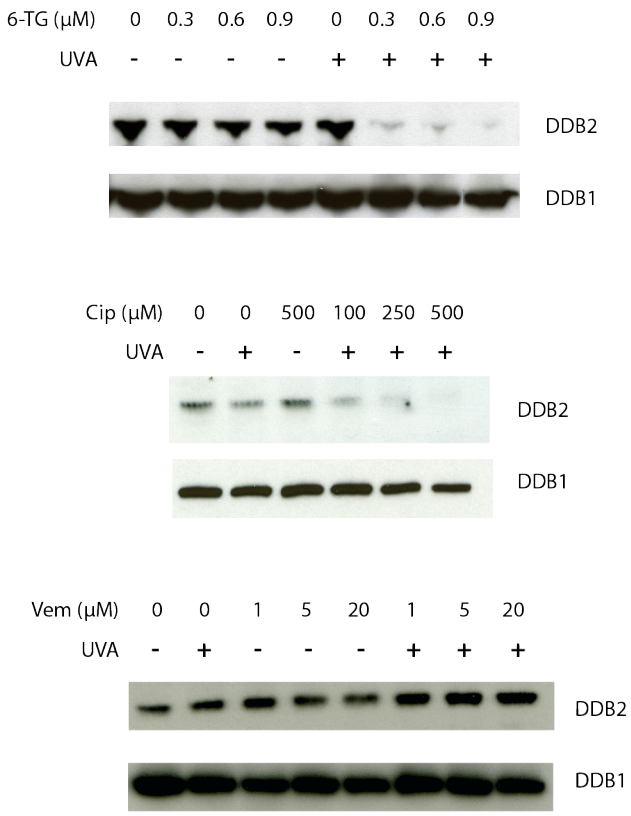


**Figure 5.3 Effect of photosensitisers on DDB2**
Extracts prepared from UVA (20kJ/m$^2$) irradiated drug-treated CEM cells (24h 6-TG and vemurafenib/1h ciprofloxacin) were analysed by western blotting.

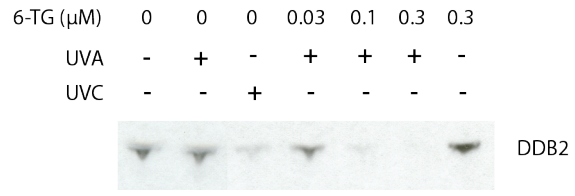


**Figure 5.4 Effects of 6-TG dose on DDB2 relocalisation**
Extracts prepared from UVC (20J/m$^2$) irradiated or UVA (20 kJ/m$^2$) irradiated 6-TG-treated (24h) CEM cells were analysed by western blotting.

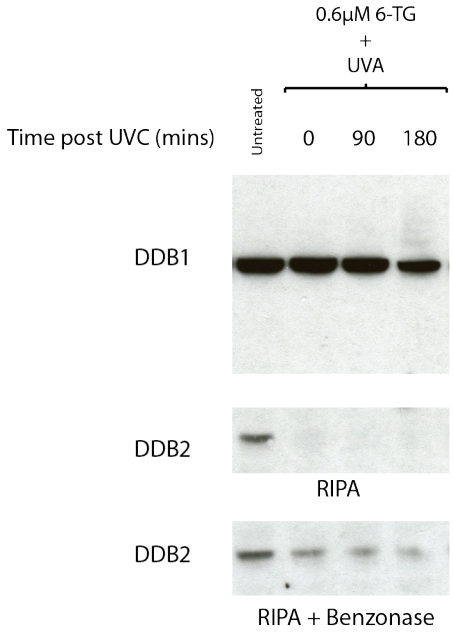


**Figure 5.5 Kinetics of DDB2 localisation induced by 6-TG**
Cells were treated with 6-TG (0.6μM/24h) and UVA (20kJ/m$^2$) and extracts were prepared at the times indicated. Cells were harvested and divided into two fractions that were extracted in the presence or absence of Benzonase (>2.5 U/μL).

CPD and (6-4)PP induction was therefore examined by ELISA. Figure 5-6 (top) shows that ciprofloxacin/UVA is a significant source of CPDs in UVA-irradiated CEM cells. CPD induction was dose-dependent over the concentration range examined and levels were approximately equivalent to UVC doses of 5-20 J/m$^2$. The same assay showed that UVA alone induces barely detectable CPDs at the doses relevant to these experiments whilst CPDs were undetectable following 6-TG/UVA treatment. UVC induced the expected dose dependent increase in (6-4)PPs (Figure 5-6, bottom). Treatment with ciprofloxacin/UVA, 6-TG/UVA or UVA alone did not yield detectable (6-4)PPs.

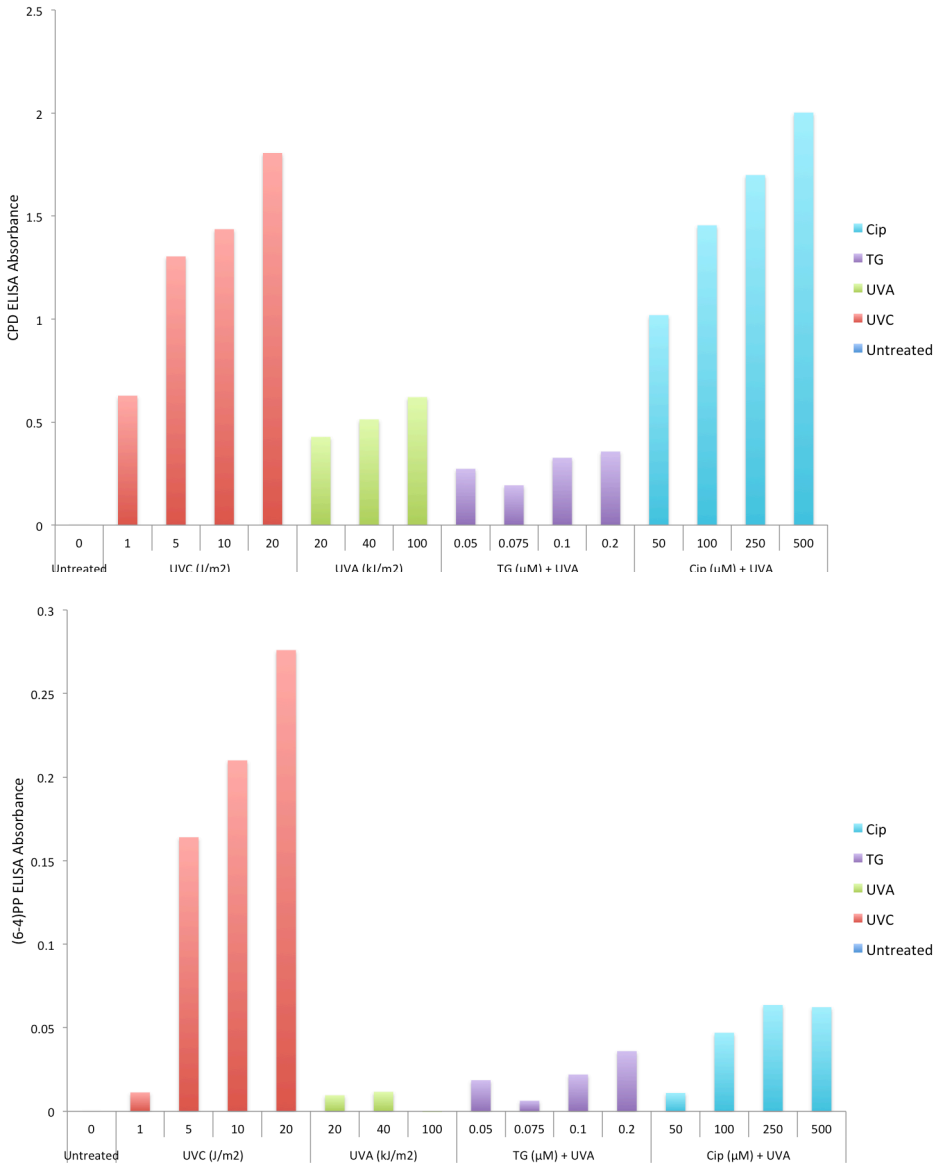


**Figure 5.6 CPD and (6-4)PP ELISA absorbance after UVC, UVA, 6-TG and ciprofloxacin treatment.**
**Top:** CPD and **Bottom:** (6-4)PP ELISAs were performed on genomic DNA from CEM cells treated with UVC, UVA, 6-TG/UVA, or Ciprofloxacin/UVA as indicated.

The ELISA data place ciprofloxacin in the group of FQs that photosensitise T<>T CPD formation by UVA. To establish whether this photochemical DNA damage is responsible for DDB2 relocalisation, I compared CPD induction and DDB2 relocalisation in the same cells treated with ciprofloxacin/UVA or ofloxacin/UVA. As positive controls I included the fluoroquinolones lomefloxacin and norfloxacin as both are reported to induce CPDs with UVA (Cuquerella et al. 2011). Figure 5.7 (top) shows

that ciprofloxacin, norfloxacin and lomefloxacin all induced DDB2 relocalisation when combined with UVA radiation. In contrast, ofloxacin had a barely detectable effect on the yield of extractable DDB2. ELISA (Figure 5.7, bottom) confirmed that ciprofloxacin, norfloxacin and lomefloxacin induce significant levels of CPDs in cellular DNA whereas ofloxacin is much less effective in this regard. I conclude that relocalisation of DDB2 by UVA activated FQs reflects their ability to induce CPDs, which may lead to direct competition for NER recognition with UVB-induced DNA lesions. Importantly, 6-TG/UVA does not generate CPDs (or (6-4)PPs) main lesions recognised by DDB2. This treatment does, however, cause DDB2 relocalisation. I therefore examined possible binding of DDB2 to DNA 6-TG photoproducts.

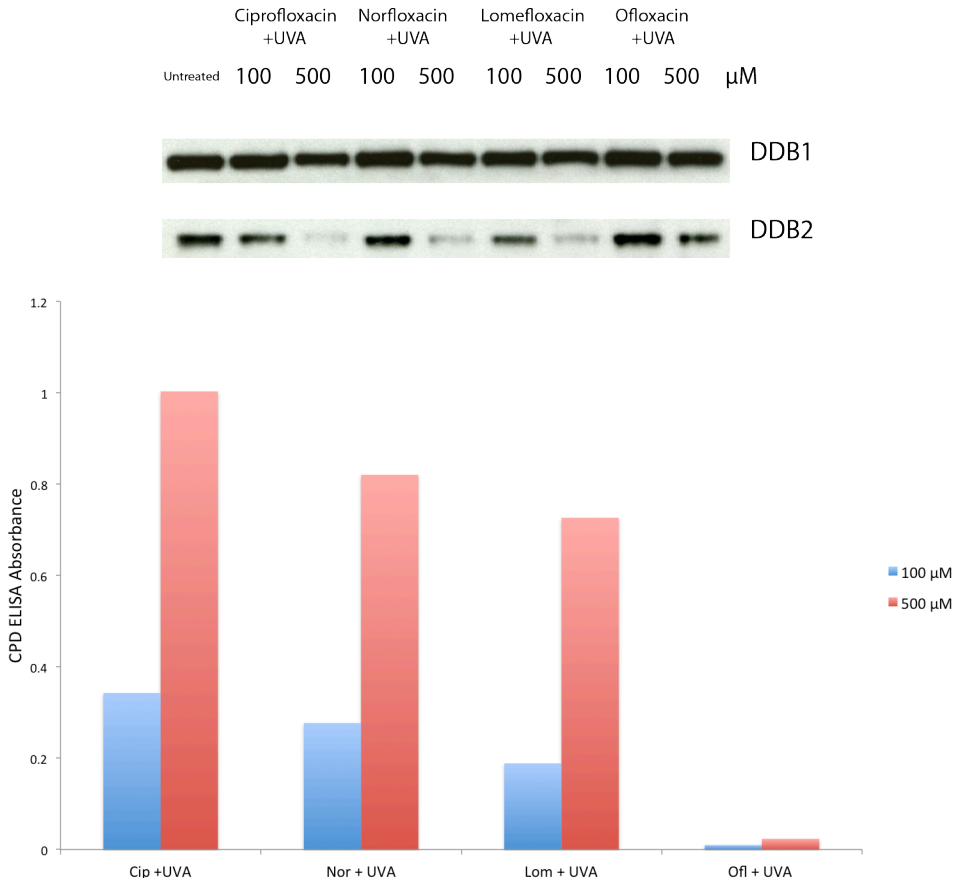


**Figure 5.7 Comparison of CPD induction with DDB2 extractability for FQs**
CEM cells were treated with FQs for 1h at the doses indicated and then irradiated with UVA (20 kJ/m$^2$). Cells were split into two fractions. From one half, DNA was extracted and a CPD ELISA was performed (top). The other half was extracted and Western blot analysis for DDB2 was performed.

### 5.2.4 DDB2 binding 6-TG photoproducts

I used two approaches to investigate possible DDB2 binding to DNA 6-TG photoproducts. In the first, genomic DNA from untreated and 6-TG/UA treated cells was immobilised on a nylon membrane and used as a bait for DDB2 binding. Following blocking and extensive washing, membranes were exposed to cell extracts. After further washing, membranes were probed with anti-DDB2 antibody. DNA binding was checked Sybr Green staining. Figure 5.8 (top) shows a comparison of binding to DNA from untreated and from 6-TG/UVA treated cells. At 1µg DNA, a DDB2 signal is seen for both untreated and treated samples, consistent with the known high DDB2 affinity for DNA even in the absence of damage(Wittschieben et al. 2005). At 100ng DNA from 6-TG/UVA cells recruits more DDB2 than undamaged DNA. Figure 5.8 (bottom) reveals that differential DDB2 binding could also be observed to DNA from UVC-treated and ciprofloxacin/UVA- treated cells. Since the extracts used were from naïve cells that had not been exposed to damaging treatment, DNA lesion recognition is a more likely explanation for these findings than, for example, an oxidative activating DDB2 modification.

In a second approach, I used EMSA analysis to explore the possible identity of lesions provoking DDB2 recruitment. A 30mer oligonucleotide containing a single 6-TG and its non 6-TG-containing counterpart were end-labelled and either UVC (25kJ/$m^2$) or UVA (20kJ/$m^2$) irradiated. After annealing to a complementary oligonucleotide, the duplex probes were incubated with a CEM cell extract. Figure 5.9 (top) shows that the reaction conditions (originally developed to investigate DDB2 binding(Wittschieben et al. 2005)) reveal binding by CEM cell extracts that produces a shift in migration of the UVC-irradiated probe. A retarded complex with similar migration was apparent with the UVA-irradiated 6-TG containing duplex. No binding was observed in the absence of irradiation or to the non-6-TG probe irradiated with UVA.

In the experiment shown in the lower panel of Figure 5.9, a third probe is included in which the 6-TG was stoichiometrically converted to $G^{SO3}$ by treatment with the mild

oxidising agent, magnesium monoperoxyphthalate (MMPP). Binding was more pronounced than to the same oligonucleotide irradiated with UVA. Since UVA irradiation generates a mixture of 6-TG photoproducts and not exclusively $G^{SO3}$, this observation suggests that $G^{SO3}$ is a likely target for DDB2 binding. Inclusion of a 25-fold excess of unlabelled UVC competitor in the binding assay abolished the low level binding to the UVA-irradiated 6-TG duplex. This concentration of competitor oligonucleotide had little impact on the more extensive binding to the MMPP-treated substrate. It also had only a minor effect on the UVC-irradiated complex, however.

Taken together, the filter binding and EMSA experiments indicate that a damaged-DNA binding protein, most likely DDB2, recognises and binds to DNA 6-TG photoproducts. This case is further strengthened by the observation that chemical oxidation of the DNA 6-TG with MMPP, which does not react with canonical bases and has previously been used to quantitatively generate $G^{SO3}$(X. Zhang et al. 2007) increases binding. This indicates that the $G^{SO3}$ photoproduct is a good substrate for DDB2 binding and for possible irreversible sequestration in cells treated with 6-TG and UVA.

In summary, although these observations should be regarded as preliminary, they are consistent with sequestration of DDB2 by non-productive binding to 6-TG photoproducts, most likely $G^{SO3}$, that are not NER substrates.

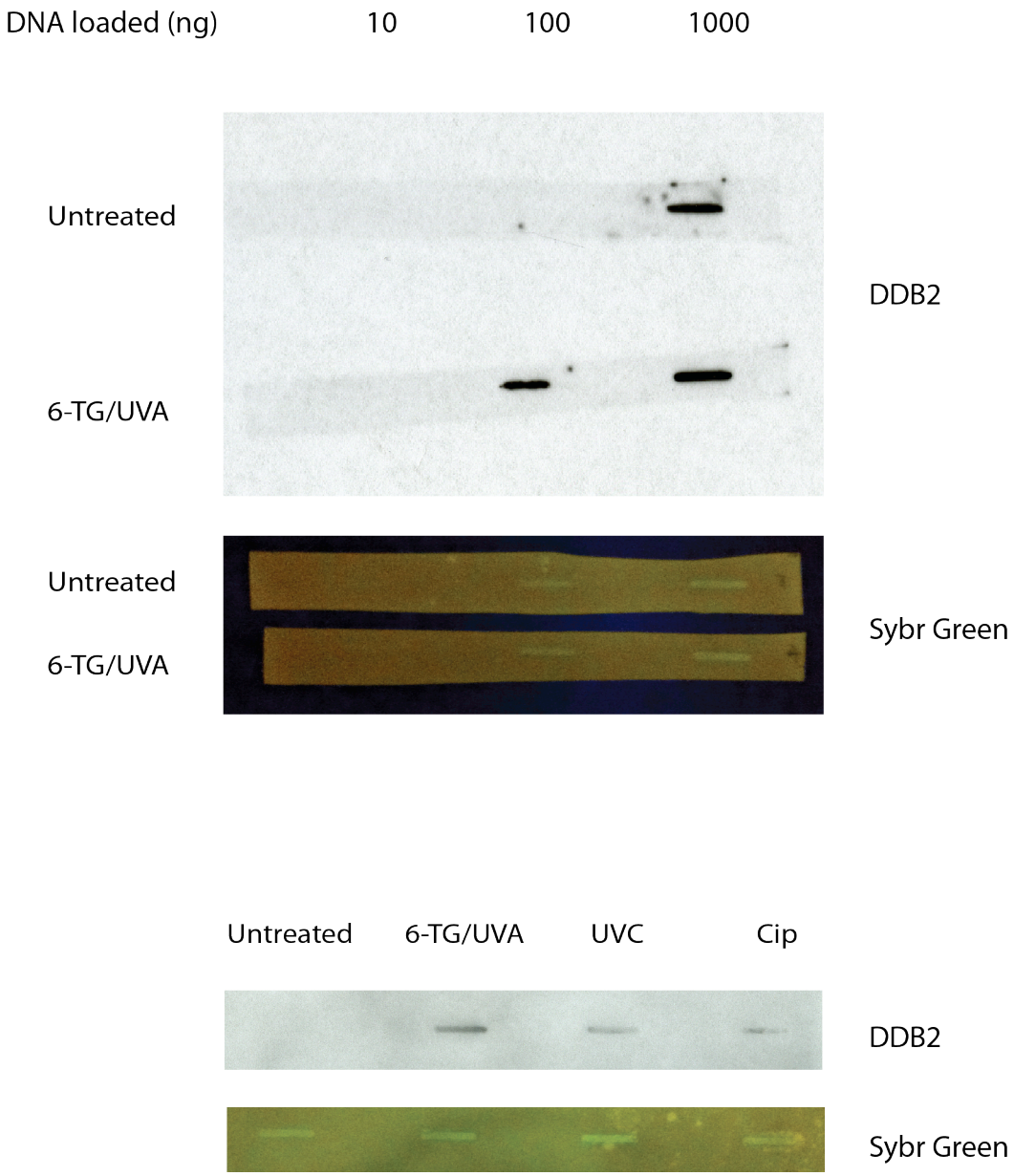


**Figure 5.8 Binding of DDB2 by membrane bound genomic DNA**
**Top:** Genomic DNA from untreated cells and cells treated with 0.6μM 6-TG/ 24 h and UVA (20kJ/m$^2$) was slot blotted onto a nylon membrane. The membrane was exposed to a whole cell extract in 1% Triton X-100-HEPES buffer (Materials and Methods). After blocking and washing, membrane strips were probed with anti-DDB2. DNA loading was checked by Sybr Green staining (lower panel). **Bottom:** The procedure was carried out as above with the inclusion of DNA from UVC (100J/m$^2$) and ciprofloxacin/UVA treated cells (500μM/1h) at a fixed DNA loading of 250 ng.

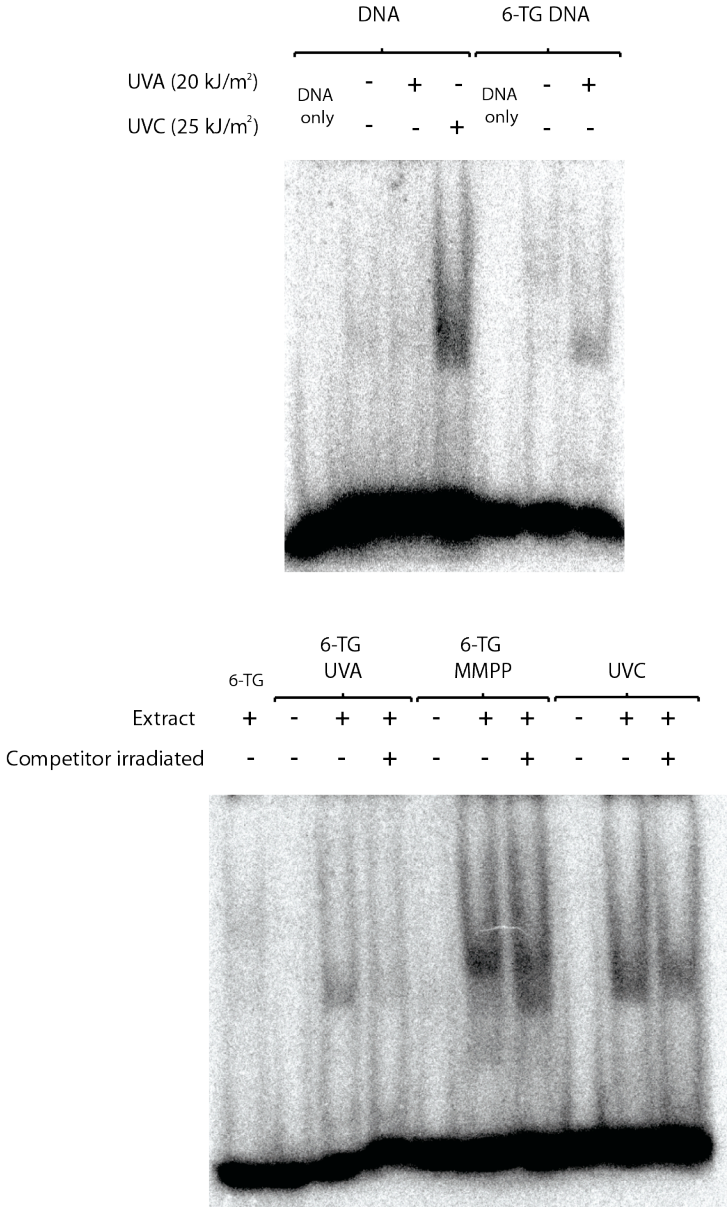


**Figure 5.9 EMSA for irradiated 6-TG containing oligonucleotide**
**Top:** $^{32}$P end-labelled 30 mer single stranded oligonucleotides with or without 6-TG were irradiated with UVC (25kJ/m$^2$) or UVA (20kJ/m$^2$) and annealed to a complementary strand. The radiolabelled double stranded probe was incubated with CEM cell extract for 30 mins at room temperature in the presence of 1µg poly(dA:dT). **Bottom:** As above with a third probe: a 6-TG oligonucleotide oxidised chemically with 10 fold-molar excess of MMPP. A 25-fold excess of non-radioactive competitor oligonucleotide that was irradiated with UVC where indicated was included. Buffers and conditions can be found in Materials and Methods.

## 5.3 Discussion

### 5.3.1 The effect of photosensitisation on DDB2 localisation

Despite more than two decades of study, a full understanding of the role played by DDB2 in NER remains elusive. It was initially linked to NER by the inability of XP-E cell extracts to delay the migration of UVC-damaged DNA in EMSA assays(Chu & E. Chang 1988). There exists a broadly accepted consensus that upon UV-DDB binding, a lesion is rendered more attractive to XPC due to amplified helical distortion. Concurrently the ubiquitin ligase activity of DDB1-CUL4-RBX1 is stimulated leading to ubiquitination of DDB2, XPC and nearby histones, serving to target DDB2 for degradation, increase XPC's affinity for DNA and relax the local chromatin structure, respectively. The recruitment of a number of other chromatin remodelling factors has been also reported(Marteijn et al. 2014). There are some seemingly dissenting reports that complicate the picture including a 2 minute DNA retention time for DDB2 as judged by FRAP and the fact that its dissociation from DNA is independent of XPC(Luijsterburg et al. 2007; Alekseev et al. 2008), which both speak against a handover mechanism. There is also the puzzling issue of DDB2 being degraded before CPD repair is complete and at a time when it is presumably most needed. An alternative mechanism has been proposed wherein a transient DNA-independent association between DDB2 and XPC allows the former to target the latter to damage although this does not appear to have gained widespread acceptance(Fei et al. 2011). I have interpreted my observations in the context of the majority opinion that the primary function of DDB2 is to bind UV photoproducts and facilitate their recognition by XPC.

UVC irradiation of CEM induces loss of extractable DDB2 in agreement with previously published data(Rapić-Otrin et al. 2002; Fitch, Cross, et al. 2003a) and consistent with its recruitment to chromatin. Levels of extractable DDB2 could be affected by numerous factors including the cell type used, the UVR dose and the composition of the extraction buffer(Rapić-Otrin et al. 2002). DDB2 is targeted for degradation immediately following UVC irradiation (half-life ~2 hours (Luijsterburg et al. 2007)) and its expression is induced by p53 around 24 hours after irradiation(Rapić-Otrin et al. 2002). The near-quantitative recruitment of DDB2 to DNA is compatible

with the expected number of lesions. A UVC dose of 20 J/m$^2$ is estimated to induce around 2.6 x 10$^6$ CPDs and 6.4 x 10$^5$ (6-4)PPs(Perdiz et al. 2000), which far exceeds the number of DDB2 molecules in a cell, which is estimated to be ~1 x 10$^5$ (Beck et al. 2011; Keeney et al. 1993).

The return of extractable DDB2 seen 3 hours after UVC treatment in my experiments is somewhat surprising considering it should be earmarked for degradation. Fitch et al reported return of extractable DDB2 at 4 hours in human fibroblasts whilst Rapic-Otrin reported absence of extractable DDB2 until 18 hours after irradiation in monkey TC-7 cells. The UV dose was equal in both cases (10 J/m$^2$) thus an explanation may lie in the extraction conditions used. The former study used an SDS-containing lysis buffer whilst the latter used a high salt (0.5 M NaCl) in combination with freeze-thaw; the RIPA buffer used in my experiments more closely resembles the extraction conditions of Fitch et al. Curiously, Rapic-Ortin et al previously used the same extraction technique to show a recovery of lost UV-DDB binding activity in extracts 3-6 hours after irradiation(Otrin et al. 1997), which seems entirely contradictory to their later paper. Another explanation could be the expression of high levels of proteasomal subunits in CEM cells(Kumatori et al. 1990) which may accelerate the cycle of degradation and expression.

The effect of photosensitisers on DDB2 does not appear to have been considered before aside from one report of which found that psoralen-UVA-induced crosslinks are not recognised by DDB2 and XP-E cells are not sensitive to psoralen/UVA(Muniandy et al. 2009). The results for vemurafenib and FQs are in keeping with my findings in Chapter 4 and previous reports. FQs induce CPDs through type I photosensitisation provided the energy of the excited triplet state is sufficiently high(Cuquerella et al. 2011). Although not previously reported for ciprofloxacin, the significant induction of CPDs is compatible with its ranking as a more potent photosensitiser than ofloxacin, which does not induce CPDs to any significant degree. That ofloxacin/UVA treatment does not result in significant DDB2 recruitment suggests that the effects of ciprofloxacin are related to CPD induction rather than to the effects of $^1O_2$. Although little is known of the effects of vemurafenib on DNA, its highly lipophilic nature suggests it will mainly

localise to membranes and organelles, perhaps reducing its ability to affect DNA(Benov et al. 2010). Photosensitised CPD induction, whilst by no means exclusive to FQs, is not a feature of the majority of photosensitisers and thus it is unlikely that vemurafenib would possess this attribute.

The recruitment of DDB2 after 6-TG treatment was unexpected; DDB2 had recently been reported to dimerise upon DNA binding(Yeh et al. 2012) so dimer crosslinking was the expected outcome. Binding is rapid and seems qualitatively different to the UVC-induced binding in that DDB2 does not return to an extractable form after 3 hours. This could reflect higher levels of damage or lesions that are slower, or indeed, impossible to repair. 6-TG had never been noted as an inducer of CPDs, and this was confirmed by ELISA (Figure 5-6). This suggested that the recruitment was either caused by recognition of 6-TG photoproducts or *via* some cellular process resulting from 6-TG photosensitisation (for example, post translational modification of DDB2).

### 5.3.2 DDB2 binding 6-TG photoproducts

The ability of membrane immobilised genomic DNA from 6-TG/UVA treated cells to recruit DDB2 from untreated cells more efficiently than DNA from untreated cells supports a DNA lesion-binding interpretation. This is a somewhat insensitive technique. Nevertheless, DDB2 recruitment by DNA from UVC and ciprofloxacin treated cells provides some validation.

Data from the EMSA assays are also consistent with recognition of a UVA/6-TG induced photoproduct. Binding can be competed by an excess of UVC damaged DNA in an assay designed to reveal DDB2 binding to photoproducts. The substrate for binding was generated by irradiation of a single stranded oligonucleotide containing 6-TG. This was then annealed to a complementary strand. This procedure obviates any complications from protein crosslinks or ICLSs. Under the conditions of my assay, DDB2-mediated binding generates the major band for EMSA of UVC-damaged DNA(Chu & E. Chang 1988). $G^{SO3}$ is a minor product after UVA irradiation(Ren et al. 2010) but the exclusive product of MMPP oxidation under the conditions I used. The

much larger shift seen after MMPP treatment is consistent with the recognised lesion being $G^{SO3}$. The relative effectiveness of UVC-irradiated DNA as a competitor for UVA- and MMPP-treated 6-TG oligonucleotides is also compatible with this interpretation. Performing the assay with XP-E cell extracts would provide a definitive answer.

The effect of 6-TG-mediated DDB2 recruitment in cells, if any, will be determined by a variety of factors. Firstly, $G^{SO3}$ is not currently considered an NER substrate therefore stable recruitment without processing could result in persistent depletion of UV-DDB. The classification of $G^{SO3}$ as NER intractable is based on the insensitivity of CSB, XP-G and XP-A cells to 6-TG/UVA treatment(Brem et al. 2011; Li 2010). In view of the near complete abolition of NER after 6-TG/UVA treatment, the NER status of a cell line may be unimportant in determining 6-TG/UVA toxicity. A $G^{SO3}$ containing substrate for the *in vitro* NER assay could resolve the matter.
The total number of DNA $G^{SO3}$ relative to the number of UV-DDB molecules will determine the extent of depletion. $G^{SO3}$ is the minor product of 6-TG oxidation upon irradiation by UVA and accounts for around 10% of total 6-TG at the dose of 20kJ/m$^2$ used in my experiments(Ren et al. 2010). Substitution of guanine is normally between 0.1-1% depending on dosage and guanine constitutes 20% of the genome. Therefore, taking the number of bases in a diploid human cell as $6 \times 10^9$, the substitution of guanine as 0.1% and the UVA dose of 20kJ/m$^2$, the predicted number of $G^{SO3}$ per cell is around $1.2 \times 10^5$ ($6 \times 10^9 \times 0.2 \times 0.001 \times 0.1$). This is around equal to the total number of DDB2 molecules thus accounting for the total loss extractable DDB2 observed after 6-TG/UVA treatment and suggesting that depletion could be highly relevant. Finally, the ratio of photoproducts to $G^{SO3}$ could influence the extent to which competition occurs. As stated above, in cultured cells, a UVC dose of 20 J/m$^2$ is estimated to induce around $2.6 \times 10^6$ CPDs and $6.4 \times 10^5$ (6-4)PPs suggesting UV-DDB is quickly exhausted and that NER proceeds via XPC until increased DDB2 expression begins around 6 hours after irradiation(Fitch, Cross, et al. 2003a). In human skin, CPD levels will be influenced by skin type and sun exposure; Mouret et al found that one MED of either UVA or UVB induced around an average 30 CPD per $10^6$ bases in patient skin or $3 \times 10^4$ per cell(S. E. P. Mouret et al. 2011b). At the 6-TG substitution level of 0.02%

seen in patients, the predicted $G^{SO3}$ per cell is 2.4 x $10^4$ (exchanging 0.0002 for 0.001 in the above calculation) so levels are certainly comparable.

As judged by microinjection of UV-DDB into XP-E cells, CPD repair can function with around 10% of total DDB2(Keeney et al. 1994). This may mean that sequestration of UV-DDB by $G^{SO3}$ is insignificant although the stage at which NER is abandoned or blocked is unknown and therefore more limiting factors such as XPC may also be sequestered. There is a precedent for sequestration of NER factors leading to a repair defect. Recently, sequestration of RPA at stalled replication forks was shown to reduce NER capacity(Tsaalbi-Shtylik et al. 2014). As 6-TG/UVA treatment also causes replication blockage, RPA sequestration as a possible contributor to NER inhibition is currently under investigation in the lab. Cells from patients with the Hutchinson-Gilford progeria syndrome exhibit accumulation of mutated lamin proteins, which specifically sequester XPA resulting in an NER defect(Musich & Y. Zou 2009).

Increasing cellular DDB2 levels offers protection from UVB induced-carcinogenesis in mice. This is seen after knockout of Cul4A (which prevents polyubiquitination leading to accumulation) (L. Liu et al. 2009) or overexpression via transfection with a ectopic construct(Alekseev 2005) both of which restore CPD repair in mice and delay the onset of UVB-induced tumours. If the converse is true, and loss of a significant fraction of free DDB2 effectively induces a transient XP-E-like state then this may exert further genomic stress on cells that are already subject to protein oxidation and DNA damage.

## 5.4 Summary

6-TG/UVA treatment results in the recruitment of DDB2 to DNA in a manner reminiscent of the UVC DNA damage response. Ciprofloxacin gives a similar response likely due to its ability to induce CPDs via type I photosensitisation. 6-TG treatment results in neither CPDs nor (6-4)PPs thus its recruitment is mediated by a different lesion. 6-TG containing probes irradiated with UVA or oxidised chemically are gel shifted by incubation with extracts and the binding of 6-TG/UVA can be reduced by inclusion of a UVC irradiated cold competitor. This suggests that the 6-TG/UVA and

UVC damage are bound by the same factor, which is likely UV-DDB, via the DDB2 subunit.

The data presented in this chapter are very preliminary and hence the above interpretation requires extensive validation under different conditions and in different cell lines before any firm conclusions can be drawn. If my conclusions are substantiated, this may represent yet another facet of 6-TG's, and by extension azathioprine's, carcinogenic potential.

# Chapter 6. Discussion

The results presented in this thesis span two established areas of research, protein oxidation and DNA repair, that have overlapped surprisingly little to date. Although protein oxidation is by no means a nascent field (initial characterisation of amino acid oxidation products was performed at the turn of the 20$^{th}$ century(Dakin 1906)), consideration of its biological effects awaited the development, in the 1990's, of reliable techniques to detect oxidised proteins in biological samples(Hensley & Floyd 2002). Because genetic information has to be faithfully transferred to the next generation, DNA has historically been considered the most important target for damage by cellular RS. In contrast, the ease of replacement of damaged proteins suggests that oxidative stress presents less of a hazard to the proteome. In this final discussion, I aim to address differences in photosensitisation, why certain proteins are susceptible to photosensitised damage, the putative link between protein oxidation and carcinogenesis and the applicability of these findings to patients, especially with regards to therapy-related cancer in immunosuppressed individuals.

The data presented in Chapter 4 indicate that different photosensitisers can have dramatically different effects on protein oxidation. This is most strikingly illustrated by the properties of vemurafenib. Vemurafenib/UVA induced little or no crosslinking of PCNA or Ku. It did not effect photobleaching of RNO *in vitro*. Vemurafenib phototoxicity was associated with little RS detectable by CM-$H_2$DCFDA. These observations all indicate that vemurafenib has low type II photosensitising capability and that toxicity occurs by a type I mechanism. Of the photosensitizers I examined, vemurafenib is the most lipophilic and most likely localises to cell membranes or mitochondria(Castano et al. 2004). The phototoxic effects of vemurafenib might therefore be mediated through lipid peroxidation or release of pro-apoptotic factors following mitochondrial damage. More information regarding the photosensitisation mechanism of vemurafenib may allow co-administration with a compatible antioxidant to attenuate its adverse effects as has been achieved for doxorubicin(Deres et al. 2005) and chemo- and radiotherapy used to treat acute lymphoblastic leukaemia in children(Al-Tonbary et al. 2009).

One of the questions I wanted to address at the inception of this study was the extent to which 6-TG was a typical photosensitiser. In particular, the extent to which its photosensitisation by 6-TG requires its incorporation into DNA. Surprisingly, the FQs, which are not incorporated into DNA, replicated many of the properties of DNA 6-TG including damage to DNA repair proteins and inhibition of DNA repair. These effects most likely reflect type II photosensitization. DNA 6-TG is a mixed type I and type II photosensitizer and my findings show that compared to the FQs, its phototoxicity is associated with relatively low levels of RS. The particular effectiveness of DNA 6-TG as a type II photosensitizer may reflect its ability to serve as both a source and as a target of RS to generate potentially lethal DNA lesions. In addition, type I sensitisation of DNA 6-TG will promote the formation of additional lethal lesions in the form of ICLs and DNA-protein crosslinks.

Through the combined action of type I and II photosensitisation, UVA-induced DNA lesions will form in the immediate vicinity of DNA-6-TG. As DNA 6-TG continues to produce $^1O_2$, repair proteins that arrive to repair these lesions are in danger of inactivation by oxidation. This would confer a self-selecting component to DNA repair protein inactivation. If a suitable identification method can be developed, it would be interesting to examine the cross section of oxidised proteins from 6-TG/UVA vs. FQs/UVA to see if the former damages a higher proportion of DNA replication/repair proteins.

6-TG/UVA treatment abrogates the cell's ability to repair DSBs in G1 phase and to remove (6-4)PPs and 8-oxoG(Gueranger et al. 2014). These observations are complemented by *in vitro* assays for NHEJ, NER and BER that reveal defects in the functions of Ku, RPA and OGG-1 respectively. By contrast, the removal of DNA-uracil by cells and the *in vitro* activity of the UNG DNA glycosylase are not detectably changed by supra-lethal treatment with 6-TG/UVA. The structures of the UNG and OGG-1 DNA glycosylases provide a tentative explanation for the greater sensitivity of OGG-1 to oxidizing conditions (Figure 6.1). OGG-1 can be inactivated by thiol oxidising treatments *in vitro* and activity is restored by treatment with reducing agents(Bravard et al. 2006). It has an active site cysteine that is constitutively

deprotonated(Banerjee et al. 2005) and assists in the stabilisation of 8-oxoG binding in the active site(Bruner et al. 2000)(highlighted in red, Figure 6.1, left).

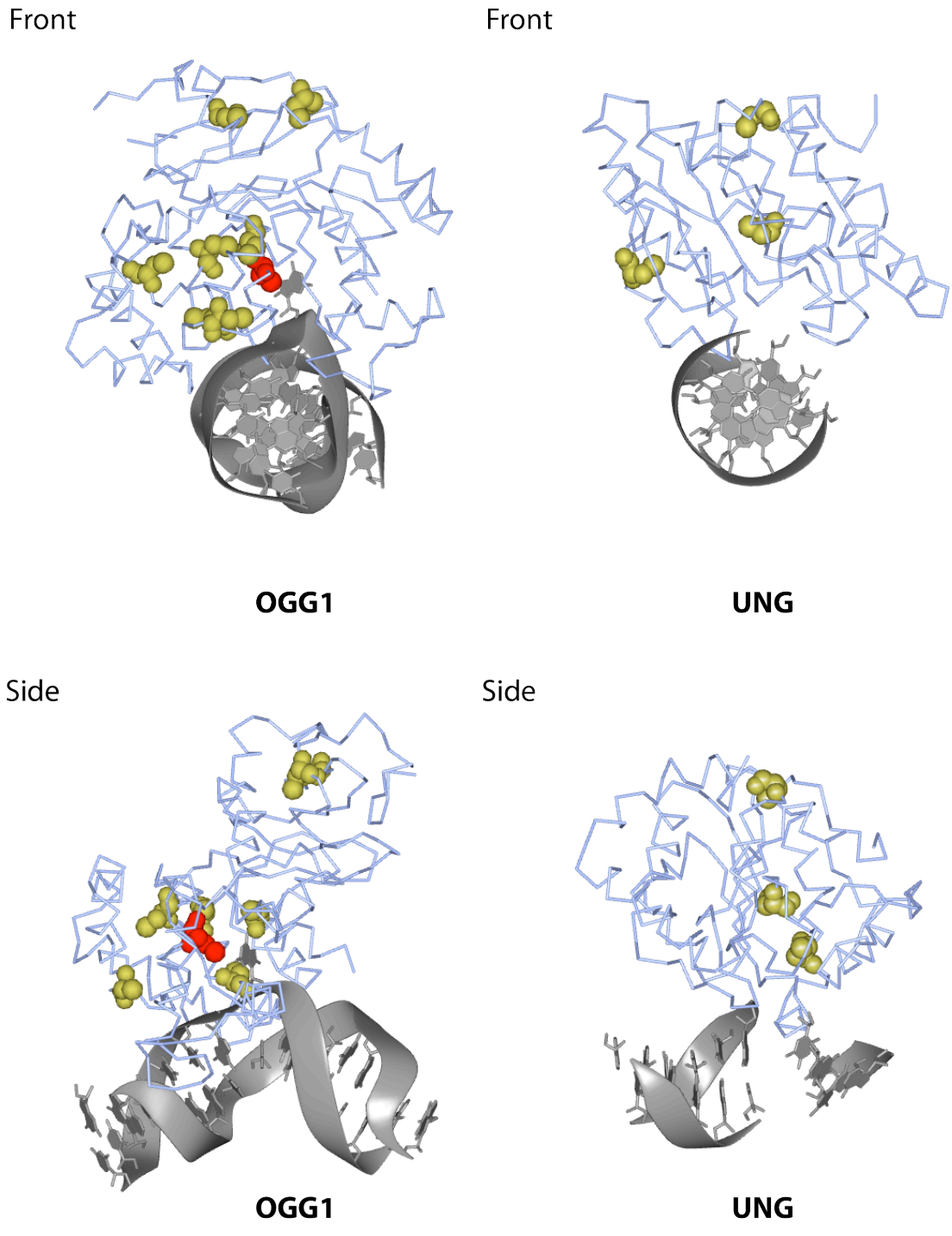


**Figure 6.1 Structures of OGG1 and UNG with highlighted cysteines**
3D models of OGG-1 and UNG2 binding to DNA. Cysteines are shown in space-filling mode. Active site thiolate Cys253 in OGG-1 is highlighted in red. OGG-1 structural data from Bruner et al (Bruner et al. 2000), UNG2 structural data from Parker et al(Parker et al. 2007). Image rendered using CCP4mg (McNicholas et al. 2011).

Molecular modelling suggests that replacing the active site cysteine with a bulky residue would dramatically decrease catalytic activity(Lukina et al. 2013). Similarly, formation of an additional disulphide or sulphur oxyacid would probably also have an adverse effect on active site conformation. By contrast, no redox sensitivity has been reported for UNG. The enzyme has only three cysteines, none of which are in or proximate to the active site; uracil binding is stabilised by stacking with a conserved phenylalanine(Krokan et al. 1997).

Ku(Bennett et al. 2009) and RPA(Men et al. 2007) are also susceptible to thiol oxidation-dependent inactivation *in vitro*. It may not be coincidental that the proteins I identified as susceptible to photosensitised inactivation exhibit thiol redox modulation. Optimising a more tractable system for identifying proteins with susceptible thiols may be a productive direction in which to continue this investigation; exploiting the biotinylated sulfenic acid probe would be a good starting point(Leonard et al. 2009).

Based on my experience, I suspect that carbonylation, whilst a good measure of general oxidation, may not be the optimal tool for addressing the fates of susceptible proteins. That is to say, by the time protein carbonylation becomes detectable, thiol modification may already be extensive. In addition to the aforementioned proteins, other DNA repair factors including MGMT(Laval & Wink 1994) and XRCC3(Girard et al. 2013) are also inactivated by thiol oxidation. XPA, TFIIH and Ligase III all contain a zinc finger domain, and XPD has a Fe-S cluster, suggesting that other NER factors may also be susceptible to inactivation. Quite why this functional vulnerability has evolved is unclear as it would appear antithetical to an efficient DNA damage response.

The idea that oxidation of repair factors may lead to increased fixation of mutations has been considered previously. Inflammatory cytokine treatment of adenocarcinoma cells induces nitric oxide synthase activity, leading to inactivation of OGG-1 and has been proposed as a link between inflammation and cancer(Jaiswal et al. 2000). Barry Halliwell, a leading figure in the biology of RS, downplayed the concept in a 2007 review on the basis that most cancers retain repair capabilities(Halliwell 2007). An impact on mutagenesis and carcinogenesis does not require that repair is completely or

permanently inactivated, however. Transient abrogation or a chronic slight reduction in DNA repair capacity may, over many years also contribute to cancer risk. Consistent with this possibility, DNA repair capacity can be modulated by polymorphisms of repair genes(Spitz et al. 2001) and these variants may be associated with a higher risk of NMSC(Vogel et al. 2001).

A link between protein oxidation and repair capacity has been established by the work from the laboratories of Radman and of Daly (for review see Slade and Radman(Slade & Radman 2011) and Daly (Daly 2009). In several publications, (Daly et al. 2010; Daly et al. 2007; Krisko & Radman 2010), these authors demonstrated a connection between the extraordinary radiation resistance of extremophiles and efficient non-enzymatic antioxidant protection of the proteome (Krisko & Radman 2010). More recently, they showed that increasing the susceptibility of cellular proteins to endogenous RS results in diminished repair capacity and a concomitant mutator phenotype(Krisko & Radman 2013). These results support a role for protein oxidation in promoting genomic instability. Although these investigations were largely confined to bacteria, enhanced protein protection extends to other organisms(Krisko et al. 2012) and appears to be an adaptation to desiccation –a process that is known to be associated with the wholesale production of RS(Fredrickson et al. 2008). Since the chemistry of RS and proteins is independent of the organism, the concept warrants further study with regards to human carcinogenesis.

My experiments for the first time demonstrate that protein oxidation is widespread in cultured cells treated with 6-TG and UVA. My findings, together with those of my laboratory colleagues, indicate that this oxidation decreases DNA repair capacity. Can these findings be extrapolated to patients taking the immunosuppressant azathioprine? Azathioprine treatment is associated with a huge increased skin cancer risk. Analysis of mutations from azathioprine-associated skin tumours does not provide evidence for a novel mutational mechanism (McGregor et al. 1997; Harwood et al. 2008). Instead, as in sporadic skin tumours, the majority of mutations are UVB signatures - consistent with less than optimal NER of sunlight-induced DNA lesions. The important parameters for 6-TG photosensitization are the level of DNA substitution and the incident UVA

dose. The steady state 6-TG substitution in patients' skin is around 0.02% of DNA guanine(O'Donovan et al. 2005). My experiments were designed to amplify any phototoxic effects that might occur in patients' skin and I estimate that they represent levels of DNA substitution around 10-fold higher than the clinical situation. The UVA doses used were mild and within reasonable exposure levels (equivalent to around 20-30 minutes of midday sun in British summer time). These combinations were sufficient to completely inhibit UVC photoproduct removal by NER. Two caveats should be added, however. The $O_2$ concentration in cultured cells is likely to be significantly higher than in skin. In addition, cultured cells lack the protective effect of the stratum corneum. Thus, the levels of RS generated in patient skin will inevitably be less than in my experiments. On the other hand, the high, localised RS concentrations associated with photosensitisation may hinder effective detoxification by antioxidants. Overall, although complete NER inhibition by photosensitised DNA 6-TG in patients' skin is unlikely, significant attenuation remains a possibility. In PCNA and Ku crosslinking, and now loss of extractable DDB2, we have a number of sensitive measures that denote the effects of DNA 6-TG photosensitisation and $^1O_2$ production. These may be exploited to provide an indication of the severity of 6-TG photosensitisation in samples taken from patients. If repair capacity is significantly compromised in sun exposed skin of patients taking azathioprine, topical application of molecules that counteract these effects (Yarosh et al. 2001) might increase protection against therapy-related cancer.

# Reference List

Adamo, A. et al., 2010. Preventing nonhomologous end joining suppresses DNA repair defects of Fanconi anemia. *Molecular Cell*, 39(1), pp.25–35.

Aguilera, A. & Gómez-González, B., 2008. Genome instability: a mechanistic view of its causes and consequences. *Nature Reviews Genetics*, 9(3), pp.204–217.

Al-Tonbary, Y. et al., 2009. Vitamin E and N-Acetylcysteine as Antioxidant Adjuvant Therapy in Children with Acute Lymphoblastic Leukemia. *Advances in Hematology*, 2009(7), pp.1–5.

Alam, M. & Ratner, D., 2001. Cutaneous squamous-cell carcinoma. *The New England journal of medicine*, 344(13), pp.975–983.

Alekseev, S., 2005. Enhanced DDB2 Expression Protects Mice from Carcinogenic Effects of Chronic UV-B Irradiation. *Cancer research*, 65(22), pp.10298–10306.

Alekseev, S. et al., 2008. Cellular Concentrations of DDB2 Regulate Dynamic Binding of DDB1 at UV-Induced DNA Damage. *Molecular and cellular biology*, 28(24), pp.7402–7413.

Andersson, M.I., 2003. Development of the quinolones. *Journal of Antimicrobial Chemotherapy*, 51(90001), pp.1–11.

Andrews, B.J., Lehman, J.A. & Turchi, J.J., 2006. Kinetic analysis of the Ku-DNA binding activity reveals a redox-dependent alteration in protein structure that stimulates dissociation of the Ku-DNA complex. *The Journal of biological chemistry*, 281(19), pp.13596–13603.

Archier, E. et al., 2012. Carcinogenic risks of Psoralen UV-A therapy and Narrowband UV-B therapy in chronic plaque psoriasis: a systematic literature review. *Journal of the European Academy of Dermatology and Venereology*, 26, pp.22–31.

Attard, N.R. & Karran, P., 2011. UVA photosensitization of thiopurines and skin cancer in organ transplant recipients. *Photochemical & photobiological sciences : Official journal of the European Photochemistry Association and the European Society for Photobiology*, 11(1), p.62.

Avkin, S. et al., 2002. Quantitative measurement of translesion replication in human cells: evidence for bypass of abasic sites by a replicative DNA polymerase. *Proceedings of the National Academy of Sciences of the United States of America*, 99(6), pp.3764–3769.

Bacsi, A. et al., 2005. Modulation of DNA-dependent protein kinase activity in chlorambucil-treated cells. *Free radical biology & medicine*, 39(12), pp.1650–1659.

Bae, S.I., Zhao, R. & Snapka, R.M., 2008. PCNA damage caused by antineoplastic drugs. *Biochemical pharmacology*, 76(12), pp.1653–1668.

Bahner, J.D. & Bordeaux, J.S., 2013. Non-melanoma skin cancers: Photodynamic therapy, cryotherapy, 5-fluorouracil, imiquimod, diclofenac, or what? Facts and controversies. *Clinics in Dermatology*, 31(6), pp.792–798.

Baker, A. & Kanofsky, J.R., 1992. Quenching of singlet oxygen by biomolecules from L1210 leukemia cells. *Photochemistry and photobiology*, 55(4), pp.523–528.

Balasubramanian, D., Du, X. & Zigler, J.S., 1999. The reaction of singlet oxygen with proteins, with special reference to crystallins. *Photochemistry and photobiology*, 52(4), pp.761–768.

Banerjee, A. et al., 2005. Structure of a repair enzyme interrogating undamaged DNA elucidates recognition of damaged DNA. *Nature*, 434(7033), pp.612–618.

Banyasz, A. et al., 2011. Base Pairing Enhances Fluorescence and Favors Cyclobutane Dimer Formation Induced upon Absorption of UVA Radiation by DNA. *Journal of the American Chemical Society*, 133(14), pp.5163–5165.

Baraibar, M.A., Ladouce, R. & Friguet, B., 2013. Proteomic quantification and identification of carbonylated proteins upon oxidative stress and during cellular aging. *Journal of proteomics*, 92(C), pp.63–70.

Barzilay, G. & Hickson, I.D., 1995. Structure and function of apurinic/apyrimidinic endonucleases. *Bioessays*, 17(8), pp.713–719.

Bastian, B.C., 2014. The Molecular Pathology of Melanoma: An Integrated Taxonomy of Melanocytic Neoplasia. *Annual Review of Pathology: Mechanisms of Disease*, 9(1), pp.239–271.

Baty, J.W., Hampton, M.B. & Winterbourn, C.C., 2002. Detection of oxidant sensitive thiol proteins by fluorescence labeling and two-dimensional electrophoresis. *PROTEOMICS*, 2(9), pp.1261–1266.

Baumann, P. & West, S.C., 1998. DNA end-joining catalyzed by human cell-free extracts. *Proceedings of the National Academy of Sciences of the United States of America*, 95(24), pp.14066–14070.

Beck, M. et al., 2011. The quantitative proteome of a human cell line. *Molecular Systems Biology*, 7, pp.1–8.

Beckman, J.S., 1994. Peroxynitrite versus Hydroxyl Radical: The Role of Nitric Oxide in Superoxide-Dependent Cerebral Injurya. *Annals of the New York Academy of Sciences*, 738(1), pp.69–75.

Bennett, S.M. et al., 2009. Molecular analysis of Ku redox regulation. *BMC Molecular Biology*, 10, p.86.

Benov, L., Craik, J. & Batinic-Haberle, I., 2010. Protein damage by photo-activated Zn(II) N-alkylpyridylporphyrins. *Amino Acids*, 42(1), pp.117–128.

Bentley, J. et al., 2009. Papillary and muscle invasive bladder tumors with distinct genomic stability profiles have different DNA repair fidelity and KU DNA-binding activities. *Genes, Chromosomes and Cancer*, 48(4), pp.310–321.

Berlett, B.S. & Stadtman, E.R., 1997. Protein oxidation in aging, disease, and oxidative stress. *The Journal of biological chemistry*, 272(33), pp.20313–20316.

Bethea, D. et al., 1999. Psoralen photobiology and photochemotherapy: 50 years of science and medicine. *Journal of dermatological science*, 19(2), pp.78–88.

Biertümpfel, C. et al., 2010. Structure and mechanism of human DNA polymerase η. *Nature*, 465(7301), pp.1044–1048.

Bigelow, D.J. & Squier, T.C., 2011. Thioredoxin-dependent redox regulation of cellular signaling and stress response through reversible oxidation of methionines. *Molecular BioSystems*, 7(7), p.2101.

Bisby, R.H. et al., 1999. Quenching of Singlet Oxygen by Trolox C, Ascorbate, and Amino Acids: Effects of pH and Temperature. *The Journal of Physical Chemistry A*, 103(37), pp.7454–7459.

Blondeau, J.M., 2004. Fluoroquinolones: mechanism of action, classification, and development of resistance. *Survey of Ophthalmology*, 49(2), pp.S73–S78.

Bollag, G. et al., 2012. Vemurafenib: the first drug approved for BRAF-mutant cancer. pp.1–14.

Bollineni, R.C., Hoffmann, R. & Fedorova, M., 2014. Proteome-wide profiling of carbonylated proteins and carbonylation sites in HeLa cells under mild oxidative stress conditions. *Free radical biology & medicine*, 68(C), pp.186–195.

Boonstra, J. & Post, J.A., 2004. Molecular events associated with reactive oxygen species and cell cycle progression in mammalian cells. *Gene*, 337, pp.1–13.

Borutaite, V. & Brown, G.C., 2001. Caspases are reversibly inactivated by hydrogen peroxide. *FEBS letters*, 500(3), pp.114–118.

Bota, D.A. & Davies, K.J.A., 2002. Lon protease preferentially degrades oxidized mitochondrial aconitase by an ATP-stimulated mechanism. *Nature Cell Biology*, 4(9), pp.674–680.

Boudon, S.M. et al., 2013. Characterization of Vemurafenib Phototoxicity in a Mouse Model. *Toxicological Sciences*, 137(1), pp.259–267.

Bracchitta, G. et al., 2013. Investigation of the phototoxicity and cytotoxicity of naproxen, a non-steroidal anti-inflammatory drug, in human fibroblasts. *Photochemical & photobiological sciences : Official journal of the European*

*Photochemistry Association and the European Society for Photobiology*, 12(5), p.911.

Bravard, A. et al., 2006. Redox Regulation of Human OGG1 Activity in Response to Cellular Oxidative Stress. *Molecular and cellular biology*, 26(20), pp.7430–7436.

Breen, A.P. & Murphy, J.A., 1995. Reactions of oxyl radicals with DNA. *Free radical biology & medicine*, 18(6), pp.1033–1077.

Brem, R. & Karran, P., 2011. Multiple forms of DNA Damage Caused by UVA Photoactivation of DNA 6-Thioguanine. *Photochemistry and photobiology*, 88(1), pp.5–13.

Brem, R. & Karran, P., 2012. Oxidation-Mediated DNA Cross-Linking Contributes to the Toxicity of 6-Thioguanine in Human Cells. *Cancer research*, 72(18), pp.4787–4795.

Brem, R. et al., 2010. DNA breakage and cell cycle checkpoint abrogation induced by a therapeutic thiopurine and UVA radiation. *Oncogene*, 29(27), pp.3953–3963.

Brem, R., Daehn, I. & Karran, P., 2011. Efficient DNA interstrand crosslinking by 6-thioguanine and UVA radiation. *DNA repair*, 10(8), pp.869–876.

Brem, R., Li, F. & Karran, P., 2009. Reactive oxygen species generated by thiopurine/UVA cause irreparable transcription-blocking DNA lesions. *Nucleic Acids Research*, 37(6), pp.1951–1961.

Breusing, N. et al., 2009. Inverse correlation of protein oxidation and proteasome activity in liver and lung. *Mechanisms of ageing and development*, 130(11-12), pp.748–753.

Brodie, A.E. & Reed, D.J., 1987. Reversible oxidation of glyceraldehyde 3-phosphate dehydrogenase thiols in human lung carcinoma cells by hydrogen peroxide. *Biochemical and biophysical research communications*, 148(1), pp.120–125.

Bruner, S.D., Norman, D.P. & Verdine, G.L., 2000. Structural basis for recognition and repair of the endogenous mutagen 8-oxoguanine in DNA. *Nature*, 403(6772), pp.859–866.

Bucciantini, M. et al., 2002. Inherent toxicity of aggregates implies a common mechanism for protein misfolding diseases. *Nature*, 416(6880), pp.507–511.

Buell, J.F., Gross, T.G. & Woodle, E.S., 2005. Malignancy after Transplantation. *Transplantation*, 80(Supplement), pp.S254–S264.

Bunting, S.F. & Nussenzweig, A., 2013. End-joining, translocations and cancer. pp.1–12.

Burkitt, M.J., 2003. Chemical, biological and medical controversies surrounding the Fenton reaction. *Progress in Reaction Kinetics and Mechanism*, 28(1), pp.75–103.

Burney, S. et al., 1999. The chemistry of DNA damage from nitric oxide and peroxynitrite. *Mutation research*, 424(1-2), pp.37–49.

Cadet, J. & Douki, T., 2011. Oxidatively Generated Damage to DNA by UVA Radiation in Cells and Human Skin. *Journal of Investigative Dermatology*, 131(5), pp.1005–1007.

Cadet, J. et al., 2012. Photoinduced Damage to Cellular DNA: Direct and Photosensitized Reactions†. *Photochemistry and photobiology*, 88(5), pp.1048–1065.

Cadet, J. et al., 2006. Singlet Oxygen Oxidation of Isolated and Cellular DNA: Product Formation and Mechanistic Insights. *Photochemistry and photobiology*, 82(5), p.1219.

Cantwell-Dorris, E.R., O'Leary, J.J. & Sheils, O.M., 2011. BRAFV600E: Implications for Carcinogenesis and Molecular Therapy. *Molecular Cancer Therapeutics*, 10(3), pp.385–394.

Carraro, C. & Pathak, M.A., 1988. Studies on the nature of in vitro and in vivo photosensitization reactions by psoralens and porphyrins. *The Journal of investigative dermatology*, 90(3), pp.267–275.

Carter, M.J., 2004. Guidelines for the management of inflammatory bowel disease in adults. *Gut*, 53(suppl_5), pp.v1–v16.

Castano, A.P., Demidova, T.N. & Hamblin, M.R., 2004. Mechanisms in photodynamic therapy: part one—photosensitizers, photochemistry and cellular localization. *Photodiagnosis and Photodynamic Therapy*, 1(4), pp.279–293.

Centre, H.A.S.C.I., 2013. Prescription Cost Analysis - England, 2012 Report Prescribing & P. C. Team, eds. pp.1–659.

Chance, B., Sies, H. & Boveris, A., 1979. Hydroperoxide metabolism in mammalian organs. *Physiological reviews*, 59(3), pp.527–605.

Chang, Y.-C. et al., 2010. Mapping protein cysteine sulfonic acid modifications with specific enrichment and mass spectrometry: An integrated approach to explore the cysteine oxidation. *PROTEOMICS*, 10(16), pp.2961–2971.

Chapman, J.R., Taylor, M.R.G. & Boulton, S.J., 2012. Playing the End Game: DNA Double-Strand Break Repair Pathway Choice. *Molecular Cell*, 47(4), pp.497–510.

Chapman, P.B. et al., 2011. Improved Survival with Vemurafenib in Melanoma with BRAF V600E Mutation. *The New England journal of medicine*, 364(26), pp.2507–2516.

Chavez, J.D., Bisson, W.H. & Maier, C.S., 2010. A targeted mass spectrometry-based approach for the identification and characterization of proteins containing α-aminoadipic and γ-glutamic semialdehyde residues. *Analytical and Bioanalytical*

*Chemistry*, 398(7-8), pp.2905–2914.

Chiruvella, K.K., Liang, Z. & Wilson, T.E., 2013. Repair of Double-Strand Breaks by End Joining. *Cold Spring Harbor Perspectives in Biology*, 5(5), pp.a012757–a012757.

Chu, G. & Chang, E., 1988. Xeroderma pigmentosum group E cells lack a nuclear factor that binds to damaged DNA. *Science (New York, NY)*, 242(4878), pp.564–567.

Clauson, C., Scharer, O.D. & Niedernhofer, L., 2013. Advances in Understanding the Complex Mechanisms of DNA Interstrand Cross-Link Repair. *Cold Spring Harbor Perspectives in Biology*, 5(10), pp.a012732–a012732.

Cocciolo, A. et al., 2012. Decreased expression and increased oxidation of plasma haptoglobin in Alzheimer disease Insights from redox proteomics. *Free radical biology & medicine*, 53(10), pp.1868–1876.

Conklin, L.S. et al., 2012. 6-mercaptopurine transport in human lymphocytes: Correlation with drug-induced cytotoxicity. *Journal of Digestive Diseases*, 13(2), pp.82–93.

Conte, Lo, M. & Carroll, K.S., 2012. Chemoselective Ligation of Sulfinic Acids with Aryl-Nitroso Compounds. *Angewandte Chemie International Edition*, 51(26), pp.6502–6505.

Conte, Lo, M. & Carroll, K.S., 2013. The Chemistry of Thiol Oxidation and Detection. In *Oxidative Stress and Redox Regulation*. Springer, pp. 1–42.

COOKE, M.S. et al., 2008. Measurement and Meaning of Oxidatively Modified DNA Lesions in Urine. *Cancer Epidemiology Biomarkers & Prevention*, 17(1), pp.3–14.

Cosentino-Gomes, D., Rocco-Machado, N. & Meyer-Fernandes, J.R., 2012. Cell Signaling through Protein Kinase C Oxidation and Activation. *International Journal of Molecular Sciences*, 13(12), pp.10697–10721.

Courdavault, S. et al., 2005. Repair of the three main types of bipyrimidine DNA photoproducts in human keratinocytes exposed to UVB and UVA radiations. *DNA repair*, 4(7), pp.836–844.

Coyle, C.H. et al., 2006. Mechanisms of H2O2-induced oxidative stress in endothelial cells. *Free radical biology & medicine*, 40(12), pp.2206–2213.

Cuquerella, M.C. et al., 2011. Photosensitised pyrimidine dimerisation in DNA. *Chemical Science*, 2(7), p.1219.

Dajee, M. et al., 2003. NF-kappaB blockade and oncogenic Ras trigger invasive human epidermal neoplasia. *Nature*, 421(6923), pp.639–643.

Dakin, H.J., 1906. The Oxidation of Amido-Acids with the Production of Substances of

Biological Importance. (1), pp.171–176.

Dalle-Donne, I. et al., 2009. Protein carbonylation: 2,4-dinitrophenylhydrazine reacts with both aldehydes/ketones and sulfenic acids. *Free radical biology & medicine*, 46(10), pp.1411–1419.

Dalle-Donne, I. et al., 2007. S-glutathionylation in protein redox regulation. *Free radical biology & medicine*, 43(6), pp.883–898.

Dall'Acquaa, F. et al., 2007. Photoinduced modifications by fluoroquinolone drugs in bovine serum albumin (BSA) and ribonuclease A (RNAse) as model proteins. *Arkivoc*, 8, pp.231–244.

Daly, M.J., 2009. A new perspective on radiation resistance based on Deinococcus radiodurans. *Nature reviews. Microbiology*, 7(3), pp.237–245.

Daly, M.J. et al., 2007. Protein Oxidation Implicated as the Primary Determinant of Bacterial Radioresistance. *PLoS Biology*, 5(4), p.e92.

Daly, M.J. et al., 2010. Small-Molecule Antioxidant Proteome-Shields in Deinococcus radiodurans M. Otto, ed. *PloS one*, 5(9), p.e12570.

Davies, H. et al., 2002. Mutations of the BRAF gene in human cancer. *Nature*, 417(6892), pp.949–954.

Davies, M.J., 2004. Reactive species formed on proteins exposed to singlet oxygen. *Photochemical & photobiological sciences : Official journal of the European Photochemistry Association and the European Society for Photobiology*, 3(1), pp.17–25.

Davies, M.J., 2003. Singlet oxygen-mediated damage to proteins and its consequences. *Biochemical and biophysical research communications*, 305(3), pp.761–770.

Davies, M.J., 2005. The oxidative environment and protein damage. *Biochimica et biophysica acta*, 1703(2), pp.93–109.

Davies, M.J. & Truscott, R.J., 2001. Photo-oxidation of proteins and its role in cataractogenesis. *Journal of photochemistry and photobiology B, Biology*, 63(1-3), pp.114–125.

de Gruijl, F.R. & Rebel, H., 2008. Early Events in UV Carcinogenesis—DNA Damage, Target Cells and Mutant p53 Foci†. *Photochemistry and photobiology*, 84(2), pp.382–387.

de Gruijl, F.R. & van der Leun, J.C., 2000. Environment and health: 3. Ozone depletion and ultraviolet radiation. *CMAJ : Canadian Medical Association journal = journal de l'Association medicale canadienne*, 163(7), pp.851–855.

de Laat, W.L. et al., 1998. DNA-binding polarity of human replication protein A positions nucleases in nucleotide excision repair. *Genes & Development*, 12(16),

pp.2598–2609.

De Zwaan, S.E. & Haass, N.K., 2009. Genetics of basal cell carcinoma. *Australasian Journal of Dermatology*, 51(2), pp.81–92.

Deres, P. et al., 2005. Prevention of doxorubicin-induced acute cardiotoxicity by an experimental antioxidant compound. *Journal of cardiovascular pharmacology*, 45(1), pp.36–43.

Derheimer, F.A. et al., 2009. Psoralen-Induced DNA Interstrand Cross-Links Block Transcription and Induce p53 in an Ataxia-Telangiectasia and Rad3-Related-Dependent Manner. *Molecular Pharmacology*, 75(3), pp.599–607.

DeRosa, M.C. & Crutchley, R.J., 2002. Photosensitized singlet oxygen and its applications. *Coordination Chemistry Reviews*, 233, pp.351–371.

Dessinioti, C. et al., 2010. Basal cell carcinoma: what's new under the sun. *Photochemistry and photobiology*, 86(3), pp.481–491.

Devasagayam, T.P. et al., 1991. Activity of thiols as singlet molecular oxygen quenchers. *Journal of photochemistry and photobiology B, Biology*, 9(1), pp.105–116.

Di Mascio, P. et al., 1990. Carotenoids, tocopherols and thiols as biological singlet molecular oxygen quenchers. *Biochemical Society transactions*, 18(6), pp.1054–1056.

Diffey, B.L., 1991. Solar ultraviolet radiation effects on biological systems. *Physics in medicine and biology*, 36(3), pp.299–328.

DiGiovanna, J.J. & Kraemer, K.H., 2012. Shining a Light on Xeroderma Pigmentosum. *Journal of Investigative Dermatology*, 132(3), pp.785–796.

Dimon-Gadal, S. et al., 2000. Increased oxidative damage to fibroblasts in skin with and without lesions in psoriasis. *The Journal of investigative dermatology*, 114(5), pp.984–989.

Dizdaroglu, M. & Jaruga, P., 2012. Mechanisms of free radical-induced damage to DNA. *Free radical research*, 46(4), pp.382–419.

Dizdaroglu, M., Kirkali, G. & Jaruga, P., 2008. Formamidopyrimidines in DNA: Mechanisms of formation, repair, and biological effects. *Free radical biology & medicine*, 45(12), pp.1610–1621.

Dolan, D. et al., 2013. Systems Modelling of NHEJ Reveals the Importance of Redox Regulation of Ku70/80 in the Dynamics of DNA Damage Foci D. C. Samuels, ed. *PloS one*, 8(2), p.e55190.

Douki, T. et al., 2003. Bipyrimidine Photoproducts Rather than Oxidative Lesions Are the Main Type of DNA Damage Involved in the Genotoxic Effect of Solar UVA

Radiation †. *Biochemistry*, 42(30), pp.9221–9226.

Drucker, A.M. & Rosen, C.F., 2011. Drug-induced photosensitivity: culprit drugs, management and prevention. *Drug safety : an international journal of medical toxicology and drug experience*, 34(10), pp.821–837.

Dummer, R., Rinderknecht, J. & Goldinger, S.M., 2012. Ultraviolet A and photosensitivity during vemurafenib therapy. *The New England journal of medicine*, 366(5), pp.480–481.

Edmunds, C.E., Simpson, L.J. & Sale, J.E., 2008. PCNA Ubiquitination and REV1 Define Temporally Distinct Mechanisms for Controlling Translesion Synthesis in the Avian Cell Line DT40. *Molecular Cell*, 30(4), pp.519–529.

Emmert, S., Schön, M.P. & Haenssle, H.A., 2013. Molecular Biology of Basal and Squamous Cell Carcinomas.

Epstein, E.H., 2008. Basal cell carcinomas: attack of the hedgehog. *Nature reviews Cancer*, 8(10), pp.743–754.

Euvrard, S. et al., 1995. Comparative epidemiologic study of premalignant and malignant epithelial cutaneous lesions developing after kidney and heart transplantation. *Journal of the American Academy of Dermatology*, 33(2 Pt 1), pp.222–229.

Euvrard, S., Kanitakis, J. & Claudy, A., 2003. Skin cancers after organ transplantation. *The New England journal of medicine*, 348(17), pp.1681–1691.

Evans, M.D., Saparbaev, M. & COOKE, M.S., 2010. DNA repair and the origins of urinary oxidized 2'-deoxyribonucleosides. *Mutagenesis*, 25(5), pp.433–442.

Falnes, P.Ø., Johansen, R.F. & Seeberg, E., 2002. AlkB-mediated oxidative demethylation reverses DNA damage in Escherichia coli. *Nature*, 419(6903), pp.178–182.

Fasani, E. et al., 1997. The photochemistry of lomefloxacin. An aromatic carbene as the key intermediate in photodecomposition. *Chemical Communications*, (14), pp.1329–1330.

Fattman, C., Schaefer, L. & Oury, T., 2003. Extracellular superoxide dismutase in biology and medicine. *Free radical biology & medicine*, 35(3), pp.236–256.

Fei, J. et al., 2011. Regulation of Nucleotide Excision Repair by UV-DDB: Prioritization of Damage Recognition to Internucleosomal DNA J. H. J. Hoeijmakers, ed. *PLoS Biology*, 9(10), p.e1001183.

Ferguson, J., 1995. Fluoroquinolone photosensitization: a review of clinical and laboratory studies. *Photochemistry and photobiology*, 62(6), pp.954–958.

Ferguson, J. & Dawe, R., 1997. Phototoxicity in quinolones: comparison of

ciprofloxacin and grepafloxacin. *Journal of Antimicrobial Chemotherapy*, 40(suppl 1), pp.93–98.

Fischer, E.S. et al., 2011. The Molecular Basis of CRL4 DDB2/CSA Ubiquitin Ligase Architecture, Targeting, and Activation. *Cell*, 147(5), pp.1024–1039.

Fitch, M.E., Cross, I.V., et al., 2003a. The DDB2 nucleotide excision repair gene product p48 enhances global genomic repair in p53 deficient human fibroblasts. *DNA repair*, 2(7), pp.819–826.

Fitch, M.E., Nakajima, S., et al., 2003b. In Vivo Recruitment of XPC to UV-induced Cyclobutane Pyrimidine Dimers by the DDB2 Gene Product. *Journal of Biological Chemistry*, 278(47), pp.46906–46910.

Folkes, L.K., Candeias, L.P. & Wardman, P., 1995. Kinetics and mechanisms of hypochlorous acid reactions. *Archives of biochemistry and biophysics*, 323(1), pp.120–126.

Fredrickson, J.K. et al., 2008. Protein oxidation: key to bacterial desiccation resistance? *The ISME Journal*, 2(4), pp.393–403.

Freeman, A.K., Ritt, D.A. & Morrison, D.K., 2013. Effects of Raf Dimerization and Its Inhibition on Normal and Disease-Associated Raf Signaling. *Molecular Cell*, 49(4), pp.751–758.

Friedberg, E.C. et al., 2004. *DNA Repair and Mutagenesis* 2nd ed, ASM Press.

Frit, P. et al., 2014. Alternative end-joining pathway(s): Bricolage at DNA breaks. *DNA repair*, 17, pp.81–97.

Fu, Y.V. et al., 2011. Selective Bypass of a Lagging Strand Roadblock by the Eukaryotic Replicative DNA Helicase. *Cell*, 146(6), pp.931–941.

Gaboriau, F. et al., 1995. Involvement of singlet oxygen in ultraviolet A-induced lipid peroxidation in cultured human skin fibroblasts. *Archives of dermatological research*, 287(3-4), pp.338–340.

Gaetke, L., 2003. Copper toxicity, oxidative stress, and antioxidant nutrients. *Toxicology*, 189(1-2), pp.147–163.

Gaillard, H. & Aguilera, A., 2013. Transcription coupled repair at the interface between transcription elongation and mRNP biogenesis. *BBA - Gene Regulatory Mechanisms*, 1829(1), pp.141–150.

Girard, P.-M. et al., 2013. Oxidative Stress in Mammalian Cells Impinges on the Cysteines Redox State of Human XRCC3 Protein and on Its Cellular Localization J. Choi, ed. *PloS one*, 8(10), p.e75751.

Girard, P.M. et al., 2011. UVA-induced damage to DNA and proteins: direct versusindirect photochemical processes. *Journal of Physics: Conference Series*,

261, p.012002.

Godar, D.E., 1999. Light and death: photons and apoptosis. *The journal of investigative dermatology. Symposium proceedings / the Society for Investigative Dermatology, Inc. [and] European Society for Dermatological Research*, 4(1), pp.17–23.

Grulich, A.E. et al., 2007. Incidence of cancers in people with HIV/AIDS compared with immunosuppressed transplant recipients: a meta-analysis. *Lancet*, 370(9581), pp.59–67.

Gueranger, Q. et al., 2011. Crosslinking of DNA repair and replication proteins to DNA in cells treated with 6-thioguanine and UVA. *Nucleic Acids Research*, 39(12), pp.5057–5066.

Gueranger, Q. et al., 2014. Protein Oxidation and DNA Repair Inhibition by 6-Thioguanine and UVA Radiation. *Journal of Investigative Dermatology*, 134(5), pp.1408–1417.

Gutteridge, J., 1986. Iron promoters of the Fenton reaction and lipid peroxidation can be released from haemoglobin by peroxides. *FEBS letters*, 201(2), pp.291–295.

Halliwell, B., 2008. Are polyphenols antioxidants or pro-oxidants? What do we learn from cell culture and in vivo studies? *Archives of biochemistry and biophysics*, 476(2), pp.107–112.

Halliwell, B., 1998. Can oxidative DNA damage be used as a biomarker of cancer risk in humans? Problems, resolutions and preliminary results from nutritional supplementation studies. *Free radical research*, 29(6), pp.469–486.

Halliwell, B., 2007. Oxidative stress and cancer: have we moved forward? *The Biochemical journal*, 401(1), p.1.

Halliwell, B. & Gutteridge, J.M., 2007. *Free Radicals in Biology and Medicine* 4 ed, New York: Oxford University Press.

Hammerman, P.S. et al., 2012. Comprehensive genomic characterization of squamous cell lung cancers. *Nature*, 489(7417), pp.519–525.

Hanawalt, P.C. & Spivak, G., 2008. Transcription-coupled DNA repair: two decades of progress and surprises. *Nature reviews Molecular cell biology*, 9(12), pp.958–970.

Hart, C.A. & Beeching, N.J., 2001. Prophylactic treatment of anthrax with antibiotics. *BMJ (Clinical research ed.)*, 323(7320), pp.1017–1018.

Harwood, C.A. et al., 2012. A Surveillance Model for Skin Cancer in Organ Transplant Recipients: A 22-Year Prospective Study in an Ethnically Diverse Population. *American Journal of Transplantation*, 13(1), pp.119–129.

Harwood, C.A. et al., 2008. PTCH mutations in basal cell carcinomas from azathioprine-treated organ transplant recipients. *British Journal of Cancer*, 99(8),

pp.1276–1284.

Hashimoto, M. et al., 2003. DNA-PK: the major target for wortmannin-mediated radiosensitization by the inhibition of DSB repair via NHEJ pathway. *Journal of radiation research*, 44(2), pp.151–159.

Hensley, K. & Floyd, R.A., 2002. Reactive Oxygen Species and Protein Oxidation in Aging: A Look Back, A Look Ahead. *Archives of biochemistry and biophysics*, 397(2), pp.377–383.

Hicks, L.A., Taylor, T.H., Jr. & Hunkler, R.J., 2013. U.S. Outpatient Antibiotic Prescribing, 2010. *The New England journal of medicine*, 368(15), pp.1461–1462.

Holt, R.B., McLane, C.K. & Oldenberg, O., 1948. Ultraviolet Absorption Spectrum of Hydrogen Peroxide. *The Journal of Chemical Physics*, 16(3), p.225.

Holzer, A.M., Athar, M. & Elmets, C.A., 2010. The Other End of the Rainbow: Infrared and Skin. *Journal of Investigative Dermatology*, 130(6), pp.1496–1499.

Höhn, A., Jung, T. & Grune, T., 2014. Pathophysiological importance of aggregated damaged proteins. *Free radical biology & medicine*, 71(C), pp.70–89.

Hwang, B.J. et al., 1999. Expression of the p48 xeroderma pigmentosum gene is p53-dependent and is involved in global genomic repair. *Proceedings of the National Academy of Sciences of the United States of America*, 96(2), pp.424–428.

Ibbotson, S.H., 2011. Adverse effects of topical photodynamic therapy. *Photodermatology, photoimmunology & photomedicine*, 27(3), pp.116–130.

Ide, H. et al., 2011. Repair and biochemical effects of DNA-protein crosslinks. *Mutation research*, 711(1-2), pp.113–122.

Ischiropoulos, H. & al-Mehdi, A.B., 1995. Peroxynitrite-mediated oxidative protein modifications. *FEBS letters*, 364(3), pp.279–282.

Itoh, T. et al., 2005. The photocarcinogenesis of antibiotic lomefloxacin and UVA radiation is enhanced in xeroderma pigmentosum group A gene-deficient mice. *The Journal of investigative dermatology*, 125(3), pp.554–559.

Jaiswal, M. et al., 2000. Inflammatory cytokines induce DNA damage and inhibit DNA repair in cholangiocarcinoma cells by a nitric oxide-dependent mechanism. *Cancer research*, 60(1), pp.184–190.

Jayaraman, S.S. et al., 2013. Mutational Landscape of Basal Cell Carcinomas by Whole-Exome Sequencing. 134(1), pp.213–220.

Jiménez, I., Lissi, E.A. & Speisky, H., 2000. Free-radical-induced inactivation of lysozyme and carbonyl residue generation in protein are not necessarily associated. *Archives of biochemistry and biophysics*, 381(2), pp.247–252.

Jing, Y., Kao, J.F. & Taylor, J.S., 1998. Thermodynamic and base-pairing studies of matched and mismatched DNA dodecamer duplexes containing cis-syn, (6-4) and Dewar photoproducts of TT. *Nucleic Acids Research*, 26(16), pp.3845–3853.

Jiricny, J., 2013. Postreplicative Mismatch Repair. *Cold Spring Harbor Perspectives in Biology*, 5(4), pp.a012633–a012633.

Jung, T., Bader, N. & Grune, T., 2007. Oxidized proteins: Intracellular distribution and recognition by the proteasome. *Archives of biochemistry and biophysics*, 462(2), pp.231–237.

Kalinski, P., 2011. Regulation of Immune Responses by Prostaglandin E2. *The Journal of Immunology*, 188(1), pp.21–28.

Kansanen, E. et al., 2013. The Keap1-Nrf2 pathway_ Mechanisms of activation and dysregulation in cancer. *Redox Biology*, 1(1), pp.45–49.

Karran, P. & Attard, N., 2008. Thiopurines in current medical practice: molecular mechanisms and contributions to therapy-related cancer. *Nature reviews Cancer*, 8(1), pp.24–36.

Kasiske, B.L. et al., 2009. KDIGO clinical practice guideline for the care of kidney transplant recipients: a summary. *Kidney International*, 77(4), pp.299–311.

Keeney, S. et al., 1994. Correction of the DNA repair defect in xeroderma pigmentosum group E by injection of a DNA damage-binding protein. *Proceedings of the National Academy of Sciences of the United States of America*, 91(9), pp.4053–4056.

Keeney, S., Chang, G.J. & Linn, S., 1993. Characterization of a human DNA damage binding protein implicated in xeroderma pigmentosum E. *The Journal of biological chemistry*, 268(28), pp.21293–21300.

Kehrer, J.P., 2000. The Haber-Weiss reaction and mechanisms of toxicity. *Toxicology*, 149(1), pp.43–50.

Keyer, K. & Imlay, J.A., 1996. Superoxide accelerates DNA damage by elevating free-iron levels. *Proceedings of the National Academy of Sciences of the United States of America*, 93(24), pp.13635–13640.

Khanna, K.K. & Jackson, S.P., 2001. DNA double-strand breaks: signaling, repair and the cancer connection. *Nature genetics*, 27(3), pp.247–254.

Kielbassa, C., Roza, L. & Epe, B., 1997. Wavelength dependence of oxidative DNA damage induced by UV and visible light. *Carcinogenesis*, 18(4), pp.811–816.

Kirouac, K.N. & Ling, H., 2011. Unique active site promotes error-free replication opposite an 8-oxo-guanine lesion by human DNA polymerase iota. *Proceedings of the National Academy of Sciences of the United States of America*, 108(8), pp.3210–3215.

Kirschner, K. & Melton, D.W., 2010. Multiple roles of the ERCC1-XPF endonuclease in DNA repair and resistance to anticancer drugs. *Anticancer research*, 30(9), pp.3223–3232.

Klatt, P. et al., 1999. Redox regulation of c-Jun DNA binding by reversible S-glutathiolation. *The FASEB journal : official publication of the Federation of American Societies for Experimental Biology*, 13(12), pp.1481–1490.

Klecak, G., Urbach, F. & Urwyler, H., 1997. Fluoroquinolone antibacterials enhance UVA-induced skin tumors. *Journal of photochemistry and photobiology B, Biology*, 37(3), pp.174–181.

Klivenyi, P. et al., 2000. Mice deficient in cellular glutathione peroxidase show increased vulnerability to malonate, 3-nitropropionic acid, and 1-methyl-4-phenyl-1, 2, 5, 6-tetrahydropyridine. *The Journal of Neuroscience*, 20(1), pp.1–7.

Klotz, L.-O., Kr ncke, K.-D. & Sies, H., 2003. Singlet oxygen-induced signaling effects in mammalian cells. *Photochemical & photobiological sciences : Official journal of the European Photochemistry Association and the European Society for Photobiology*, 2(2), p.88.

Korichneva, I., 2005. Redox regulation of cardiac protein kinase C. *Experimental and clinical cardiology*, 10(4), pp.256–261.

Kraljić, I. & Mohsni, S.E., 1978. A new method for the detection of singlet oxygen in aqueous solutions. *Photochemistry and photobiology*, 28(4-5), pp.577–581.

Krasikova, Y.S. et al., 2010. Localization of xeroderma pigmentosum group A protein and replication protein A on damaged DNA in nucleotide excision repair. *Nucleic Acids Research*, 38(22), pp.8083–8094.

Krisko, A. & Radman, M., 2013. Phenotypic and Genetic Consequences of Protein Damage P. H. Viollier, ed. *PLoS Genetics*, 9(9), p.e1003810.

Krisko, A. & Radman, M., 2010. Protein damage and death by radiation in Escherichia coli and Deinococcus radiodurans. *Proceedings of the National Academy of Sciences of the United States of America*, 107(32), pp.14373–14377.

Krisko, A. et al., 2012. Extreme anti-oxidant protection against ionizing radiation in bdelloid rotifers. *Proceedings of the National Academy of Sciences*, 109(7), pp.2354–2357.

Krokan, H.E. & Bjoras, M., 2013. Base Excision Repair. *Cold Spring Harbor Perspectives in Biology*, 5(4), pp.a012583–a012583.

Krokan, H.E., Standal, R. & Slupphaug, G., 1997. DNA glycosylases in the base excision repair of DNA. *The Biochemical journal*, 325 ( Pt 1), pp.1–16.

Kumatori, A. et al., 1990. Abnormally high expression of proteasomes in human leukemic cells. *Proceedings of the National Academy of Sciences of the United*

*States of America*, 87(18), pp.7071–7075.

Lacouture, M.E. et al., 2013. Analysis of Dermatologic Events in Vemurafenib-Treated Patients With Melanoma. *The Oncologist*, 18(3), pp.314–322.

Laval, F. & Wink, D.A., 1994. Inhibition by nitric oxide of the repair protein, O6-DNA-methyltransferase. *Carcinogenesis*, 15(3), pp.443–447.

Lee, J.-W. & Helmann, J.D., 2006. The PerR transcription factor senses H2O2 by metal-catalysed histidine oxidation. *Nature Cell Biology*, 440(7082), pp.363–367.

Legrini, O., Oliveros, E. & Braun, A.M., 1993. Photochemical processes for water treatment. *Chemical reviews*, 93(2), pp.671–698.

Lehmann, A.R., 2011. DNA polymerases and repair synthesis in NER in human cells. *DNA repair*, 10(7), pp.730–733.

Leonard, S.E., Reddie, K.G. & Carroll, K.S., 2009. Mining the thiol proteome for sulfenic acid modifications reveals new targets for oxidation in cells. *ACS chemical biology*, 4(9), pp.783–799.

Levine, R.L. et al., 1990. Determination of carbonyl content in oxidatively modified proteins. *Methods in enzymology*, 186, pp.464–478.

Li, F., 2010. DNA damage and UVA-induced oxidation of DNA 6-thioguanine. *PhD Thesis, The University of London, London*, pp.1–221.

Lieber, M.R., 2010. The Mechanism of Double-Strand DNA Break Repair by the Nonhomologous DNA End-Joining Pathway. *Annual review of biochemistry*, 79(1), pp.181–211.

Lindahl, T., 1993. Instability and decay of the primary structure of DNA. *Nature*, 362(6422), pp.709–715.

Linetsky, M. et al., 2003. Effect of UVA light on the activity of several aged human lens enzymes. *Investigative ophthalmology & visual science*, 44(1), pp.264–274.

Liu, B., Chen, Y. & St Clair, D.K., 2008. ROS and p53: A versatile partnership. *Free radical biology & medicine*, 44(8), pp.1529–1535.

Liu, L. et al., 2009. CUL4A Abrogation Augments DNA Damage Response and Protection against Skin Carcinogenesis. *Molecular Cell*, 34(4), pp.451–460.

Liu, Y. et al., 2011. Probing for DNA damage with β-hairpins: Similarities in incision efficiencies of bulky DNA adducts by prokaryotic and human nucleotide excision repair systems in vitro. *DNA repair*, 10(7), pp.684–696.

Lopez, M.F. et al., 2000. A comparison of silver stain and SYPRO Ruby Protein Gel Stain with respect to protein detection in two-dimensional gels and identification by peptide mass profiling. *Electrophoresis*, 21(17), pp.3673–3683.

Luijsterburg, M.S. et al., 2007. Dynamic in vivo interaction of DDB2 E3 ubiquitin ligase with UV-damaged DNA is independent of damage-recognition protein XPC. *Journal of Cell Science*, 120(15), pp.2706–2716.

Lukina, M.V. et al., 2013. DNA Damage Processing by Human 8-Oxoguanine-DNA Glycosylase Mutants with the Occluded Active Site. *Journal of Biological Chemistry*, 288(40), pp.28936–28947.

Lundeen, R.A. & McNeill, K., 2013. Reactivity Differences of Combined and Free Amino Acids: Quantifying the Relationship between Three-Dimensional Protein Structure and Singlet Oxygen Reaction Rates. *Environmental Science & Technology*, 47(24), pp.14215–14223.

Luo, J. et al., 2006. Inactivation of primary antioxidant enzymes in mouse keratinocytes by photodynamically generated singlet oxygen. *Antioxidants & redox signaling*, 8(7-8), pp.1307–1314.

Luo, S. & Wehr, N.B., 2009. Protein carbonylation: avoiding pitfalls in the 2,4-dinitrophenylhydrazine assay. *Redox report : communications in free radical research*, 14(4), pp.159–166.

Ma, Q., 2013. Role of Nrf2 in Oxidative Stress and Toxicity. *Annual Review of Pharmacology and Toxicology*, 53(1), pp.401–426.

Madian, A.G. & Regnier, F.E., 2010. Proteomic identification of carbonylated proteins and their oxidation sites. *Journal of proteome research*, 9(8), pp.3766–3780.

Marampon, F. et al., 2011. MEK/ERK Inhibitor U0126 Increases the Radiosensitivity of Rhabdomyosarcoma Cells In vitro and In vivo by Downregulating Growth and DNA Repair Signals. *Molecular Cancer Therapeutics*, 10(1), pp.159–168.

Marechal, A. & Zou, L., 2013. DNA Damage Sensing by the ATM and ATR Kinases. *Cold Spring Harbor Perspectives in Biology*, 5(9), pp.a012716–a012716.

Marteijn, J.A. et al., 2014. Understanding nucleotide excision repair and its roles in cancer and ageing. *Nature reviews Molecular cell biology*, 15(7), pp.465–481.

Martindale, J.L. & Holbrook, N.J., 2002. Cellular response to oxidative stress: Signaling for suicide and survival. *Journal of Cellular Physiology*, 192(1), pp.1–15.

Martínez, L.J., Sik, R.H. & Chignell, C.F., 1998. Fluoroquinolone antimicrobials: singlet oxygen, superoxide and phototoxicity. *Photochemistry and photobiology*, 67(4), pp.399–403.

Mathieu, N. et al., 2013. DNA Quality Control by a Lesion Sensor Pocket of the Xeroderma Pigmentosum Group D Helicase Subunit of TFIIH. *Current biology : CB*, 23(3), pp.204–212.

McCubrey, J.A. et al., 2007. Roles of the Raf/MEK/ERK pathway in cell growth, malignant transformation and drug resistance. *Biochimica et Biophysica Acta (BBA)*

- *Molecular Cell Research*, 1773(8), pp.1263–1284.

McCulloch, S.D. et al., 2004. Preferential cis-syn thymine dimer bypass by DNA polymerase eta occurs with biased fidelity. *Nature*, 428(6978), pp.97–100.

McGregor, J.M. et al., 1997. p53 mutations implicate sunlight in post-transplant skin cancer irrespective of human papillomavirus status. *Oncogene*, 15, pp.1737–1740.

McIlwraith, M.J. et al., 2005. Human DNA Polymerase η Promotes DNA Synthesis from Strand Invasion Intermediates of Homologous Recombination. *Molecular Cell*, 20(5), pp.783–792.

McLeod, H.L. et al., 2000. Genetic polymorphism of thiopurine methyltransferase and its clinical relevance for childhood acute lymphoblastic leukemia. *Leukemia*, 14(4), pp.567–572.

McNicholas, S. et al., 2011. Presenting your structures: the CCP4mg molecular-graphics software. *Acta Cryst (2011). D67, 386-394 [doi:10.1107/S0907444911007281]*, pp.1–9.

Men, L. et al., 2007. Redox-dependent formation of disulfide bonds in human replication protein A. *Rapid communications in mass spectrometry : RCM*, 21(16), pp.2743–2749.

Meng, T.-C., Fukada, T. & Tonks, N.K., 2002. Reversible oxidation and inactivation of protein tyrosine phosphatases in vivo. *Molecular Cell*, 9(2), pp.387–399.

Michaelis, M. et al., 2014. Differential effects of the oncogenic BRAF inhibitor PLX4032 (vemurafenib) and its progenitor PLX4720 on ABCB1 function. *Journal of pharmacy & pharmaceutical sciences : a publication of the Canadian Society for Pharmaceutical Sciences, Société canadienne des sciences pharmaceutiques*, 17(1), pp.154–168.

Min, J.-H. & Pavletich, N.P., 2007. Recognition of DNA damage by the Rad4 nucleotide excision repair protein. *Nature*, 449(7162), pp.570–575.

Mirzaei, H. & Regnier, F., 2008. Protein:protein aggregation induced by protein oxidation. *Journal of Chromatography B*, 873(1), pp.8–14.

Montaner, B. et al., 2007. Reactive oxygen-mediated damage to a human DNA replication and repair protein. *EMBO reports*, 8(11), pp.1074–1079.

Morliere, P., Moysan, A. & Tirache, I., 1995. Action spectrum for UV-induced lipid peroxidation in cultured human skin fibroblasts. *Free radical biology & medicine*, 19(3), pp.365–371.

Moser, J. et al., 2005. The UV-damaged DNA binding protein mediates efficient targeting of the nucleotide excision repair complex to UV-induced photo lesions. *DNA repair*, 4(5), pp.571–582.

Mouret, S. et al., 2006. Cyclobutane pyrimidine dimers are predominant DNA lesions in whole human skin exposed to UVA radiation. *Proceedings of the National Academy of Sciences of the United States of America*, 103(37), pp.13765–13770.

Mouret, S. et al., 2010. UVA-induced cyclobutane pyrimidine dimers in DNA: a direct photochemical mechanism? *Organic & biomolecular chemistry*, 8(7), p.1706.

Mouret, S., Forestier, A. & Douki, T., 2011a. The specificity of UVA-induced DNA damage in human melanocytes. *Photochemical & photobiological sciences : Official journal of the European Photochemistry Association and the European Society for Photobiology*, 11(1), p.155.

Mouret, S.E.P. et al., 2011b. Individual Photosensitivity of Human Skin and UVA-Induced Pyrimidine Dimers in DNA. *Journal of Investigative Dermatology*, 131(7), pp.1539–1546.

Mudigonda, T. et al., 2012. Incidence, Risk Factors, and Preventative Management of Skin Cancers in Organ Transplant Recipients: A Review of Single- and Multicenter Retrospective Studies from 2006 to 2010. *Dermatologic Surgery*, 39(3pt1), pp.345–364.

Muniandy, P.A. et al., 2009. Repair of Laser-localized DNA Interstrand Cross-links in G1 Phase Mammalian Cells. *Journal of Biological Chemistry*, 284(41), pp.27908–27917.

Murray, C.I. & Van Eyk, J.E., 2012. Chasing Cysteine Oxidative Modifications: Proteomic Tools for Characterizing Cysteine Redox Status. *Circulation: Cardiovascular Genetics*, 5(5), pp.591–591.

Musich, P.R. & Zou, Y., 2009. Genomic instability and DNA damage responses in progeria arising from defective maturation of prelamin A. *Aging*, 1(1), pp.28–37.

Narayanan, D.L., Saladi, R.N. & Fox, J.L., 2010. Ultraviolet radiation and skin cancer. *International journal of dermatology*, 49(9), pp.978–986.

Neeley, W.L. & Essigmann, J.M., 2006. Mechanisms of Formation, Genotoxicity, and Mutation of Guanine Oxidation Products. *Chemical research in toxicology*, 19(4), pp.491–505.

Negre-Salvayre, A. et al., 2008. Advanced lipid peroxidation end products in oxidative damage to proteins. Potential role in diseases and therapeutic prospects for the inhibitors. *British Journal of Pharmacology*, 153(1), pp.6–20.

Neuzil, J., Gebicki, J.M. & Stocker, R., 1993. Radical-induced chain oxidation of proteins and its inhibition by chain-breaking antioxidants. *The Biochemical journal*, 293 ( Pt 3), pp.601–606.

Nishi, R. et al., 2009. UV-DDB-dependent regulation of nucleotide excision repair kinetics in living cells. *DNA repair*, 8(6), pp.767–776.

O'Donovan, P. et al., 2005. Azathioprine and UVA Light Generate Mutagenic Oxidative DNA Damage. *Science (New York, NY)*, 309(5742), pp.1871–1874.

Oleinick, N.L. et al., 2009. Identifying initial molecular targets of PDT: protein and lipid oxidation products. In D. H. Kessel, ed. 12th World Congress of the International Photodynamic Association. SPIE, pp. 738008–738008–11.

Oliveira, C.S. et al., 2011. Major determinants of photoinduced cell death: Subcellular localization versus photosensitization efficiency. *Free radical biology & medicine*, 51(4), pp.824–833.

Otrin, V.R. et al., 1997. Translocation of a UV-damaged DNA binding protein into a tight association with chromatin after treatment of mammalian cells with UV light. *Journal of Cell Science*, 110 ( Pt 10), pp.1159–1168.

Pacher, P., Beckman, J.S. & Liaudet, L., 2007. Nitric oxide and peroxynitrite in health and disease. *Physiological reviews*, 87(1), pp.315–424.

Panier, S. & Boulton, S.J., 2013. Double-strand break repair: 53BP1 comes into focus. *Nature reviews Molecular cell biology*, 15(1), pp.7–18.

Parker, J.B. et al., 2007. Enzymatic capture of an extrahelical thymine in the search for uracil in DNA. *Nature*, 449(7161), pp.433–437.

Parkin, D.M., Mesher, D. & Sasieni, P., 2011. 13. Cancers attributable to solar (ultraviolet) radiation exposure in the UK in 2010. *British Journal of Cancer*, 105(S2), pp.S66–S69.

Pattison, D.I., Rahmanto, A.S. & Davies, M.J., 2011. Photo-oxidation of proteins. *Photochemical & photobiological sciences : Official journal of the European Photochemistry Association and the European Society for Photobiology*, 11(1), p.38.

Pavlov, Y.I. et al., 1994. DNA replication fidelity with 8-oxodeoxyguanosine triphosphate. *Biochemistry*, 33(15), pp.4695–4701.

Payne, A. & Chu, G., 1994. Xeroderma pigmentosum group E binding factor recognizes a broad spectrum of DNA damage. *Mutation research*, 310(1), pp.89–102.

Perdiz, D. et al., 2000. Distribution and repair of bipyrimidine photoproducts in solar UV-irradiated mammalian cells. Possible role of Dewar photoproducts in solar mutagenesis. *Journal of Biological Chemistry*.

Peus, D. et al., 1999. UVB activates ERK1/2 and p38 signaling pathways via reactive oxygen species in cultured keratinocytes. *Journal of Investigative Dermatology*, 112(5), pp.751–756.

Pignatelli, B. et al., 2001. Nitrated and oxidized plasma proteins in smokers and lung cancer patients. *Cancer research*, 61(2), pp.778–784.

Polte, T. & Tyrrell, R.M., 2004. Involvement of lipid peroxidation and organic peroxides in UVA-induced Matrix Metalloproteinase-1 expression. *Free radical biology & medicine*, 36(12), pp.1566–1574.

Poon, H.F. et al., 2007. Improving image analysis in 2DGE-based redox proteomics by labeling protein carbonyl with fluorescent hydroxylamine. *Biological procedures online*, 9, pp.65–72.

Poon, H.F. et al., 2004. Quantitative proteomics analysis of specific protein expression and oxidative modification in aged senescence-accelerated-prone 8 mice brain. *Neuroscience*, 126(4), pp.915–926.

Poulikakos, P.I. et al., 2011. RAF inhibitors transactivate RAF dimers and ERK signalling in cells with wild-type BRAF. *Nature*, 464(7287), pp.427–430.

Pourzand, C. et al., 1999. Ultraviolet A radiation induces immediate release of iron in human primary skin fibroblasts: the role of ferritin. *Proceedings of the National Academy of Sciences of the United States of America*, 96(12), pp.6751–6756.

Prasad, R. et al., 2011. A review of recent experiments on step-to-step "hand-off" of the DNA intermediates in mammalian base excision repair pathways. *Molecular Biology*, 45(4), pp.536–550.

Pullar, J.M., Vissers, M.C. & Winterbourn, C.C., 2000. Living with a killer: the effects of hypochlorous acid on mammalian cells. *IUBMB life*, 50(4-5), pp.259–266.

Radhakrishnan, S.K., Jette, N. & Lees-Miller, S.P., 2014. Non-homologous end joining: Emerging themes and unanswered questions. *DNA repair*, 17, pp.2–8.

Radi, R., 2004. Nitric oxide, oxidants, and protein tyrosine nitration. *Proceedings of the National Academy of Sciences of the United States of America*, 101(12), pp.4003–4008.

Rapić-Otrin, V. et al., 2002. Sequential binding of UV DNA damage binding factor and degradation of the p48 subunit as early events after UV irradiation. *Nucleic Acids Research*, 30(11), pp.2588–2598.

Redmond, R.W. & Kochevar, I.E., 2006. Spatially Resolved Cellular Responses to Singlet Oxygen. *Photochemistry and photobiology*, 82(5), p.1178.

Regensburger, J. et al., 2012. Fatty acids and vitamins generate singlet oxygen under UVB irradiation. *Experimental Dermatology*, 21(2), pp.135–139.

Ren, X. et al., 2010. Guanine sulphinate is a major stable product of photochemical oxidation of DNA 6-thioguanine by UVA irradiation. *Nucleic Acids Research*, 38(6), pp.1832–1840.

Renkawitz, J., Lademann, C.A. & Jentsch, S., 2014. Mechanisms and principles of homology search during recombination. *Nature reviews Molecular cell biology*, pp.1–15.

Requena, J.R. et al., 2001. Glutamic and aminoadipic semialdehydes are the main carbonyl products of metal-catalyzed oxidation of proteins. *Proceedings of the National Academy of Sciences of the United States of America*, 98(1), pp.69–74.

Reynolds, P. et al., 2012. The dynamics of Ku70/80 and DNA-PKcs at DSBs induced by ionizing radiation is dependent on the complexity of damage. *Nucleic Acids Research*, 40(21), pp.10821–10831.

Rhee, S.G., 2003. Cellular Regulation by Hydrogen Peroxide. *Journal of the American Society of Nephrology*, 14(90003), pp.211S–215.

Rhee, S.G. et al., 2005. Controlled elimination of intracellular H2O2: regulation of peroxiredoxin, catalase, and glutathione peroxidase via post-translational modification. *Antioxidants & redox signaling*, 7(5-6), pp.619–626.

Rhee, S.G. et al., 2000. Hydrogen Peroxide: A Key Messenger That Modulates Protein Phosphorylation Through Cysteine Oxidation. *Science Signaling*, 2000(53), pp.pe1–pe1.

Rhie, G. et al., 2001. Aging- and photoaging-dependent changes of enzymic and nonenzymic antioxidants in the epidermis and dermis of human skin in vivo. *The Journal of investigative dermatology*, 117(5), pp.1212–1217.

Roberts, P.J. & Der, C.J., 2007. Targeting the Raf-MEK-ERK mitogen-activated protein kinase cascade for the treatment of cancer. *Oncogene*, 26(22), pp.3291–3310.

Robertson, A.B. et al., 2009. DNA Repair in Mammalian Cells. *Cellular and molecular life sciences : CMLS*, 66(6), pp.981–993.

Romero-Graillet, C. et al., 1996. Ultraviolet B Radiation Acts through the Nitric Oxide and cGMP Signal Transduction Pathway to Stimulate Melanogenesis in Human Melanocytes. *Journal of Biological Chemistry*, 271(45), pp.28052–28056.

Rudeck, M. et al., 2000. Ferritin oxidation in vitro: implication of iron release and degradation by the 20S proteasome. *IUBMB life*, 49(5), pp.451–456.

Runchel, C., Matsuzawa, A. & Ichijo, H., 2011. Mitogen-Activated Protein Kinases in Mammalian Oxidative Stress Responses. *Antioxidants & redox signaling*, 15(1), pp.205–218.

Sage, E., Girard, P.-M. & Francesconi, S., 2011. Unravelling UVA-induced mutagenesis. *Photochemical & photobiological sciences : Official journal of the European Photochemistry Association and the European Society for Photobiology*, 11(1), p.74.

Sakharov, D.V. et al., 2003. Photodynamic treatment and H2O2-induced oxidative stress result in different patterns of cellular protein oxidation. *European Journal of Biochemistry*, 270(24), pp.4859–4865.

Sale, J.E., Lehmann, A.R. & Woodgate, R., 2012. Y-family DNA polymerases and their

role in tolerance of cellular DNA damage. *Nature reviews Molecular cell biology*, 13(3), pp.141–152.

Sander, C.S. et al., 2002. Photoaging is associated with protein oxidation in human skin in vivo. *Journal of Investigative Dermatology*, 118(4), pp.618–625.

Saran, A., 2010. Basal cell carcinoma and the carcinogenic role of aberrant Hedgehog signaling. *Future Oncology*, 6(6), pp.1003–1014.

Sauvaigo, S. et al., 2001. Analysis of fluoroquinolone-mediated photosensitization of 2'-deoxyguanosine, calf thymus and cellular DNA: determination of type-I, type-II and triplet-triplet energy transfer mechanism contribution. *Photochemistry and photobiology*, 73(3), pp.230–237.

Scharer, O.D., 2013. Nucleotide Excision Repair in Eukaryotes. *Cold Spring Harbor Perspectives in Biology*, 5(10), pp.a012609–a012609.

Schipler, A. & Iliakis, G., 2013. DNA double-strand-break complexity levels and their possible contributions to the probability for error-prone processing and repair pathway choice. *Nucleic Acids Research*, 41(16), pp.7589–7605.

Schwertman, P., Vermeulen, W. & Marteijn, J.A., 2013. UVSSA and USP7, a new couple in transcription-coupled DNA repair. *Chromosoma*, 122(4), pp.275–284.

Scrima, A. et al., 2008. Structural basis of UV DNA-damage recognition by the DDB1-DDB2 complex. *Cell*, 135(7), pp.1213–1223.

Shachar, S. et al., 2009. Two-polymerase mechanisms dictate error-free and error-prone translesion DNA synthesis in mammals. *The EMBO journal*, 28(4), pp.383–393.

Shen, H.-R., Spikes, J.D., Smith, C.J. & Kopeček, J., 2000a. Photodynamic cross-linking of proteins: IV. Nature of the His–His bond (s) formed in the rose bengal-photosensitized cross-linking of N-benzoyl-L-histidine. *Journal of Photochemistry and Photobiology A: Chemistry*, 130(1), pp.1–6.

Shen, H.-R., Spikes, J.D., Smith, C.J. & Kopeček, J., 2000b. Photodynamic cross-linking of proteins: V. Nature of the tyrosine–tyrosine bonds formed in the FMN-sensitized intermolecular cross-linking of N-acetyl-L-tyrosine. *Journal of Photochemistry and Photobiology A: Chemistry*, 133(1), pp.115–122.

Shen, H.R. et al., 1996. Photodynamic crosslinking of proteins. I. Model studies using histidine- and lysine-containing N-(2-hydroxypropyl)methacrylamide copolymers. *Journal of photochemistry and photobiology B, Biology*, 34(2-3), pp.203–210.

Shindo, Y. & Hashimoto, T., 1997. Time course of changes in antioxidant enzymes in human skin fibroblasts after UVA irradiation. *Journal of dermatological science*, 14(3), pp.225–232.

Shindo, Y. et al., 1994. Dose-response effects of acute ultraviolet irradiation on antioxidants and molecular markers of oxidation in murine epidermis and dermis.

*The Journal of investigative dermatology*, 102(4), pp.470–475.

Silvester, J.A., Timmins, G.S. & Davies, M.J., 1998. Protein hydroperoxides and carbonyl groups generated by porphyrin-induced photo-oxidation of bovine serum albumin. *Archives of biochemistry and biophysics*, 350(2), pp.249–258.

Sirbu, B.M. & Cortez, D., 2013. DNA Damage Response: Three Levels of DNA Repair Regulation. *Cold Spring Harbor Perspectives in Biology*, 5(8), pp.a012724–a012724.

Sitte, N., Merker, K. & Grune, T., 1998. Proteasome-dependent degradation of oxidized proteins in MRC-5 fibroblasts. *FEBS letters*, 440(3), pp.399–402.

Slade, D. & Radman, M., 2011. Oxidative Stress Resistance in Deinococcus radiodurans. *Microbiology and Molecular Biology Reviews*, 75(1), pp.133–191.

Smith, J. et al., 2010. *Chapter 3 - The ATM-Chk2 and ATR-Chk1 Pathways in DNA Damage Signaling and Cancer* 1st ed, Elsevier Inc.

Sonntag, Von, C., 2006. *Free-Radical-Induced DNA Damage and Its Repair: A Chemical Perspective*, Springer.

Sosman, J.A. et al., 2012. Survival in BRAF V600-mutant advanced melanoma treated with vemurafenib. *The New England journal of medicine*, 366(8), pp.707–714.

South, A.P. et al., 2014. NOTCH1 Mutations Occur Early during Cutaneous Squamous Cell Carcinogenesis. pp.1–9.

Souza, J.M., 2000. Dityrosine Cross-linking Promotes Formation of Stable alpha - Synuclein Polymers. IMPLICATION OF NITRATIVE AND OXIDATIVE STRESS IN THE PATHOGENESIS OF NEURODEGENERATIVE SYNUCLEINOPATHIES. *Journal of Biological Chemistry*, 275(24), pp.18344–18349.

Spencer, J.P. et al., 2000. Nitrite-induced deamination and hypochlorite-induced oxidation of DNA in intact human respiratory tract epithelial cells. *Free radical biology & medicine*, 28(7), pp.1039–1050.

Spitz, M.R. et al., 2001. Modulation of nucleotide excision repair capacity by XPD polymorphisms in lung cancer patients. *Cancer research*, 61(4), pp.1354–1357.

Stadtman, E.R. & Levine, R.L., 2001. Protein oxidation. *Annals of the New York Academy of Sciences*, 899, pp.191–208.

Steenken, S. & Jovanovic, S.V., 1997. How easily oxidizable is DNA? One-electron reduction potentials of adenosine and guanosine radicals in aqueous solution. *Journal of the American Chemical Society*, 119(3), pp.617–618.

Su, F. et al., 2012. RAS mutations in cutaneous squamous-cell carcinomas in patients treated with BRAF inhibitors. *The New England journal of medicine*, 366(3),

pp.207–215.

Sugasawa, K., 2006. UV-induced ubiquitylation of XPC complex, the UV-DDB-ubiquitin ligase complex, and DNA repair. *Journal of Molecular Histology*, 37(5-7), pp.189–202.

Sugasawa, K. et al., 2005. UV-Induced Ubiquitylation of XPC Protein Mediated by UV-DDB-Ubiquitin Ligase Complex. *Cell*, 121(3), pp.387–400.

Svobodová, A. & Vostálová, J., 2010. Solar radiation induced skin damage: Review of protective and preventive options. *International Journal of Radiation Biology*, 86(12), pp.999–1030.

Swann, P.F. et al., 1996. Role of postreplicative DNA mismatch repair in the cytotoxic action of thioguanine. *Science (New York, NY)*, 273(5278), pp.1109–1111.

Szokalska, A. et al., 2009. Proteasome Inhibition Potentiates Antitumor Effects of Photodynamic Therapy in Mice through Induction of Endoplasmic Reticulum Stress and Unfolded Protein Response. *Cancer research*, 69(10), pp.4235–4243.

Tamarit, J. et al., 2012. Analysis of oxidative stress-induced protein carbonylation using fluorescent hydrazides. *Journal of proteomics*, 75(12), pp.3778–3788.

Telci, A. et al., 2000. Oxidative protein damage in plasma of type 2 diabetic patients. *Hormone and Metabolic Research*, 32(01), pp.40–43.

Temple, A., Yen, T.-Y. & Gronert, S., 2006. Identification of specific protein carbonylation sites in model oxidations of human serum albumin. *Journal of the American Society for Mass Spectrometry*, 17(8), pp.1172–1180.

Tsaalbi-Shtylik, A. et al., 2014. Persistently stalled replication forks inhibit nucleotide excision repair in trans by sequestering Replication protein A. *Nucleic Acids Research*, 42(7), pp.4406–4413.

Tsai, J. et al., 2008. Discovery of a selective inhibitor of oncogenic B-Raf kinase with potent antimelanoma activity. *Proceedings of the National Academy of Sciences of the United States of America*, 105(8), pp.3041–3046.

Tsaytler, P.A. et al., 2008. Immediate protein targets of photodynamic treatment in carcinoma cells. *Journal of proteome research*, 7(9), pp.3868–3878.

Tyrrell, R.M., 2011. Modulation of gene expression by the oxidative stress generated in human skin cells by UVA radiation and the restoration of redox homeostasis. *Photochemical & photobiological sciences : Official journal of the European Photochemistry Association and the European Society for Photobiology*, 11(1), p.135.

Valko, M. et al., 2006. Free radicals, metals and antioxidants in oxidative stress-induced cancer. *Chemico-biological interactions*, 160(1), pp.1–40.

Vasquez-Vivar, J., 2000. Mitochondrial Aconitase Is a Source of Hydroxyl Radical. An electron spin resonance investigation. *Journal of Biological Chemistry*, 275(19), pp.14064–14069.

Vile, G.F. & Tyrrell, R.M., 1995. UVA radiation-induced oxidative damage to lipids and proteins in vitro and in human skin fibroblasts is dependent on iron and singlet oxygen. *Free radical biology & medicine*, 18(4), pp.721–730.

Vistoli, G. et al., 2013. Advanced glycoxidation and lipoxidation end products (AGEs and ALEs): an overview of their mechanisms of formation. *Free radical research*, 47(S1), pp.3–27.

Vogel, U. et al., 2001. Polymorphisms of the DNA repair gene XPD: correlations with risk of basal cell carcinoma revisited. *Carcinogenesis*, 22(6), pp.899–904.

Walker, J.R., Corpina, R.A. & Goldberg, J., 2001. Structure of the Ku heterodimer bound to DNA and its implications for double-strand break repair. *Nature*, 412(6847), pp.607–614.

Wang, N.J. et al., 2011. Loss-of-function mutations in Notch receptors in cutaneous and lung squamous cell carcinoma. *Proceedings of the National Academy of Sciences of the United States of America*, 108(43), pp.17761–17766.

Wang, P. & Powell, S.R., 2010. Decreased sensitivity associated with an altered formulation of a commercially available kit for detection of protein carbonyls. *Free radical biology & medicine*, 49(2), pp.119–121.

Wardman, P., 2007. Fluorescent and luminescent probes for measurement of oxidative and nitrosative species in cells and tissues: Progress, pitfalls, and prospects. *Free radical biology & medicine*, 43(7), pp.995–1022.

Waters, C.A. et al., 2014. Nonhomologous end joining: A good solution for bad ends. *DNA repair*, 17, pp.39–51.

Wellbrock, C., Karasarides, M. & Marais, R., 2004. The RAF proteins take centre stage. *Nature reviews Molecular cell biology*, 5(11), pp.875–885.

Weterings, E., 2003. The role of DNA dependent protein kinase in synapsis of DNA ends. *Nucleic Acids Research*, 31(24), pp.7238–7246.

Whittier, J.E., 2004. Hsp90 Enhances Degradation of Oxidized Calmodulin by the 20 S Proteasome. *Journal of Biological Chemistry*, 279(44), pp.46135–46142.

Wilkinson, F. & Brummer, J.G., 1981. Rate constants for the decay and reactions of the lowest electronically excited singlet state of molecular oxygen in solution. *Journal of Physical and Chemical Reference Data*, 10(4), pp.809–999.

Winterbourn, C.C., 2008. Reconciling the chemistry and biology of reactive oxygen species. *Nature Chemical Biology*, 4(5), pp.278–286.

Wittschieben, B.O., Iwai, S. & Wood, R.D., 2005. DDB1-DDB2 (Xeroderma Pigmentosum Group E) Protein Complex Recognizes a Cyclobutane Pyrimidine Dimer, Mismatches, Apurinic/Apyrimidinic Sites, and Compound Lesions in DNA. *Journal of Biological Chemistry*, 280(48), pp.39982–39989.

Wohlkonig, A. et al., 2010. Structural basis of quinolone inhibition of type IIA topoisomerases and target-mediated resistance. *Nature Publishing Group*, 17(99), pp.1152–1153.

Wondrak, G.T., Jacobson, M.K. & Jacobson, E.L., 2006. Endogenous UVA-photosensitizers: mediators of skin photodamage and novel targets for skin photoprotection. *Photochemical & photobiological sciences : Official journal of the European Photochemistry Association and the European Society for Photobiology*, 5(2), p.215.

Woo, H.A. & Rhee, S.G., 2010. Immunoblot detection of proteins that contain cysteine sulfinic or sulfonic acids with antibodies specific for the hyperoxidized cysteine-containing sequence. *Mary Ann Liebert, Inc*, p.275.

Wu, R.W.K. et al., 2011. Photodynamic therapy (PDT) – Initiation of apoptosis via activation of stress-activated p38 MAPK and JNK signal pathway in H460 cell lines. *Photodiagnosis and Photodynamic Therapy*, 8(3), pp.254–263.

Wu, S. et al., 2014. Long-term Ultraviolet Flux, Other Potential Risk Factors, and Skin Cancer Risk: A Cohort Study. *Cancer Epidemiology Biomarkers & Prevention*, 23(6), pp.1080–1089.

Xu, G. & Chance, M.R., 2007. Hydroxyl radical-mediated modification of proteins as probes for structural proteomics. *Chemical reviews*, 107(8), pp.3514–3543.

Yaar, M. & Gilchrest, B.A., 2007. Photoageing: mechanism, prevention and therapy. *The British journal of dermatology*, 157(5), pp.874–887.

Yano, K.-I. et al., 2009. Molecular Mechanism of Protein Assembly on DNA Double-strand Breaks in the Non-homologous End-joining Pathway. *Journal of radiation research*, 50(2), pp.97–108.

Yarosh, D. et al., 2001. Effect of topically applied T4 endonuclease V in liposomes on skin cancer in xeroderma pigmentosum: a randomised study. Xeroderma Pigmentosum Study Group. *Lancet*, 357(9260), pp.926–929.

Yeeles, J.T.P. et al., 2013. Rescuing Stalled or Damaged Replication Forks. *Cold Spring Harbor Perspectives in Biology*, 5(5), pp.a012815–a012815.

Yeh, J.I. et al., 2012. Damaged DNA induced UV-damaged DNA-binding protein (UV-DDB) dimerization and its roles in chromatinized DNA repair. *Proceedings of the National Academy of Sciences of the United States of America*, 109(41), pp.E2737–46.

Yoon, J.H., Prakash, L. & Prakash, S., 2010. Error-free replicative bypass of (6-4)

photoproducts by DNA polymerase  in mouse and human cells. *Genes & Development*, 24(2), pp.123–128.

Zastrow, L. et al., 2009. UV, visible and infrared light. *Der Hautarzt*, 60(4), pp.310–317.

Zhang, F., Fu, L. & Wang, Y., 2013. 6-Thioguanine Induces Mitochondrial Dysfunction and Oxidative DNA Damage in Acute Lymphoblastic Leukemia Cells. *Molecular & Cellular Proteomics*, 12(12), pp.3803–3811.

Zhang, X. et al., 2007. Novel DNA lesions generated by the interaction between therapeutic thiopurines and UVA light. *DNA repair*, 6(3), pp.344–354.

Zhang, Y., Zhou, J. & Lim, C.U., 2006. The role of NBS1 in DNA double strand break repair, telomere stability, and cell cycle checkpoint control. *Cell Research*, 16(1), pp.45–54.

Zhao, B. et al., 2010. Detection and prevention of ocular phototoxicity of ciprofloxacin and other fluoroquinolone antibiotics. *Photochemistry and photobiology*, 86(4), pp.798–805.

Zilfou, J.T. & Lowe, S.W., 2009. Tumor Suppressive Functions of p53. *Cold Spring Harbor Perspectives in Biology*, 1(5), pp.a001883–a001883.